Wheat non-specific Lipid Transfer Proteins: identification and characterisation of nuclear-encoded fertility restorer genes

By

Allan Kouidri

Thesis submitted in fulfilment of the requirements for the degree of Doctorate of Philosophy in the Faculty of Sciences at The University of Adelaide

School of Agriculture, Food and Wine

THE UNIVERSITY of ADELAIDE

June 2018

Wheat non-specific Lipid Transfer Proteins: identification and characterisation of nuclear-encoded fertility restorer genes

By

Allan Kouidri

Supervised by:

Dr Ute Baumann

Research Scientist

Bioinformatics Group Leader

Plant Genomics Centre

The University of Adelaide, AUS

Dr Ryan Whitford

Research Scientist

Plant Genomics Centre

The University of Adelaide, AUS

Table of contents

Abstract

Plant non-specific lipid transfer proteins (nsLTPs) constitute a large protein family found in all land plants. NsLTPs are involved in a wide range of biological processes, however, only few members have been functionally characterised. The aim of this project was to investigate the biological function of TaMs1, a wheat glycosylphosphatidylinositol (GPI)-anchored nsLTP. *TaMs1* was identified as a dominant wheat fertility gene necessary for pollen exine development and proposed for use in the efficient bulking of male-sterile lines required for hybrid wheat seed production. Additionally, we identified and analysed nsLTP members in bread wheat on a genome-wide scale, providing a valuable resource aimed at elucidating the function of these genes in wheat development.

Firstly, to investigate the biological function of TaMs1, we conducted expression analysis of its three homeoalleles (A, B, and D sub-genomes) on a series of wheat tissues collected at different developmental stages. *TaMs1* transcripts were detected exclusively in anthers during early microspore development, and we only observed expression of the B-genome-derived *TaMs1* (Chapter 3). Additionally, we observed that previously reported genes deemed necessary for pollen exine formation were not differentially regulated in *ms1* deletion mutants (*ms1c,* cv. Cornerstone) relative to Wild-Type, suggesting an independent function for TaMs1 from these genes during pollen development. Moreover, we showed that the encoded protein TaMs1 is targeted to the plasma membrane.

For a commercially viable hybrid wheat production platform, complete penetrance of the *ms1*-induced male sterility is critical. Here, we observed male sterility penetrance to be variable depending upon *ms1* mutation type and genotypic background (Chapter 5). The single nucleotide polymorphism (SNP mutant) *ms1d* (cv. Chris), showed near-complete male sterility in various backgrounds, whilst partial to full fertility (incomplete penetrance) was observed for the homozygous *ms1c* deletion mutant. To identify possible loci involved with this incomplete penetrance, we used a genotyping-by-sequencing (GbS)-SNP-based linkage map followed by analysis of quantitative trait loci (QTL) for selfed-seed set in the homozygous mutant *ms1c*. Two QTLs, on chromosome 4AL and 2BS respectively, were identified to be associated with selfed-seed set. The 4AL QTL spans 36 cM and contains three *nsLTPs*, including the *TaMs1-A* homeologue, whereas the 2BS QTL spans 42.5 cM and contains four *nsLTPs*.

Finally, to study the evolution of *nsLTPs* we conducted a genome-wide identification of this gene family in wheat (Chapter 4). A total of 461 putative *nsLTPs* were identified from the wheat genome (*TaLTPs*) (cv. Chinese Spring). The evolutionary relationships of the retrieved *TaLTPs* with rice and *A.thaliana nsLTPs* revealed an expansion of this family in the wheat genome, emerging mainly from tandem duplications. We showed that wheat *nsLTP* transcripts were detected in most tissues and stages of wheat development, which is in accordance with the diverse reported roles of this gene family. We further refined the expression profile of anther-expressed *nsLTPs* to provide additional male fertility gene sequences that can be used for the generation of alternative male-sterile wheat mutants.

The present work contributes towards an understanding of the biological role for *TaMs1* in male fertility, providing valuable information to help the development of large-scale and cost-effective multiplication of *ms1* male-steriles. Furthermore, this project provides groundwork for future fundamental research in wheat focussing on the role of *nsLTPs* in wheat development.

Thesis declaration

I certify that this work contains no material which has been accepted for the award of any other degree or diploma in my name, in any university or other tertiary institution and, to the best of my knowledge and belief, contains no material previously published or written by another person, except where due reference has been made in the text. In addition, I certify that no part of this work will, in the future, be used in a submission in my name, for any other degree or diploma in any university or other tertiary institution without the prior approval of the University of Adelaide and where applicable, any partner institution responsible for the joint-award of this degree.

I give consent to this copy of my thesis, when deposited in the University Library, being made available for loan and photocopying, subject to the provisions of the Copyright Act 1968.

I also give permission for the digital version of my thesis to be made available on the web, via the University's digital research repository, the Library Search and also through web search engines, unless permission has been granted by the University to restrict access for a period of time.

Allan Kouidri

30/05/2018

Acknowledgments

This dissertation would not have been possible without the guidance and help of several individuals who, in one way or another, contributed and extended their valuable assistance throughout the duration of this study.

First, it is with sincere gratitude that I would like to acknowledge the continual help and support of my supervisors, Dr Ute Baumann and Dr Ryan Whitford. The patience they have shown during encountered obstacles, along with the inspiration and expertise they provided will not be forgotten. The completion of this work would not have been possible without their recommendations and assurances.

I would also wish to thank all the current and past members of the hybrid group; I would especially like to thank Mathieu Baes for his support, helpful discussions and passionate debates. I would like to thank Margie Pallotta, Dr Takashi Okada and Elise Tucker for the insightful discussions, in addition to their guidance and knowledge regarding experimental work. Thanks to Patricia Warner, Taj Arndell, Anzu Okada and Sue Manning for their technical support.

I would like to thank the bioinformatics group, their knowledge and assistance was essential to this study. Thanks to Gwen Mayo for her microscopy assistance, to the transformation team, and Yuan Li for help provided with the qRT-PCR experiments. I wish to thank my independent advisor Dr Matthew Tucker for his valuable input early on in my project.

I gratefully acknowledge the funding sources that made my Ph.D. work possible. My scholarship was provided by the University of Adelaide and the Australian and Centre for Plant Functional Genomics (ACPFG). My work was also supported by DuPont Pioneer.

My time at the University of Adelaide was made pleasant in large part due to the many friends that became part of my life, Mathieu, Juan, Marie, Vahid, Alberto, Jessica, Nick, Fabio, Bart, Caterina, Matteo, William, Amelie, Abdel, Taj, Simon and Margaret.

I would like to express my deepest gratitude to my parents for their supports in all my pursuits.

Finally, my special thanks go to Pauline Thomelin, my loving, supportive, encouraging, and patient partner who made this journey far easier and more enjoyable.

List of abbreviations

8CM	eight cysteine motif
aa	amino acid
ABA	Abscisic Acid
AP2	APETALA2
Ba	Blue aleurone
bp	base pair
cDNA	complementary DNA
CDS	Coding Sequence
CHA	Chemical Hybridizing Agent
cM	CentiMorgan
CMS	Cytoplasmic Male Sterility
CO_2	Carbon Dioxide
CS	Chinese Spring
Cys	Cysteine
DH	Doubled Haploid
DNA	Deoxyribonucleic Acid
EGMS	Environment-Sensitive Genetic Male Sterility
EMS	Ethyl-methanesulfonate
ER	Endoplasmic Reticulum
ERF	Ethylene Response Factor
FAO	Food and Agriculture Organization
FPKM	Fragments Per Kilobase of exon per Million fragments mapped
GA_3	Gibberellic Acid
GFP	Green Flurorescent Protein
GM	Genetically Modified
GPI	Glycosylphosphatidylinositol
GS	Genomic Selection
GUS	β-Glucuronidase
IWGSC	International Wheat Genome Sequencing Consortium
JA	Jasmonic Acid
Ka	nonsynonymous
KASP	Kompetitive allele specific PCR
kDa	kilo Dalton
Ks	synonymous
LBD	Lipid Binding Domain
LZ	Lanzhou
M	Molar
MAS	Marker Assisted Selection
Mbp	Mega base pairs

mCh	mCherry
mRNA	messenger RNA
ms	male sterility
MW	Molecular Weight
MYA	Million Years Ago
NMS	Nuclear Male Sterility
nsLTP	non-specific Lipid Transfer Protein
PCD	Program Cell Death
PCR	Polymerase Chain Reaction
PGMS	Photoperiod-Sensitive Genetic Male Sterility
pI	Isoelectric point
PMC	Pollen Mother Cell
PR	Pathogenesis- Related
PTGMS	Photothermal-Sensitive Genetic Male Sterility
qRT-PCR	quantitative Reverse Transcription -PCR
QTL	Quantitative Trait Loci
Rf	fertility restorer
Rf^{multi}	Restoration of fertility in multiple CMS systems
RFP	Red Fluorescent Protein
RNA	Ribonucleic Acid
RNAi	RNA interference
SAR	Systemic Acquired Resistance
SNP	Single Nucleotide Polymorphisms
SP	Signal Peptide
SPT	Seed Production Technology
St	Stage
TFBS	Transcription Factor Binding Sites
TGMS	Thermosensitive Genetic Male Sterility
WT	Wild Type

Chapter 1

General introduction

Chapter 1
General introduction

1.1 Context of the thesis

The 20th century has seen spectacular technological advances and scientific discoveries, which have resulted in an outstanding increase in agriculture productivity. The "green revolution" led to substantially higher crop yields resulting in enough food produced to meet population demand. However, considering the earth's rapid increase in human population growth, global food security remains a central challenge of the 21st century and much needs to be done:

- To date, around two billion people are food insecure according to the FAO's food security definition (Wheeler and Braun, 2013).
- In 2014-16, 797 million people were unable to acquire sufficient food to meet the necessary dietary energy requirements, representing 11% of the worldwide population (FAO *et al.*, 2015).
- Nearly half of all deaths in children under 5 are attributable to undernutrition (UNICEF *et al.*, 2016).
- In 2016, stunting (low height for age) affected 22.9 % of children under 5 due to a lack of food, representing a total of 154.8 million children. One in two stunted children are living in South Asia and one in three in sub-Saharan Africa (UNICEF *et al.*, 2016).
- Additionally, 52 million children under the age of five exhibit wasting (low weight for height) of which 17 million were severely wasted (UNICEF *et al.*, 2016).
- Food insecurity and starvation often cause more deaths than direct violence (Liu, 2017). Between 2007 and 2012, an estimated 70,000 people lost their life due to conflicts and terrorism (GDAVD, 2015). In contrast, starvation caused 250,000 death in Somalia alone between 2010 and 2012 (FAO, 2013).

Regrettably, current and future projected trends are not favourable towards solving these issues. Firstly, population growth is expected to result in large increases in staple food demands. Secondly, we will be confronted by a likely rise in the occurrence of natural disasters, as new records in average temperature have been beaten consecutively in the years 2014, 2015 and 2016 (Earth Observatory, 2016). This rising temperature and multiplication of climate-related disasters will increasingly jeopardize food security (FAO, 2015). As a result, climate change is projected to put an additional 120 million people at risk of undernourishment by 2050 (Liu, 2017). To tackle such issues, increasing the current crop yield gain and yield stability will provide an important part of the solution towards sustainable food security.

1.2 Structure of the thesis

The thesis presented consists of six chapters, including a series of three papers (Figure 1). Two manuscripts have been submitted, and the remaining chapter has been written in manuscript format. Chapter 1 (this chapter) provides a broad overview of the thesis background, and research objectives are briefly discussed. Chapter 2 provides a comprehensive review of the literature for the work presented, giving support for the research objectives. Chapter 3, 4 and 5 are three experimental papers following the standard manuscript format that includes: Abstract, Introduction, Materials and Methods, Results, Discussion and References. The thesis will conclude in Chapter 6, which provides a general discussion of the findings reported in this thesis, summary of contributions of knowledge and considerations for future research directions.

This thesis also contain one appendix:

Tucker, E. J., Baumann, U., Kouidri, A., Suchecki, R., Baes, M., Garcia, M., Okada, T., Dong, C., Wu, Y., Sandhu, A., Singh, M., Langridge, P., Wolters, P., Albertsen, M. C., Cigan, A. M., & Whitford, R. (2017). Molecular identification of the wheat male fertility gene Ms1 and its prospects for hybrid breeding. *Nature Communications*, *8*(1), 869.

The data reported in this manuscript served as fundamentals for designing this PhD research project in wheat. The experimental data was in part generated and prepared for publication during the course of the PhD candidature.

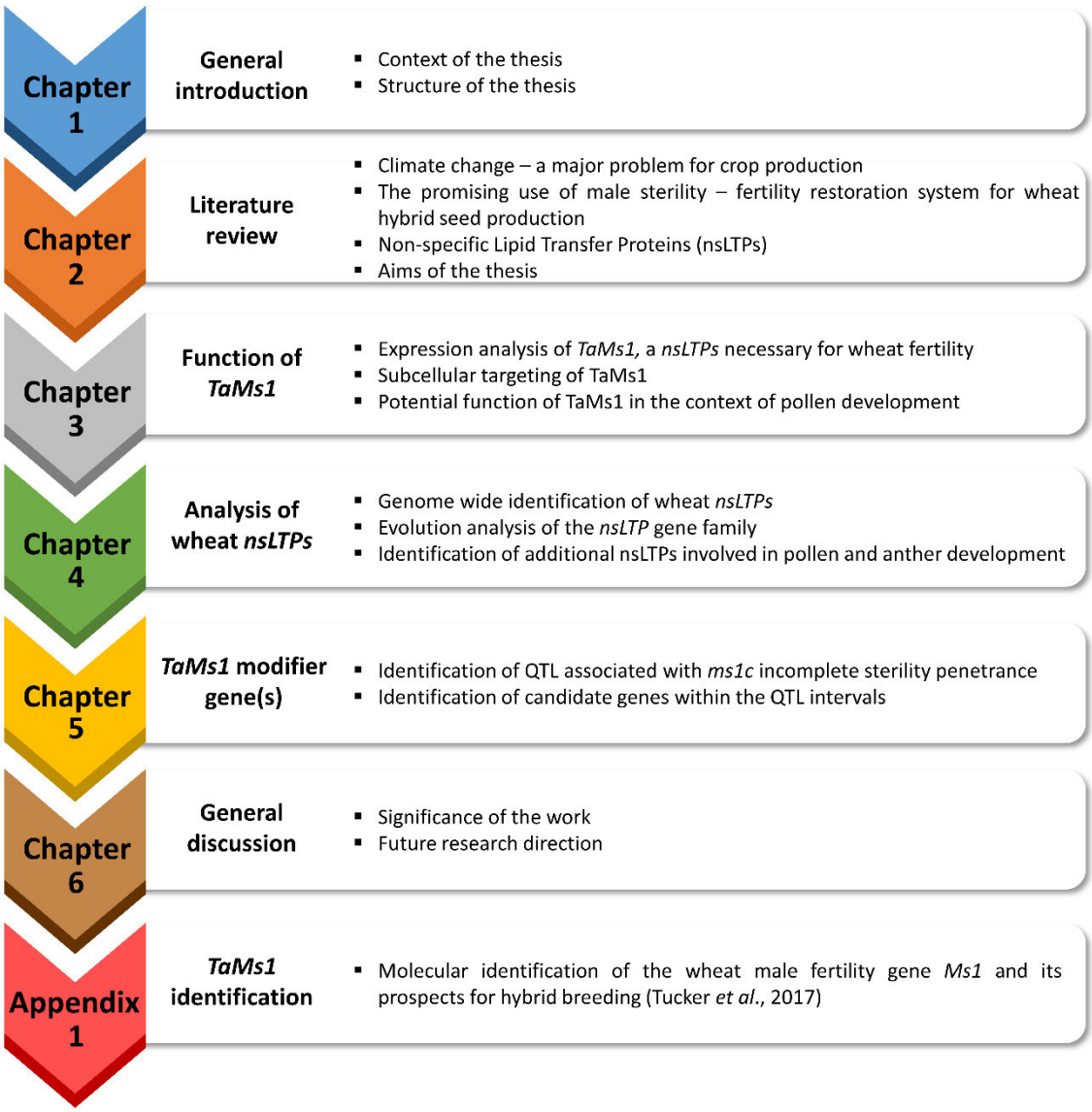

Figure 1 | Schematic structure of the thesis.

Chapter 2

Literature review

Chapter 2
Literature review

2.1 Increasing cereal production under a changing climate

2.1.1 Production and economic importance of wheat

The cultivation of bread wheat (*Triticum aestivum* L.) started nearly 10,000 years ago in the fertile crescent, which stretches throughout the middle east an includes countries now known as Iraq, Jordan, Israel, Palestine, Egypt, Turkey and Iran (Brown *et al.*, 2009). To date, wheat is cultivated in 128 countries and is considered as one of the most important staple crops for human consumption. Wheat accounts for 11 % of the total agricultural output with about 750 million of tonnes produced in 2016 (Liu, 2017) and it is the most widely cultivated plant, representing 16 % of the total area under cultivation. In addition, wheat is the most traded commodity with 23 % of the total production exported (160 million tonnes) compared to 12 % for maize and 5 % for rice (Liu, 2017). As a consequence, wheat availability and price fluctuation could have a large impact on food security. The importance of wheat also relates to its nutritional value, providing a total 20 % of daily protein and food calories.

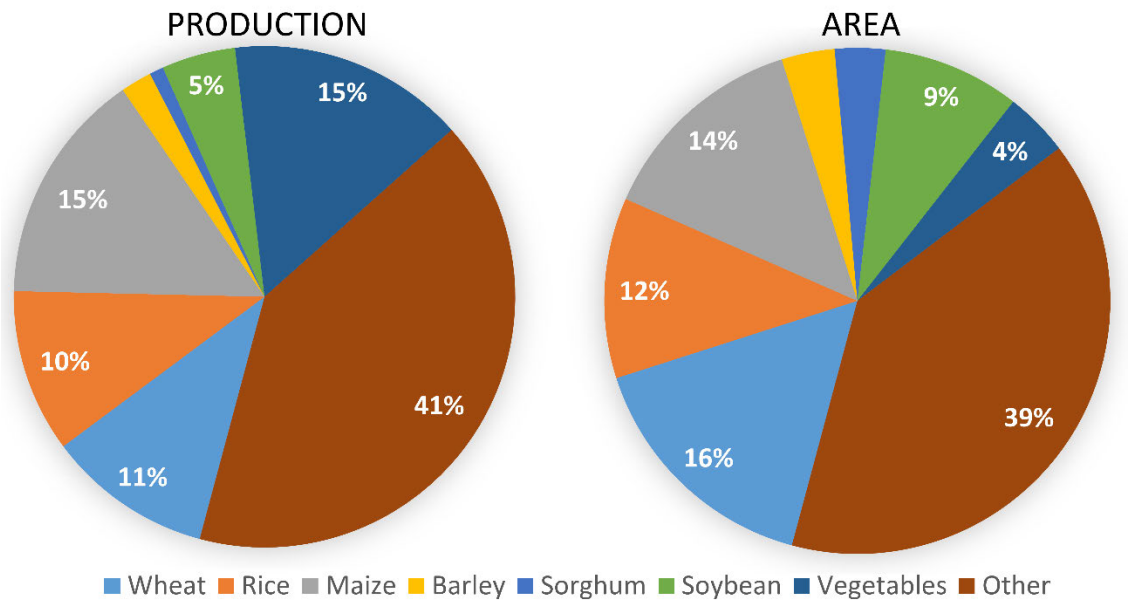

Figure 1 | Comparison of major crop production and cultivated area in 2016. Data from FAOSTAT, 2017.

2.1.2 Climate change is predicted to negatively affect food production

The world population is projected to reach 9.7 billion by 2050 (Alexandratos and Bruinsma, 2012). Accordingly, global demand for food, feed and biofuel, is predicted to increase by 50 %

from 2012 to 2050 (FAOSTAT, 2017). To meet this demand, agricultural output would need to more than double by 2050 in sub-Saharan and South Asia (Alexandratos and Bruinsma, 2012; FAOSTAT, 2017). In the rest of the world, an increase of over 30 % to the 2017 level would be required. However, in the past 40 years, climate change has affected crop production counteracting a portion of the yield gain increase arising from genetic progress and technology (Lobell *et al.*, 2011). For instance, in Australia, climate trends are suggested to account for stalled wheat yields since 1990 (Hochman *et al.*, 2017). In addition, climate change is predicted to increase the frequency of extreme climatic events such as drought, heat, flood and frost (Coumou and Rahmstorf, 2012). Such extreme weather disasters were shown to significantly reduce cereal production by 9 - 10 % (Lesk *et al.*, 2016). Across the United States of America (USA), maize yields are predicted to decline by 20 % to 40 % by 2050 (Leng and Huang, 2017). For wheat, mean yields are also projected to decrease under climate change, with global wheat yield predicted to decline between 4.1 % and 6.4 % for each degree of further temperature increase (Asseng *et al.*, 2015; Liu *et al.*, 2016). Studies looking at the impact of climate change on agriculture outputs were combined by Porter (2014) in a meta-analysis of 1090 studies. This meta-analysis, focussing predominantly on wheat, maize, rice and soybeans yields under different climate trend predictions, led to the conclusion that there will be a significant fall in global yield over the long term (Figure 2).

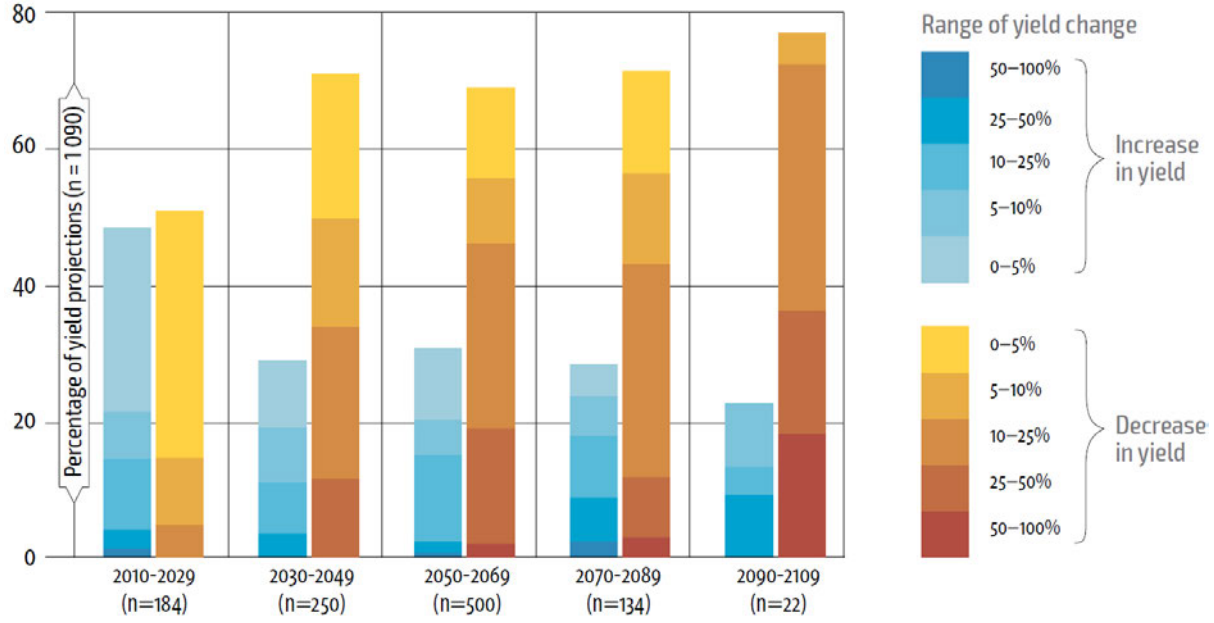

Figure 2 | Projected changes in crop yields owing to climate change (Porter, 2014; FAOSTAT, 2017).

2.1.3 Increasing crop yield would require improvement in breeding and selection technologies

Since the introduction of the Green Revolution crops in the 1960's, cereal yield has been boosted, and total cereal production has, on average, achieved a linear increase from 1 billion to 2.5 billion tonnes (FAOSTAT, 2017). This gradual increase of the total crop production is due to important agriculture innovations combining: (i) extension of the land water supply system; (ii) extensive use of fertilizers; (iii) adoption of modern improved varieties through the development of breeding technologies. However, agronomic practices to improve yield such as fertilizers and water inputs are limited and the amount of land that can be devoted to agriculture is restricted. Consequently, from now on, the best approach to increase yield is likely to rely on the improvement of breeding and selection technologies.

In wheat, over the past 60 years, five conventional methods of wheat breeding have consistently contributed to a steady rate of 1% yield gain increase per year (Fischer *et al.*, 2014). These breeding techniques, affected by the inbreeding nature of wheat, include: pedigree selection, single seed descent, doubled haploid (DH), bulk selection and backcross breeding (Bentley and Mackay, 2017). However, with the reported stagnation of wheat yield gain and the projected negative impact of a changing climate on global production, there is an urgent need to develop new breeding techniques to rapidly increase wheat's yield potential, improve its yield stability and increase the sustainability of its production systems. New promising breeding techniques with the potential to increase the rate of yield gain in wheat have been proposed. These include, marker assisted selection (MAS) and genomic selection (GS), genetic engineering, genome editing, mutation breeding, and F1 hybrid breeding (Bentley and Mackay, 2017). Here, we will focus on the potential of hybrid wheat breeding for improving the rates of genetic gain and therefore yield.

2.2 Hybrid wheat breeding

2.2.1 Heterosis

Heterosis or outbreeding performance is the improvement of agronomical characteristics of the offspring relative to both parents (Shull, 1908). Heterosis refers to the phenomenon in which the offspring shows better yield, biotic and abiotic stress resistance than either parent. This is in part due to superior combinations of parental alleles. The extent of the heterotic effect is related to the genetic divergence between the two parents. Generally, the more

divergent the parents are genetically, the greater the heterotic effect (Reif *et al.*, 2005). This effect is important in the F_1 generation and decreases in subsequent generations. This phenomenon is known as inbreeding depression.

The exploitation of heterosis has resulted in important economic benefits for many crops. Over half of the production from major crops is derived from hybrid varieties, including rice, maize, sorghum, rapeseed and sunflower (Martín *et al.*, 2010). In the USA and China, hybrid maize accounts for more than 95% of the total maize produced (Chen and Liu, 2014; USDA, 2018). Yield improvement associated with heterosis was estimated to be 55% in rice, 11% in barley, 68 % in foxtail millet, 263 % in tomato and 200 % in brassica oil crops (Fu *et al.*, 1990; Siles *et al.*, 2004; Jain *et al.*, 2007; Longin *et al.*, 2012; Mühleisen *et al.*, 2014). In wheat, estimates of heterotic yield gain range from 3.5 % to 15 % (Longin *et al.*, 2012). Over the past century modern plant breeding has restricted cultivated wheat's genetic diversity (Fu and Somers, 2009). The ability to capture heterosis will require the creation of genetically divergent groups, also known as heterotic groups.

2.2.2 Hybrid breeding systems

2.2.2.1 Prerequisites

Commercial hybrid seed production has several prerequisites. Firstly, yield gains through hybrid breeding necessitate a panel of genetically diverse parental lines (Fisher, 1972). These genetically diverse lines that underpin the heterotic effect must first be evaluated, with optimal combinations thereof requiring field testing.

In order to produce the hybrid seed, effective pollination control is required. Cost-effective production systems for hybrid seed need to prevent unwanted self-pollination with no deleterious effect on plant growth or vigor, more specifically impairing the male organs of the mother line without affecting either the female organs or seed development. Wheat, however, is a strong self-pollinator with male (anther, pollen) and female reproductive organs (stigma, ovary) being small and co-localized within one floret (Figure 3). As a consequence, hand emasculation is highly impractical for commercial production of hybrid wheat seed.

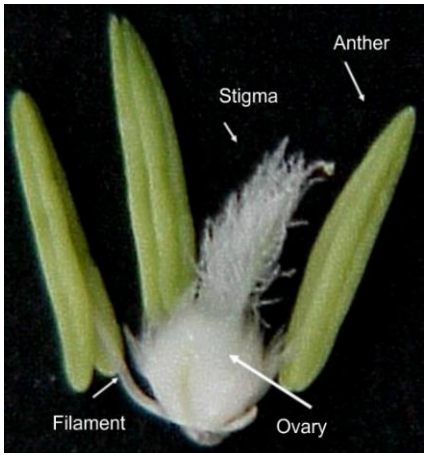

Figure 3 | Wheat reproductive organs.

In addition, when seeds are the end use product (e.g. all cereals), the fertility of sterile plants must be fully restored in order to exploit the optimal yield potential in the hybrid progeny. For this purpose, male sterility must be counteracted by fertility restorer (*Rf*) genes. *Rfs* should ideally possess the following characteristics:

(i) Completely restore fertility to male steriles in a wide range of genetic backgrounds:

- Seed yield derived from F1 plants can be compromised if the *Rf*(s) only partially restore fertility; an efficiency of 100% fertility restoration is required when using sterility inducing systems, to make it both cost effective and efficient.
- The system must work across all wheat germplasm.

(ii) Be non-conditional: a conditional fertility restorer gene can restrict the use of sterility systems to geographical regions in which there is predictable day length and/or temperature variations. Non-conditional *Rfs* permit hybrid breeding in all environments.

Several approaches have been successfully applied for hybrid wheat breeding and these are described in more detail below.

2.2.2.2 Cytoplasmic Male Sterility (CMS)

CMS is a maternally inherited trait resulting from the conflict between nuclear and mitochondrial encoded genomes. In wheat, CMS is mostly based on the sterilizing ability of the *Triticum timopheevii* Zhuk. cytoplasm (Wilson and Ross, 1962). The sterilizing cytoplasm was transferred from *T. timopheevii* to *T. aestivum* via backcrossing and resulted in male-sterile *T. aestivum cyt. T. timopheevii* alloplasmic lines.

However, despite the development of this system across various wheat germplasms, no optimum CMS system for hybrid seed production was successfully established in wheat (Whitford *et al.*, 2013). This led to the search for additional cytoplasm – fertility restorer gene systems, aside from *T. timopheevi*, that could also be used to induce male sterility in wheat. Among them, they include *Rfv1* gene for *Aegilops kotschyi* (Mukai and Tsunewaki, 1979), *Rfm1* for *Aegilops mutica* and *Rfn1* for *Aegilops uniaristata* (Tsujimoto and Tsunewaki, 1984).

In all three cytoplasms male sterility was observed when the normal bread wheat chromosome 1BS was replaced with 1RS (1RS.1BL translocation) (cv. Salmon). However, 1RS.1BL translocation affected negatively on wheat quality (Mukai and Tsunewaki, 1979). The bread wheat landrace Chinese Spring was reported to contain a “Restoration of fertility in

multiple CMS systems" (*Rf*^{multi}) locus, which contains *Rf* genes for these three cytoplasms clustered within a 2.9 cM interval of chromosome 1BS (Tsunewaki, 2015). This cluster of *Rf* genes enabled engineering the *Rf*^{multi} on 1BS with a 2.8cM insert derived from 1RS. This faciliates the development of wheat hybrids without being penalised in terms of baking quality based on the presence of the entire 1RS arm (Hohn and Lukaszewski, 2016). Additionally, a system that results from the incompatibility between *T. aestivum* cytoplasm and the cytoplasmic genome of the wild barley, *Hordeum chilense Roem. et Schultz.* was reported and termed the msH1 CMS system (Castillo *et al.*, 2015).

Towards large-scale commercial deployment of wheat hybrids, this approach requires significant improvement especially in terms of fertility restoration. Current methods do not allow the production of fully fertile wheat across all genetic backgrounds, given that CMS-based fertility restorers can be restricted to specific germplasm. Another problem associated with the deployment of CMS is the negative effects on plant vigour and yield derived from the "alien" cytoplasm.

2.2.2.3 Chemical Hybridizing Agent (CHA)

CHA refers to a group of chemicals able to induce male sterility in plants. Several chemicals have shown gametocidal activity, these include auxins/anti-auxins (Hoagland *et al.*, 1953; Porter and Wiese, 1961; Rowell and Miller, 1971), arsenicals and halogenated aliphatic acids (Roux and Chirinian, 1959). Most of the chemical agents have shown strong phytotoxic effects. Consequently, in Europe, sintofen (CROISOR®100) produced by Saaten Union Research (Germany) is the only deregulated chemical currently approved for use in commercial hybrid wheat seed production. More recently, a pyridazinecarboxylic acid compound called SQ-1 was reported to be an efficient chemical hybridising agent for inducing wheat male sterility, attracting interest for hybrid seed production, mainly in China (Liu *et al.*, 2018; Wang *et al.*, 2018).

The use of CHAs allows a large number of parent combinations to be tested for hybrid seed production. This system also simplifies seed production given that it does not require breeding and use of a maintainer line for female parent propagation, or the identification and tracking of fertility restorer genes in the male parent. However, CHA-based systems have several

drawbacks, such as (i) phytotoxicity (ii) difficulties in field application, due to rain, heat and wind events that can reduce the chemical agent's efficacy and (iii) potential reduction of seed set in the treated female parent.

2.2.2.4 Environment-Sensitive Genetic Male Sterility (EGMS)

The term EGMS refers to the pollen fertility affected by either temperature (thermosensitive genetic male sterility, TGMS), or day length (photoperiod-sensitive genetic male sterility, PGMS), or both (photothermal-sensitive genetic male sterility, PTGMS). The first reported case of EGMS was identified in pepper, which showed male sterility under greenhouse conditions but restored fertility in the field (Martin and Grawford, 1951). Subsequently, EGMS was reported in several species, including wheat (Fisher, 1972), maize (Duvick, 1966), barley (Batch and Morgan, 1974), tomato (Rick and Boynton, 1967) and in rice (Cheng *et al.*, 2007). In practice, rice EGMS systems have been problematic in terms of stability of the male-sterile phenotype or incomplete restoration of fertility to the F_1 progenies. In wheat, TGMS line BS366 is reported to exhibit aberrant cytokinesis during meiosis under low temperature (Xu *et al.*, 2013). The sterility of BS366 under cold stress was determined to result from an upregulation of *TaPaO1*, a pheophorbide *a* oxygenase (PaO) encoding gene that is involved in chlorophyll degradation (Yuan *et al.*, 2018). In contrast to CMS, EGMS systems can take advantage of a wider range of germplasm, which provides potential for greater development and exploitation of heterotic pools. However, EGMS sterility expression is restricted to specific regions and seasons (Huang *et al.*, 2014).

2.2.2.5 Nuclear Male Sterility (NMS)

Nuclear Male Sterility involves nuclear mutations that impair pollen and anther development but do not affect female reproductive development. NMS is often monogenic recessive and found in many crop species including maize, tomato, sorghum, barley, rice and wheat (Kaul, 1988). NMS-based systems exploit these recessive mutations in the development of maintainer lines. One such NMS-based system uses a maintainer line which is completely male fertile but has the capacity to produce 100% male-sterile progenies when used as a pollinator of male-sterile plants (Perez-Prat and van Lookeren Campagne, 2002). Such a method was first described by Driscoll, 1972 who outlined a fertility control system based on a fertility restoring

alien addition chromosome. A maintainer line containing this alien chromosome is used for up-scaling production of male-sterile female inbred parents. This was first called the XYZ system for hybrid wheat breeding. Subsequently, alternative names for such a system have been proposed:

- 4E-*ms* system

The principle of XYZ system was realized in 2006 with the development of the 4E-*ms* system (Zhou *et al.*, 2006). This approach simplified the selection of male-sterile populations by cytogenetic-chromosomal manipulation. In this system the Lanzhou (LZ) male sterile mutant (*ms1g*) is complemented by the presence of an additional 4E chromosome derived from *Agropyron elongatum spp ruthenicum*. Generation of this stock was achieved by a cross between the LZ male-sterile mutant and a 4E disomic addition line male.

The most important improvement comes from the use of a marker gene because the 4E chromosome possesses both a fertility restorer and a visual marker, blue aleurone, which causes the seeds to appear blue in colour (Figure 5). The blue aleurone *1* (*Ba1*) trait allows easy seed selection depending upon dose whereby increased addition in chromosome number induces a deeper blue hue. So, 4E disomic addition line (2n=44) seeds are deep blue, 4E monosomic addition lines (2n=43) seeds are light blue and LZ (2n=42) seeds are white.

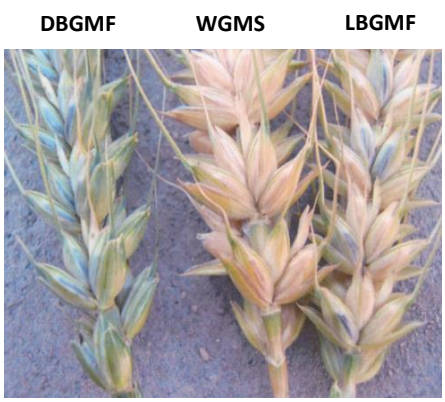

Figure 5 | Blue aleurone trait used in the 4E-ms system. (Zhou et al, 2006) Left, DBGMF: Deep Blue Grain Male Fertile; middle, WGWS: White Grain Male Sterile; right, LBGMF: Light Blue Male Fertile.

For a commercially-viable application of this system, the recessive male-sterile mutant must have 100% phenotypic penetrance, otherwise selfed female inbred progenies known as “rouges” could reduce hybrid seed purity and therefore compromise hybrid yield. However, the major drawback to this system is the unknown linkage between the fertility restorer locus and the marker gene, with a possibility of meiotic instability of the 4E-monosomic addition that could result in chromosome breakage at the centromere. While *Ba1* was mapped on distal region of the long arm of chromosome 4E, the position of the fertility restorer locus

remains to be identified. Therefore, systems using genetic male sterility complemented by alien chromosome(s) might not be ideal for commercial seed production.

- Genetically modified (GM) plants

An alternative solution for propagating male-sterile lines using maintainer lines is described by Wu *et al*., 2016 (Figure 6). These authors propose a system which introduces a genetic construct (*Ms:P:S*) into a male sterile plant (*ms*/*ms*). The transgenic maintainer locus (SPT transgene, *Ms:P:S*) includes three components:

- A fertility restorer gene that can render the male sterile mutant plant male fertile (*Ms)*
- Two genes linked to the fertility restorer gene
    - A screenable marker gene, which permits easy visual selection of seeds (*S*).
    - A pollination disruption gene, that prevents the inheritance of the transgene (*P*)

The plant containing the GM event is called the "SPT maintainer" (*ms*/*ms*; *Ms:P:S*). Its use for propagating male sterile plants is described in Figure 6.

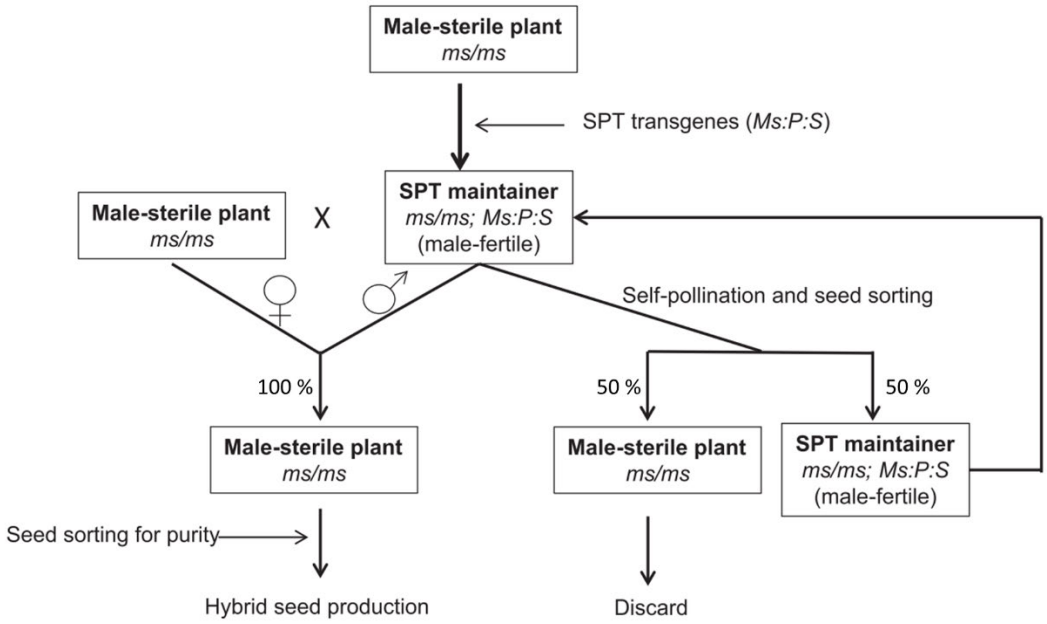

Figure 6 | Propagation of male-sterile (*ms*) plants. *Ms*, male fertility gene; *P*, pollination disruption gene; *S*, seed screenable marker gene; SPT, Seed Production Technology (Wu *et al.*, 2016).

The system is based on a GM event whereby a fertility restorer gene is physically linked on the same construct as a pollen lethality gene. The maintainer line contains the SPT construct to a hemizygous state. Consequently, 50 % of the produced pollen grains would lack the SPT construct and therefore be fertile, while 50 % would be non-viable as they contain the

pollination disruption gene. This effectively prevents the transmission of the STP construct to progenies via pollen. A cross between male sterile female plants (*ms*/*ms*) and pollen lethality gene-containing maintainer plants (*ms*/*ms*; *Ms:P:S*) produce 100% male-sterile progenies. In parallel, the multiplication of SPT maintainer lines is based on the presence of a visual marker linked to the fertility restorer gene. Visual marker-based maintainer lines produce both viable (*ms*/*ms*) and non-viable (*ms*/*ms*; *Ms:P:S*) pollen grains. Progenies resulting from self-pollination segregate 1:1 for the SPT transgene (*Ms:P:S*) due to viable transmission of the transgene via female gametes, with seeds carrying the transgene being coloured. Seed sorting facilitates separation of non-coloured non-transgenic male sterile seed as well as the SPT maintainer line seed stock.

NMS mutants and their respective fertility restorers are important components for developing such a transgenic construct driven non-GM fertility control system. The major limitations towards the development of such a system in wheat are isolation of gene sequences capable of completely restoring fertility to a homozygous recessive male-sterile mutant.

2.2.3 Wheat genic male sterility loci

2.2.3.1 Candidate male sterile mutants

As previously mentioned, for agronomic utilization of a NMS-based fertility control system, the fertility restorer should be non-conditional, dominant and be able to fully restore fertility to a completely penetrant homozygous recessive male sterile mutant. In the literature, several loci have been described in wheat that are essential for male fertility (Whitford *et al.*, 2013). Only two of these loci meet most of the requirements for developing an NMS-based fertility control system. These are *Ms1* (see Table 1 for references and description of the mutant alleles generated to date) and *Ms5* (Klindworth *et al.*, 2002).

Research to date indicates that the male-sterility phenotype resulting from the *ms5* (3AL) mutation is unlikely to be completely penetrant across a range of genetic backgrounds (Pallotta *et al.*, unpublished data), indicating that *Ms5* may not be an ideal candidate for developing a NMS-based fertility control system. For this reason, *ms1* (4BS), a more penetrant recessive non-conditional male sterility locus represents a better candidate for developing a NMS-based wheat fertility control system. However, a thorough assessment of the degree of *ms1* male sterility penetrance across broad germplasm is needed.

Table 1 | Allele variation of the known *ms1* mutants

***Ms1* mutant allele(s)**	**Germplasm**	**Reference**
ms1a	cv. Pugsley's spontaneous male sterile mutant	(Pugsley and Oram, 1959)
ms1b	cv. Probus radiation induced deletion (RID) mutant: interstitial deletion of chromosome arm 4BS	(Fossati and Ingold, 1970)
ms1c	cv. Cornerstone RID mutant. The deletion is larger than that of Probus. The deleted portion is distally located on chromosome arm 4BS, representing ~16% of the arm.	(Driscoll, 1977)
ms1d - e	EMS (Ethyl Methanesulfonate) derived mutants (cv. Chris)	(Klindworth *et al.*, 2002)
ms1g	cv. Lanzhou spontaneous male sterile mutant	(Zhou *et al.*, 2007)
ms1h	EMS derived mutants (cv. Gladius)	(Tucker *et al.*, 2017)
ms1h-q	EMS derived mutants (cv. Ningchun)	(Wang *et al.*, 2017)

2.2.3.2 *ms1* male sterility penetrance

The penetrance of *ms1* refers to the proportion of plants homozygous for this mutation that express a male-sterility phenotype. Complete penetrance refers to all *ms1/ms1* homozygote individuals being completely sterile. Analysis of F_2 phenotypic segregation ratios can help to determine whether single or multiple loci are likely involved in phenotypic expression, in this case the ratio of fertile- versus sterile plants. Ratios that are distorted from 3:1, could be explained by the presence of "modifier gene(s)" that are non-allelic to *ms1* and capable of restoring fertility to the male sterile. Another explanation could be the presence of a segregation distortion gene (meiotic drive), which produces a distortion in normal segregation in favor of either the dominant or the recessive restorer gene (*Ms1)*.

Penetrance tests have been performed by crossing *ms1d/ms1d* homozygote plants (point mutation) with a series of six wheat Australian varieties. For each of these crosses, the F_2 fertile:sterile segregation fitted the expected 3:1 ratio (Chapter 5). These results indicate that the *ms1d* mutant phenotype is likely to be controlled by a single recessive gene in the genetic backgrounds tested.

Penetrance has also been evaluated for the *ms1c* deletion mutant. Surprisingly, in some F_2 populations the phenotypic segregation ratio deviated from 3:1 (fertile:sterile) (Islam and

Driscoll, 1984). This phenotypic distortion may indicate that the *ms1c* mutant phenotype is not fully penetrant. One hypothesis to explain this incomplete penetrance could be that the *ms1c* mutation is complemented by a "modifier gene" that is present at *Ms1* homoeloci (4AL or 4DS) or at another position in the genome. This incomplete sterility penetrance can be a major drawback toward the deployment of a commercially-viable hybrid seed production platform and knowledge of its genetic basis may assist in identifying alternative strategies for ensuring fully penetrant sterility.

2.2.3.3 *TaMs1:* a putative non-specific Lipid Transfer Protein (nsLTP)

Tucker *et al.* (2017) first reported the identification of *TaMs1*. Using a map-based cloning approach that included the *ms1b* and *ms1c* deletion mutants that carry deletions differing in size and a biparental F_2 mapping population involving an EMS-derived mutant (*ms1d* x Gladius), *TaMs1* was located to a 251 Kb region predicted to contain 10 genes. Among those predicted genes, a putative GPI-anchored Lipid Transfer Protein (TaLTPg) was identified as a strong candidate based on tissue-specific expression data and functional annotation. Sequence analysis of the candidate gene across an EMS-derived mutant allele series (*ms1d, ms1e, ms1f* and *ms1h*) revealed critical point mutations in the coding region for each of the mutant alleles. Further, *TaMs1* was shown by transgenic complementation to fully restore male fertility to *ms1d*.

The identification of TaLTPg as *TaMs1* was also reported by Wang *et al.* (2017) who, similarly, used a positional cloning approach to determine the *TaMs1* gene sequence. In this study the authors generated 10 additional *ms1* alleles using an EMS-mutagenized population of cv. Ningchun. These include four stop-codon mutant alleles *(ms1h*, *ms1l*, *ms1m*, *ms1q*), three non-synonymous mutations within the predicted lipid binding domain (*ms1n*, *ms1o*, *ms1p*), two splice-site mutants (*ms1i* and *ms1k*) and one non-synonymous mutation at C-terminal region of TaMs1 (S195F) predicted to affect the site of GPI-anchor addition (Chapter 3).

Taken together, these findings strongly suggest that the identified *TaLTPg* gene sequence is the male fertility gene sequence for *Ms1*.

2.2.4 Non-specific Lipid Transfer Proteins (*nsLTPs*)

nsLTPs consist of a large gene family present across all plant species, with 79 members in *A. thaliana*, 58 in sorghum, 63 in *Brassica*, 91 in cotton, 77 in rice, 63 in maize and 156 in wheat (Boutrot *et al.*, 2008; Li *et al.*, 2014, 2016; Wei and Zhong, 2014).

2.2.4.1 Structural characterization of plant *nsLTPs*

Plant nsLTPs are small (7-10 kDa), stable proteins with a highly conserved consensus motif of 8 cysteines (8CM) of the general form C–Xn–C–Xn–CC–Xn–CXC–Xn–C–Xn–C, whereby "X" denotes any amino acid and n denotes any number of amino acids (Figure 7). These eight cysteines are cross-linked by four disulfide bonds, thus resulting in resistance of nsLTPs to high temperature and denaturing agents (Lindorff-Larsen and Winther, 2001). This inter-connectivity stabilizes the tertiary structure and forms a hydrophobic cavity, capable of binding a broad range of lipidic compounds *in vitro*. Such activity facilitates lipid transport between inter-cellular membranes (Vergnolle *et al.*, 1992). Most nsLTPs possess an N-terminal signal peptide of 20-30 amino acids that target the protein to the secretory pathway (Figure 7) (Petersen *et al.*, 2011).

MERSRGLLLVAGLLAALLPAAAAQPGAPCEPALLATQVALFCAPDMPTAQCCEPVVAAVDLGGGVPCLCRVAA
EPQLVMAGLNATHLLTLYSSCGGLRPGGAHLAAACEGPAPPAAVVSSPPPPPPPSAAPRRKQPAHDAPPPPPP
SSEKPSSPPPSQDHDGAAPRAKAAPAQAATSTLAPAAAATAPPPQAPHSAAPTAPSKAAFFFVATAMLGLYIIL

Figure 7: The amino acid sequence of TaMs1. Amino acids highlighted in purple are the N-terminal signal peptide. The eight cysteines are represented in yellow. The pro-peptide GPI-anchored domain is shown in red.

Moreover, some nsLTPs such as TaMs1, possess an additional membrane-anchoring signal at the C-terminal region (Figure 7) (Eisenhaber *et al.*, 2003). The C-terminal signal sequence possesses an attachment/cleavage site (termed omega site), which is subject to post-translational modification whereby glycosylphosphatidylinositol (GPI) is transferred onto the C-terminal end of the protein (GPI-anchor). GPI-anchored proteins are therefore able to attach to the cell plasma membrane by integration of the phosphatidylinositol moiety within the plasma membrane (Paulick and Bertozzi, 2008) (Figure 8). The protein can be released from the anchor by cleavage from phospholipase C activity (Paulick and Bertozzi, 2008).

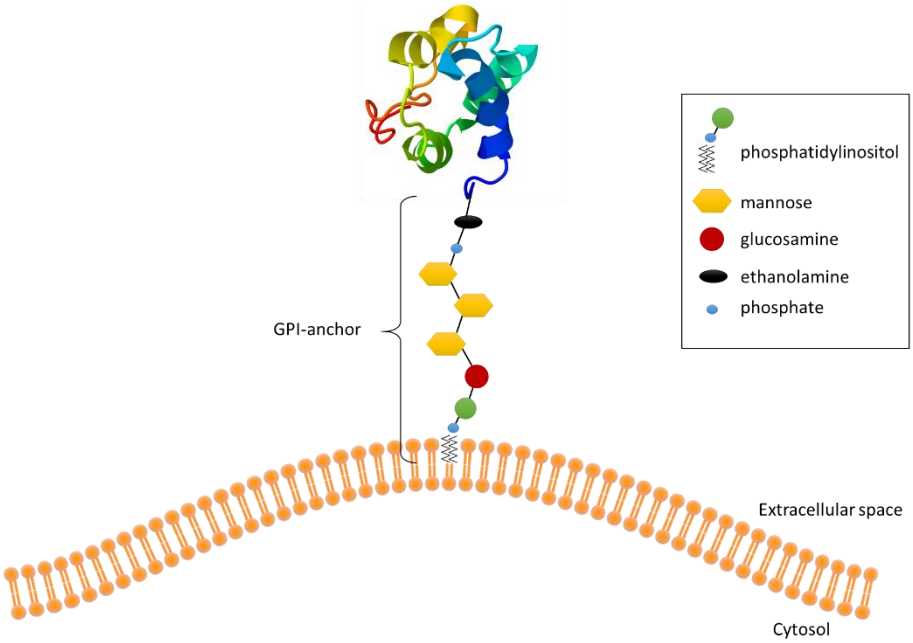

Figure 8 | A nsLTPg tethered to the plasma membrane via a GPI-anchor.

2.2.4.2 Classification and nomenclature of nsLTPs

nsLTPs were initially classified into two types based on their molecular mass, whereby nsLTP1 are 9 kDa and nsLTP2 are 7 kDa (Kalla *et al.*, 1994). However, after the identification of nsLTPs with molecular masses that differ from the proposed 7 kDa and 9 kDa, a novel classification dividing nsLTPs into 11 types (I, II, III, IV, V, VI, VII, VIII, IX, X, and Y) based on sequence similarity was proposed (Boutrot *et al.*, 2008; Liu *et al.*, 2010). Nevertheless, this classification was shown to be unsuitable for categorizing nsLTPs from early diverging plants (Edstam *et al.*, 2011) and therefore a third classification system was introduced. This system categorized nsLTPs into five major types (LTP1, LTP2, LTPc, LTPd and LTPg) and four minor types that have few members (LTPe, LTPf, LTPh, LTPj, LTPk) (Edstam *et al.*, 2011). Here the classification is based on the intron-exon pattern, which is suggested to carry the imprint of the evolution of the gene family (Del Campo *et al.*, 2013). This system also considers sequence similarity and the presence or absence of a GPI-anchor pro-peptide.

2.2.4.3 Function of nsLTPs

nsLTPs are part of the very large class of pathogenesis- related (PR) proteins constituting the PR-14 family (Sels *et al.*, 2008). *A. thaliana* DIR1 was the first nsLTP reported to be involved in disease resistance. DIR1 functions in systemic resistance signalling against *Pseudomonas syringe* (Maldonado *et al.*, 2002). A related function was found for the *A. thaliana* nsLTP AZELAIC ACID INDUCED 1 (AZL1), with *azi1* resulting in the loss of signal translocation of systemic acquired resistance (SAR) triggered by pathogen infections (Jung *et al.*, 2009). Additionally, wheat nsLTPs were shown to have an anti-fungal activity toward wheat and non-wheat pathogens *in vitro* (Sun *et al.*, 2008). A similar anti-fungal effect was shown for rice LTP110 (Ge *et al.*, 2003). Because no correlation was observed between the toxicity of nsLTPs and their ability to bind and transport lipids, one could speculate that that nsLTPs inhibitory effects result from an alteration of the pathogen membrane permeability.

nsLTPs are also reported to be involved in cuticular wax accumulation. In *A. thaliana*, a knock-down mutant line for *AtLTPG1* resulted in reduced wax accumulation of the stem surface (Figure 9a) (Debono *et al.*, 2009). AtLTPG2, of the same nsLTP class, was reported to functionally overlap AtLTPG1; with a double mutant *Atltpg1/Atltpg2* having a significantly lower cuticular wax load than each single mutant. In *Brassica napus,* overexpression of *BnLTP1,* caused in a decrease of cuticle wax on the leaf surface (Liu *et al.*, 2014). Other than being important for wax deposition, some evidence suggests nsLTPs are also involved in root suberin synthesis (Figure 9b) (Edstam *et al.*, 2013).

Additionally, nsLTPs were reported to be necessary for pollen development. In rice, the nsLTP *OsC6*, an anther-specific gene, was shown to be required for postmeiotic anther development (Zhang *et al.*, 2010). More evidence of nsLTP function for pollen development was studied *in planta,* using anther-specific genes from *A. thaliana* (*At5g62080* and *At5g07230*) (Figure 9c) (Huang *et al.*, 2013). These AtLTPs were shown to be secreted from the tapetum to become constituents of developing microspores. More recently, wheat *TaMs1* encoding a nsLTPg was demonstrated to be necessary for pollen exine formation and male fertility (Tucker *et al.*, 2017; Wang *et al.*, 2017).

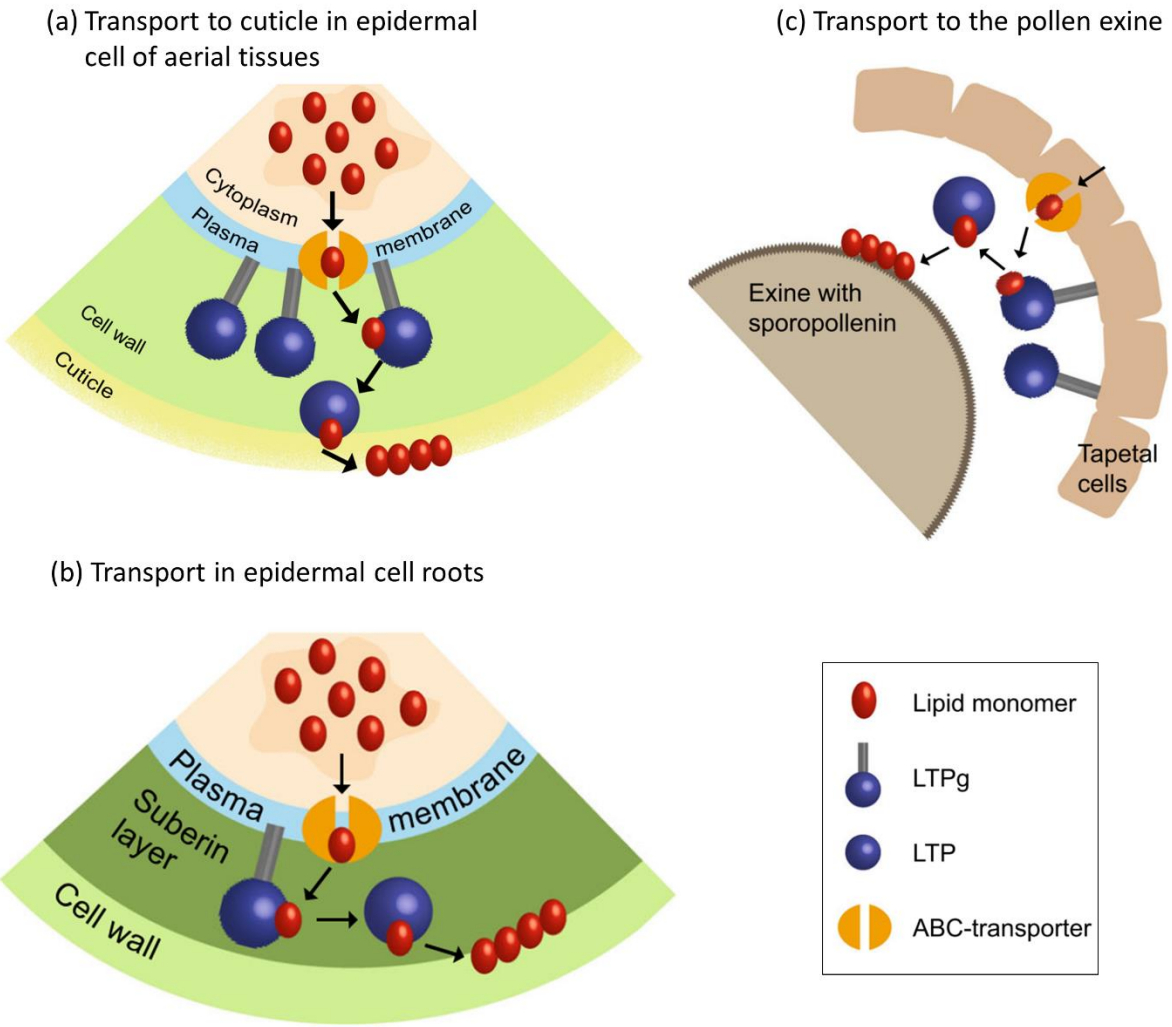

Figure 9 | A schematic model of nsLTP function for (a) cuticle, (b) root suberin synthesis and (c) pollen formation. (Image modified from (Salminen *et al.*, 2016).

2.3 Aims of the thesis

The main aim of this study was to achieve a deeper understanding of the function of TaLTPs for wheat growth and development. In addition, TaMs1 function in wheat male fertility was investigated further. Such knowledge could provide valuable information towards the development of a large-scale and cost-effective hybrid wheat seed production platform. Therefore, a number of experiments were conducted with the following objectives:

1. To understand the biological role of TaMs1 for pollen exine development.
2. To investigate the variability of *ms1*-induced male sterility penetrance and identify candidate genes for *ms1c* incomplete sterility penetrance.
3. To identify, analyse and study the evolution of all *nsLTPs* within the wheat genome (cv. Chinese Spring).
4. To identify additional wheat *nsLTPs* involved in pollen and anther development.

2.4 References (Chapter 1 and 2)

Alexandratos N, Bruinsma J. 2012. WORLD AGRICULTURE TOWARDS 2030 / 2050 The 2012 Revision. Food and Agriculture Organization of the United Nations, 146.

Asseng S, Ewert F, Martre P, *et al.* 2015. Rising temperatures reduce global wheat production. Nature Climate Change **5**, 143–147.

Batch JJ, Morgan DG. 1974. Male sterility induced in barley by photoperiod. Nature **250**, 165.

Bentley RA, Mackay I. 2017. *Advances in wheat breeding techniques* (P Langridge, Ed.).

Boutrot F, Chantret N, Gautier M-F. 2008. Genome-wide analysis of the rice and Arabidopsis non-specific lipid transfer protein (nsLtp) gene families and identification of wheat nsLtp genes by EST data mining. BMC genomics **9**, 86.

Brown TA, Jones MK, Powell W, Allaby RG. 2009. The complex origins of domesticated crops in the Fertile Crescent. Trends in Ecology and Evolution **24**, 103–109.

Del Campo EM, Casano LM, Barreno E. 2013. Evolutionary implications of intron-exon distribution and the properties and sequences of the RPL10A gene in eukaryotes. Molecular Phylogenetics and Evolution **66**, 857–867.

Castillo A, Rodríguez-Suárez C, Martín AC, Pistón F. 2015. Contribution of Chromosomes 1H S to Fertility Restoration in the Wheat msH1 CMS System under Different Environmental Conditions. PLoS ONE.

Chen L, Liu Y-G. 2014. Male Sterility and Fertility Restoration in Crops. Annual Review of Plant Biology **65**, 579–606.

Cheng S-H, Zhuang J-Y, Fan Y-Y, Du J-H, Cao L-Y. 2007. Progress in Research and Development on Hybrid Rice: A Super-domesticate in China. Annals of Botany **100**, 959–966.

Coumou D, Rahmstorf S. 2012. A decade of weather extremes. Nature Climate Change **2**, 491–496.

Debono A, Yeats TH, Rose JKC, Bird D, Jetter R, Kunst L, Samuels L. 2009. Arabidopsis LTPG is a glycosylphosphatidylinositol-anchored lipid transfer protein required for export of lipids to the plant surface. The Plant cell **21**, 1230–1238.

Driscoll CJ. 1972. XYZ system of producing hybrid wheat. Crop Science **12**, 516–517.

Driscoll CJ. 1977. Registration of cornerstone male sterile wheat germplasm (reg. no. GP 74). Crop Science **17**, 190.

Duvick DN. 1966. Influence of morphology and sterility on breeding methodology (KJ FREY, Ed.). Plant breeding. A symposium held at Iowa state University., 85–138.

Earth Observatory. 2016. Visualizing the Warmest August in 136 Years. Earth Observatory, online edition, 12 September 2016 (available at http://earthobservatory.nasa.gov/ blogs/earthmatters/2016/09/12/ heres-how-the-warmest-august- in-136-years-looks-in-chart-form).

Edstam MM, Blomqvist K, Eklöf A, Wennergren U, Edqvist J. 2013. Coexpression patterns indicate that GPI-anchored non-specific lipid transfer proteins are involved in accumulation of

cuticular wax, suberin and sporopollenin. Plant molecular biology **83**, 625–49.

Edstam MM, Viitanen L, Salminen TA, Edqvist J. 2011. Evolutionary history of the non-specific lipid transfer proteins. Molecular Plant **4**, 947–964.

Eisenhaber B, Wildpaner M, Schultz CJ, Borner GH, Dupree P, Eisenhaber F. 2003. Glycosylphosphatidylinositol lipid anchoring of plant proteins. Sensitive prediction from sequence- and genome-wide studies for Arabidopsis and rice. Plant Physiol **133**, 1691–1701.

FAO. 2013. Food and Agriculture Organization of the United Nations. FAOSTAT, http://faostat.fao.org.

FAO, IFAD, WFP. 2015. *The State of Food Insecurity in the World: Meeting the 2015 international hunger targets: taking stock of uneven progress.*

FAOSTAT. 2017. http://www.fao.org/faostat/en/#data/RF.

Fischer RA, Byerlee D, Edmeades G. 2014. Crop yields and global food security—will yield increase continue to feed the world? ACIAR Monograph No. 158. Australian Centre for International Agricultural Research: Canberra. ACIAR Monograph No. 158. Australian Centre for International Agricultural Research: Canberra.

Fisher JE. 1972. The Transformation of Stamens to Ovaries and of Ovaries to Inflorescences in Triticum aestivum L. Under Short-Day Treatment. Botanical Gazette **133**, 78–85.

Fossati A, Ingold M. 1970. A male-sterile mutant in Triticum aestivum. Wheat Information Service (Kyoto), 8–10.

Fu Y-B, Somers DJ. 2009. Genome-Wide Reduction of Genetic Diversity in Wheat Breeding. Crop Science **49**, 161.

Fu T, Yang G, Yang X. 1990. Studies on “three line” Polima cytoplasmic male sterility developed in Brassica napus. Plant Breeding, 115–120.

GDAVD Geneva Declaration on Armed Violence and Development. 2015. Global Burden of Armed Violence 2015: Every body counts. Geneva (available at www.genevadeclaration.org/ measurability/global-burden-of- armed-violence/global-burden-of- armed-violence-2015.html).

Ge X, Chen J, Sun C, Cao K. 2003. Preliminary study on the structural basis of the antifungal activity of a rice lipid transfer protein. Protein engineering **16**, 387–390.

Hoagland A, Elliott F, Rasmussen L. 1953. Some histological and morphological effects of maleic hydrazide on spring wheat. Agronomy Journal, 468–472.

Hochman Z, Gobbett DL, Horan H. 2017. Climate trends account for stalled wheat yields in Australia since 1990. Global Change Biology **23**, 2071–2081.

Hohn CE, Lukaszewski AJ. 2016. Engineering the 1BS chromosome arm in wheat to remove the Rfmultilocus restoring male fertility in cytoplasms of Aegilops kotschyi, Ae. uniaristata and Ae. mutica. Theoretical and Applied Genetics.

Huang M-D, Chen T-LL, Huang AHC. 2013. Abundant Type III Lipid Transfer Proteins in Arabidopsis Tapetum Are Secreted to the Locule and Become a Constituent of the Pollen

Exine. Plant Physiology **163**, 1218–1229.

Huang JZ, E ZG, Zhang HL, Shu QY. 2014. Workable male sterility systems for hybrid rice: Genetics, biochemistry, molecular biology, and utilization. Rice **7**, 1–14.

Islam A, Driscoll C. 1984. Latent male fertility in 'Cornerstone' chromosome 4A. Can. J. Genet. Cytol. **26**, 98–99.

Jain M, Prasad PVV, Boote KJ, Hartwell AL, Chourey PS. 2007. Effects of season-long high temperature growth conditions on sugar-to-starch metabolism in developing microspores of grain sorghum (Sorghum bicolor L. Moench). Planta **227**, 67–79.

Jung HW, Tschaplinski TJ, Wang L, Glazebrook J, Greenberg JT. 2009. Priming in Systemic Plant Immunity. Science **324**, 89 LP-91.

Kalla R, Ko S, Robert P, Stein NP, Casper L, Odd-Arne O. 1994. The promoter of the barley aleurone-specific gene encoding a putative 7 kDa lipid transfer protein confers aleurone cell-specific expression in transgenic rice. The Plant Journal **6**, 849–860.

Kaul ML. 1988. Male Sterility in Higher Plants. Monographs on Theoretical and Applied Genetics.

Klindworth DL, Williams ND, Maan SS. 2002. Chromosomal Location of Genetic Male Sterility Genes in Four Mutants of Hexaploid Wheat. Crop Science **42**, 1447.

Leng G, Huang M. 2017. Crop yield response to climate change varies with crop spatial distribution pattern. Scientific Reports **7**, 1–10.

Lesk C, Rowhani P, Ramankutty N. 2016. Influence of extreme weather disasters on global crop production. Nature **529**, 84–87.

Li F, Fan K, Ma F, *et al.* 2016. Genomic Identification and Comparative Expansion Analysis of the Non-Specific Lipid Transfer Protein Gene Family in Gossypium. Scientific Reports **6**, 38948.

Li J, Gao G, Xu K, Chen B, Yan G, Li F, Qiao J, Zhang T, Wu X. 2014. Genome-wide survey and expression analysis of the putative non-specific lipid transfer proteins in Brassica rapa L. PLoS ONE **9**.

Lindorff-Larsen K, Winther JR. 2001. Surprisingly high stability of barley lipid transfer protein, LTP1, towards denaturant, heat and proteases. FEBS Letters **488**, 145–148.

Liu P. 2017. *The future of food and agriculture: Trends and challenges.*

Liu B, Asseng S, Müller C, *et al.* 2016. Similar estimates of temperature impacts on global wheat yield by three independent methods. Nature Climate Change **6**, 1130–1136.

Liu W, Huang D, Liu K, Hu S, Yu J, Gao G, Song S. 2010. Discovery, Identification and Comparative Analysis of Non-Specific Lipid Transfer Protein (nsLtp) Family in Solanaceae. Genomics, Proteomics and Bioinformatics **8**, 229–237.

Liu F, Xiong X, Wu L, Fu D, Hayward A, Zeng X, Cao Y, Wu Y, Li Y, Wu G. 2014. BraLTP1, a lipid transfer protein gene involved in epicuticular wax deposition, cell proliferation and flower development in Brassica napus. PLoS ONE **9**, 1–12.

Liu H, Zhang G, Wang J, Li J, Song Y, Qiao L, Niu N, Wang J, Ma S, Li L. 2018. Chemical

hybridizing agent SQ-1-induced male sterility in Triticum aestivum L.: a comparative analysis of the anther proteome. BMC Plant Biology.

Lobell BD, Schlenker W, Costa-Roberts J. 2011. Climate Trends and Global Crop Production Since 1980. Science **331**, 1207–1210.

Longin CFH, Mühleisen J, Maurer HP, Zhang H, Gowda M, Reif JC. 2012. Hybrid breeding in autogamous cereals. Theoretical and Applied Genetics **125**, 1087–1096.

Maldonado AM, Doerner P, Dixon RA, Lamb CJ, Cameron RK. 2002. A putative lipid transfer protein involved in systemic resistance signalling in *Arabidopsis*. Nature **419**, 399–403.

Martín a C, Atienza SG, Ramírez MC, Barro F, Martín a. 2010. Molecular and cytological characterization of an extra acrocentric chromosome that restores male fertility of wheat in the msH1 CMS system. TAG. Theoretical and applied genetics. Theoretische und angewandte Genetik **121**, 1093–101.

Martin J, Grawford J. 1951. Several types of sterility in Capsicum frutescens. Proceedings of the Society for Horticultural Science, 335–338.

Mühleisen J, Piepho HP, Maurer HP, Longin CFH, Reif JC. 2014. Yield stability of hybrids versus lines in wheat, barley, and triticale. Theoretical and Applied Genetics.

Mukai Y, Tsunewaki K. 1979. Basic studies on hybrid wheat breeding. VIII. A new male sterility-fertility restoration system in common wheat utilizing the cytoplasm of Aegilops kotschyi and Ae. variabilis. Theoretical and Applied Genetics, 153–160.

Paulick MG, Bertozzi CR. 2008. The Glycosylphosphatidylinositol Anchor : A Complex Membrane-Anchoring. , 6991–7000.

Perez-Prat E, van Lookeren Campagne MM. 2002. Hybrid seed production and the challenge of propagating male-sterile plants. Trends in plant science **7**, 199–203.

Petersen TN, Brunak S, Von Heijne G, Nielsen H. 2011. SignalP 4.0: Discriminating signal peptides from transmembrane regions. Nature Methods **8**, 785–786.

Porter. 2014. Part A: Global and Sectoral Aspects. (Contribution of Working Group II to the Fifth Assessment Report of the Intergovernmental Panel on Climate Change). Climate Change 2014: Impacts, Adaptation, and Vulnerability., 1132.

Porter K, Wiese A. 1961. Evaluation of certain chemicals on selective gametocides for wheat. Crop Science **1**, 381–382.

Pugsley A, Oram R. 1959. Genic male sterility in wheat. Australian Plant Breeding and Genetics Newsletter **14**, 10–11.

Reif JC, Hailauer AR, Melchinger AE. 2005. Heterosis and heterotic patterns in maize. Maydica **50**, 215–223.

Rick MC, Boynton EJ. 1967. A TEMPERATURE-SENSITIVE MALE-STERILE MUTANT OF THE TOMATO. American Journal of Botany **54**, 601–611.

Roux J, Chirinian G. 1959. Essais d'induction de la sterilite male sterile sur le Cotonier. Fibres Trop, 363–631.

Rowell P, Miller D. 1971. Induction of male sterility in wheat with z-chloro- ethylphosphonic acid (Ethrel). Crop Science, 629–631.

Salminen TA, Blomqvist K, Edqvist J. 2016. Lipid transfer proteins: classification, nomenclature, structure, and function. Planta **244**, 971–997.

Sels J, Mathys J, De Coninck BMA, Cammue BPA, De Bolle MFC. 2008. Plant pathogenesis-related (PR) proteins: A focus on PR peptides. Plant Physiology and Biochemistry **46**, 941–950.

Shull G. 1908. The composition of a field of maize. Journal of Heredity **4**, 296–301.

Siles MM, Russell WK, Baltensperger DD, Nelson LA, Johnson B, Van Vleck LD, Jensen SG, Hein G. 2004. Heterosis for grain yield and other agronomic traits in foxtail millet. Crop Science **44**, 1960–1965.

Sun J-Y, Gaudet DA, Lu Z-X, Frick M, Puchalski B, Laroche A. 2008. Characterization and Antifungal Properties of Wheat Nonspecific Lipid Transfer Proteins. Molecular Plant-Microbe Interactions **21**, 346–360.

Tsujimoto H, Tsunewaki K. 1984. Gametocidal genes in wheat and its relatives. I. Genetic analyses in common wheat of a gametocidal gene derived from Aegilops speltoides. Canadian Journal of Genetics and Cytology **26**, 78–84.

Tsunewaki K. 2015. Fine mapping of the first multi-fertility-restoring gene, Rfmulti, of wheat for three Aegilops plasmons, using 1BS-1RS recombinant lines. Theoretical and Applied Genetics.

Tucker EJ, Baumann U, Kouidri A, *et al.* 2017. Molecular identification of the wheat male fertility gene Ms1 and its prospects for hybrid breeding. Nature Communications **8**, 869.

UNICEF, World Health Organization, World Bank Group. 2016. Levels and trends in child malnutrition. , 1–8.

USDA. 2018. United States Department of Agriculture https://www.ers.usda.gov/topics/crops/corn-and-other-feedgrains/background/.

Vergnolle C, Arondel V, Jolliot A, Kader J-C. 1992. Phospholipid transfer proteins from higher plants. In: Dennis EA,, In: ennis E. Vance, eds. Methods in Enzymology. Phospholipid Biosynthesis. Academic Press, 522–530.

Wang Z, Li J, Chen S, *et al.* 2017. Poaceae-specific *MS1* encodes a phospholipid-binding protein for male fertility in bread wheat. Proceedings of the National Academy of Sciences, 201715570.

Wang S, Zhang Y, Song Q, *et al.* 2018. Mitochondrial Dysfunction Causes Oxidative Stress and Tapetal Apoptosis in Chemical Hybridization Reagent-Induced Male Sterility in Wheat. Frontiers in Plant Science.

Wei K, Zhong X. 2014. Non-specific lipid transfer proteins in maize. BMC plant biology **14**, 281.

Wheeler T, Braun J von. 2013. Climate Change Impacts on Global Food Security. SCIENCE **341**, 479–485.

Whitford R, Fleury D, Reif JC, Garcia M, Okada T, Korzun V, Langridge P. 2013. Hybrid

breeding in wheat: technologies to improve hybrid wheat seed production. Journal of experimental botany **64**, 5411–28.

Wilson J, Ross W. 1962. Male sterility interaction of the Triticum aestivum nucleus and Triticum timopheevii cytoplasm. Wheat Information Service (Kyoto), 29–30.

Wu Y, Fox TW, Trimnell MR, Wang L, Xu R ji, Cigan AM, Huffman GA, Garnaat CW, Hershey H, Albertsen MC. 2016. Development of a novel recessive genetic male sterility system for hybrid seed production in maize and other cross-pollinating crops. Plant Biotechnology Journal **14**, 1046–1054.

Xu C, Liu Z, Zhang L, Zhao C, Yuan S, Zhang F. 2013. Organization of actin cytoskeleton during meiosis I in a wheat thermo-sensitive genic male sterile line. Protoplasma.

Yuan G, Wang Y, Yuan S, *et al.* 2018. Functional Analysis of Wheat TaPaO1 Gene Conferring Pollen Sterility Under Low Temperature. J. Plant Biol **61**, 25–32.

Zhang D, Liang W, Yin C, Zong J, Gu F, Zhang D. 2010. OsC6, encoding a lipid transfer protein, is required for postmeiotic anther development in rice. Plant physiology **154**, 149–62.

Zhou K, Wang S, Feng Y, Ji W, Wang G. 2007. A new male sterile mutant LZ in wheat (Triticum aestivum L.). Euphytica **159**, 403–410.

Zhou K, Wang S, Feng Y, Liu Z, Wang G. 2006. The 4E- System of Producing Hybrid Wheat. Crop Science **46**, 250.

Chapter 3

Wheat TaMs1 is a glycosylphosphatidylinositol-anchored Lipid Transfer Protein necessary for pollen development

Statement of Authorship

Title of Paper	Wheat TaMs1 is a glycosylphosphatidylinositol-anchored Lipid Transfer Protein necessary for pollen development
Publication Status	☐ Published ☐ Accepted for Publication ☑ Submitted for Publication ☐ Unpublished and Unsubmitted work written in manuscript style
Publication Details	Manuscript prepared in accordance with the guidelines of BMC Plant Biology.

Principal Author

Name of Principal Author (Candidate)	Allan Kouidri
Contribution to the Paper	Conceived and designed the experiments, performed experiments, analysed data and wrote the manuscript.
Overall percentage (%)	75 %
Certification:	This paper reports on original research I conducted during the period of my Higher Degree by Research candidature and is not subject to any obligations or contractual agreements with a third party that would constrain its inclusion in this thesis. I am the primary author of this paper.
Signature	Date 28/05/2018

Co-Author Contributions

By signing the Statement of Authorship, each author certifies that:

i. the candidate's stated contribution to the publication is accurate (as detailed above);

ii. permission is granted for the candidate in include the publication in the thesis; and

iii. the sum of all co-author contributions is equal to 100% less the candidate's stated contribution.

Name of Co-Author	Dr. Ute Baumann
Contribution to the Paper	Supervised development of the work, help in data interpretation. Reviewed and edited the manuscript.
Signature	Date 28/05/2018

Name of Co-Author	Mathieu Baes
Contribution to the Paper	Assisted for cloning vectors, GUS-staining and analysing the data.
Signature	Date 28/05/2018

Name of Co-Author	Elise J. Tucker		
Contribution to the Paper	Assisted with designing the experiments and designed *TaMs1*-homeolog-specific primers qPCR-experiment.		
Signature		Date	28.5.18

Name of Co-Author	Dr. Ryan Whitford		
Contribution to the Paper	Supervised development of the work, help in data interpretation. Reviewed and edited the manuscript and acting as corresponding author.		
Signature		Date	27/5/2018.

Chapter 3

Wheat TaMs1 is a glycosylphosphatidylinositol-anchored Lipid Transfer Protein necessary for pollen development

Allan Kouidri[1], Ute Baumann[1], Mathieu Baes[1], Elise J. Tucker[1,2], Ryan Whitford[1*]

[1]University of Adelaide, School of Agriculture, Food and Wine, Waite Campus, Urrbrae, South Australia 5064, Australia.

[2]Current address Commonwealth Scientific and Industrial Research Organization, Agriculture and Food, Waite Campus, Urrbrae, South Australia 5064, Australia

[*]Correspondence: ryan.whitford@adelaide.edu.au

Keywords: Wheat, LTP, Glycosylphosphatidylinositol-anchored lipid transfer protein, Sporopollenin, Pollen exine, Male sterility.

3.1 Abstract

Background

In flowering plants, lipid biosynthesis and transport within anthers is essential for male reproductive success. *TaMs1,* a dominant wheat fertility gene located on chromosome 4BS, has been previously fine mapped and identified to encode a glycosylphosphatidylinositol (GPI)-anchored non-specific lipid transfer protein (nsLTP). Although this gene is critical for pollen exine development, details of its function remains poorly understood.

Results

In this study, we report that *TaMs1* is only expressed from the B sub-genome, with highest transcript abundance detected in anthers containing microspores undergoing pre-meiosis through to meiosis. *β-glucuronidase* transcriptional fusions further revealed that *TaMs1* is expressed throughout all anther cell-types. *TaMs1* was identified to be expressed at an earlier stage of anther development relative to genes reported to be necessary for sporopollenin precursor biosynthesis. In anthers missing a functional *TaMs1* (*ms1c* deletion mutant), these same genes were not observed to be mis-regulated, indicating an independent function for

TaMs1 in pollen development. Exogenous hormone treatments on GUS reporter lines suggest that *TaMs1* expression is increased by both indole-3-acetic acid (IAA) and abscisic acid (ABA). Translational fusion constructs showed that TaMs1 is targeted to the plasma membrane.

Conclusions

In summary, *TaMs1* is a wheat fertility gene, expressed early in anther development and encodes a GPI-LTP targeted to the plasma membrane. The work presented provides a new insight into the process of wheat pollen development.

3.2 Introduction

Wheat (*Triticum aestivum* L.) is one of the most staple food crops and accounts for 20% of human daily protein and food calories (FAOSTAT, 2017). The demand for wheat is predicted to increase 60 % by 2050 compared with 2010. Thus, an increase of the global yield gain from the current rate of 1 % (2001-2010) to 1.6 % per year (2010-2050) is required. Male reproductive development is a key factor for grain yield. Pollen grains are encapsulated by a complex multiple-layered cell wall termed exine, which forms a physical barrier against a variety of biotic and abiotic stresses (Ariizumi and Toriyama, 2011). Pollen exine mainly consists of sporopollenin, a highly resistant biopolymer providing a rigid exoskeleton, which in grass species is additionally covered by tryphine, a mixture of phenolic, protein and fatty acid derivatives (Scott *et al.*, 2004; Blackmore *et al.*, 2007).

The highly recalcitrant nature of sporopollenin to chemical degradation has proven a great challenge in unravelling its biochemical composition. However, the underlying genetics of pollen wall development has been intensively investigated through the use of exine-defective mutants in model plants such as *Arabidopsis* and *rice* among other species (Ariizumi and Toriyama, 2011). These genetic analyses indicate that sporopollenin biosynthesis consists of three conserved metabolic pathways and transport processes. The first of these involves

production of waxes and various lipid-based compounds from precursors including phospholipids, fatty acids and alcohols. This pathway includes fatty acid hydroxylases such CYP703A3 (Morant *et al.*, 2007; Aya *et al.*, 2009) and CYP704B2 (Li *et al.*, 2010) from the conserved P450 gene family. Additionally, MALE STERILITY 2 (MS2) from *Arabidopsis* (de Azevedo Souza *et al.*, 2009) and its rice orthologue DEFECTIVE IN POLLEN WALL (DPW) (Shi *et al.*, 2011*a*) encode fatty acid reductases which have been shown to be essential for pollen exine formation.

The second conserved pathway involves phenolic compound biosynthesis, an important component of exine and tryphine (Quilichini *et al.*, 2015). Phenolics are synthesized from fatty acid substrates by fatty-acyl-CoA synthetases (ACOS5) (de Azevedo Souza *et al.*, 2009), polyketide synthetases (OsPKS1) and tetraketide α-pyrone reductases (TKPR) (Grienenberger *et al.*, 2010).

The third conserved pathway involves polysaccharide metabolism whereby the timing of callose biosynthesis and degradation facilitates pollen coat formation (Hird *et al.*, 1993; Wang *et al.*, 2012).

Newly synthesized sporopollenin precursors are then translocated from the tapetal cell layer to developing microspores. How sporopollenin precursors are allocated for pollen coat formation remains unclear. Studies reveal ABCG15, encoding an ATP-binding cassette (ABC) transport protein, in addition to non-specific lipid transfer proteins, play roles in sporopollenin precursor transport (Qin *et al.*, 2013). Additionally, it was shown that *A. thaliana* type III-LTPs allocate and incorporate lipidic compounds to the pollen wall (Huang *et al.*, 2013). More recently, a wheat gene termed *TaMs1* encoding a glycosylphophatidylinositol (GPI) Lipid Transfer Protein was demonstrated to be required for wheat male fertility (Tucker *et al.*, 2017).

Members of the non-specific lipid transfer protein (nsLTP) gene family have been identified in most plant species. They exhibit a range of expression patterns across different developmental stages. This is reflected by their potential involvement in numerous biological processes, including cutin biosynthesis (Sterk *et al.*, 1991), pathogen defense response (Isaac Kirubakaran *et al.*, 2008), long distance signaling (Maldonado *et al.*, 2002; Lascombe *et al.*, 2008), seed maturation (Thoma *et al.*, 1994), and pollen tube adhesion (Park *et al.*, 2000).

nsLTPs have the ability to shuttle lipids between membranes *in vitro* (Kader, 1975). They are part of a plant specific prolamin superfamily, identifiable by an eight conserved cysteine motif (8CM) backbone, low molecular mass and 4 to 5 alpha-helices (Shin *et al.*, 1995; Gomar *et al.*, 1996). The conserved cysteine domain has the following pattern: C-Xn-C-Xn-CC-Xn-CXC-Xn-C-Xn-C, with cysteine residues required for the formation of four disulphide bridges (José-Estanyol *et al.*, 2004). In this context the disulfide bridges stabilize a hydrophobic cavity with the ability to bind various lipids and other hydrophobic compounds *in vitro* (Zachowski *et al.*, 1998). Most nsLTPs also possess an N-terminal signal peptide targeting the proteins to the apoplastic space via the vesicular secretory pathway. nsLTPs can also contain a conserved C-terminal motif subject to post-translational modification. This motif is recognised by glycophosphatidylinositol (GPI) transamidases in the *lumen* of the *endoplasmic reticulum* (*ER*) whereby it is cleaved and replaced by a GPI moiety. This GPI moiety anchors the protein to the extracellular side of the plasma membrane. GPI-anchored nsLTPs can be released from the membrane by specific phospholipases that cleave the GPI molecule (Paulick and Bertozzi, 2008).

Genome wide analysis of nsLTPs in rice and *Arabidopsis* reported 77 and 79 nsLTPs, respectively (Wei and Zhong, 2014). In wheat 156 putative nsLTPs were retrieved by EST data mining (Boutrot *et al.*, 2008). nsLTPs are categorized into at least nine types, distinguished

based on intron position, inter-cysteine spacing and the presence of a GPI-anchor motif (Boutrot *et al.*, 2008; Edstam *et al.*, 2011). Among the nine reported types, GPI-anchored nsLTPs, type G, are the most represented in rice and *Arabidopsis* (Wei and Zhong, 2014).

In this study, we - investigated the biological function of TaMs1 during pollen exine formation. We report evidence for spatio-temporally restricted expression of *TaMs1* in anthers undergoing microsporogenesis. TaMs1 is shown to be expressed earlier than many genes required for sporopollenin-biosynthesis. Finally, we demonstrate the importance of both signal peptide and pro-peptide GPI anchor for TaMs1 subcellular localization as indicative of a role in lipidic transport. Our results provide new insights into mechanisms of pollen development.

3.3 Materials and Methods

3.3.1 Plant materials and growth conditions

Wheat cultivars Chris and Chris-EMS mutagenized lines FS2 (*ms1d*) were used for cytological examination and expression profiling (Sasakuma *et al.*, 1978). Plants were sown at 5 to 6 plants per 6 L (8 inches diameter) pot containing soil mix. The soil mix consisted of 75 % (v/v) Coco Peat, 25 % (v/v) nursery cutting sand (sharp), 750 mg/L $CaSO_4.2H_2O$ (gypsum) 750 mg/L $Ca(H_2PO_4)_2.H20$ (superphosphate), 1.9 g/L $FeSO_4$, 125 mg/L FeEDTA, 1.9 g/L $Ca(NO_3)$, 2.750 mg/L Scotts Micromax micronutrients, and 2.5 g/L Osmocote Plus slow release fertilizer (16:3:9) (Scotts Australia Pty. Ltd.). pH was adjusted to between 6.0 and 6.5 using 2 parts agricultural lime to 1 part hydrated lime. Potted plants were grown either in controlled environment growth rooms at 23 °C (day) and 16 °C (night) or similarly temperature moderated glasshouses in which photoperiod was extended using 400 W high pressure sodium lamps in combination with metal halide lamps to 12 hours over winter months.

3.3.2 Expression analysis by qRT-PCR

Total RNA was isolated using ISOLATE II *RNA* Mini Kit (Bioline, Sydney, Australia) from wheat tissues: roots, shoot and glume, lemma, palea, pistil, and anthers containing microspores from pre-meiosis to maturity. Quantitative real-time PCR was perform according to Burton *et al.,* (2004) using the primer combinations shown in Additional File 1. Anthers containing developing microspores were staged by acetocarmine staining. 0.6 µg of RNA was used to synthesise oligo(dT)-primed first strand cDNA using the superscript IV reverse transcriptase (Thermo Fisher Scientific, Melbourne, Australia). 2 µL of the RT product diluted 1:20 was then used as template for conventional and quantitative real-time PCR. *TaGAPdH, TaActin and Ta14-3-3* were used as reference genes.

3.3.3 Histochemical GUS staining and cytological examination

The construct pTOOL36-*TaMs1::gusplus* (Tucker *et al.*, 2017) was transformed into wheat (cv. Fielder) using *Agrobacterium tumefaciens* according to Ismagul *et al.*, (2014). GUS activity in transgenic lines from leaves, roots and anthers containing microspores at pre-meiosis to maturity were analysed by histochemical staining using 5-Bromo-4-chloro-3-indolyl-beta-D-glucuronic acid (Gold Biotechnology, Inc). Samples were incubated in a 1 mM X-Gluc solution in 100 mM sodium phosphate, pH 7.0, 10 mM sodium ethylenediaminetetraacetate, 2 mM $FeK_3(CN)_6$, 2 mM $K_4Fe(CN)_6$ and 0.1 % Triton X-100. After vacuum infiltration at 2600 Pa for 20 min, samples were incubated 72 hours at 37 °C.

Samples were incubated in fixative solution of 4 % sucrose, 1x PBS, 4 % paraformaldehyde, 0.25 % glutaraldehyde, at 4 °C overnight. Samples were subsequently dehydrated in an ethanol series of increasing concentration (30 %, 50 %, 70 %, 85 %, 90 %, 95 % and 100 %). Tissues were then embedded in *Technovit®* resin, microtome sectioned at 8-14 µm, counter-

stained with ruthenium red and then mounted in DPX solution (Sigma, St. Louis, MO). Sections were observed using standard light microscopy on a LEICA DM1000 microscope coupled with a CCD camera. The precipitated product from the β-glucuronidase reaction appears blue under bright field and pink under dark field.

3.3.4 Promoter analysis

NewPLACE (Higo *et al.*, 1999), an online database of plant *cis*-acting regulatory DNA elements (*cis*-element) was used to identify putative *cis*-elements in the promoter regions of *TaMs1* and its homeologues.

3.3.5 Hormone and drought response assays

Plants were treated with indole-3-acetic acid (IAA) (PytoTechnology Lab., Lenexa, USA) and abscisic acid (ABA) (Sigma-Aldrich, Sidney, Australia). Hormone stock solutions were made with 100 % ethanol. Wheat tillers were collected and dipped in hormone solutions for 9 hours containing either 100 µM IAA or 100 µM ABA, to a final concentration of 0.05 % ethanol. A 0.05 % ethanol solution was used as a control treatment. For the drought treatment, plants were well watered until the stage of flag leaf emergence and water withheld until wilting. After sample collection, plants were re-watered. The effects of the cyclic drought treatment was assessed from the percentage of fertility of three spikes from well-watered and treated plants calculated according to Tucker *et al*. (2017).

GUS activity in anthers from treated transgenic lines was analyzed by histochemical staining using X-gluc as previously described. Anthers containing developing microspores were staged by acetocarmine staining. Six spikes were used for each treatments.

3.3.6 Amino-acid sequence analysis

TaMs1 amino acid sequence were tested for the presence of a putative signal peptide using SignalP 4.1 (Nielsen, 2017). Additionally, the presence of a GPI-anchor domain was

predicted using big-PI plant predictor (Eisenhaber *et al.*, 2003), PredGPI (Pierleoni *et al.*, 2008) and GPI-SOM (Fankhauser and Mäser, 2005).

3.3.7 Subcellular localization of TaMs1

The fusion construct mCherry-TaMs1 was synthetized by GeneScript® and inserted between the BamHI and KpnI sites of pUC57-Kan to generate pUC57-mCh-TaMs1. *TaMs1* coding sequence from wheat cv. Chris was used as template and the mCherry reporter was inserted between Q24 and P25 of the TaMs1 protein. pUC57-mCh-TaMs1 was digested by BamHI/KpnI and the fragment containing mCh-TaMs1 was inverted and inserted between the maize ubiquitin promoter (ZmUbi) and RuBisCo terminator resulting in p*ZmUbipro*::mCh-TaMs1. The constructed p*ZmUbipro*::mCh-TaMs1 was used for transient expression in epidermal onion cells as well as wheat protoplasts according to Bart *et al*., 2006 and Shan *et al*., 2014. p*ZmUbipro*::mCh was used as a transformation control. Confocal images were captured with a Nikon A1R laser scanning microscope (Nikon Instruments Inc, U.S.) coupled to a DS-Ri1 CCD camera. A 488 nm laser was used for GFP fluorescence (excitation: 488.0 nm; emission: 525.0 nm) detection and the 561 nm laser for RFP fluorescence (excitation: 561.1 nm; emission: 595 nm) detection. Plasmolysis was performed using 0.8 M mannitol.

3.4 Results

3.4.1 *TaMs1* is an anther-specific gene expressed early during anther development

TaMs1 transcripts were not detected in pistils, shoots, roots, glume, lemma or palea, however, transcripts were enriched in anther tissues with their abundance peaking when microspores were at pre- to early meiosis to meiosis, stage (st) 2 to 4 (Fig. 1a). *TaMs1* expression decreased significantly in anthers containing uninucleate microspores (st 5 and 6). Additionally, only the B homeologue was detected, indicating only this sub-genome is transcribed.

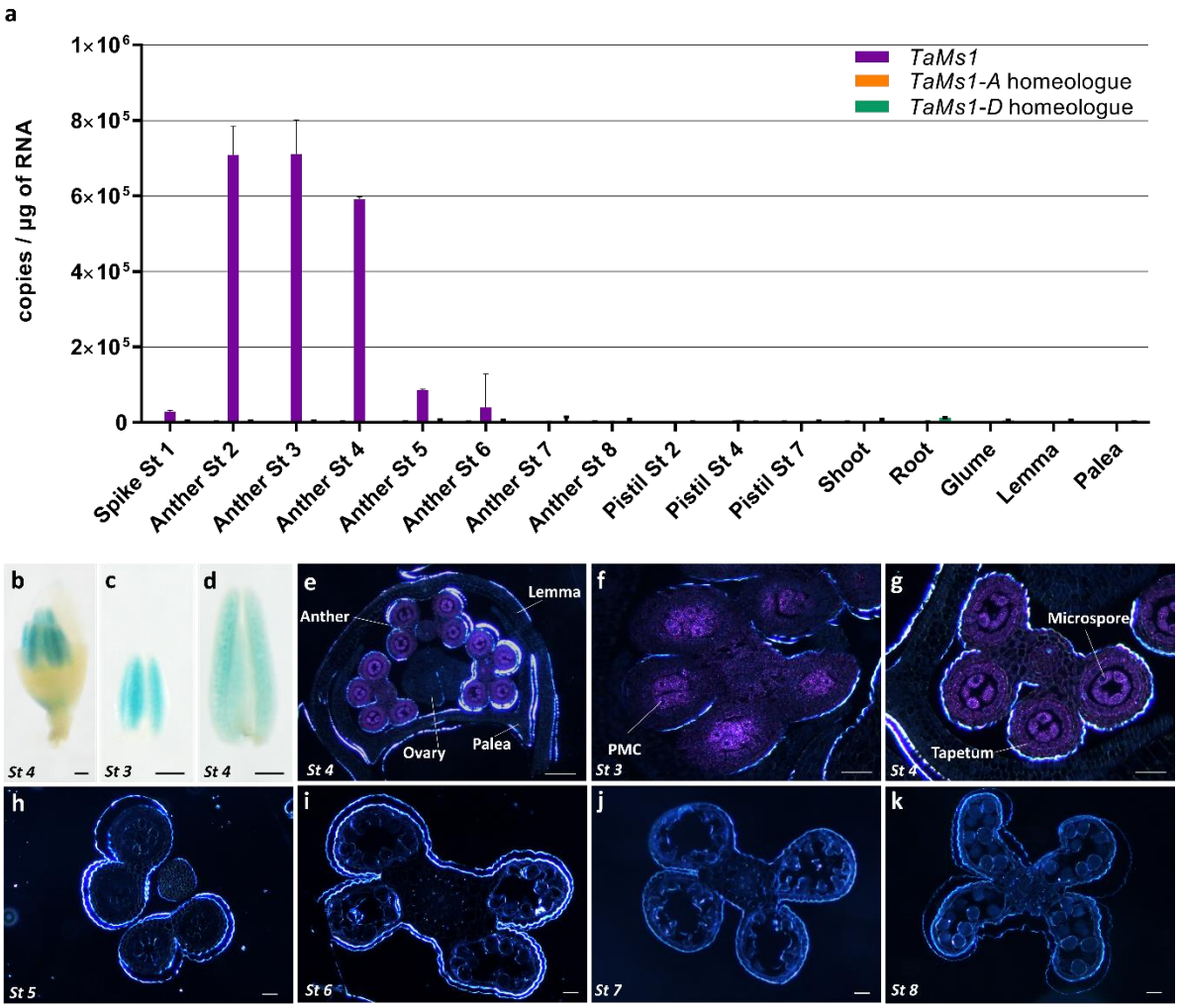

Figure 1 | *TaMs1* expression is anther-specific and predominantly within pre-meiotic to meiotic microspores. qRT-PCR expression profiling of *TaMs1* and its homeologues (a) in anthers containing pre-meiotic microspores to mature pollen, pistil, shoots, roots, glume, lemma and palea. St1, Spike white anthers; St2, archesporial cells; St3, pre-meiotic pollen mother cells; St4, meiotic microspores; St5, early uninucleate; St6, late uninucleate; St7, binucleate; St8, mature pollen. Error bars reflect standard error of three independent tissue replicates (n=3). GUS activity in whole mount tissue samples (b-d), transverse section of floret (e) and anthers (f-k) in transgenics expressing *TaMs1::gusplus*. Scale bars: b-d, 100 µm; d, 200 µm; e-j, 50 µm.

Furthermore, analyses of *TaMs1* promoter activity in transgenic wheat cv. *Fielder* were performed using *TaMs1::gusplus* transcriptional fusion constructs. Similar to the qRT-PCR results, GUS activity was observed exclusively in anthers containing microspores at pre-meiosis (st 3) till meiosis (st 4) (Fig. 1b to 1g). Transverse sections of anthers containing pre-meiotic microspores (st 3) revealed GUS activity predominantly in Pollen Mother Cells (PMCs)

with weak detection in all other anther cell types (Fig. 1f). Whereas, in anthers containing early meiotic microspores (st 4), high GUS activity was detected both in microspores and tapetal cells, and to a lesser extent in other tissues of the anther (Fig. 1g). No GUS activity was detected in anther transverse sections from uninucleate microspores to pollen maturity (st 5 to 8) (Fig. 1h to 1k).

3.4.2 Effect of exogenous hormones on *TaMs1* expression

To investigate the regulation of *TaMs1* present on chromosome 4B, we identified *in silico* putative *cis*-regulatory elements in the 2 kb the promoter region of *TaMs1* and its homeologues (Fig. 2). Two types of *cis*-elements related to pollen specific expression, GTGA motif and POLLEN1LELAT52 (Zhou, 1999), were detected using the newPLACE tool (Higo *et al.*, 1999). All three homeologues contained putative GTGA motif and POLLEN1LELAT52 elements in their promoter regions. The GTGA motif was enriched in the *TaMs1-A* promoter region with 16 occurrences, while 11 and five occurrences were identified in *TaMs1-D and TaMs1-B,* respectively. *TaMs1-A and TaMs1-B* contained respectively 12 and ten copies of POLLEN1LELAT52 element, while only four copies were identified in *TaMs1-D* promoter region.

Two hormone responsive elements were identified in *TaMs1-B* promoter region, including two GCCCORE-boxes, a jasmonate/ethylene responsive element, located at -103 bps and -155 bps from the start codon, and ABREOSRAB21, an ABA responsive element activator of transcription (Busk, 1998), at -234 bps. Interestingly, the ABREOSRAB21 was identified only on *TaMs1-B* promoter region. In addition, *TaMs1-D* promoter region contained only one putative GCCCORE element located at -237 bps and none were identified in the *TaMs1-A* promoter region.

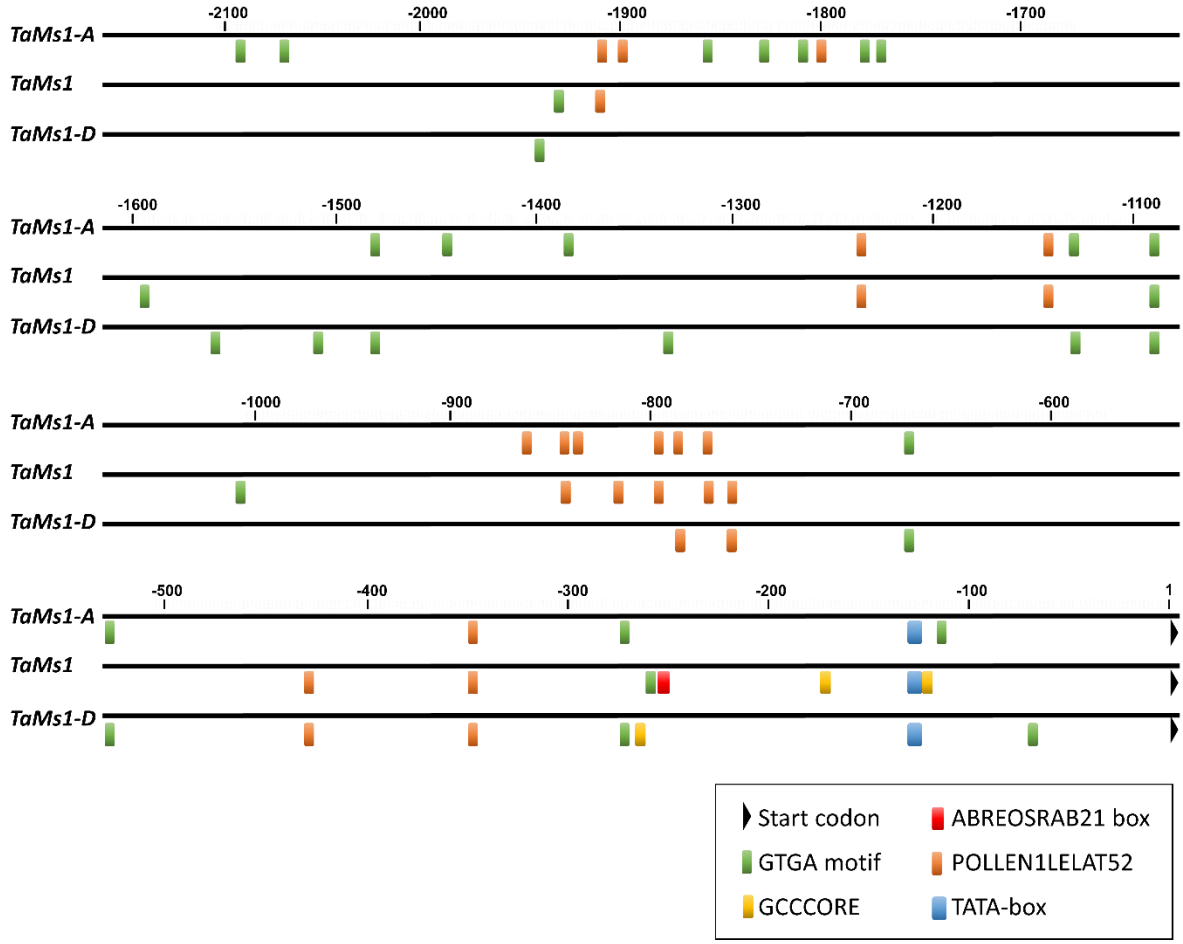

Figure 2 | Distribution of some *cis*-acting elements in the promoter sequence of *TaMs1* and its homeologues. Selected pollen specific and hormone responsive *cis*-acting were retrieved in 2 kb *TaMs1* and its homeologues promoter sequences. The three homeologue promoter regions were annotated after sequence alignments. Start codons and putative GTGA motifs, ABREOSRAB21 and GCCCORE, TATA-boxes, POLLEN1LELAT52 *cis*-elements are represented by the different symbol as indicated. Numbering is from the first base of translations start site (+1).

Because the distribution of hormone response *cis*-elements in *TaMs1* promoter region differed relative to its homeologues, we first investigated the effects of exogenous hormones on *TaMs1* expression using *TaMs1::gusplus* lines. Differences in GUS activity between treatments was determined by altering staining time. Firstly, blue color saturation for the untreated *TaMs1::gusplus* line was found to occur at approximately 72 h, therefore GUS staining for treatments was stopped when differences between these and the control were

first observed. This typically occurred at approximately 48 hours of GUS staining. *TaMs1::gusplus* anthers containing pre-meiotic and meiotic microspores were more intensely stained after nine hours of indole-3-acetic acid (IAA) and abscisic acid (ABA) treatment relative to mock treated controls (Fig. 3), suggesting *TaMs1* is transcriptionally activated by these hormones. No differences in GUS activity were observed in response to jasmonic acid (JA) and gibberellic acid (GA_3) treatments (data not shown).

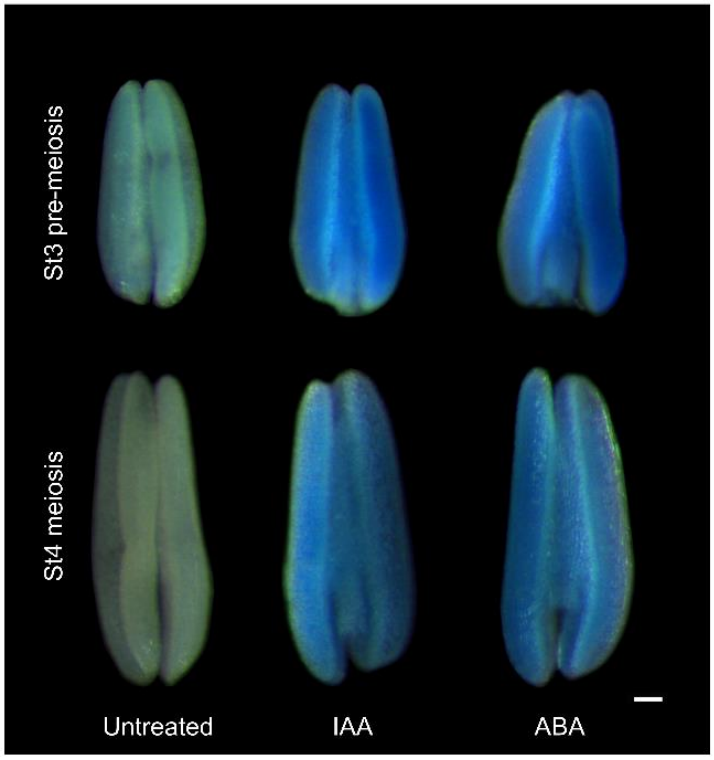

Figure 3 | *TaMs1* promoter activity in response to exogenous IAA and ABA treatment. GUS activity in whole mount anther samples in transgenic expressing *TaMs1::gusplus* in response to hormonal treatment using IAA and ABA. St3, pre-meiotic pollen mother cells; St4, meiotic microspores. Scale bars: 100 µm.

3.4.3 *TaLTPG1* is expressed earlier than other genes deemed necessary for pollen exine formation

TaMs1 is expressed within anthers containing sporogenous cells (stage 2), an early stage of anther development (Fig. 1f). To better understand *TaMs1*'s function, we investigated the timing of its expression relative to wheat orthologues of rice sporopollenin-biosynthetic genes such as *TaABCG15, TaCYP703A3*, *TaCYP704B2*, *TaDPW* and *TaPSK1* (Morant *et al.*, 2007; Aya

et al., 2009; Li *et al.*, 2010) (Fig. 4). Transcripts for each of these genes were preferentially detected in anther samples containing meiotic to uni-nucleate microspores (stage 4 and 5).

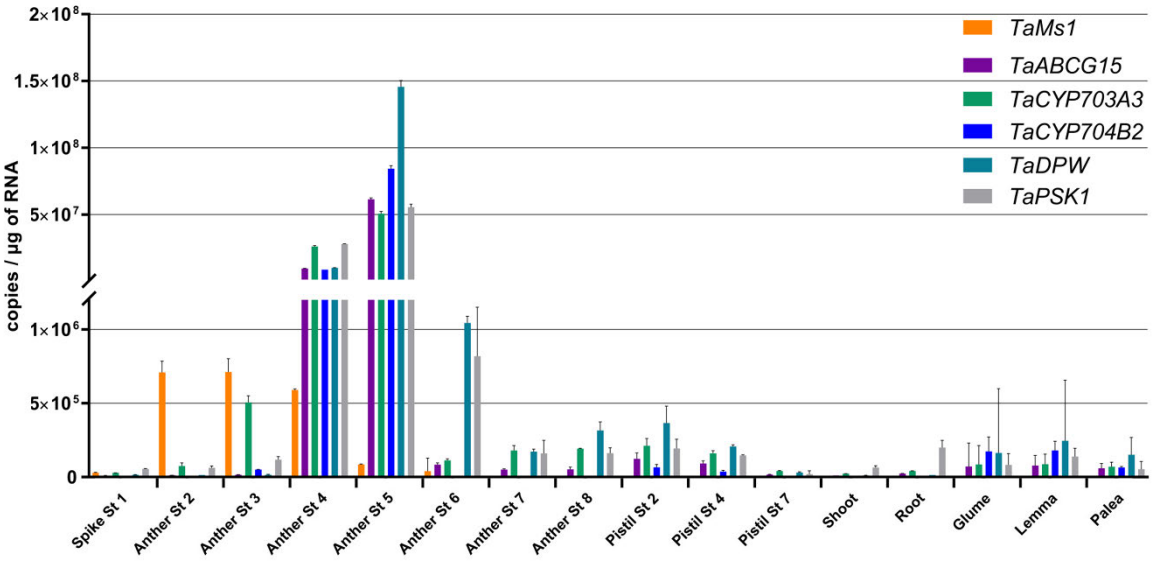

Figure 4 | Sporopollenin biosynthetic genes *TaABCG15, TaCYP703A3, TaCYP704B2, TaDPW* and *TaPSK1*, are expressed in anthers after *TaMs1*. qRT-PCR expression profile of *TaABCG15, TaCYP703A3, TaCYP704B2, TaDPW and TaPSK1* in anthers containing pre-meiotic microspores to mature pollen, pistil, shoot, root, glume, lemma and palea. St1, Spike white anthers; St2, archesporial cells; St3, pre-meiotic pollen mother cells; St4, meiotic microspores; St5, early uninucleate; St6, late uninucleate; St7, binucleate; St8, mature pollen. Error bars reflect standard error of three independent tissue replicates (n=3).

3.4.4 *TaMs1* knock-out does not affect the expression level of genes involved in anthers and pollen wall development at meiosis stage.

Inter-dependent regulatory relationships of genes during male reproductive development have been reported in rice amongst other species. For example, rice mutants for genes deemed necessary for pollen formation typically show differential expression patterns for many genes identified to be involved in pollen exine formation (Lin *et al.*, 2017). We aimed to determine if this holds true in wheat, by examining gene expression profiles, in Wild Type (WT) versus *ms1* anthers, for 20 putative wheat orthologues to rice sporopollenin biosynthetic genes reported to be necessary for male fertility. Genes were identified firstly based on reports of male sterility mutations in rice, and then based on whether they had been

functionally characterized and shown to be essential for anther development and pollen wall formation (Fig. 5; Additional File 2; Fig. 6).

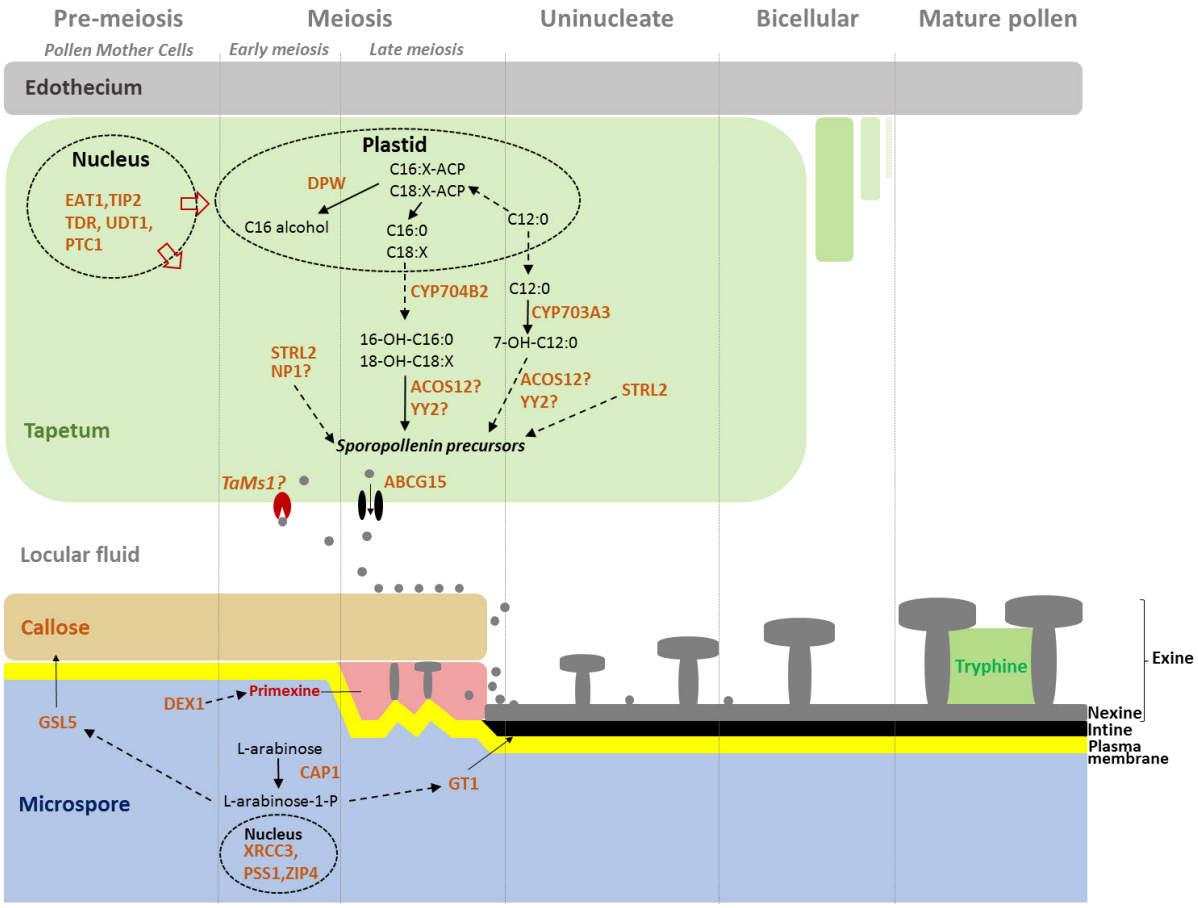

Figure 5 | Current model of pollen development and metabolic network of exine formation in rice and *Arabidopsis*. (Adapted from Ariizumi and Toriyama (2011) and Zhang *et al.* (2016) with modification (License number: 4286200743277 and 4286240859506). For full names of the genes/enzymes refer to Additional file 2.

Surprisingly, none of the selected genes displayed abnormal expression in *ms1* anthers containing meiotic microspores (stage 4), with the exception of *TaMs1* (Fig. 6). In *ms1* anthers containing uni-nucleate microspores (stage 5), only *UNDEVELOPED TAPETUM1* (*TaUDT1)* was significantly down-regulated relative to WT. However, its expression was not altered across other stages of pollen development. No significant difference in gene expression could be observed for the other sporopollenin biosynthetic genes at this stage. The rice *UDT1,* a bHLH transcription factor, has been reported to be critical for early tapetum development and PMC

meiosis (Jung, 2005). At stage 6 and 7, expression levels of sporopollenin biosynthetic genes were not affected by the *Tams1* mutation.

Taken together, *TaMs1*'s expression relative to the 20 putative wheat orthologues to sporopollenin biosynthetic genes, would suggest that the TaMs1 protein's production proceeds the availability of sporopollenin precursors.

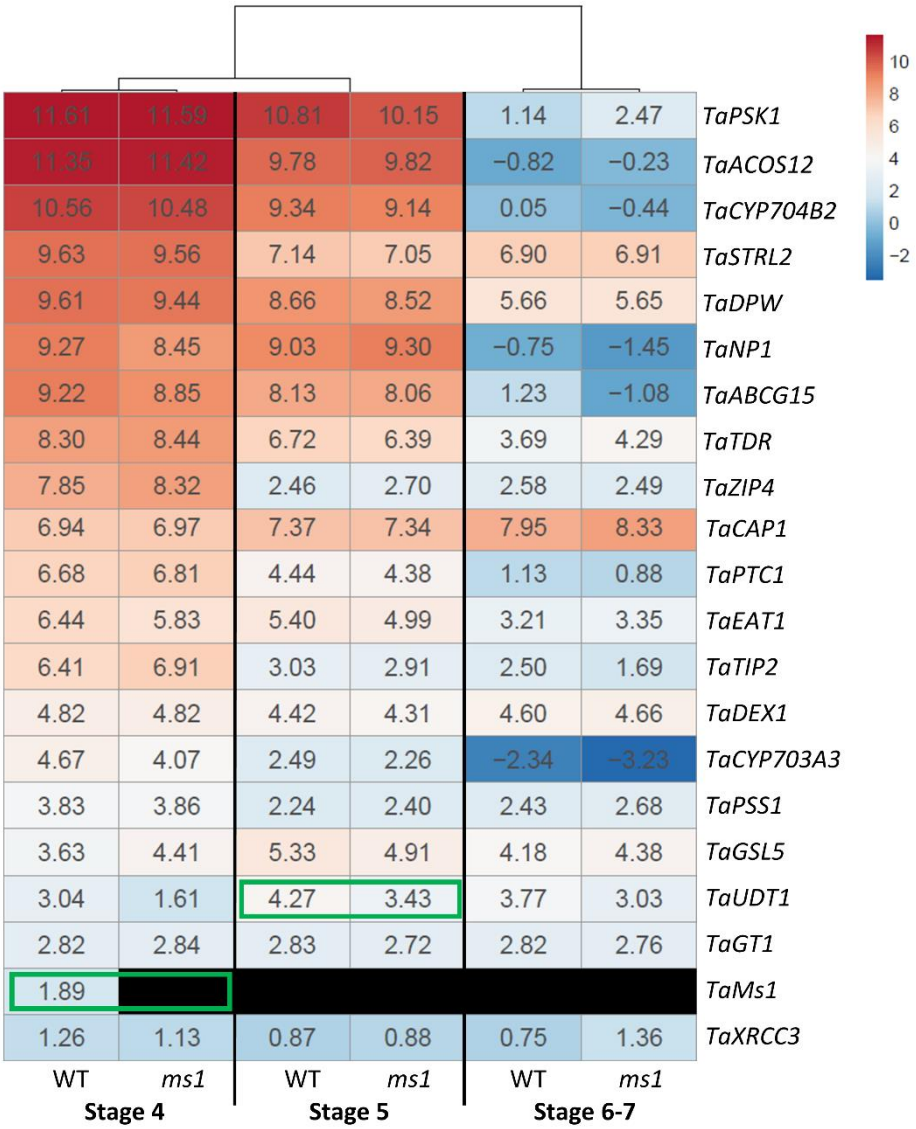

Figure 6 | Expression analysis of genes related to anther and pollen wall synthesis between Wild-Type and ms1. Expression value indicates log2 FPKM from RNA-seq data. The color bar represents the relative signal intensity value, red indicates higher while blue represents lower expression and black indicates no expression detected. Stage 4, meiotic microspores; Stage 5, early uninucleate; Stage 6, late uninucleate. Stage 7, binucleate. Hierarchical clustering of samples was obtained using McQuitty correlation. Green squares denote the values significantly different between WT and ms1 ($P < 0.05$) by t-test analysis.

3.4.5 TaMs1 protein is localized to the plasma membrane

Computational analysis of TaMs1 primary polypeptide predicts the presence of (i) an N-terminal signal secretory peptide (SP) 23 amino acids in length that is expected to target the mature protein to the secretory pathway, (ii) followed by an eight cysteine motif characteristic of LTPs' lipid binding domain (LBD) consensus, (iii) and a C-terminal transmembrane domain that is predicted to be post-translationally cleaved and replaced with a GPI-anchor (Fig. 7a). The TaMs1 protein defined by its three putative motifs, SP-LBD-GPI, is predicted to be secreted via the vesicular pathway and tethered to the extracellular side of the plasma membrane by a GPI moiety. In order to confirm TaMs1's sub-cellular localization *in vivo*, TaMs1 was fused with mCherry (mCh) and transiently expressed in onion epidermal cells.

Free mCh Fluorescence was observed to be diffuse within the cytoplasm (Fig. 7b). mCh-TaMs1 signal was observed at the cell periphery and co-localized with the PIP_2A-GFP plasma membrane marker (Nelson *et al.*, 2006) (Fig. 7c). This co-localization was confirmed in plasmolysed epidermal onion cells which allows the distinction between the plasma membrane and cell wall.

The requirement for each of the putative TaMs1 motifs (SP-LBD-GPI) for secretion and cell surface tethering was also demonstrated using truncated translation fusions transiently expressed in onion epidermal cells. We first tested the function of the N-terminal signal peptide (SP) using Ms1_SP. Ms1_SP fluorescence accumulated in the apoplast (Fig. 7d). This suggests that TaMs1 is targeted to the secretory pathway by the presence of the N-terminal signal peptide.

Finally, we studied the function of the pro-peptide GPI-anchor using Ms1ΔLBD and Ms1ΔGPI. Onion cells co-transformed with TaMs1 lacking the LBD and the plasma membrane intrinsic protein 2A- (PIP_2A-GFP) plasma membrane marker expressed fluorescence only at the outer

surface of the plasma-membrane (Fig. 7e). Post plasmolysis treatment, RFP signal was detected both at the retracted cell membrane and on Hechtian strands which form a membrane-cell-wall continuum. In the absence of the pro-peptide GPI-anchor, Ms1ΔLBD fluorescence was co-localized with the plasma membrane marker pre- and post-plasmolysis (Fig. 7f). Surprisingly, we additionally observed fluorescence within the cytosol. We interpret these findings to mean the GPI-anchor is required for specific targeting of TaMs1 to the plasma-membrane.

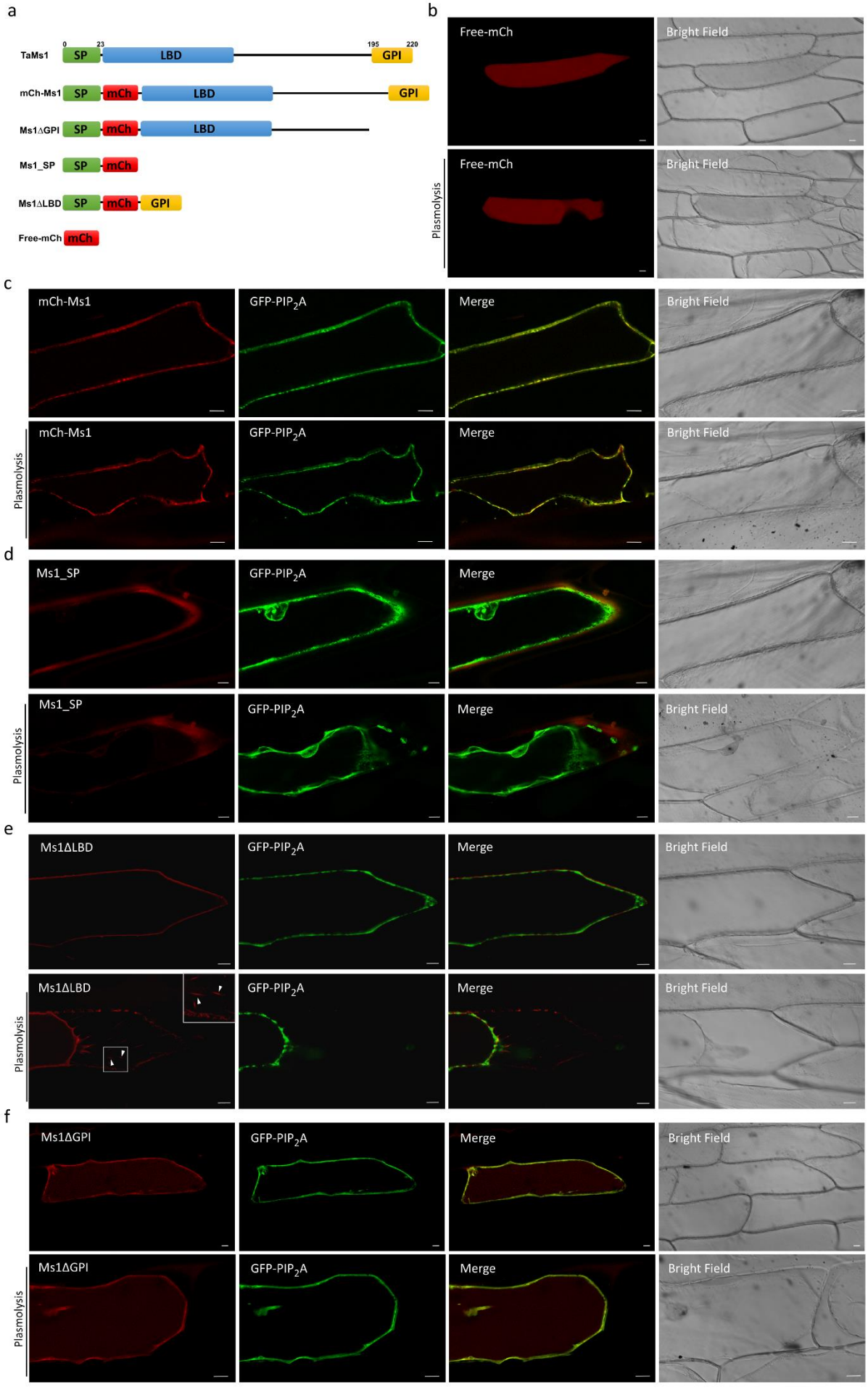
a
TaMs1
SP
LBD
GPI
0
23
195
220
mCh-Ms1
mCh
Ms1ΔGPI
Ms1_SP
Ms1ΔLBD
Free-mCh
b
Free-mCh
Bright Field
Plasmolysis
c
mCh-Ms1
GFP-PIP2A
Merge
Bright Field
d
Ms1_SP
e
Ms1ΔLBD
f
Ms1ΔGPI

Figure 7 | TaMs1 is targeted to the plasma membrane. (a) Schematic representation of the TaMs1 full length pre-protein and translational reporter fusion constructs used for epidermal onion cell transient expression assay (b) Cytosolic fluorescence of free mCh. (c) to (f) Co-expression of GFP- PIP_2A plasma membrane marker and TaMs1 full length or truncated proteins with and without plasmolysis. Scale bars = 20 µm.

3.5 Discussion

3.5.1 *TaMs1* is an anther specific gene expressed during pre-meiosis

We previously reported the identification of *TaMs1*, a dominant wheat fertility gene sequence located on chromosome 4BS (Tucker *et al.*, 2017). *TaMs1* was shown to be necessary for pollen exine formation. The phenotype for abnormal exine formation commonly leads to reduced fertility or complete male sterility. Pollen exine defective mutants have been reported to be a consequence of (i) defects in tapetal cell layer development, such as *tdr, tip2, eat1, ptc1* and *udt1* (Jung, 2005; Zhang *et al.*, 2008; Li *et al.*, 2011; Niu *et al.*, 2013; Ranjan *et al.*, 2017), (ii) disruption of the sporopollenin precursor synthesis and transport pathways, including *acos12, strl2, cyp703a3, psk1, dpw* and *abcg15* (Aya *et al.*, 2009; Shi *et al.*, 2011*b*; Qin *et al.*, 2013; Yang *et al.*, 2017; Zou *et al.*, 2017) (iii) disruption of callose formation (*gls5)* (Shi *et al.*, 2015), (iv) abnormal intine and premixine formation, such as *gt1, cap1 and dex1* (Moon *et al.*, 2013; Ueda *et al.*, 2013; Yu *et al.*, 2016), (v) and meiotic defects, including *xrcc3*, *zip4* and *pss1* (Zhou *et al.*, 2011; Shen *et al.*, 2012; Zhang *et al.*, 2015). These genes, whilst involved in different pathways, have demonstrated interdependent expression. For instance, rice *dpw* exhibits abnormal expression of *CYP704B2* (Shi *et al.*, 2011*b*) , *np1* is misregulated in *TDR*, *DPW*, *CYP703A3, CYP704B2* and *ABCG15* expression (Chang *et al.*, 2016), and loss-of-function mutants for *CYP703A3* were reported to have reduced expression of *DPW* and *CYP704B2* (Yang *et al.*, 2014). Furthermore, *TDR*, *EAT*, and *PTC1* had reduced expression in *tip2* (Li *et al.*, 2011) , whereas abnormal expression of *CYP704B2, PTC1*, *PSK1,* and *DPW* was detected in *ptc1* anthers (Li *et al.*, 2011). In order to determine whether *TaMs1* expression is

dependent upon sporopollenin biosynthesis, we analyzed expression of wheat orthologues as well as rice sporopollenin biosynthetic genes in *ms1* anthers relative to WT. We determined that *TaMs1* was expressed earlier than sporopollenin precursor biosynthesis. However, to our surprise, the *ms1* mutation did not affect transcription levels of the biosynthetic genes during stages where they have previously reported to be essential for pollen development (Fig. 6; Additional File 2). Because *TaMs1's* expression proceeds that of genes involved in sporopollenin biosynthesis temporally, further experimentation is necessary to determine whether the TaMs1 protein itself persists past meiosis, the time of last detectable transcript expression, to coincide with the expression of these key sporopollenin biosynthetic genes. Importantly the timing of expression of these wheat orthologues is in accordance with that reported in rice.

To date, wheat male sterile mutants linked to these rice genes have not yet been identified, with the exception of *TaCYP704B* (Singh *et al.*, 2017); this can in part be explained by genic redundancy embedded within wheat's allohexaploid genome. However, given the advent of new genome-editing technologies with the capability of simultaneously generating loss-of-function mutants in a single transgenic event, there is the possibility of uncovering additional genes necessary for sporopollenin biosynthesis.

Phytohormones play an essential role in the regulation of stamen and pollen development (Chandler, 2011). Here, we show the *TaMs1-B* promoter when compared to its homeologues contains several unique motifs with homology to ABA responsive (ABREOSRAB21), and jasmonate/ethylene responsive (GCCCORE-box) *cis*-elements (Fig. 2). We show that *TaMs1* expression is enhanced by ABA (Fig. 3), but not by JA exogenous treatment whereas treatments with hormones IAA and GA_3 revealed *TaMs1* to be responsive only to auxin. Importantly, auxin has been reported as a key regulator at both early and latter

stages of male gametogenesis, where it has been shown to be important for cellular differentiation, cell elongation and division (Sundberg and Østergaard, 2009). ABA on the other hand, is suggested to act as a potential signal leading to male sterility (Kovaleva and Voronkov, 2017). Confirmation of the importance of such *cis*-elements in hormone response signaling during microsporogenesis requires further experimentation.

It is generally assumed that protein trafficking plays a central role for protein function. Here, we identified TaMs1 to contain two putative signal sequences: an N-terminal signal peptide (SP) and a C-terminal GPI-anchor pro-peptide (Fig. 7a). The SP is expected to target TaMs1 for translocation across the ER allowing the protein to enter the vesicular pathway (von Heijne, 1990), whereas the GPI anchor is expected to retain the mature protein at the extracellular side of the plasma membrane (Debono *et al.*, 2009). As expected, using transient expression of a TaMs1 translational fusion with mCherry in onion epidermal cells, we determined TaMs1 to be localized at the plasma membrane (Fig. 7c). In order to validate function of TaMs1's predicted signal sequences for transport, we used truncated TaMs1 translational fusion proteins. The signal peptide alone was determined to induce protein secretion (Fig. 7d). Despite TaMs1 lacking the GPI-anchor pro-peptide, the truncated protein remained targeted to the plasma membrane, but was also detected to a lesser extent in the cytosol (Fig. 7f). This contrasts with AtLTP1 which, despite the absence of a GPI anchor, has only been identified at the plasma membrane (Potocka *et al.*, 2012). Despite the fact that TaMs1's GPI-anchor was not necessary for the protein to be targeted to the plasma membrane, it appears to be essential for its function. This is supported by the finding that *ms1j*, which contains a SNP converting Serine 195 to a Phenylalanine (S195F) is male sterile (Wang *et al.*, 2017). Importantly, this residue is predicted to be at the omega cleavage site of the GPI-anchor pro-peptide and this point mutation results in the loss of potential C-terminal GPI-modification

site (Additional file 3). Why TaMs1's GPI-anchor pro-peptide is essential for the protein activity could be explained by the unique properties of GPI-anchors: (i) it has been proposed that the functional importance of the GPI anchor could be related to its characteristic to allow greater three-dimensional flexibility for the protein at the cellular surface (Paulick and Bertozzi, 2008). (ii) Additionally, unlike transmembrane proteins, such GPI-anchored proteins have the potential to also be released from the cell surface via the activity of phospholipases (Müller *et al.*, 2012). Considering these properties, it is reasonable to assume that TaMs1 would be secreted from both the tapetal cell layer and developing microspores, and be tethered to the cell surface of each. Upon GPI-anchor cleavage by a phospholipase, TaMs1 could deliver sporopollenin precursors from the tapetal cell surface to the developing microspore surface. At this point, microspore derived TaMs1 proteins could potentially act as precursor receivers and therefore be responsible for the local deposition of exine at the cell surface. It is interesting that in a similar study, Wang *et al.* (2017), reported TaMs1 to be localized to mitochondria in onion epidermal cells. Relative to our findings of TaMs1 being localized at the cell surface, it is clear that further experimentation is necessary to determine where TaMs1 is localized *in planta*, particularly in wheat as opposed to interpretations based on an orthologous system like onion epidermal cells. Furthermore, validation of lipid binding by the TaMs1 fluorescent protein translational fusions is needed, as well as determining whether the translational fusions have the capacity to complement (i.e. restore male fertility) *ms1* mutants.

In this study, we attempted to further understand the role of TaMs1 in relation to pollen exine formation. Our results provide new insight into the importance of GPI-anchored LTPs at the early stages of anther development. We also identified putative wheat orthologues of rice sporopollenin biosynthetic genes. Future studies on the functional role of TaMs1 *in vivo* are

required to understand how this protein controls sporopollenin deposition onto the microspore in wheat.

3.6 References

Ariizumi T, Toriyama K. 2011. Genetic regulation of sporopollenin synthesis and pollen exine development. Annual review of plant biology **62**, 437–460.

Aya K, Ueguchi-Tanaka M, Kondo M, Hamada K, Yano K, Nishimura M, Matsuoka M. 2009. Gibberellin Modulates Anther Development in Rice via the Transcriptional Regulation of GAMYB. the Plant Cell Online **21**, 1453–1472.

de Azevedo Souza C, Kim SS, Koch S, Kienow L, Schneider K, McKim SM, Haughn GW, Kombrink E, Douglas CJ. 2009. A Novel Fatty Acyl-CoA Synthetase Is Required for Pollen Development and Sporopollenin Biosynthesis in Arabidopsis. the Plant Cell Online **21**, 507–525.

Blackmore S, Wortley AH, Skvarla JJ, Rowley JR. 2007. Pollen wall development in flowering plants. New Phytologist **174**, 483–498.

Boutrot F, Chantret N, Gautier M-F. 2008. Genome-wide analysis of the rice and Arabidopsis non-specific lipid transfer protein (nsLtp) gene families and identification of wheat nsLtp genes by EST data mining. BMC genomics **9**, 86.

Busk PK. 1998. Regulation of abscisic acid-induced transcription. Plant Molecular Biology **37**, 425–435.

Chandler JW. 2011. The Hormonal Regulation of Flower Development. Journal of Plant Growth Regulation **30**, 242–254.

Chang Z, Chen Z, Wang N, Xie G, Lu J, Yan W, Zhou J, Tang X, Deng XW. 2016. Construction of a male sterility system for hybrid rice breeding and seed production using a nuclear male sterility gene. Proceedings of the National Academy of Sciences, 201613792.

Debono A, Yeats TH, Rose JKC, Bird D, Jetter R, Kunst L, Samuels L. 2009. Arabidopsis LTPG is a glycosylphosphatidylinositol-anchored lipid transfer protein required for export of lipids to the plant surface. The Plant cell **21**, 1230–1238.

Edstam MM, Viitanen L, Salminen TA, Edqvist J. 2011. Evolutionary history of the non-specific lipid transfer proteins. Molecular Plant **4**, 947–964.

Eisenhaber B, Wildpaner M, Schultz CJ, Borner GH, Dupree P, Eisenhaber F. 2003. Glycosylphosphatidylinositol lipid anchoring of plant proteins. Sensitive prediction from

sequence- and genome-wide studies for Arabidopsis and rice. Plant Physiol **133**, 1691–1701.

Fankhauser N, Mäser P. 2005. Identification of GPI anchor attachment signals by a Kohonen self-organizing map. Bioinformatics **21**, 1846–1852.

FAOSTAT. 2017. http://www.fao.org/faostat/en/#data/RF.

Gomar J, Petit MC, Sodano P, Sy D, Marion D, Kader JC, Vovelle F, Ptak M. 1996. Solution structure and lipid binding of a nonspecific lipid transfer protein extracted from maize seeds. Protein science : a publication of the Protein Society **5**, 565–77.

Grienenberger E, Kim SS, Lallemand B, Geoffroy P, Heintz D, Souza C de A, Heitz T, Douglas CJ, Legrand M. 2010. Analysis of *TETRAKETIDE α-PYRONE REDUCTASE* Function in *Arabidopsis thaliana* Reveals a Previously Unknown, but Conserved, Biochemical Pathway in Sporopollenin Monomer Biosynthesis. The Plant Cell **22**, 4067–4083.

von Heijne G. 1990. The Signal peptide. J Membr Biol **115**, 195–201.

Higo K, Ugawa Y, Iwamoto M, Korenaga T. 1999. Plant cis-acting regulatory DNA elements (PLACE) database: 1999. Nucleic Acids Research **27**, 297–300.

Hird DL, Worrall D, Hodge R, Smartt S, Paul W, Scott R. 1993. The anther-specific protein encoded by the Brassica napus and Arabidopsis thaliana A6 gene displays similarity to beta-1,3-glucanases. The Plant journal : for cell and molecular biology **4**, 1023–33.

Huang M-D, Chen T-LL, Huang AHC. 2013. Abundant type III lipid transfer proteins in Arabidopsis tapetum are secreted to the locule and become a constituent of the pollen exine. Plant physiology **163**, 1218–29.

Isaac Kirubakaran S, Begum SM, Ulaganathan K, Sakthivel N. 2008. Characterization of a new antifungal lipid transfer protein from wheat. Plant Physiology and Biochemistry **46**, 918–927.

Ismagul A, Mazonka I, Callegari C, Eliby S. 2014. Agrobacterium-Mediated Transformation of Barley (Hordeum vulgare L.). Methods in molecular biology (Clifton, N.J.) **1145**, 203–211.

José-Estanyol M, Gomis-Rüth FX, Puigdomènech P. 2004. The eight-cysteine motif, a versatile structure in plant proteins. Plant Physiology and Biochemistry **42**, 355–365.

Jung K-H. 2005. Rice Undeveloped Tapetum1 Is a Major Regulator of Early Tapetum Development. the Plant Cell Online **17**, 2705–2722.

Kader JC. 1975. Proteins and the intracellular exchange of lipids. Biochimica et Biophysica Acta (BBA) - Lipids and Lipid Metabolism **380**, 31–44.

Kovaleva L V, Voronkov AS. 2017. ABA and IAA control microsporogenesis in Petunia hybrida L .

Lascombe M, Larue RY, Marion D, Blein J. 2008. The structure of ‘“ defective in induced resistance ”’ protein of Arabidopsis thaliana , DIR1 , reveals a new type of lipid transfer protein. Protein Science **17**, 1522–1530.

Li H, Pinot F, Sauveplane V, *et al.* 2010. Cytochrome P450 Family Member CYP704B2 Catalyzes the -Hydroxylation of Fatty Acids and Is Required for Anther Cutin Biosynthesis and Pollen Exine Formation in Rice. The Plant Cell **22**, 173–190.

Li H, Yuan Z, Vizcay-Barrena G, Yang C, Liang W, Zong J, Wilson ZA, Zhang D. 2011. PERSISTENT TAPETAL CELL1 Encodes a PHD-Finger Protein That Is Required for Tapetal Cell Death and Pollen Development in Rice. Plant Physiology **156**, 615–630.

Lin H, Yu J, Pearce S, Zhang D, Wilson Z. 2017. RiceAntherNet: a gene co-expression network for identifying anther and pollen development genes. The Plant Journal, n/a-n/a.

Maldonado AM, Doerner P, Dixon RA, Lamb CJ, Cameron RK. 2002. A putative lipid transfer protein involved in systemic resistance signalling in *Arabidopsis*. Nature **419**, 399–403.

Moon S, Kim S-R, Zhao G, Yi J, Yoo Y, Jin P, Lee S-W, Jung K -h., Zhang D, An G. 2013. Rice GLYCOSYLTRANSFERASE1 Encodes a Glycosyltransferase Essential for Pollen Wall Formation. Plant Physiology **161**, 663–675.

Morant M, Jørgensen K, Schaller H, Pinot F, Møller BL, Werck-Reichhart D, Bak S. 2007. CYP703 is an ancient cytochrome P450 in land plants catalyzing in-chain hydroxylation of lauric acid to provide building blocks for sporopollenin synthesis in pollen. The Plant cell **19**, 1473–1487.

Müller A, Klöppel C, Smith-Valentine M, Van Houten J, Simon M. 2012. Selective and programmed cleavage of GPI-anchored proteins from the surface membrane by phospholipase C. Biochimica et Biophysica Acta - Biomembranes **1818**, 117–124.

Nelson CJ, Hegeman AD, Harms AC, Sussman MR. 2006. A Quantitative Analysis of *Arabidopsis* Plasma Membrane Using Trypsin-catalyzed ^{18} O Labeling. Molecular & Cellular Proteomics **5**, 1382–1395.

Nielsen H. 2017. Protein Function Prediction. **1611**, 59–73.

Niu N, Liang W, Yang X, Jin W, Wilson ZA, Hu J, Zhang D. 2013. EAT1 promotes tapetal cell death by regulating aspartic proteases during male reproductive development in rice. Nature Communications **4**, 1445.

Park SY, Jauh GY, Mollet JC, Eckard KJ, Nothnagel EA, Walling LL, Lord EM. 2000. A lipid transfer-like protein is necessary for lily pollen tube adhesion to an in vitro stylar matrix. The Plant cell **12**, 151–64.

Paulick MG, Bertozzi CR. 2008. The Glycosylphosphatidylinositol Anchor : A Complex Membrane-Anchoring. , 6991–7000.

Pierleoni A, Martelli P, Casadio R. 2008. PredGPI: a GPI-anchor predictor. BMC Bioinformatics **9**, 392.

Potocka I, Baldwin TC, Kurczynska EU. 2012. Distribution of lipid transfer protein 1 (LTP1) epitopes associated with morphogenic events during somatic embryogenesis of Arabidopsis thaliana. Plant Cell Reports **31**, 2031–2045.

Qin P, Tu B, Wang Y, Deng L, Quilichini TD, Li T, Wang H, Ma B, Li S. 2013. ABCG15 encodes an ABC transporter protein, and is essential for post-meiotic anther and pollen exine development in rice. Plant and Cell Physiology **54**, 138–154.

Quilichini TD, Grienenberger E, Douglas CJ. 2015. The biosynthesis, composition and assembly of the outer pollen wall: A tough case to crack. Phytochemistry **113**, 170–182.

Ranjan R, Khurana R, Malik N, Badoni S, Parida SK, Kapoor S, Tyagi AK. 2017. bHLH142 regulates various metabolic pathway-related genes to affect pollen development and anther dehiscence in rice. Scientific Reports **7**, 43397.

Sasakuma T, Maan SS, Williams ND. 1978. EMS-Induced Male-Sterile Mutants in Euplasmic and Alloplasmic Common Wheat1. Crop Science **18**, 850.

Scott RJ, Spielman M, Dickinson HG. 2004. Stamen structure and function. The Plant cell **16 Suppl**, S46–S60.

Shen Y, Tang D, Wang K, Wang M, Huang J, Luo W, Luo Q, Hong L, Li M, Cheng Z. 2012. ZIP4 in homologous chromosome synapsis and crossover formation in rice meiosis. Journal of Cell Science **125**, 2581–2591.

Shi X, Sun X, Zhang Z, Feng D, Zhang Q, Han L, Wu J, Lu T. 2015. GLUCAN SYNTHASE-LIKE 5 (GSL5) plays an essential role in male fertility by regulating callose metabolism during microsporogenesis in rice. Plant and Cell Physiology **56**, 497–509.

Shi J, Tan H, Yu X-H, *et al.* 2011*a*. Defective pollen wall is required for anther and microspore development in rice and encodes a Fatty acyl carrier protein reductase. The Plant cell **23**, 2225–2246.

Shi J, Tan H, Yu X-H, *et al.* 2011*b*. Defective pollen wall is required for anther and microspore

development in rice and encodes a Fatty acyl carrier protein reductase. The Plant cell **23**, 2225–2246.

Shin DH, Lee JY, Hwang KY, Kyu Kim K, Suh SW. 1995. High-resolution crystal structure of the non-specific lipid-transfer protein from maize seedlings. Structure **3**, 189–199.

Singh M, Kumar M, Thilges K, Cho MJ, Cigan AM. 2017. MS26/CYP704B is required for anther and pollen wall development in bread wheat (Triticum aestivum L.) and combining mutations in all three homeologs causes male sterility. PLoS ONE **12**, 1–16.

Sterk P, Booij H, Schellekens G a, Van Kammen a, De Vries SC. 1991. Cell-specific expression of the carrot EP2 lipid transfer protein gene. The Plant cell **3**, 907–921.

Sundberg E, Østergaard L. 2009. Distinct and dynamic auxin activities during reproductive development. Cold Spring Harbor perspectives in biology **1**, 1–15.

Thoma S, Hecht U, Kippers A, Botella J, De Vries S, Somerville C. 1994. Tissue-specific expression of a gene encoding a cell wall-localized lipid transfer protein from Arabidopsis. Plant Physiol **105**, 35–45.

Tucker EJ, Baumann U, Kouidri A, *et al.* 2017. Molecular identification of the wheat male fertility gene Ms1 and its prospects for hybrid breeding. Nature Communications **8**, 869.

Ueda K, Yoshimura F, Miyao a., Hirochika H, Nonomura K-I, Wabiko H. 2013. COLLAPSED ABNORMAL POLLEN1 Gene Encoding the Arabinokinase-Like Protein Is Involved in Pollen Development in Rice. Plant Physiology **162**, 858–871.

Wang Z, Li J, Chen S, *et al.* 2017. Poaceae-specific *MS1* encodes a phospholipid-binding protein for male fertility in bread wheat. Proceedings of the National Academy of Sciences, 201715570.

Wang M, Wan L, Chen H, Liu X, Liu J. 2012. A new fluorescent staining method for callose of microspore mother cells during meiosis. Biotechnic & Histochemistry **87**, 300–302.

Wei K, Zhong X. 2014. Non-specific lipid transfer proteins in maize. BMC Plant Biology **14**, 281.

Yang X, Liang W, Chen M, Zhang D, Zhao X, Shi J. 2017. Rice fatty acyl-CoA synthetase OsACOS12 is required for tapetum programmed cell death and male fertility. Planta **246**, 105–122.

Yang X, Wu D, Shi J, *et al.* 2014. Rice CYP703A3, a cytochrome P450 hydroxylase, is essential for development of anther cuticle and pollen exine. Journal of Integrative Plant Biology **56**, 979–994.

Yu J, Meng Z, Liang W, *et al.* 2016. A Rice Ca 2 + Binding Protein Is Required for Tapetum Function and Pollen Formation 1 [OPEN]. **172**, 1772–1786.

Zachowski A, Guerbette F, Grosbois M, Jolliot-Croquin A, Kader JC. 1998. Characterisation of acyl binding by a plant lipid-transfer protein. European Journal of Biochemistry **257**, 443–448.

Zhang D-S, Liang W-Q, Yuan Z, Li N, Shi J, Wang J, Liu Y-M, Yu W-J, Zhang D-B. 2008. Tapetum degeneration retardation is critical for aliphatic metabolism and gene regulation during rice pollen development. Molecular plant **1**, 599–610.

Zhang B, Wang M, Tang D, Li Y, Xu M, Gu M, Cheng Z, Yu H. 2015. XRCC3 is essential for proper double-strand break repair and homologous recombination in rice meiosis. Journal of Experimental Botany **66**, 5713–5725.

Zhou DX. 1999. Regulatory mechanism of plant gene transcription by GT-elements and GT-factors. Trends in Plant Science **4**, 210–214.

Zhou S, Wang Y, Li W, *et al.* 2011. Pollen semi-sterility1 encodes a kinesin-1-like protein important for male meiosis, anther dehiscence, and fertility in rice. The Plant cell **23**, 111–129.

Zou T, Li S, Liu M, *et al.* 2017. An atypical strictosidine synthase, OsSTRL2, plays key roles in anther development and pollen wall formation in rice. Scientific Reports **7**, 6863.

3.7 Declarations

3.7.1 Acknowledgements

We thank, Patricia Warner and Yuan Li for technical assistance, Dr Gwen Mayo (Adelaide Microscopy) for the of microscopy assistance, Dr Ursula Langridge for helping with glasshouse management, Dr Takashi Okada, Margaret Pallotta for project advice, and Dr Nathan S. Watson-Haigh and Juan Carlos Sanchez for their bioinformatics assistance. We are grateful for the support provided by DuPont Pioneer Hi-Bred International Inc. and the University of Adelaide.

3.7.2 Funding

This research was supported by DuPont Pioneer Hi-Bred International Inc. and the University of Adelaide

3.7.3 Availability of data and materials

The datasets used and/or analysed during the current study are available from the corresponding author on reasonable request.

3.7.4 Authors' contributions

AK designed and conducted the experiments, analysed the data and drafted the manuscript. RW and UB conceived the project, assisted with data analysis and manuscript revision. MB assisted in cloning vector and data analysis. ET assisted with project conception and assisted with the qRT-PCR experiment. All authors contributed to revisions of the manuscript.

3.7.5 Ethics approval and consent to participate

Not applicable.

3.7.6 Consent for publication

Not applicable.

3.7.7 Competing interests

The authors declare that they have no competing interests.

3.8 Additional files

Table S1 | List of primers used for qRT-PCR.

Gene	Forward primer (5' to 3')	Reverse primer (5' to 3')
TaGAPdH	TTCAACATCATTCCAAGCAGCA	CGGACAGCAAAACGACCAAG
TaActin	GACAATGGAACCGGAATGGTC	GTGTGATGCCAGATTTTCTCCAT
Ta13-3-3	ACGCAGCTACCTGTATCATTC	CGACGATGTCCACATGACC
TaMs1_B	CCTCTACATCATCCTCTGAGTCGC	GTACGAGCGGACAGAAACGATAG
TaMs1_A	CCTCTACATCATCCTCTGAGTCGC	TGAACATACTGCTGCTACCAGACACTA
TaMs1_D	CCTCTACATCATCCTCTGAGTGGC	TCCATACTCCTGCCAACGACAG
TaABCG15	CTCACCTACAACTGCGGGAG	AGAAGTAGGCGAGGAGGCG
TaCYP703A3	CGCCAGGCTCTTCCACTG	GCCTTGGGCATGGTCATC
TaCYP704B2	GTTCATCGACCCGCTGTG	ATGACGCTGTAGGTGAACTCG
TaDPW	CGCCAGCTACGTCGAGAC	CTGGTAGATGCTGCCGAGG
TaPSK1	AACACAGTCTTCTATGTGCTGGAG	CAAGATCAATCCCCACTCTTCC

Table S2 | List of selected genes reported to be required for male fertility in rice.

Pathway	Gene name	Protein encoded	Putative function based on rice orthologues	Reference
Callose biosynthesis	*GLUCAN SYNTHASE-LIKE 5 (GSL5)*	Callose synthase	Essential for callose formation during microsporogenesis	Shi *et al.*, (2015)
Primexine formation	*DEFECTIVE IN EXINE FORMATION1 (DEX1)*	Calcium-binding protein	Required for exine pattern formation	Yu et al., (2016)
Intine development	*GLYCOSYLTRANSFERASE1 (GT1)*	Glycosyl-transferases	Essential for intine formation and pollen development	Moon *et al.*, (2013)
	COLLAPSED ABNORMAL POLLEN1 (CAP1)	Arabinokinase-like protein	Involved in cell wall polysaccharides synthesis	Ueda et al., (2013)
Biosynthesis of sporopollenin	*ACYL-COA* SYNTHETASE 12 (*ACOS12*)	Fatty Acyl-CoA synthetase	Required for tapetum programmed cell death and male fertility.	Yang *et al.*, (2017)
	STRICTOSIDINE SYNTHASE 2 (STRL2)	Strictosidine synthase	Essential anther development and pollen wall formation	Zou *et al.*, (2017)
	NO POLLEN 1 (*NP1*)	Glucose-methanol-choline oxidoreductase	Essential for tapetum degeneration and pollen exine formation	Lui *et al.*, (2017)
	CYTOCHROME P450 (*CYP703A3*)	Mid-chain fatty acid hydroxylase	Catalyzes in-chain hydroxylation of saturated medium-chain fatty acids	Aya *et al.*, (2009)
	CYTOCHROME P450 (*CYP704B2*)	Fatty acid ω-hydroxylase	Catalyzes v-hydroxylation of long-chain fatty acids, implicating these molecules in sporopollenin synthesis	Li *et al.*, (2010)
	POLYKETIDE SYNTHASE1 (PKS1)	Polyketide synthase	Essential anther development and pollen wall formation	Wang *et al.*, (2013)
	DEFECTIVE POLLEN WALL (DPW)	Fatty acyl carrier protein reductase	Required for pollen exine development	Shi *et al.*, (2011)
Transporters	*ABC TRANSPORTER G FAMILY MEMBER 15 (ABCG15)*	ATP binding cassette transporter	Sporopollenin precursor transfer	Qin *et al.*, (2013)
Transcription factors	*TAPETUM DEGERATION RETARDATION (TDR)*	bHLH transcription factor	Master regulator necessary for pollen wall formation regulating tapetum development and degeneration	Zhang *et al.*, (2008)
	UNDEVELOPED TAPETUM1 (UDT1)	bHLH transcription factor	A crucial regulator of a genetic network that controls anther development and function	Jung *et al.*, (2005)
	ETERNAL TAPETUM 1 (EAT1)	bHLH transcription factor	Promotes aspartic proteases to trigger plant programmed cell death	Niu *et al.*, (2012)
	TDR INTERACTING PROTEIN2 (TIP2)	bHLH transcription factor	Promotes tapetal PCD and degeneration of callose surrounding the microspores	Ranjan *et al.*, (2017)
	PERSISTENT TAPETAL CELL1 (PTC1)	PHD finger protein	Implicated in pollen wall development by regulating tapetal PCD and breakdown.	Li *et al.*, (2011)
Chromosome pairing and recombination	*X-RAY REPAIR CROSS COMPLEMENTING 3 (XRCC3)*	DNA repair protein	Essential for proper double-strand break repair and homologous recombination during meiosis	Zhang *et al.*, (2015)
	ZRT-IRT-LIKE PROTEIN (ZIP4)	Iron and zinc transporter protein	Promotes accurate synapsis and crossover of homologous chromosomes	Shen *et al.*, (2012)
	POLLEN SEMI-STERILITY1 (PSS1)	Kinesin-1-like protein	Essential for male meiotic chromosomal dynamics	Zhou *et al.*, (2011)

Table S3 | *ms1j* results in the loss of potential GPI-modification site.

Lines	Wild Type TaMs1	*ms1j* (S195F)
Peptide sequence	MERSRGLLLVAGLLAALLPAAAAQPGAPCEPALLATQVALFCAPDMPTAQCCEPV VAAVDLGGGVPCLCRVAAEPQLVMAGLNATHLLTLYSSCGGLRPGGAHLAAACE GPAPPAAVVSSPPPPPPPSAAPRRKQPAHDAPPPPPPSSEKPSSPPPSQDHDGAA PRAKAAPAQAATSTLAPAAAATAPPPQAPH**S**AAPTAPSKAAFFFVATAMLGLYIIL	MERSRGLLLVAGLLAALLPAAAAQPGAPCEPALLATQVALFCAPDMPTAQCCEPV VAAVDLGGGVPCLCRVAAEPQLVMAGLNATHLLTLYSSCGGLRPGGAHLAAACE GPAPPAAVVSSPPPPPPPSAAPRRKQPAHDAPPPPPPSSEKPSSPPPSQDHDGAA PRAKAAPAQAATSTLAPAAAATAPPPQAPHFAAPTAPSKAAFFFVATAMLGLYIIL
Prediction of potential C-terminal GPi-modification site	Potential GPI-modification site was found. Quality of the site ..... : P Sequence position of the omega-site : **195** Score of the best site ..... : 14.83 (P Value = 8.698e-07)	**None** potential GPI-modification site was found. Among all positions checked, sequence position 197 had the best score.

TaMs1 and *Tams1j* peptide sequences were tested for prediction of potential GPI-modification site using big-PI Plant Predictor (Eisenhaber *et al*., 2003).

Chapter 4

Genome-wide identification and analysis of non-specific Lipid

Statement of Authorship

Title of Paper	Genome-wide identification and analysis of non-specific Lipid Transfer Proteins in hexaploid wheat
Publication Status	☐ Published ☐ Accepted for Publication ☑ Submitted for Publication ☐ Unpublished and Unsubmitted w ork w ritten in manuscript style
Publication Details	Manuscript prepared in accordance with the guidelines of *Scientific Report.*

Principal Author

Name of Principal Author (Candidate)	Allan Kouidri
Contribution to the Paper	Conducted the study, performed bioinformatics and expression analysis, interpreted data and wrote the manuscript.
Overall percentage (%)	80 %
Certification:	This paper reports on original research I conducted during the period of my Higher Degree by Research candidature and is not subject to any obligations or contractual agreements with a third party that would constrain its inclusion in this thesis. I am the primary author of this paper.
Signature	Date 28/05/2018

Co-Author Contributions

By signing the Statement of Authorship, each author certifies that:

i. the candidate's stated contribution to the publication is accurate (as detailed above);

ii. permission is granted for the candidate in include the publication in the thesis; and

iii. the sum of all co-author contributions is equal to 100% less the candidate's stated contribution.

Name of Co-Author	Dr. Ryan Whitford
Contribution to the Paper	Supervised development of the work, help in data interpretation. Reviewed and edited the manuscript.
Signature	Date 27/5/2018.

Name of Co-Author	Dr. Radoslaw Suchecki
Contribution to the Paper	Extracted expression data from public RNA-seq datasets.
Signature	Date 28/5/2018

Name of Co-Author	Dr. Elena Kalashyan		
Contribution to the Paper	Provided help with the identification of nsLTPs in the wheat genome.		
Signature		Date	28.05.18

Name of Co-Author	Dr. Ute Baumann		
Contribution to the Paper	Supervised development of the work, help in data interpretation. Reviewed and edited the manuscript and acting as corresponding author.		
Signature		Date	28.05.18

Chapter 4

Genome-wide identification and analysis of non-specific Lipid Transfer Proteins in hexaploid wheat

Allan Kouidri[1], Ryan Whitford[1], Radoslaw Suchecki[1,2], Elena Kalashyan[1], Ute Baumann[1]*

[1] University of Adelaide, School of Agriculture, Food & Wine, Waite Campus, Urrbrae, South Australia 5064, Australia.

[2] Commonwealth Scientific and Industrial Research Organization, Agriculture and Food, Waite Campus, Urrbrae, South Australia 5064, Australia.

* Correspondence: ute.baumann@adelaide.edu.au

4.1 Abstract

Non-specific Lipid Transfer Proteins (nsLTPs) are involved in numerous biological processes. To date, only a fraction of wheat (*Triticum aestivum* L.) nsLTPs (TaLTPs) have been identified, and even fewer have been functionally analysed. In this study, the identification, classification, phylogenetic reconstruction, chromosome distribution, functional annotation and expression profiles of *TaLTPs* were analysed. 461 putative *TaLTPs* were identified from the wheat genome and classified into five types (1, 2, C, D and G). Phylogenetic analysis of the TaLTPs along with nsLTPs from *Arabidopsis thaliana* and rice, showed that all five types were shared across species, however, some type 2 TaLTPs formed wheat-specific clades. Gene duplication analysis indicated that tandem duplications contributed to the expansion of this gene family in wheat. Analysis of RNA sequencing data showed that *TaLTPs* were expressed in most tissues and stages of wheat development. Further, we refined the expression profile of anther-enriched expressed genes, and identified potential *cis*-elements regulating their expression specificity. This analysis provides a valuable resource towards elucidating the function of TaLTP family members during wheat development, aids our understanding of the evolution and expansion of the TaLTP gene family and, additionally, provides new information for developing wheat male-sterile lines with application to hybrid breeding.

4.2 Introduction

Plant non-specific Lipid Transfer Proteins (nsLTPs) are small and soluble proteins with the ability to transfer various lipid molecules between membranes *in vitro.* nsLTPs are characterized by an eight cysteine motif (8CM) backbone with the general form C-Xn-C-Xn-CC-Xn-CXC-Xn-C-Xn-C (Salminen *et al.*, 2016). The cysteine residues are linked by four disulphide bonds stabilizing a tertiary structure composed of four or five alpha helices, with a

hydrophobic cavity where the lipid binding takes place (Finkina *et al.*, 2016). In general, nsLTPs possess an N-terminal secretory signal peptide targeting the protein to the secretory pathway. In addition, some LTPs also carry a C-terminal signal sequence whereby a glycosylphosphatidylinositol-anchor (GPI-anchor) is post-translationally attached to the protein; The GPI-anchor tethers the peptide to the extracellular side of the plasma membrane (Mayor and Riezman, 2004). nsLTPs have been reported to participate in various biological processes, such as plant signalling, plant defence against biotic and abiotic stresses, cuticular wax and cutin synthesis, seed maturation and sexual reproduction (Carvalho and Gomes, 2007).

Plant *nsLTPs* consist of a large multigene family found in all land plants and are abundantly expressed in most tissues. Initially, nsLTPs were divided into two major groups based on molecular weight of the mature protein: nsLTP1 (9kDa) and nsLTP2 (7kDa) (Douliez *et al.*, 2000). These two groups differ in the disulphide bond linkages, nsLTP1 at Cys1-Cys6 and Cys5-Cys8 and nsLTP2 at Cys1-Cys5 and Cys6-Cys8. Recently, a new classification according to intron position, presence of GPI-anchor pro-peptide domain and amino acid sequence identity was proposed by Edstam *et al*. (2011). The system classified nsLTPs into 10 types, including five major types (Type 1, 2, C, D and G) and five minor types containing fewer members (E, F, H, J and K). nsLTPs have been reported by genome-wide analysis for several members of the *Poaceae*, including maize (*Zea mays)* (63 nsLTPs), rice (*Oriza sativa*) (77 nsLTPs) and sorghum (*Sorghum bicolor*) (58 nsLTPs) (Wei and Zhong, 2014). Previously, in wheat 156 nsLTPs were identified based on EST datasets (Boutrot *et al.*, 2008).

Recent studies have revealed the importance of nsLTPs for pollen development. In *A. thaliana*, RNA interference knock-down for *AtLTPg*.*3* and *AtLTPg*.*4* displayed deformed or sterile pollen grains (Edstam and Edqvist, 2014). Of the type C *nsLTPs*, *AtLTPc.1*, *AtLTPc.2* and *AtLTPc.3* have an anther specific expression restricted to the tapetal cell layer (Huang *et al.*, 2013). AtLTPc.3 was shown to be secreted into the anther locule whereby it ultimately becomes a constituent of the microspore surface. Double RNAi silencing of *AtLTPc.1* and *AtLTPc.3* affected intine morphology, however, pollen grains showed no reduction in fertility. Similarly to *A. thaliana nsLTP* genes, the maize (*Zea mays*) *Ms44* also encodes a type C LTP specifically expressed in tapetal cells with its silencing having no effect on fertility (Fox *et al.*, 2017). However, a mutation impairing the cleavage of the *Ms44* signal peptide and therefore blocking its secretion, results in a dominant male sterility phenotype. In contrast, silencing of the rice

OsC6, an anther-specific LTP, resulted in reduced pollen fertility (Zhang *et al.*, 2010). Different to what observed in rice, wheat *TaMS1* is a *nsLTP* type G, which shows expression specifically in anthers containing pre-meiosis to meiotic microspores (Tucker *et al.*, 2017; Wang *et al.*, 2017). Detailed examination of anthers derived from several deletion mutants (*ms1a*, *ms1b*, *ms1c*) and ethyl methanesulfonate (EMS)-derived mutants (*ms1d*, *ms1e*, *ms1f* and *ms1h*) revealed male sterility is a consequence of disrupted orbicule and pollen exine structure. The determination that wheat *TaMs1* is a single locus nuclear-encoded gene necessary for wheat male fertility represented a significant advance towards developing a hybrid wheat production system similar to the maize Seed Production Technology (SPT) (Whitford *et al.*, 2013; Tucker *et al.*, 2017). In previous studies, only a small portion of nsLTPs from wheat were identified. Considering a wheat genome reference sequence is now approaching completion, an opportunity exists to initiate a genome-wide analysis of the *nsLTP* gene family for this species.

In this study we identified 461 putative nsLTPs in the bread wheat genome (cv. Chinese Spring). We conducted a comprehensive study on the phylogeny, genomic structure, chromosomal location and expression profiles of the *nsLTP* gene family in wheat. Our analysis provides new insights into the *TaLTP* gene family which will support future functional research of nsLTPs. We identified anther-enriched nsLTPs of likely involvement in pollen development. When combined with new gene-editing technologies, this opens opportunities for exploring new loci for inducing male sterility that has application to hybrid breeding.

4.3 Results

4.3.1 Identification and classification of wheat nsLTPs

A total of 461 putative wheat *nsLTPs* were identified in cv. Chinese Spring (Supplementary Table S1 online). Predicted *nsLTPs* were classified into five types according to Edstam *et al.* (2011) (Type 1, 2, C, D and G)*;* type 2 contained most members with 59.44% of wheat *nsLTPs,* followed by type G (18.66%), type D (12.36%), type 1 (8.46%) and type C (1.08%). The proportion of wheat *nsLTPs* types varies greatly from that reported in genome-wide analyses performed in *A. thaliana* (*AtLTPs*), rice (*OsLTPs*), maize (*ZmLTPs*) and sorghum (*SbLTPs*) (Table 1), mainly due to a higher proportion of type 2 *nsLTPs* in wheat.

Table 1 | A summary of nsLTP genes in wheat, maize, sorghum, rice and *A.thaliana*.

	Wheat	Maize[1]	Sorghum[1]	Rice[1]	*A.thaliana*[1]
Type 1	39	8	9	18	13
Type 2	274	9	7	13	13
Type C	5	2	2	2	3
Type D	57	16	13	14	12
Type E	0	0	0	0	2
Type G	86	26	24	27	29
Single	0	2	3	3	7
Total nsLTPs	461	63	58	77	79

[1] nsLTPs members retrieved from Wei and Zhong (2014.

The evolutionary relationship of nsLTPs between wheat, rice and *A. thaliana* was determined based on phylogenetic analysis (Figure 1, Supplementary Fig. S1 online). The tree organisation was in agreement and coherent with the organisation of the five types. For type 1 and type C, all sequences belonging to the same type were grouped and constitute monophyletic groups (i.e. clades). However, type 2, type D and Type G sequences were divided into several groups with five, three and two clades, respectively. In addition, the distribution of nsLTP members within clades was not always quantitatively homogeneous between species, with some clades containing sequences only from wheat or *A. thaliana*. These species-specific clades, such as Type 2 [0-0-9], [0-0-16] and [0-0-125] and type D [5-0-0] and [0-0-13], contained nsLTPs with proline-rich sequences at the N-terminal of the 8CM.

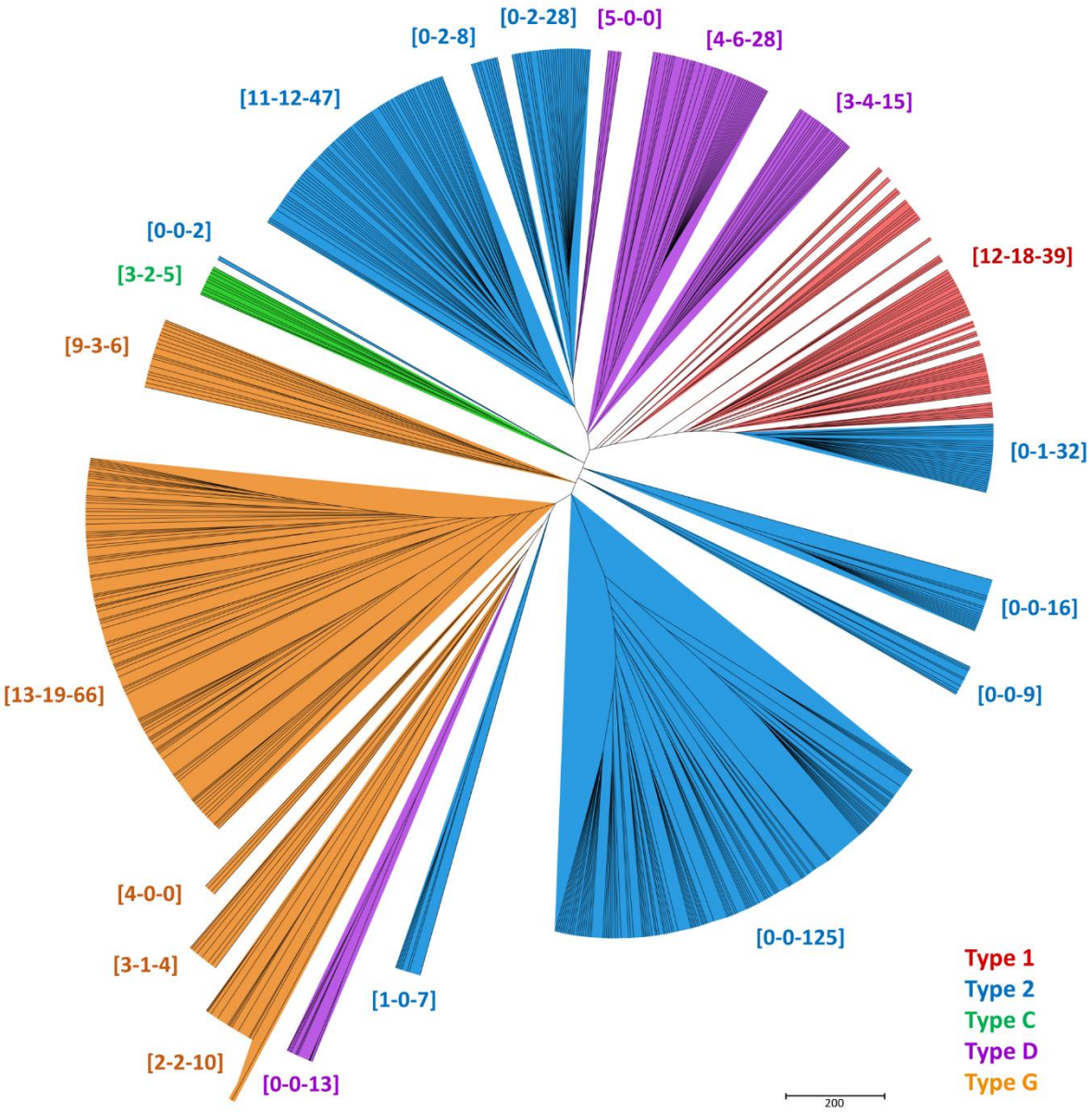

Figure 1 | Unrooted phylogenetic tree of nsLTPs from *A. thaliana*, rice and bread wheat. The phylogenetic tree was built from alignment of the predicted mature proteins. Brackets indicate number of sequences from *A. thaliana*, rice and wheat, respectively. Detailed phylogenetic tree is provided in Supplementary Fig. S1 online.

4.3.2 Gene and protein structures of the TaLTPs

Potential protein post-translational modifications of the 461 identified TaLTPs were investigated, including prediction of signal peptide domains and pre-GPI anchor transmembrane domains (Pierleoni *et al.*, 2008; Nielsen, 2017). Following cleavage of the predicted signal peptide and pre-GPI anchor domain, 418 unique mature proteins remained; among these, 386 TaLTPs possessed a unique 8CM.

nsLTPs are characterized by the highly conserved 8CM and analysis of the 8CM consensus within wheat sub-types identified a variable number of inter-cysteine amino acid residues (Table 2). Type 2 TaLTPs contained the most variable spacing across the 8CM, a likely consequence of the large number of members relative to the other sub-types. All Type C TaLTPs possessed a spacing of 12 residues between the Cys_6 and Cys_7 of the 8CM, while a spacing of 12 residues was not present in any other TaLTP class.

When analysing the 8CM spacing across all TaLTPs, we also identified conservation in the amino acids within these spaces, reflecting higher identity within, but not across sub-types. This was depicted using WebLogo3 tool (Crooks *et al.*, 2004) (Supplementary Fig. S2). For the CXC motif, hydrophobic residues at the X position were observed for most type 2 (86.1 %) and type G (87.0 %) and type C (100 %) proteins, whereas the presence of a hydrophilic residue was predominantly observed in type 1 TaLTPs (69.2%).

To better understand TaLTP protein characteristics, we analysed the isoelectric point (pI) and molecular weight (MW) for all putative TaLTPs. Their MW ranged from 6.73 kDa to 21.73 kDa. Type G nsLTPs have previously been reported to possess the highest MW due to the presence of supernumerary amino acid residues C-terminal to the 8CM. In contrast, to which has been reported in other species (*Zea mays*, *Marchantia polymorpa*, *Physcomitrella patens*, *Selaginella moellendorffi*, *Adiantum capillus-veneris*) (Edstam *et al.*, 2011; Wei and Zhong, 2014), five type D TaLTPs had a higher MW than type G TaLTPs. Furthermore, type 2 nsLTPs previously reported to be 7 kDa proteins, averaged 10.11 kDa in wheat (Douliez *et al.*, 2000).

Exon-intron structure was also used to classify wheat *nsLTPs*, based on criteria proposed by Edstam *et al*. (2011). Accordingly, type 2 *TaLTPs* were lacking introns, with the exception of 11 genes containing an intron downstream of the 8CM containing exon and classified as type 2 proteins based on peptide sequence identity (*TaLTP2.71, TaLTP2.28, TaLTP2.115, TaLTP2.127, TaLTP132, TaLTP2.135, TaLTP2.173, TaLTP2.217, TaLTP2.218, TaLTP2.220* and *TaLTP2.238*) (Supplementary Fig. S3 online). All type 1, type C and type D genes contained one intron positioned respectively at nucleotide 5, 1 and 4 after the last cysteine of the 8CM. In contrast, Type G *TaLTPs* contained up to four introns.

Table 2 | Diversity of eight cysteine motifs of TaLTPs.

Type	№	Spacing pattern									
1	39	C	X_{9}	C	$X_{13\text{-}15,19}$	CC	$X_{19\text{-}20,21}$	CXC	$X_{20\text{-}24}$	C	$X_{7,13,14,15}$
2	274	C	$X_{3,5,7,8\text{-}10,17}$	C	$X_{11,12\text{-}19,21,27}$	CC	$X_{8\text{-}13,19}$	CXC	$X_{8,10,15,18,19,21\text{-}27,36}$	C	$X_{3\text{-}9,11,13,15,16,17}$
C	5	C	X_{9}	C	$X_{14,19}$	CC	X_{9}	CXC	X_{12}	C	X_{6}
D	57	C	$X_{9,10,12\text{-}13\text{-}14}$	C	$X_{14,16\text{-}18}$	CC	$X_{9\text{-}12}$	CXC	$X_{11,17,23,24,27}$	C	$X_{4,7,9,10,11,20}$
G	86	C	$X_{6,9,10,12}$	C	$X_{8,13\text{-}18,20}$	CC	$X_{12,14,19}$	CXC	$X_{21\text{-}26,29}$	C	$X_{5,6,8\text{-}10,13,20}$

"X" represents any amino number, and the number following "X" indicates the number of amino acid residues underlined numbers indicate spacings specific for a type.

4.3.3 Chromosomal localization and duplication of TaLTPs gene family members

Of the 461 *TaLTPs*, physical location for 408 *TaLTPs* was identified within the Chinese Spring reference sequence (IWGSC Ref1.0) (Figure 2). *TaLTPs* were unevenly distributed across the 21 wheat pseudo-molecules. Chromosome 4B contained the highest number of *TaLTPs* (36), while fewest (4) were identified on chromosome 6A. In addition, *TaLTPs* distribution varied across the A (129 *nsLTPs*; 1 *TaLTP*/38.3 Mbps), B (169 *nsLTPs*, 1 *TaLTP*/30.7 Mbps) and D (110 *nsLTPs*; 1 *TaLTP*/35.9 Mbps) sub-genomes.

This uneven density of *TaLTPs* between sub-genomes is a likely consequence of ancestral translocation and duplication events. One such example is the presence of two significant clusters of tandem repeat type 2 *TaLTPs* found on both chromosome 3BS and 4BL relative to their homeologues. We identified 54 tandem duplication clusters involving a total of 200 *TaLTPs*. This suggests that some *TaLTPs* have undergone more than one round of duplication. Among the 200 duplicated genes, 144 belong to type 2 *TaLTPs.* This may explain why type 2 is found to be overrepresented in the wheat genome relative to other species.

To analyse the evolution process of type 2 *TaLTPs*, we performed nonsynonymous (Ka) and synonymous (Ks) substitution ratio analysis of the three largest *TaLTP* duplication clusters (Chr2A, TaLTP2.46-TaLTP.58; Chr3B, TaLTP2.91-TaLTP2.103 and Chr7B, TaLTP2.201-TaLTP2.211) (Supplemental Table S2 online; Figure 2). It was found that most duplicated pairs had a ratio Ka/Ks lower than one, implying that the genes evolved under influence of purifying selection with limited functional divergence after duplication. The Ka/Ks of TaLTP2.54/TaLTP2.49 gene pair was 1.0805, indicating a neutral selection pressure in evolution. Furthermore, divergence time of the duplicated genes were estimated by based on the number of non-synonymous substitution (Ks). Out of the 31 duplicated pairs analysed the Ks values were null for 38.7 % of them, indicating recent duplication events. For the remaining duplicated pairs, their corresponding duplication age were estimated to vary from 0.73 million years ago (MYA) to 53.9 MYA.

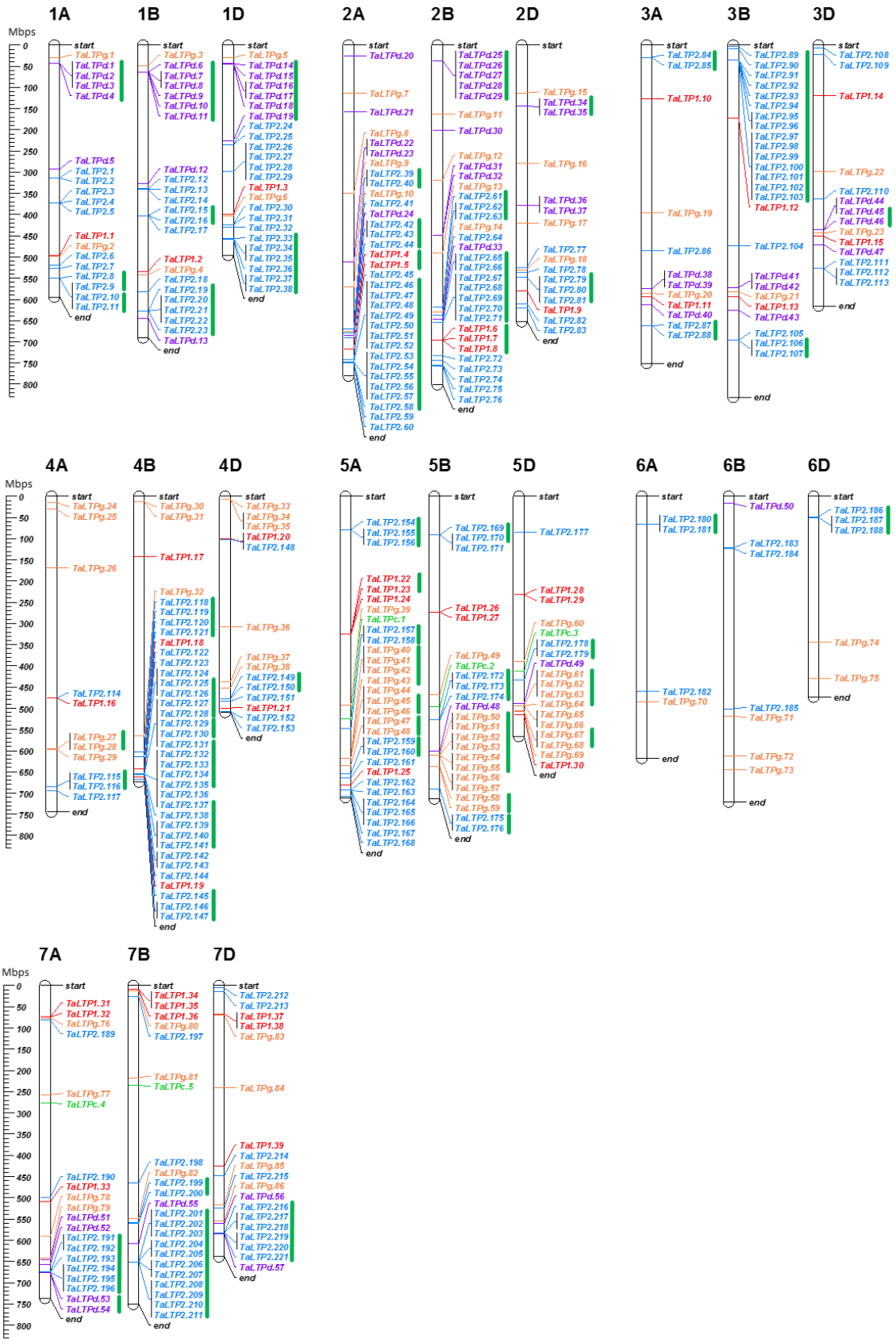

Figure 2 | Chromosomal location of TaLTPs. The scale represents megabases (Mbps). Chromosome names are indicated above each vertical bar. Green bars indicate clusters of tandemly duplicated genes.

4.3.4 Expression analysis of *TaLTPs*

The expression profiles of all 461 predicted *TaLTPs* were first analysed using public RNA-seq datasets from seven different tissues including leaves, roots, grains, stems, spikes, pistils and anthers (Figure 3, Supplementary Table S3 online). Their expression pattern varied greatly across tissues and developmental stages. No expression was detected for 30 *TaLTPs*, indicating that they are either pseudogenes or expressed in tissues or under specific environmental conditions for which RNA-seq data was not available.

Based on expression profiles, *TaLTPs* were divided in ten clusters (I to X) by hierarchical ordering (i.e. Cluster III contains anther-enriched genes while Cluster IV mostly contains genes with highly expressed in pistils). Type 1, type 2 and type G *TaLTPs* were present in most clusters, reflecting ubiquitous expression across tissues and developmental stages. In contrast, type C *TaLTPs*, only present in Cluster III, are found preferentially expressed in anthers. Comparing the proportions of *TaLTPs* per type and the proportions of TaLTP types per cluster found no significant distribution differences within Cluster VIII. In contrast, Cluster V (32 members) contained genes with expression enriched in leaf (Z23) and grain (Z85), and accounted for 56.2% of type D *TaLTPs* while overall, type D *TaLTPs* comprise only 12.4% of total *TaLTPs*.

In order to identify genes potentially involved in pollen development, we focussed on *TaLTPs* genes preferentially expressed in anthers. In total, 17 *TaLTPs* showed an anther-enriched expression profile based on the RNA-seq data. Among these, only *TaMs1,* a type G *nsLTP*, has been reported as anther-specific, and demonstrated to be involved in pollen exine development (Tucker *et al.*, 2017; Wang *et al.*, 2017). Two of the loci containing putative anther-expressed genes were found to possess only two *nsLTPs* homeologues from the three sub-genomes (TaLTPc4/TaLTPc.5 and TaLTPg.19/TaLTPg.22).

The evolutionary relationship of all identified anther-expressed genes was demonstrated using phylogenetic analysis (Figure 4). The selected *TaLTPs* were present within different clades, suggesting that these genes are derived from different ancestors. For the purpose of validating their anther-enriched expression profile, and to obtain more precise information on their expression timing during male gametogenesis, we conducted qRT-PCR across eight different wheat tissues including leaves, shoot, roots, glumes, lemmas, paleas, ovaries and anthers.

qRT-PCR results confirmed that the expression profiles for all selected genes were in agreement with the RNA-seq data (Figure 5). These anther-enriched genes were highly up-regulated in anthers containing meiotic microspores, with the exception of TaLTPg.30 (*TaMs1*) which exhibited expression in anthers deemed to contain microspores at pre-meiosis. In addition, TaLTPg.30 was the only gene to show expression on only one sub-genome, whereas all other anther-enriched LTPs showed expression across two or all three sub-genomes.

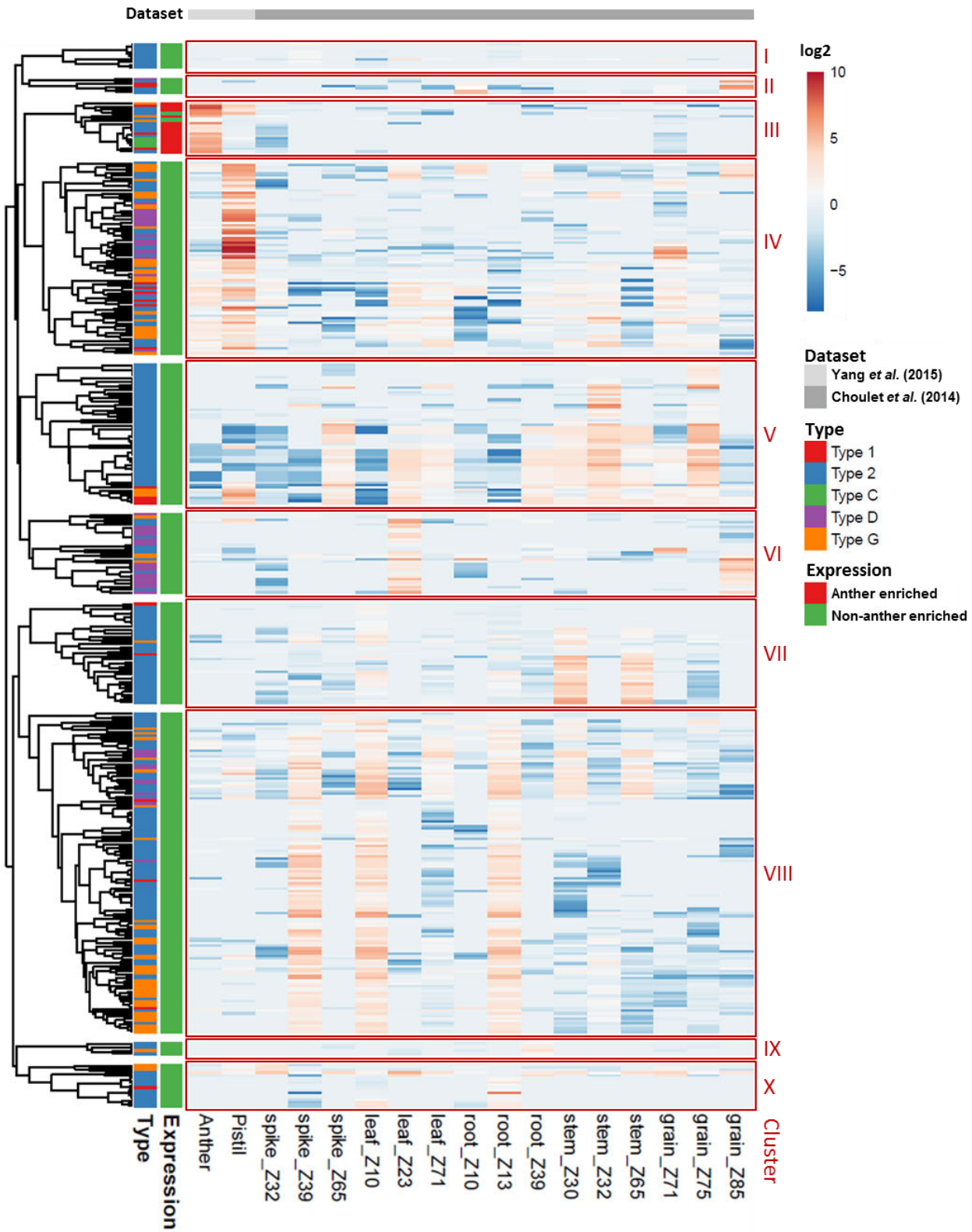

Figure 3 | Heat map representation and hierarchical clustering of transcript level of *TaLTPs* across different tissues. Data were retrieved from Choulet *et al.* (2014) and Yang *et al.* (2015). Genes were clustered by an average-linkage method (Metsalu, 2005). The transcript abundance in fragments per kilobase of exon per million fragments mapped (FPKM) of each genes is available as Supplementary Table S3 online.

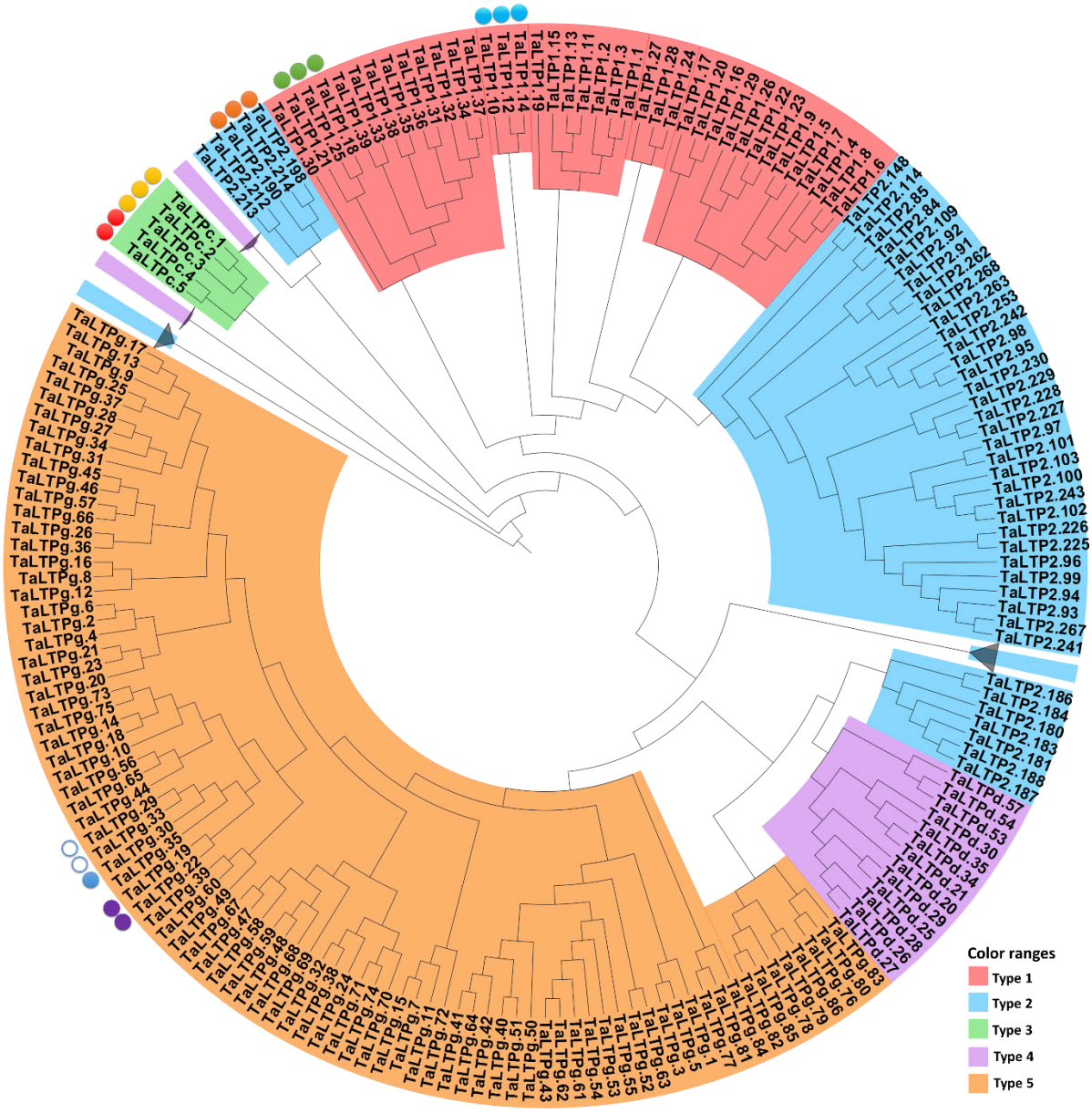

Figure 4 | Unrooted phylogenetic tree of *TaLTPs* highlighting potential anther-enriched genes. Filled circles represent anther-enriched genes identified by RNA-seq (Choulet *et al.*, 2014; Yang *et al.*, 2015), empty circles represent homeologous genes with no expression detected; different colors were used for different homeoloci. For more visibility, subtrees including sequences of the same type are grouped and represented by a grey triangle. The fully extended tree is available as Supplementary Fig. S4 online. The phylogenetic tree was built from alignment of the predicted mature proteins.

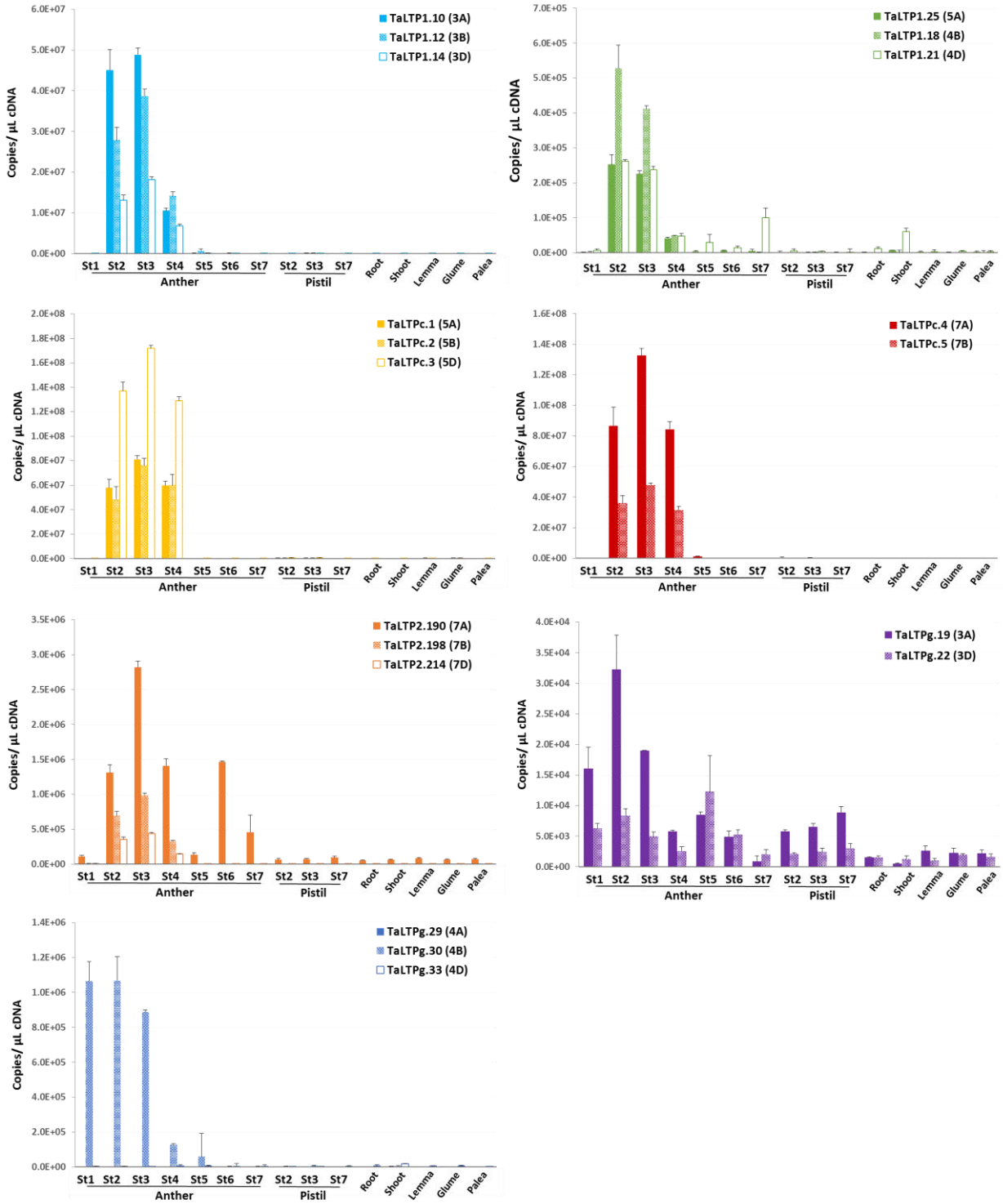

Figure 5 | Expression levels of anther-enriched expressed TaLTP candidates. Each graph represents the expression profile for one homeologue group. St1, archesporial cells; St2, pre-meiotic pollen mother cells; St3, meiotic microspores; St4, early uninucleate; St5, late uninucleate; St6, binucleate; St7, mature pollen. Error bars reflect standard error of three independent tissue replicates (n=3).

4.3.5 Promoter analysis of anther-specific *TaLTPs*

To evaluate the presence of *cis*-elements within *TaLTP* promoter regions involved in anther-specific expression, we searched for over-represented motifs in anther-specific vs non-anther-specific sequences using MEME suite (Bailey *et al.*, 2009). First, we focussed on nine boxes deemed to be associated with anther-enriched expression (Supplementary Table S4 online). Among these boxes, only the element POLLEN1LELAT52 (AGAAA) was identified to be enriched in anther-specific promoter regions (*P*-value= 6.72e-3) (Zhou, 1999). Secondly, we searched DNA motifs without *a priori* which were enriched in the anther-specific *TaLTPs* promoters relative to the remaining promoter sequence. A total of 6 motifs were identified to be significantly enriched in the anther-specific promoters (Table 3). Among these, two motifs were retrieved to be transcription factor binding sites (TFBSs); the TCTCGTAT motif (4), a putative binding site of APETALA2-ethylene response factor (AP2-ERF) (Wang *et al.*, 2016) and the ACGT core motif (6), a potential bZIP binding site (Martinez-García *et al.*, 1998).

Motif	Enrichment *P*-value [a]	Related	Logo	RC Logo
1	5.80E-10	N/A		
2	3.90E-08	N/A		
3	1.60E-07	N/A		
4	3.70E-07	SMZ (AP2-ERF)		
5	8.80E-07	N/A		
6	1.20E-06	bZIP190 (Zipper-type)		

Table 3 | List of motifs enriched in anther-specific nsLTPs promoter regions. [a] The enrichment *P*-value of the motif that are enriched in 17 anther-specific gene promoter regions compared with promoter sequences of the remaining 444 identified TaLTPs. Related, annotation of the motif; Logo, 5'-3'sequence; RC Logo, reverse-complement sequence; AP2-ERF, APETALA2-ethylene response factor; SMZ, SCHAFLMÜTZE.

4.4 Discussion

In the current study, a total of 461 *nsLTPs* were identified in the wheat genome (cv. Chinese Spring), including 39 type 1, 274 type 2, five type C, 57 type D and 86 type G. In comparison to *A. thaliana,* rice and maize, we found the wheat genome to contain over 5 times the number of *nsLTPs* (Table 1). The expansion of wheat *nsLTPs* could be due to the following reasons: (i) bread wheat is an allohexaploid species that originated from hybridization events involving three different diploid progenitors (AABBDD) (Feldman and Levy, 2012). (ii) small-scale gene duplication, including segmental and tandem duplication, may have played a significant role in *nsLTPs* gene family evolution in wheat. Genome duplication is generally accepted to be a primary source of genetic novelty through subfunctionalization and neofunctionalization and

has been central to the evolution of angiosperms, leading to species divergence (Davies *et al.*, 2004). Duplication events of *nsLTPs* have been reported in various species, such as *A. thaliana,* turnip, rice, maize and cotton (Boutrot *et al.*, 2008; Li *et al.*, 2014, 2016; Wei and Zhong, 2014). In this study, phylogenetic relationships between wheat, rice and *A. thaliana* nsLTPs showed an expansion of type 2 genes in wheat relative to rice and *A. thaliana* (Figure 1). This is reflected by the presence of type 2 clades containing only wheat sequences, mostly present in tandem repeats on the wheat pseudomolecules (Figure 2, Supplemental Table S2 online). We identified 54 tandem duplication clusters accounting for 200 *TaLTPs*, 72% of which were classified as type 2. Genic duplication and functional redundancy allows these gene sequences to accumulate mutations, increasing divergence and, over time, leading to expansion and evolution of the gene family (Conant and Wolfe, 2008). (iii) Natural selection would favour duplication of genes that results in adaptive expansion of gene families, it is suggested that retention and expansion of resistance genes in bread wheat might be the results of selection during domestication (Demuth and Hahn, 2009). Similar expansion was reported for the resistance *NBS-LRR* gene family in wheat (Gu *et al.*, 2015). The observed expansion of *nsLTP* gene family in wheat relative to rice, in addition to the estimated divergence time of the analysed some *TaLTP* duplication clusters averaging 5.28 Mya (Supplemental Table S2 online), is in accordance with an earlier divergence time of rice-*Triticeae* estimated of 50 Mya (Chalupska *et al.*, 2008). With the near complete genome assemblies of some *Triticeae* subgroups including, *Hordeum vulgare*, *Triticum Urartu*, *Aegilops tauschii* and *T. turgidum ssp dicoccoides* (Ling *et al.*, 2013; Avni *et al.*, 2017; Beier *et al.*, 2017; Luo *et al.*, 2017), new opportunities arise for a more thorough evolutionary analysis of the *nsLTP* gene family and further investigation of the duplication events that underpin the gene family expansion in wheat.

nsLTPs belong to a large family of pathogenesis-related proteins (PRPs), and are reported to play a role in defence against bacterial and fungal pathogens (Sudisha *et al.*, 2012). Some wheat nsLTPs have been shown to have an anti-fungal activity toward wheat and non-wheat fungal pathogens *in vitro* (TaLTP2.99, TaLTP2.241, TaLTP2.267, TaLTP2.227, TaLTP2.228, TaLTP2.229, TaLTP2.230, TaLTP2.242, TaLTP2.253, TaLTP2.263, TaLTP2.268, TaLTP2.109, TaLTP2.91, TaLTP2.92, TaLTP2.262, TaLTP1.22, TaLTP1.23) (Sun *et al.*, 2008). Surprisingly, no correlation was observed between their ability to inhibit pathogenic growth and lipid binding activity. However, it has been suggested that their toxicity could be derived from an alteration

of the fungal membrane permeability (Sun *et al.*, 2008). Additionally, the wheat TaLTP1.22 (100% similarity with the tandem duplicate TaLTP1.23) was reported to be associated with resistance against *Fusarium graminearum*, and its transcript level was at least 50-fold more abundant in plants carrying the resistant allele Qfhs.ifa-5A (Schweiger *et al.*, 2013). Interestingly, these previously reported *TaLTP* genes involved in abiotic stress resistance from type 1 and type 2, were all retrieved within the same phylogenetic clades (Supplemental Fig. S4 online). In addition, these *TaLTPs* demonstrated a similar expression profile based on RNA-seq analysis, and grouped within the same cluster (V), showing high expression in stems (Z30, Z32 and Z65), leaves (Z23 and Z71) and grains (Z65). Therefore, we speculate that these TaLTPs may also possess antifungal activities. In rice, similar inhibition tests using LTP110 demonstrated a critical role for the residues Tyr17 and Arg46 and Pro72 in antifungal activity (Ge *et al.*, 2003). As expected, these residues were identified as highly conserved in type 1 TaLTPs (Tyr14 and Arg50 and Pro78) (Supplementary Fig. S2 online).

In diverse crops, the use of male sterility has been exploited for production of hybrid varieties that capture the benefits of hybrid vigour. It is reported that wheat hybrid vigour offers a yield gain of over 10% and improved yield stability (Longin *et al.*, 2012). One major limitation towards developing a commercially viable hybrid seed production platform in wheat was the lack of identification of a single locus genic male-sterile mutant and its associated wild-type restorer sequence (Whitford *et al.*, 2013; Wu *et al.*, 2015). This limitation has been overcome, only recently, by the identification the dominant fertility gene *TaMs1,* and the dominant sterility gene *Ms2* (Ni *et al.*, 2017; Tucker *et al.*, 2017; Wang *et al.*, 2017; Xia *et al.*, 2017). In addition, the recent development of novel gene-editing technologies generates opportunities to generate loss-of-function mutants in a single transgenic event in wheat (Cigan *et al.*, 2017). *nsLTPs* represent potential candidates towards developing new male sterile mutants as studies have shown that defects in certain anther-expressed *nsLTPs* result in male sterility (Li and Zhang, 2010; Huang *et al.*, 2013*b*; Fox *et al.*, 2017; Tucker *et al.*, 2017). In order to identify *TaLTPs* responsible for ensuring male fertility, we analysed the expression profiles of selected *TaLTPs* using RNA-seq data and showed that most *TaLTPs* were expressed across a range of tissues and developmental stages. Interestingly, some members exhibited tissue-specific expressions, suggesting important roles in physiological processes during wheat development. This included, 16 *TaLTP* genes (7 loci) which were preferentially or specifically expressed in anthers. These include, three type 2 (single locus), six type 1 (two loci), five type C (two loci)

and 2 type G (two loci) genes. Orthologues for these wheat anther-expressed genes have been analysed in rice, maize and sorghum (Supplementary Table S5 online). Among the identified putative orthologs, only the maize type C *nsLTP (Ms44*) has been reported to be involved in male fertility (Fox *et al.*, 2017). In addition, no orthologues for *TaLTP2.190, TaLTP2.198* and *TaLTP2.214* could be retrieved for the studied species, suggesting a gain of function in wheat for male reproductive organ development. qRT-PCR analysis confirmed the expression profiles of these anther-expressed *TaLTPs* (Figure 5). Among the anther-expressed *TaLTPs,* only *TaMs1* was identified as a single homeologue expressed gene.

To understand the promoter specificity of the identified anther-specific *TaLTPs* and to also identify putative *cis*-elements controlling their spatial and temporal expression, we identified enriched DNA motifs on promoter regions for the anther-specific *TaLTPs* relative to non-anther enriched *TaLTPs* (Supplementary Table S4 online, and Table 3). A total of seven motifs were identified including three previously reported elements. (i) The first is POLLENLELAT52 (AGAAA), an enhancer element of LAT52 deemed to be essential for high level of expression in pollen (Supplementary Table S4 online, and Table 3) (Bate and Twell, 1998). (ii) The second is an AP2/ERF binding site element identified to regulate *SMZ,* involved in regulation of floral development in *A. thaliana* (Wang *et al.*, 2016). (iii) The third is a binding site element of bZIP190 (ACGT core), reported to be preferentially expressed in flowers of *Antirrhinum majus* (Martinez-García *et al.*, 1998). An analysis by promoter bashing would help to confirm functionality of these identified *cis*-elements in anther-enriched expression.

In conclusion, this is the first comprehensive and systematic analysis of nsLTPs in wheat. The structure, classification, evolutionary and expression profiles of 461 putative *TaLTPs* were analysed. The results of this study revealed the ubiquitous expression of *TaLTPs* during growth and development. The expansion of *TaLTPs* in the wheat genome was attributed to duplications during evolution. Our expression analysis may provide a solid basis for future studies of TaLTP function during wheat development. The identification of anther-expressed *TaLTPs* opens opportunities for the development of new male-sterile wheat lines for hybrid seed production.

4.5 Materials and Methods

4.5.1 Sequence retrieval and structural analysis

All nsLTP sequences of *Arabidopsis thaliana*, rice (*Oriza sativa*), sorghum (*Sorghum bicolor*) and maize (*Zea mays*) previously identified by Wei and Zhong (2014) were retrieved from phytozome (Goodstein *et al.*, 2012; Wei and Zhong, 2014). To identify wheat putative nsLTPs we first used rice protein sequences (LOC_Os10g36070.1, LOC_Os07g18750.1, LOC_Os05g47700.1, LOC_Os05g40010.1, LOC_Os03g07100.1, LOC_Os01g68580.1, LOC_Os01g59870.1, LOC_Os01g12020.1) as queries to search against the Wheat IWGSC Ref1.0 using tBLASTn with an e-value of ≤ 10. Secondly, we examined hit sequences (+/- 1000 bps) in all six DNA frames for presence of the 8CM, and all hits lacking the essential Cys residues were excluded. Then, selected genomic sequences were used for gene prediction using TriAnnot and FGENESH programs with defaults parameters (Solovyev *et al.*, 2006; Leroy *et al.*, 2012). Subsequently, all predicted genes lacking the 8CM were removed from further analysis. The remaining candidates were submitted to SUPERFAMILY 2 Beta online tool, sequences annotated as proteinase/alpha-amylase inhibitor and seed storage family, 2S albumin were discarded (http://beta.supfam.org/). Additionally, putative nsLTPs lacking NSSs (examined with SignalP 4 server (Petersen *et al.*, 2011)) were also excluded. Presence of a C-terminal GPI-anchor signal was predicted using three prediction tools PredGPI, big PI-plant predictor and GPI-SOM (Eisenhaber *et al.*, 2003; Fankhauser and Mäser, 2005; Pierleoni *et al.*, 2008). Splice junctions were predicted using Splign Transcript to Genomic Alignment tool (Kapustin *et al.*, 2008). The nsLTP nomenclature was based on guidelines from Edstam *et al.* (2011).

4.5.2 Phylogenetic analysis and gene duplications

nsLTPs sequences ID of rice (*Oriza sativa*), Sorghum (*Sorghum bicolor*), and Maize (*Zea Mays*) were retrieved from Wei and Zhong (2014). nsLTPs amino acid sequences were downloaded from ensembl plant (Kersey *et al.*, 2017). All nsLTPs 8CM sequences of the mature proteins were aligned using Clustal Omega (Sievers *et al.*, 2011). After manually refinement of the multiple sequence alignment, the phylogenetic tree was built from alignment of the predicted mature proteins by Unweighted Pair Group Method with Arithmetic mean method using the Jalview program (Waterhouse *et al.*, 2009). Trees were visualized using the iTOL web tool V4.0.3 (Letunic and Bork, 2016).

4.5.3 Gene structure analysis

In order to identify the precise splice-junction site of predicted *TaLTPs,* coding sequences (CDS) were aligned to genomic sequence using Splign alignment tool (Kapustin *et al.*, 2008). Schematic representation of *TaLTPs* gene structures was generated using the GSGS 2.0 tool (Hu *et al.*, 2018).

4.5.4 Chromosomal mapping and duplication

TaLTPs were mapped onto the 21 wheat chromosomes according to their physical position (bp), from the short arm telomere to the long arm telomere based on IWGSC reference sequence V1.0. MapChart was used to draw their location onto the physical map of each chromosome (Voorrips, 2002). To detect gene duplications, the CDS sequences of *TaLTPs* in wheat were blasted against each other and selected with the following cut-offs: 80% of coverage with the similarity of the aligned regions above 80%. Tandemly duplicated *TaLTPs* were defined as two or more adjacent homologous genes located on a single chromosome.The estimation of the evolution rates of the duplicated *TaLTPs* was calculated using KaKs_calculator 2.0 (Wang *et al.*, 2010). The divergence times (T) of *TaLTP* duplicated pairs were calculated as $T = Ks/2r \times 10^{-6}$ Mya, with a divergence rate (r) of 6.5×10^{-9} (Gaut *et al.*, 1996).

4.5.5 Gene expression profiles based on RNA-seq

Previous wheat cv. Chinese Spring transcriptome examinations were performed by RNA-seq to investigate gene expression pattern of genes during vegetative and reproductive development. The transcript abundance of each gene was estimated by fragments per kilobase of exon per million fragments mapped (FPKM). Expression data of *TaLTPs* in spikes, leaves, roots, stems and grains, each sampled at three developmental stages, were retrieved from RNA-seq data downloaded from the European Nucleotide Archive database with the study number PRJEB5314 (http://www.ebi.ac.uk/ena/data/view/PRJEB5314). *TaLTPs* expressions data in pistils and anthers were downloaded from NCBI-SRA database with accession number SRP038912.

Heatmaps were generated from log2-transformed FPKM using the ClustVis web tool (Metsalu and Vilo, 2015).

4.5.6 Quantitative RT-PCR analysis

Total RNA was isolated using ISOLATE II *RNA* Mini Kit (Bioline, Sydney, Australia) from wheat of cv. Chris tissues including roots, shoot apical meristem (SAM) and glume, lemma, palea,

ovaries, and anthers containing microspores from pre-meiosis to maturity. Microspores were cytologically examined for stage of development. The remaining two anthers from the same floret were isolated and snap frozen in liquid nitrogen. All total RNA samples were treated with DNase I (Qiagen). 0.6 µg of RNA was used to synthesise the oligo (dT)-primed first strand cDNA using the superscript IV reverse transcriptase (Thermo Fisher, Adelaide, Australia). Quantitative real-time PCR was perform according to Burton *et al.* (2004) using the primer combinations shown in Supplemental Table S6 online. Amplification products from qRT-PCR on each tissue sample, three technical replicates and three biological replicates were used to estimate the transcript abundance of genes of interest relative to TaActin, TaGAPdH and Ta13-3-3 reference transcripts.

4.5.7 Promoter analysis

For motif enrichment analysis using know *cis*-element deemed to be involved in pollen enriched expression (Supplementary Table S4 online) we used the AME web tool implemented in MEME suite (Bailey *et al.*, 2009) with the following parameter: Ranksum enrichment test with a *P*-value threshold of 0.05.

For *de novo* motif discovery and enrichment, we used the DREME web tool implemented in MEME suite (version 4.12.0) (Bailey *et al.*, 2009) with an e-value threshold of 0.05. MEME was also used to generate sequence logos for each discovered motif. Jaspar database was searched to find related transcription factor binding sites to the motifs identified using a relative profile score threshold of 80 % (Khan *et al.*, 2017).

4.6 References

Avni R, Nave M, Barad O, *et al.* 2017. Wild emmer genome architecture and diversity elucidate wheat evolution and domestication. Science **357**, 93–97.

Bailey TL, Boden M, Buske FA, Frith M, Grant CE, Clementi L, Ren J, Li WW, Noble WS. 2009. MEME Suite: Tools for motif discovery and searching. Nucleic Acids Research **37**, 202–208.

Bate N, Twell D. 1998. Functional architecture of a late pollen promoter: Pollen-specific transcription is developmentally regulated by multiple stage-specific and co-dependent activator elements. Plant Molecular Biology **37**, 859–869.

Beier S, Himmelbach A, Colmsee C, *et al.* 2017. Construction of a map-based reference genome sequence for barley, Hordeum vulgare L. Scientific Data **4**, 170044.

Boutrot F, Chantret N, Gautier M-F. 2008. Genome-wide analysis of the rice and Arabidopsis non-specific lipid transfer protein (nsLtp) gene families and identification of wheat nsLtp genes by EST data mining. BMC genomics **9**, 86.

Burton RA. 2004. The CesA Gene Family of Barley. Quantitative Analysis of Transcripts Reveals

Two Groups of Co-Expressed Genes. Plant Physiology **134**, 224–236.

Carvalho A de O, Gomes VM. 2007. Role of plant lipid transfer proteins in plant cell physiology-A concise review. Peptides **28**, 1144–1153.

Chalupska D, Lee HY, Faris JD, Evrard A, Chalhoub B, Haselkorn R, Gornicki P. 2008. Acc homoeoloci and the evolution of wheat genomes. Proceedings of the National Academy of Sciences of the United States of America **105**, 9691–6.

Choulet F, Alberti A, Theil S, *et al.* 2014. Structural and functional partitioning of bread wheat chromosome 3B. Science **345**.

Cigan AM, Singh M, Benn G, Feigenbutz L, Kumar M, Cho MJ, Svitashev S, Young J. 2017. Targeted mutagenesis of a conserved anther-expressed P450 gene confers male sterility in monocots. Plant Biotechnology Journal **15**, 379–389.

Conant GC, Wolfe KH. 2008. Turning a hobby into a job: How duplicated genes find new functions. Nature Reviews Genetics **9**, 938–950.

Crooks G, Hon G, Chandonia J, Brenner S. 2004. NCBI GenBank FTP Site\nWebLogo: a sequence logo generator. Genome Res **14**, 1188–1190.

Davies TJ, Barraclough TG, Chase MW, Soltis PS, Soltis DE, Savolainen V. 2004. Darwin's abominable mystery: Insights from a supertree of the angiosperms. Proceedings of the National Academy of Sciences **101**, 1904–1909.

Demuth JP, Hahn MW. 2009. The life and death of gene families. BioEssays **31**, 29–39.

Douliez JP, Michon T, Elmorjani K, Marion D. 2000. Structure, biological and technological functions of lipid transfer proteins and indolines, the major lipid binding proteins from cereal kernels. Journal of Cereal Science **32**, 1–20.

Edstam MM, Edqvist J. 2014. Involvement of GPI-anchored lipid transfer proteins in the development of seed coats and pollen in Arabidopsis thaliana. Physiologia Plantarum **152**, 32–42.

Edstam MM, Viitanen L, Salminen TA, Edqvist J. 2011. Evolutionary history of the non-specific lipid transfer proteins. Molecular Plant **4**, 947–964.

Eisenhaber B, Wildpaner M, Schultz CJ, Borner GH, Dupree P, Eisenhaber F. 2003. Glycosylphosphatidylinositol lipid anchoring of plant proteins. Sensitive prediction from sequence- and genome-wide studies for Arabidopsis and rice. Plant Physiol **133**, 1691–1701.

Fankhauser N, Mäser P. 2005. Identification of GPI anchor attachment signals by a Kohonen self-organizing map. Bioinformatics **21**, 1846–1852.

Feldman M, Levy AA. 2012. Genome evolution due to allopolyploidization in wheat. Genetics **192**, 763–774.

Finkina EI, Melnikova DN, Bogdanov I V., Ovchinnikova T V. 2016. Lipid transfer proteins as components of the plant innate immune system: Structure, functions, and applications. Acta Naturae **8**, 47–61.

Fox T, DeBruin J, Haug Collet K, *et al.* 2017. A single point mutation in *Ms44* results in dominant male sterility and improves nitrogen use efficiency in maize. Plant Biotechnology Journal, 1–11.

Gaut BS, Morton BR, McCaig BC, Clegg MT. 1996. Substitution rate comparisons between grasses and palms: synonymous rate differences at the nuclear gene Adh parallel rate differences at the plastid gene rbcL. Proceedings of the National Academy of Sciences **93**, 10274–10279.

Ge X, Chen J, Sun C, Cao K. 2003. Preliminary study on the structural basis of the antifungal activity of a rice lipid transfer protein. Protein engineering **16**, 387–390.

Goodstein DM, Shu S, Howson R, *et al.* 2012. Phytozome: A comparative platform for green plant genomics. Nucleic Acids Research **40**, 1178–1186.

Gu L, Si W, Zhao L, Yang S, Zhang X. 2015. Dynamic evolution of NBS–LRR genes in bread wheat and its progenitors. Molecular Genetics and Genomics **290**, 727–738.

Hu B, Jin J, Guo A, Zhang H, Luo J. 2018. Genome analysis GSDS 2 . 0 : an upgraded gene feature visualization server. **31**, 1296–1297.

Huang M-D, Chen T-LL, Huang AHC. 2013. Abundant Type III Lipid Transfer Proteins in Arabidopsis Tapetum Are Secreted to the Locule and Become a Constituent of the Pollen Exine. Plant Physiology **163**, 1218–1229.

Kapustin Y, Souvorov A, Tatusova T, Lipman D. 2008. Splign: Algorithms for computing spliced alignments with identification of paralogs. Biology Direct **3**, 1–13.

Kersey PJ, Allen JE, Allot A, *et al.* 2017. Ensembl Genomes 2018: an integrated omics infrastructure for non-vertebrate species. Nucleic Acids Research **46**, 802–808.

Khan A, Fornes O, Stigliani A, *et al.* 2017. JASPAR 2018: update of the open-access database of transcription factor binding profiles and its web framework. Nucleic Acids Research **46**, 260–266.

Leroy P, Guilhot N, Sakai H, *et al.* 2012. TriAnnot: A Versatile and High Performance Pipeline for the Automated Annotation of Plant Genomes. Frontiers in Plant Science **3**, 1–14.

Letunic I, Bork P. 2016. Interactive tree of life (iTOL) v3: an online tool for the display and annotation of phylogenetic and other trees. Nucleic acids research **44**, W242–W245.

Li F, Fan K, Ma F, *et al.* 2016. Genomic Identification and Comparative Expansion Analysis of the Non-Specific Lipid Transfer Protein Gene Family in Gossypium. Scientific Reports **6**, 38948.

Li J, Gao G, Xu K, Chen B, Yan G, Li F, Qiao J, Zhang T, Wu X. 2014. Genome-wide survey and expression analysis of the putative non-specific lipid transfer proteins in Brassica rapa L. PLoS ONE **9**.

Li H, Zhang D. 2010. Biosynthesis of anther cuticle and pollen exine in rice. Plant signaling & behavior **5**, 1121–1123.

Ling HQ, Wang J, Zhao S, *et al.* 2013. Draft genome of the wheat A-genome progenitor Triticum urartu. Nature **496**, 87–90.

Longin CFH, Mühleisen J, Maurer HP, Zhang H, Gowda M, Reif JC. 2012. Hybrid breeding in autogamous cereals. Theoretical and Applied Genetics **125**, 1087–1096.

Luo MC, Gu YQ, Puiu D, *et al.* 2017. Genome sequence of the progenitor of the wheat D genome Aegilops tauschii. Nature **551**, 498–502.

Martinez-García JF, Moyano E, Alcocer MJC, Martin C. 1998. Two bZIP proteins from Antirrhinum flowers preferentially bind a hybrid C-box/G-box motif and help to define a new sub-family of bZIP transcription factors. Plant Journal **13**, 489–505.

Mayor S, Riezman H. 2004. Sorting GPI-anchored proteins. Nature reviews. Molecular cell biology **5**, 110–20.

Metsalu T, Vilo J. 2015. ClustVis: A web tool for visualizing clustering of multivariate data using Principal Component Analysis and heatmap. Nucleic Acids Research **43**, W566–W570.

Ni F, Qi J, Hao Q, *et al.* 2017. Wheat Ms2 encodes for an orphan protein that confers male sterility in grass species. Nature Communications **8**, 15121.

Nielsen H. 2017. Protein Function Prediction. **1611**, 59–73.

Petersen TN, Brunak S, Von Heijne G, Nielsen H. 2011. SignalP 4.0: Discriminating signal peptides from transmembrane regions. Nature Methods **8**, 785–786.

Pierleoni A, Martelli P, Casadio R. 2008. PredGPI: a GPI-anchor predictor. BMC Bioinformatics **9**, 392.

Salminen TA, Blomqvist K, Edqvist J. 2016. Lipid transfer proteins: classification, nomenclature, structure, and function. Planta **244**, 971–997.

Schweiger W, Steiner B, Ametz C, *et al.* 2013. Transcriptomic characterization of two major Fusarium resistance quantitative trait loci (QTLs), Fhb1 and Qfhs.ifa-5A, identifies novel candidate genes. Molecular Plant Pathology **14**, 772–785.

Sievers F, Wilm A, Dineen D, *et al.* 2011. Fast, scalable generation of high-quality protein multiple sequence alignments using Clustal Omega. Molecular Systems Biology **7**.

Solovyev V, Kosarev P, Seledsov I, Vorobyev D. 2006. Automatic annotation of eukaryotic genes, pseudogenes and promoters. Genome biology **7 Suppl 1**, S10.1-12.

Sudisha J, Sharathchandra RG, Amruthesh KN, Kumar A, Shetty HS. 2012. Plant Defence: Biological Control. , 379–403.

Sun J-Y, Gaudet DA, Lu Z-X, Frick M, Puchalski B, Laroche A. 2008. Characterization and Antifungal Properties of Wheat Nonspecific Lipid Transfer Proteins. Molecular Plant-Microbe Interactions **21**, 346–360.

Tucker EJ, Baumann U, Kouidri A, *et al.* 2017. Molecular identification of the wheat male fertility gene Ms1 and its prospects for hybrid breeding. Nature Communications **8**, 869.

Voorrips RE. 2002. MapChart: Software for the Graphical Presentation of Linkage Maps and QTLs. Journal of Heredity **93**, 77–78.

Wang P, Cheng T, Lu M, Liu G, Li M, Shi J, Lu Y, Laux T, Chen J. 2016. Expansion and Functional Divergence of AP2 Group Genes in Spermatophytes Determined by Molecular Evolution and Arabidopsis Mutant Analysis. Frontiers in Plant Science **7**, 1–15.

Wang Z, Li J, Chen S, *et al.* 2017. Poaceae-specific *MS1* encodes a phospholipid-binding protein for male fertility in bread wheat. Proceedings of the National Academy of Sciences, 201715570.

Wang D, Zhang Y, Zhang Z, Zhu J, Yu J. 2010. KaKs_Calculator 2.0: A Toolkit Incorporating

Gamma-Series Methods and Sliding Window Strategies. Genomics, Proteomics and Bioinformatics **8**, 77–80.

Waterhouse AM, Procter JB, Martin DMA, Clamp M, Barton GJ. 2009. Jalview Version 2-A multiple sequence alignment editor and analysis workbench. Bioinformatics **25**, 1189–1191.

Wei K, Zhong X. 2014. Non-specific lipid transfer proteins in maize. BMC plant biology **14**, 281.

Whitford R, Fleury D, Reif JC, Garcia M, Okada T, Korzun V, Langridge P. 2013. Hybrid breeding in wheat: technologies to improve hybrid wheat seed production. Journal of experimental botany **64**, 5411–28.

Wu Y, Fox TW, Trimnell MR, Wang L, Xu R, Cigan a. M, Huffman G a., Garnaat CW, Hershey H, Albertsen MC. 2015. Development of a novel recessive genetic male sterility system for hybrid seed production in maize and other cross-pollinating crops. Plant Biotechnology Journal, n/a-n/a.

Xia C, Zhang L, Zou C, *et al.* 2017. A TRIM insertion in the promoter of Ms2 causes male sterility in wheat. Nature Communications **8**, 1–9.

Yang Z, Peng Z, Wei S, Liao M, Yu Y, Jang Z. 2015. Pistillody mutant reveals key insights into stamen and pistil development in wheat (Triticum aestivum L.). BMC Genomics **16**, 1–11.

Zhang D, Liang W, Yin C, Zong J, Gu F, Zhang D. 2010. OsC6, encoding a lipid transfer protein, is required for postmeiotic anther development in rice. Plant physiology **154**, 149–62.

Zhou DX. 1999. Regulatory mechanism of plant gene transcription by GT-elements and GT-factors. Trends in Plant Science **4**, 210–214.

4.7 Declarations

4.7.1 Acknowledgments

We are grateful for the support provided by DuPont Pioneer Hi-Bred International Inc. and the University of Adelaide. We thank, Juan Carlos Sanchez and Mathieu Baes for project advice, Dr. Nathan S. Watson-Haigh for his bioinformatics assistance, Yuan Li for technical assistance for the qRT-PCR experiments and, Margaret Pallotta and Dr. Takashi Okada for critical discussions and reading of the manuscript.

4.7.2 Author contributions

Conceived and designed the research: AK, RW and UB. Computational analysis and data collection: AK, EK, RS and UB. Contributed to the qRT-PCR experiments: AK. Analysed the data: AK, RW and UB. Manuscript preparation and editing: AK, RW, RS, EK and UB.

4.7.3 Additional Information

Competing Interests: The authors declare no competing interests.
Data availability: The datasets generated during and/or analysed during the current study are available from the corresponding author on reasonable request.

4.8 Additional files

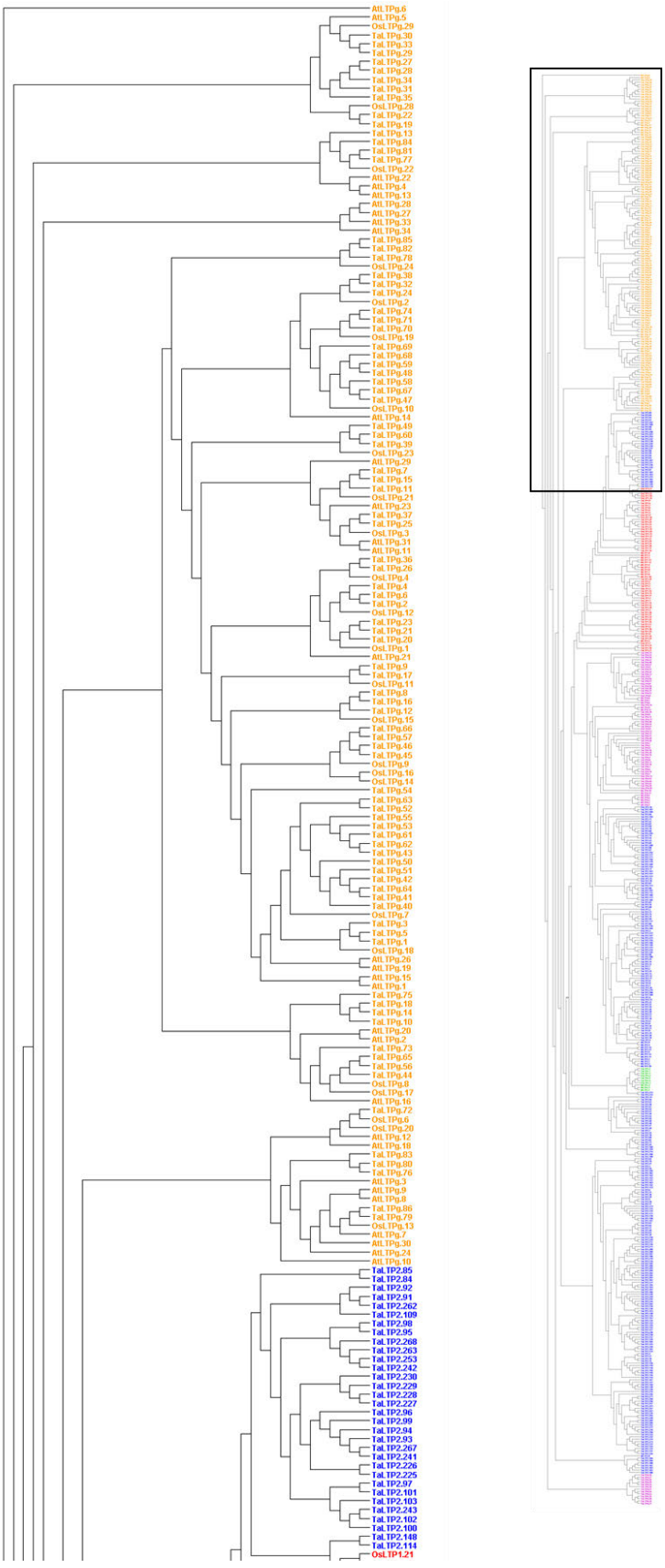

Figure S1 (1/4) |Phylogenetic relationship of the wheat, rice and *A.thaliana* nsLTP proteins.

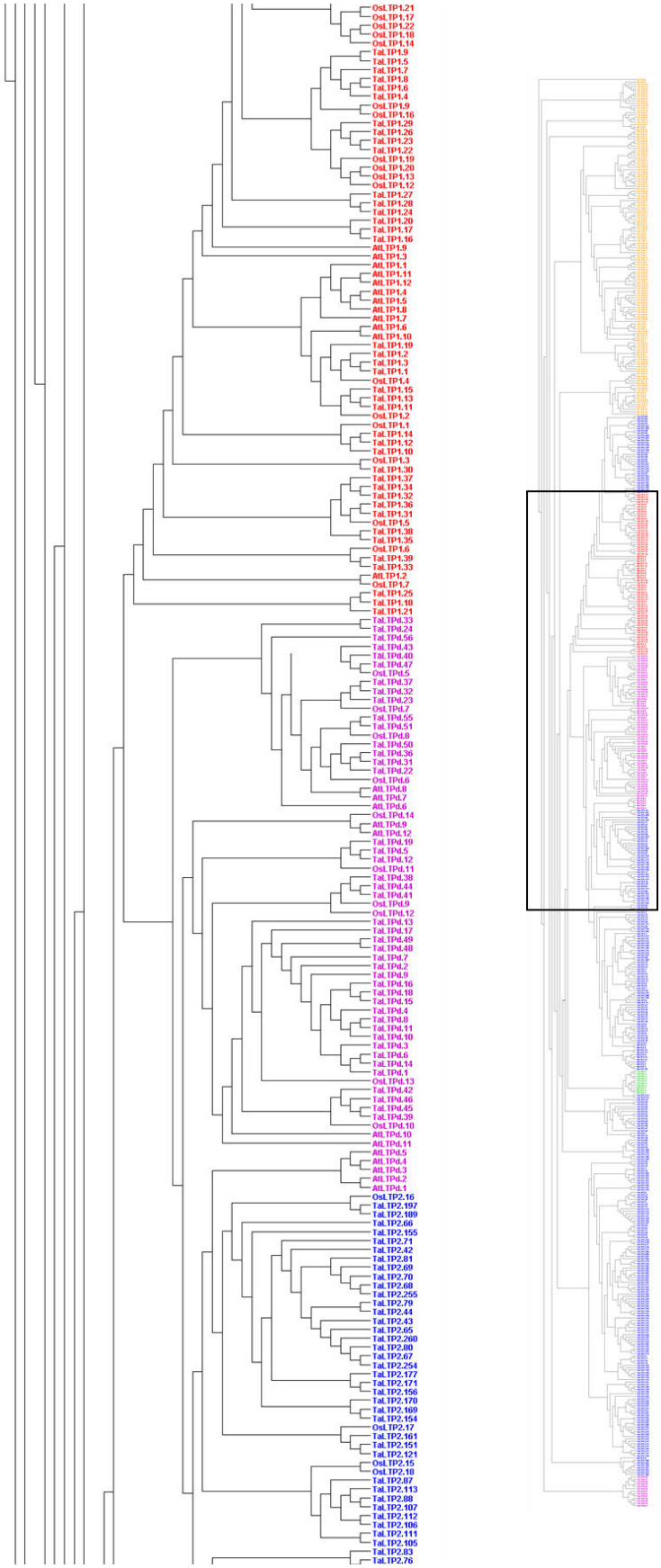

Figure S1 (2/4) |Phylogenetic relationship of the wheat, rice and *A.thaliana* nsLTP proteins.

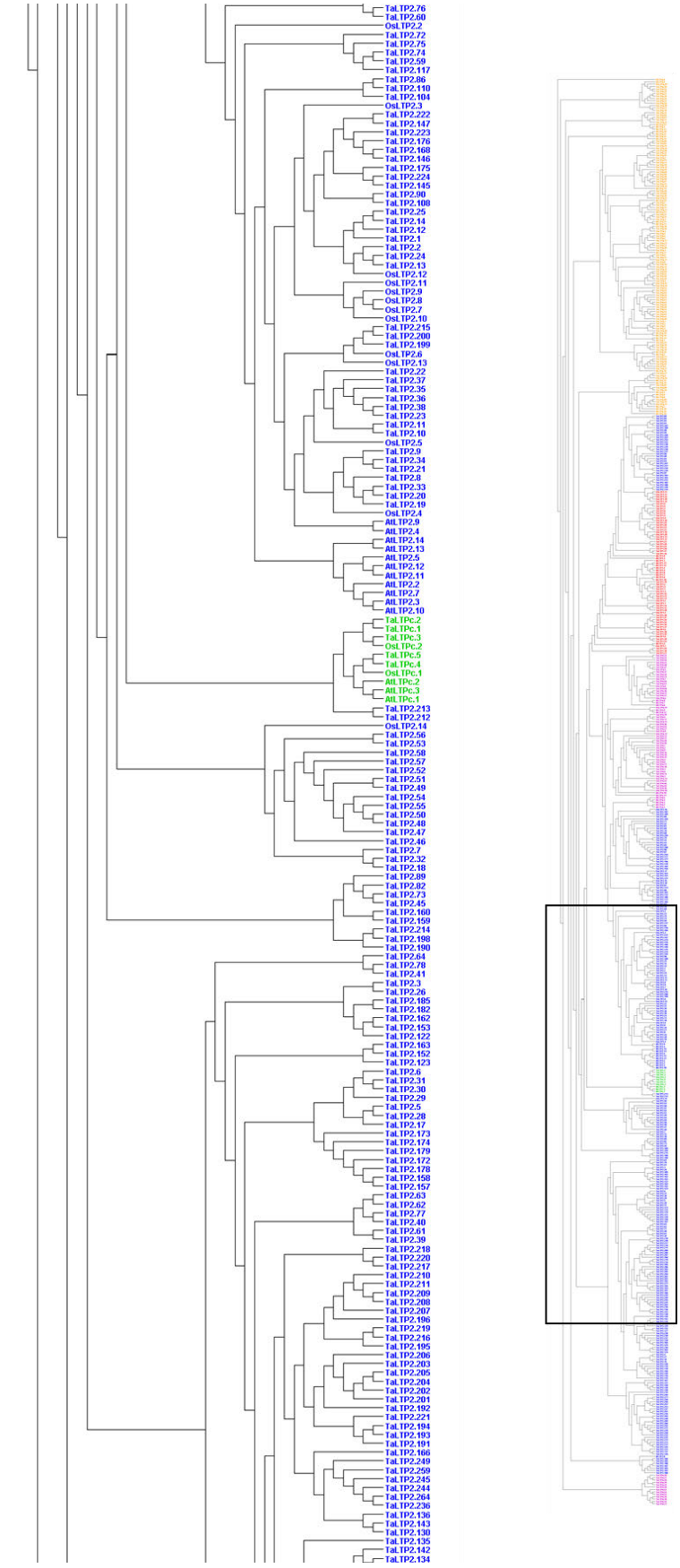

Figure S1 (3/4) | Phylogenetic relationship of the wheat, rice and *A.thaliana* nsLTP proteins.

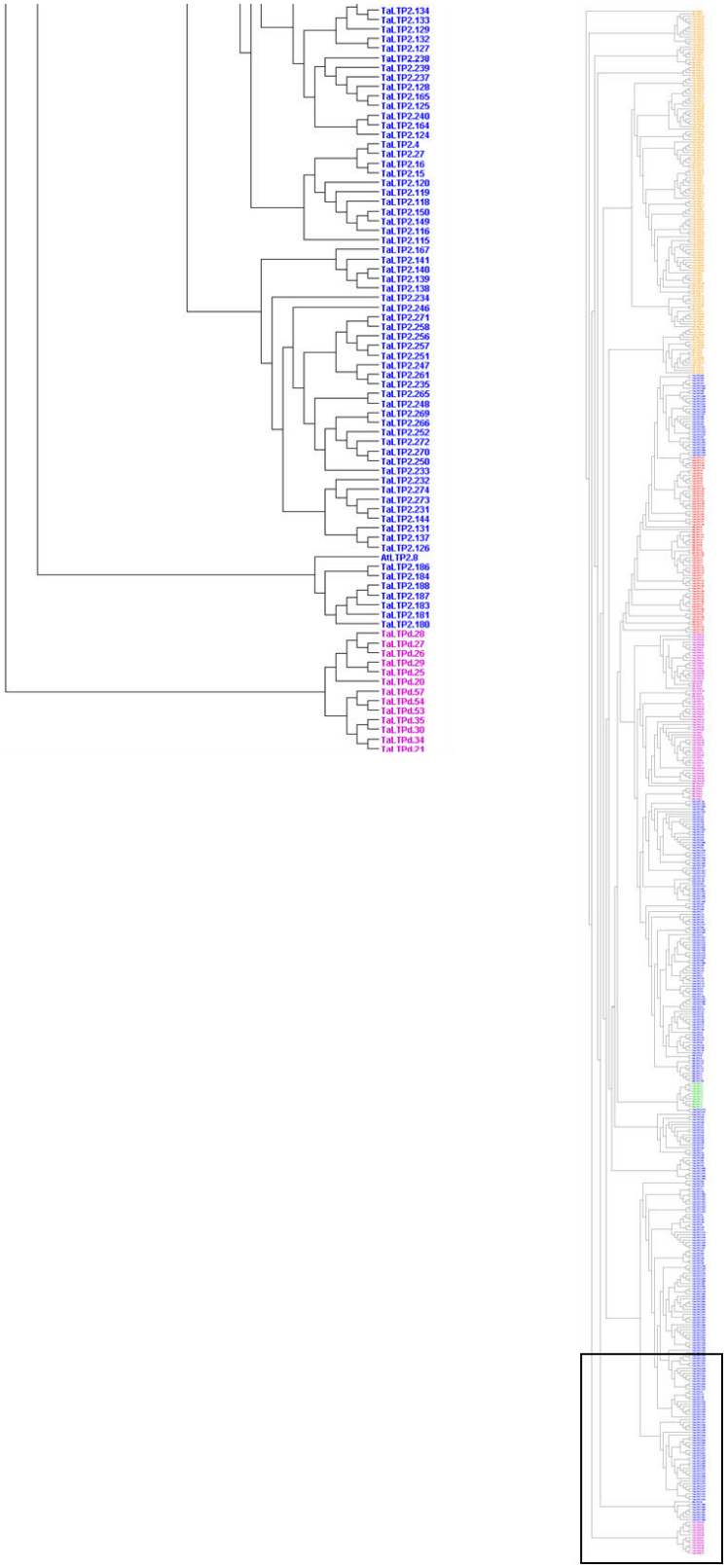

Figure S1 (4/4) | Phylogenetic relationship of the wheat, rice and A.thaliana nsLTP proteins. Unrooted phylogenetic tree of nsLTPs mature protein sequences from Wheat (TaLTP), Rice (OsLTP) and Arabidopsis (AtLTP). Red, Type 1; Blue, Type 2; Green, Type C; Purple, Type D; Type G, Orange.

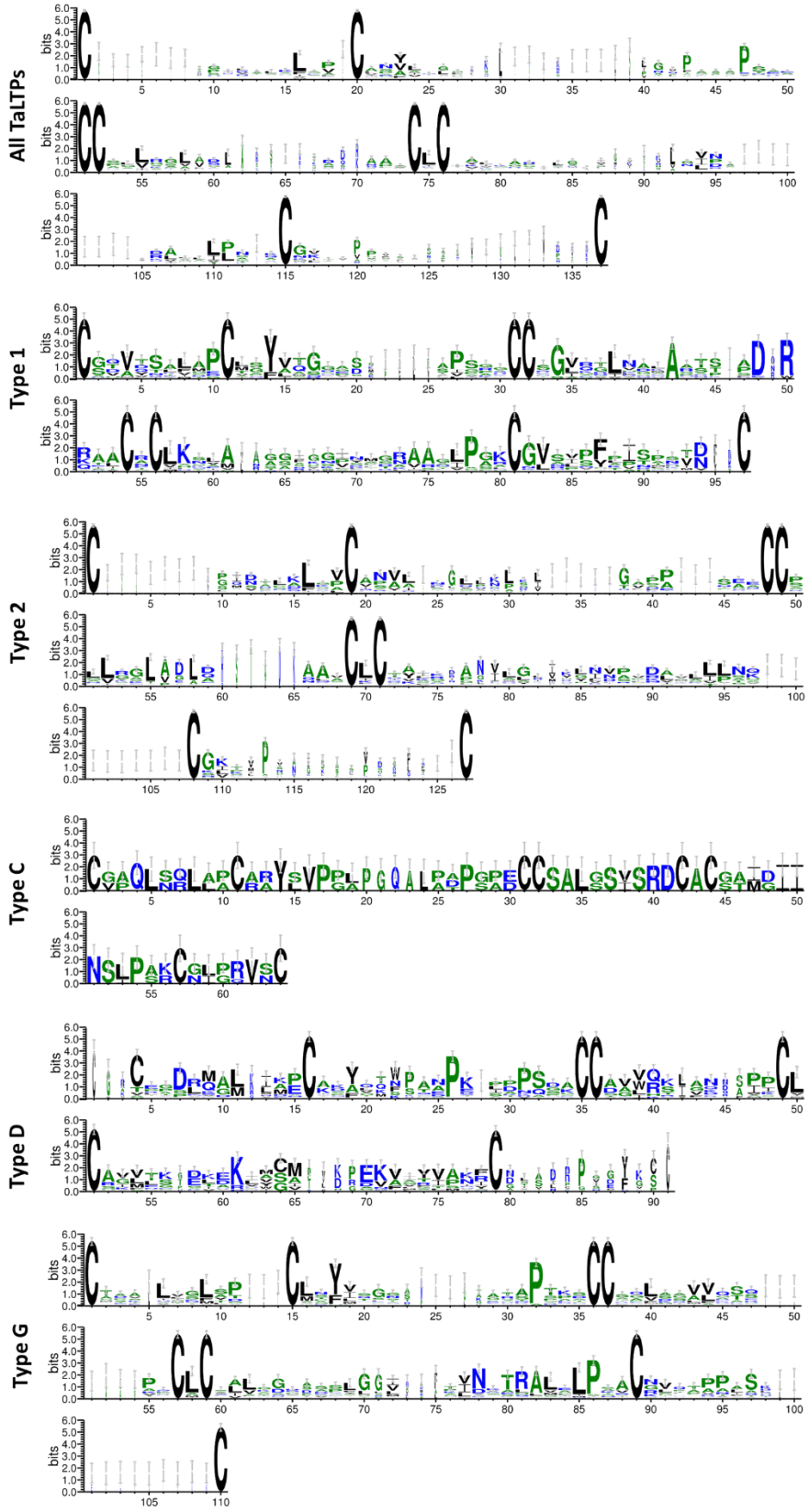

Figure S2 | Conserved domai analysis of the nsLTPs using the WebLogo3 program. The height of the letter designating the amino acid residue at each position represents the degree of conservation. The numbers on the x-axis represent the sequence positions in the corresponding conserved domains. The y-axis represents the information content measured in bits.

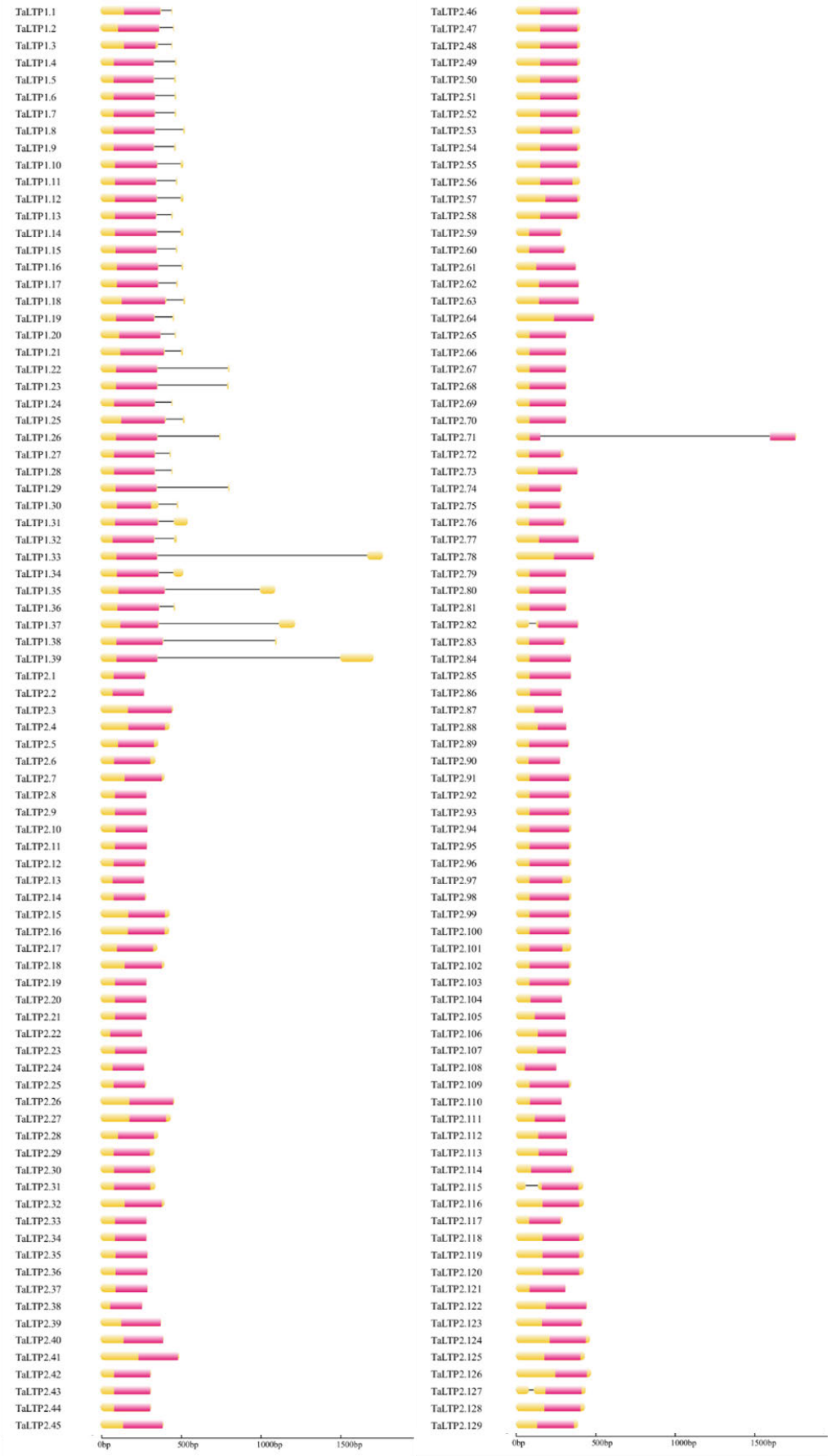

Figure S3 (1/3) | Gene structures of the Wheat nsLTP genes.

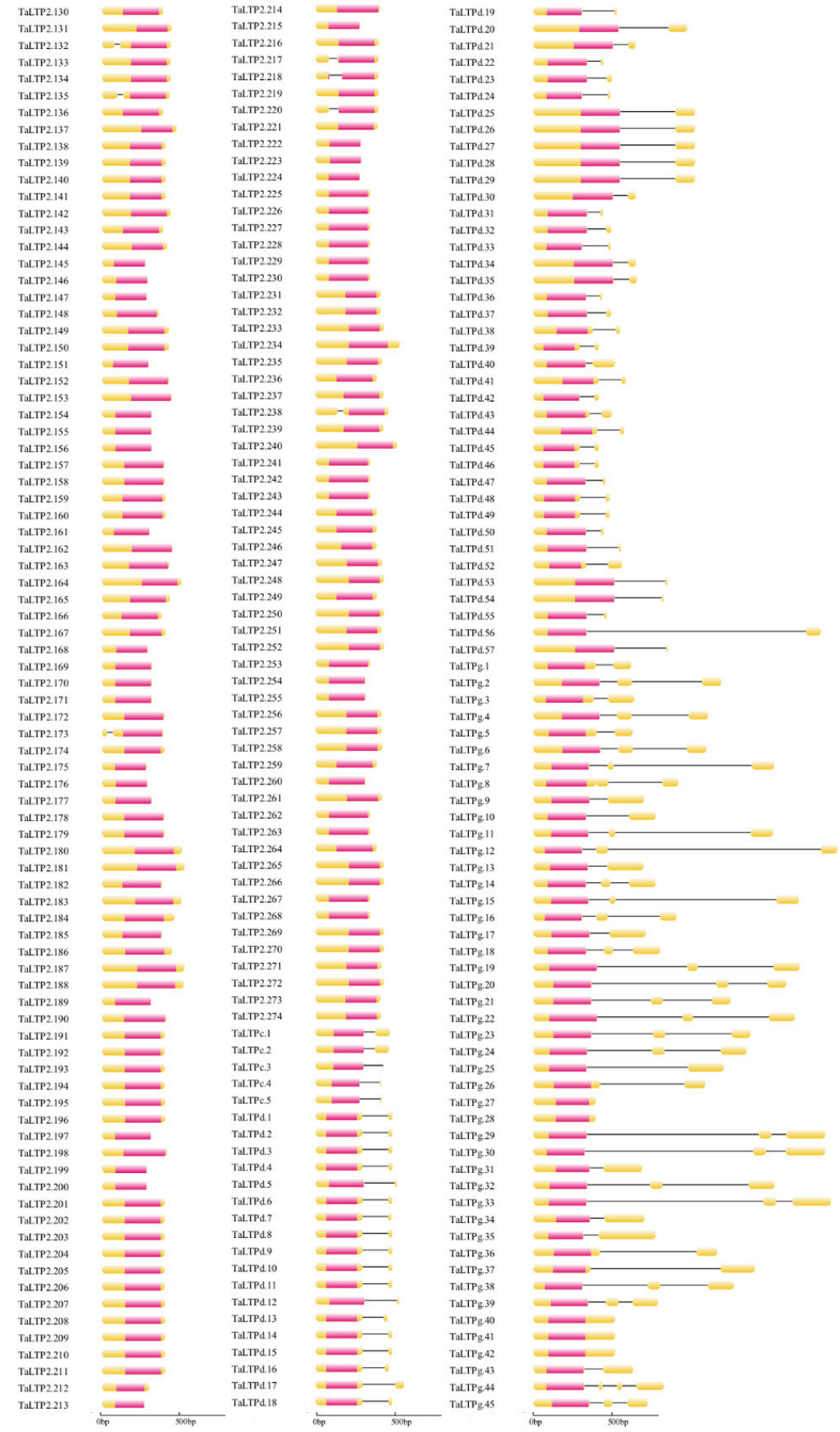

Figure S3 (2/3) | Gene structures of the Wheat nsLTP genes.

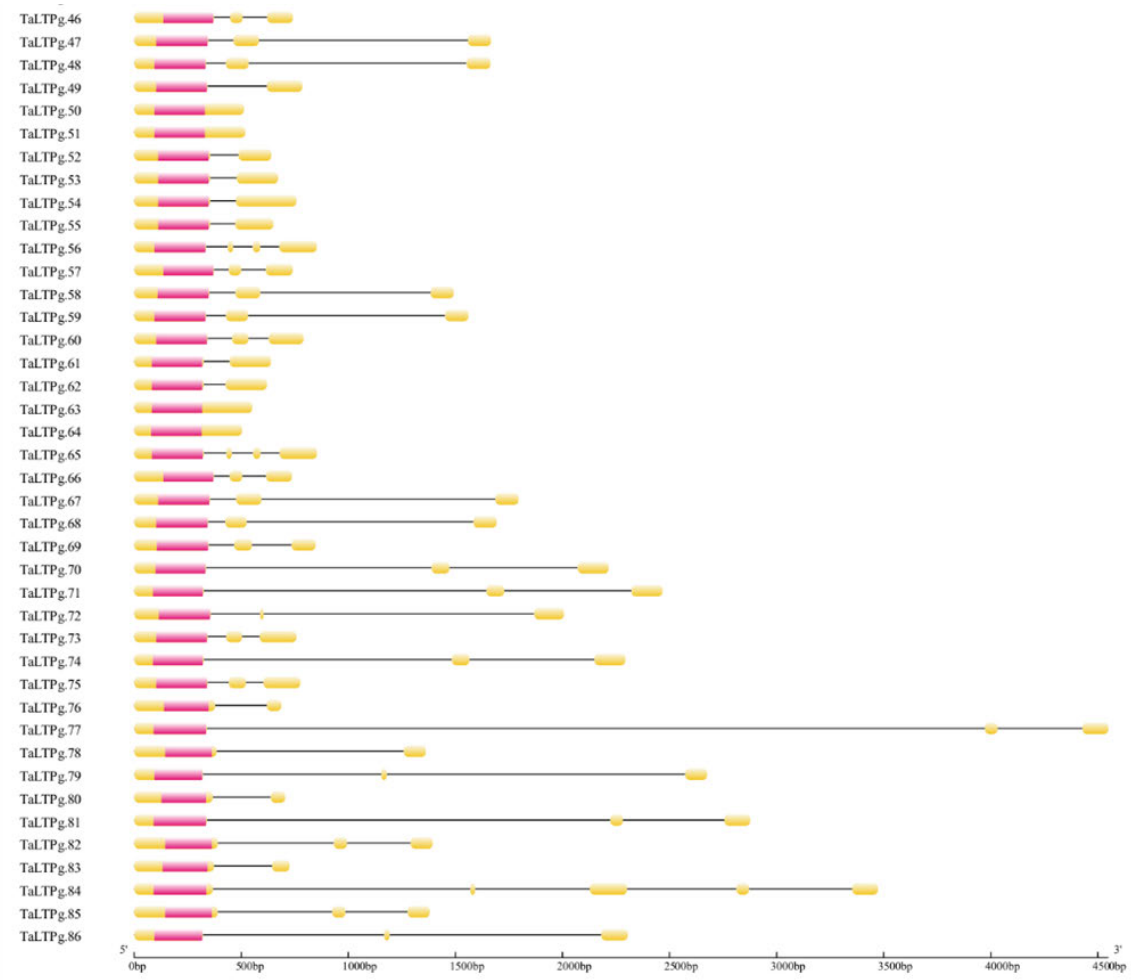

Figure S3 (3/3) | Gene structures of the Wheat nsLTP genes. The size of the each motif can be estimated using the scale at the bottom. Genes structures of nsLTPs were predicted with the GSDS software. The exons are indicated by yellow boxes, 8CM by pink boxes ans the introns are indicated by black lines.

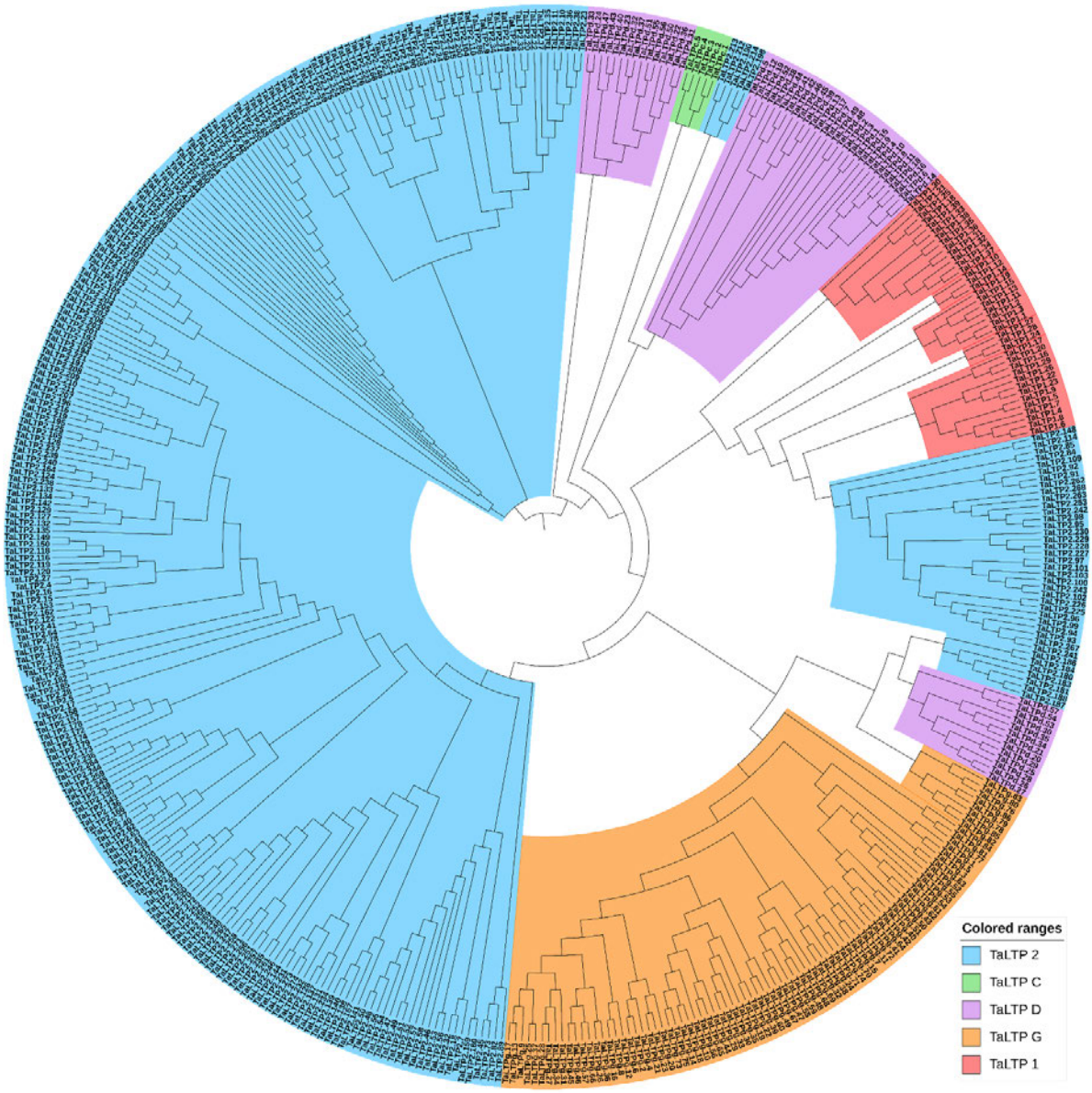

Figure S4 |Unrooted phylogenetic tree of the wheat nsLTPs gene family. The evolutionary distances were computed using the Poisson correction method (Zuckerkandl and Pauling, 1965). The analysis involved 461 amino acid sequences of the predicted mature proteins. All positions containing gaps and missing data were eliminated. There were a total of 24 positions in the final dataset. Evolutionary analyses were conducted in MEGA7 (Kumar *et al.,* 2017).

Table S1 | The locations of Non-specific Lipid Transfer Proteins in wheat IWGSC Ref 1.0, and their protein features.

		Position				Signal peptide	Mature protein		
Name	Chromosome	Start	End	Strand	8CM pattern[1]	AA[2]	AA	Mw[3]	pI[4]
TaLTP1.1	chr1A	495284357	495284829	1	M-38-C-9-C-13-CC-19-C-1-C-23-C-13-C-3	37	92	9.31	10.96
TaLTP1.2	chr1B	533406182	533406642	1	M-35-C-9-C-13-CC-19-C-1-C-23-C-13-C-3	34	92	9.41	11.51
TaLTP1.3	chr1D	398044523	398048444	1	M-32-C-9-C-13-CC-19-C-1-C-23-C-13-C-3	31	92	9.31	10.96
TaLTP1.4	chr2A	716544323	716544799	-1	M-26-C-9-C-14-CC-19-C-1-C-20-C-13-C-4	20	96	9.43	9.99
TaLTP1.5	chr2A	716549208	716549949	-1	M-26-C-9-C-14-CC-19-C-1-C-20-C-13-C-4	25	91	8.98	10.64
TaLTP1.6	chr2B	695928027	695928501	-1	M-26-C-9-C-14-CC-19-C-1-C-22-C-13-C-4	20	98	9.73	9.99
TaLTP1.7	chr2B	695992511	695992985	-1	M-26-C-9-C-14-CC-19-C-1-C-22-C-13-C-4	25	93	9.23	10.43
TaLTP1.8	chr2B	696080662	696081190	-1	M-26-C-9-C-14-CC-19-C-1-C-22-C-13-C-4	20	98	9.68	10.28
TaLTP1.9	chr2D	579060097	579065485	-1	M-26-C-9-C-14-CC-19-C-1-C-20-C-13-C-4	25	91	8.90	10.38
TaLTP1.10	chr3A	126035274	126035793	1	M-29-C-9-C-15CC-19-C-1-C-23-C-13-C-7	28	98	9.86	4.36
TaLTP1.11	chr3A	594349103	594349584	-1	M-29-C-9-C-13-CC-19-C-1-C-23-C-13-C-4	29	92	9.56	9.87
TaLTP1.12	chr3B	171701364	171701884	1	M-29-C-9-C-15-CC-19-C-1-C-22-C-13-C-7	28	97	9.80	4.36
TaLTP1.13	chr3B	592867387	592867840	-1	M-29-C-9-C-13-CC-19-C-1-C-23-C-13-C-4	29	92	9.56	9.87
TaLTP1.14	chr3D	119404001	119404521	1	M-29-C-9-C-15-CC-19-C-1-C-22-C-13-C-7	28	97	9.84	4.36
TaLTP1.15	chr3D	451234522	451235003	-1	M-30-C-9-C-13-CC-19-C-1-C-23-C-13-C-4	29	93	9.63	9.87
TaLTP1.16	chr4A	476145519	476146036	-1	M-33-C-9-C-14-CC-19-C-1-C-22-C-13-C-4	31	94	9.32	10.45
TaLTP1.17	chr4B	142541428	142541912	1	M-33-C-9-C-14-CC-19-C-1-C-22-C-13-C-4	31	94	9.39	10.44
TaLTP1.18	chr4B	642168978	642169391	1	M-43-C-9-C-19-CC-20-C-1-C-21-C-13-C-2	32	106	10.67	6.52
TaLTP1.19	chr4B	661641797	661642258	1	M-31-C-9-C-13-CC-19-C-1-C-23-C-7-C-4	30	87	9.06	11.43
TaLTP1.20	chr4D	100319858	100320221	1	M-33-C-9-C-14-CC-19-C-1-C-22-C-13-C-20	31	110	11.22	9.01
TaLTP1.21	chr4D	499312458	499312937	1	M-40-C-9-C-19-CC-20-C-1-C-21-C-13-C-27	31	129	13.50	6.64
TaLTP1.22	chr5A	324403095	324403903	-1	M-31-C-9-C-14-CC-19-C-1-C-22-C-13-C-4	30	93	9.48	10.45
TaLTP1.23	chr5A	324479786	324480589	-1	M-31-C-9-C-14-CC-19-C-1-C-22-C-13-C-4	30	93	9.48	10.45
TaLTP1.24	chr5A	325184136	325184588	-1	M-27-C-9-C-13-CC-19-C-1-C-22-C-13-C-3	27	90	9.67	9.23
TaLTP1.25	chr5A	680105615	680106025	1	M-42-C-9-C-19-CC-20-C-1-C-21-C-13-C-2	31	106	10.83	8.27
TaLTP1.26	chr5B	273147041	273147794	-1	M-31-C-9-C-14-CC-19-C-1-C-22-C-13-C-4	30	93	9.48	10.75
TaLTP1.27	chr5B	273458906	273459346	-1	M-27-C-9-C-13-CC-19-C-1-C-22-C-13-C-3	27	90	9.61	9.4
TaLTP1.28	chr5D	231788218	231788670	1	M-27-C-9-C-13-CC-19-C-1-C-22-C-13-C-3	27	90	9.48	7.1
TaLTP1.29	chr5D	232011275	232012084	1	M-30-C-9-C-14-CC-19-C-1-C-22-C-13-C-4	30	92	9.47	10.29
TaLTP1.30	chr5D	515641574	515642061	-1	M-33-C-9-C-15-CC-19-C-1-C-21-C-13-C-4	24	101	10.16	9.94
TaLTP1.31	chr7A	73746568	73747115	1	M-29-C-9-C-14-CC-19-C-1-C-24-C-14-C-32	25	127	13.24	4.32
TaLTP1.32	chr7A	74132167	74132646	1	M-24-C-9-C-14-CC-19-C-1-C-22-C-14-C-7	20	100	10.84	9.68
TaLTP1.33	chr7A	508650558	508650920	1	M-32-C-9-C-14-CC-19-C-1-C-21-C-13-C-34	29	124	12.94	4.07
TaLTP1.34	chr7B	8917078	8917597	-1	M-33-C-9-C-14-CC-19-C-1-C-22-C-14-C-22	29	115	12.60	9.22
TaLTP1.35	chr7B	8927933	8929029	-1	M-36-C-9-C-19-CC-21-C-1-C-24-C-15-C-33	32	136	14.52	9.39
TaLTP1.36	chr7B	8988470	8988937	-1	M-34-C-9-C-14-CC-19-C-1-C-22-C-14-C-4	30	97	9.86	3.91
TaLTP1.37	chr7D	66817216	66818437	-1	M-33-C-9-C-14-CC-19-C-1-C-22-C-14-C-35	29	128	13.90	9.69
TaLTP1.38	chr7D	66832500	66833605	-1	M-32-C-9-C-19-CC-21-C-1-C-24-C-15-C-4	25	110	12.10	5.8
TaLTP1.39	chr7D	424643201	424644915	-1	M-32-C-9-C-14-CC-19-C-1-C-21-C-13-C-71	29	161	16.86	4.49
TaLTP2.1	chr1A	313006783	313007070	-1	M-26-C-7-C-13-CC-8-C-1-C-23-C-6-C-2	26	70	7.14	9.6

TaLTP2.2	chr1A	313161875	313162150	-1	M-24-C-7-C-13-CC-8-C-1-C-23-C-6-C-0	25	67	7.06	11.17
TaLTP2.3	chr1A	372241197	372241652	-1	M-56-C-9-C-27-CC-13-C-1-C-25-C-9-C-2	33	119	11.59	8.91
TaLTP2.4	chr1A	372287159	372287593	-1	M-57-C-9-C-19-CC-13-C-1-C-24-C-3-C-9	21	124	12.68	8
TaLTP2.5	chr1A	372467568	372467930	-1	M-35-C-9-C-18-CC-13-C-1-C-24-C-3-C-8	20	101	10.58	7.77
TaLTP2.6	chr1A	518682557	518682901	-1	M-27-C-9-C-18-CC-13-C-1-C-24-C-3-C-10	22	93	9.83	8.13
TaLTP2.7	chr1A	526923822	526924223	1	M-49-C-10-C-15-CC-11-C-1-C-24-C-9-C-5	32	102	11.09	8.51
TaLTP2.8	chr1A	549637965	549638255	1	M-29-C-7-C-13-CC-8-C-1-C-23-C-6-C-0	29	68	7.09	9.78
TaLTP2.9	chr1A	549666495	549666785	1	M-29-C-7-C-13-CC-8-C-1-C-23-C-6-C-0	29	68	7.07	10.12
TaLTP2.10	chr1A	549670654	549670950	1	M-30-C-7-C-13-CC-9-C-1-C-23-C-6-C-0	30	69	7.19	10.58
TaLTP2.11	chr1A	549695442	549695735	1	M-29-C-7-C-13-CC-9-C-1-C-23-C-6-C-0	29	69	7.19	10.58
TaLTP2.12	chr1B	338430229	338430516	-1	M-26-C-7-C-13-CC-8-C-1-C-23-C-6-C-2	26	70	7.10	9.23
TaLTP2.13	chr1B	339364373	339364648	-1	M-24-C-7-C-13-CC-8-C-1-C-23-C-6-C-0	25	67	6.98	10.71
TaLTP2.14	chr1B	340367218	340367505	1	M-26-C-7-C-13-CC-8-C-1-C-23-C-6-C-2	26	70	7.11	8.3
TaLTP2.15	chr1B	401763150	401763584	-1	M-57-C-9-C-19-CC-13-C-1-C-24-C-3-C-9	21	124	12.71	9.03
TaLTP2.16	chr1B	401991935	401992366	-1	M-56-C-9-C-19-CC-13-C-1-C-24-C-3-C-9	21	123	12.61	9.03
TaLTP2.17	chr1B	402050747	402051103	-1	M-33-C-9-C-18-CC-13-C-1-C-24-C-3-C-8	20	99	10.41	7.77
TaLTP2.18	chr1B	580543508	580543909	1	M-49-C-10-C-15-CC-11-C-1-C-24-C-9-C-5	32	102	10.66	6.28
TaLTP2.19	chr1B	626506996	626507286	-1	M-29-C-7-C-13-CC-8-C-1-C-23-C-6-C-0	29	68	7.11	9.53
TaLTP2.20	chr1B	626595085	626595375	1	M-29-C-7-C-13-CC-8-C-1-C-23-C-6-C-0	29	68	7.11	9.78
TaLTP2.21	chr1B	626601013	626601303	1	M-29-C-7-C-13-CC-8-C-1-C-23-C-6-C-0	29	68	7.08	10.38
TaLTP2.22	chr1B	626610333	626610596	1	M-19-C-7-C-13-CC-9-C-1-C-23-C-6-C-0	19	69	7.27	10.86
TaLTP2.23	chr1B	626649118	626649411	1	M-29-C-7-C-13-CC-9-C-1-C-23-C-6-C-0	29	69	7.26	10.86
TaLTP2.24	chr1D	234528369	234528644	1	M-24-C-7-C-13-CC-8-C-1-C-23-C-6-C-0	25	67	6.99	11.2
TaLTP2.25	chr1D	234656387	234656674	1	M-26-C-7-C-13-CC-8-C-1-C-23-C-6-C-2	26	70	7.12	8.3
TaLTP2.26	chr1D	298573883	298574347	-1	M-59-C-9-C-27-CC-13-C-1-C-25-C-9-C-2	34	121	11.82	8.14
TaLTP2.27	chr1D	298603863	298604303	-1	M-59-C-9-C-19-CC-13-C-1-C-24-C-3-C-9	21	126	12.76	8
TaLTP2.28	chr1D	298619764	298620126	-1	M-35-C-9-C-18-CC-13-C-1-C-24-C-3-C-8	20	101	10.58	7.77
TaLTP2.29	chr1D	298635624	298635962	1	M-26-C-9-C-18-CC-13-C-1-C-24-C-3-C-9	22	91	9.73	7.14
TaLTP2.30	chr1D	422736634	422736978	-1	M-27-C-9-C-18-CC-13-C-1-C-24-C-3-C-10	22	93	9.97	8.15
TaLTP2.31	chr1D	422819751	422820095	-1	M-27-C-9-C-18-CC-13-C-1-C-24-C-3-C-10	22	93	9.94	8.14
TaLTP2.32	chr1D	429506893	429507294	1	M-49-C-10-C-15-CC-11-C-1-C-24-C-9-C-5	32	102	10.69	5.34
TaLTP2.33	chr1D	456132463	456132753	1	M-29-C-7-C-13-CC-8-C-1-C-23-C-6-C-0	29	68	7.12	9.78
TaLTP2.34	chr1D	456199792	456200082	1	M-29-C-7-C-13-CC-8-C-1-C-23-C-6-C-0	29	68	7.08	10.38
TaLTP2.35	chr1D	456203134	456203430	1	M-30-C-7-C-13-CC-9-C-1-C-23-C-6-C-0	30	69	7.27	10.86
TaLTP2.36	chr1D	456251729	456252025	1	M-30-C-7-C-13-CC-9-C-1-C-23-C-6-C-0	30	69	7.28	10.86
TaLTP2.37	chr1D	457033363	457033659	1	M-30-C-7-C-13-CC-9-C-1-C-23-C-6-C-0	30	69	7.26	10.86
TaLTP2.38	chr1D	457044170	457044433	1	M-19-C-7-C-13-CC-9-C-1-C-23-C-6-C-0	19	69	7.26	10.86
TaLTP2.39	chr2A	669567532	669567912	-1	M-42-C-9-C-18-CC-13-C-1-C-25-C-9-C-0	24	103	10.60	9.14
TaLTP2.40	chr2A	669619546	669619941	-1	M-47-C-9-C-18-CC-13-C-1-C-25-C-9-C-0	24	108	10.99	9.59
TaLTP2.41	chr2A	678831247	678831741	-1	M-78-C-9-C-19-CC-13-C-1-C-24-C-9-C-2	23	142	14.17	8.92
TaLTP2.42	chr2A	691116103	691116420	1	M-27-C-9-C-16-CC-9-C-1-C-26-C-7-C-1	28	78	8.20	9.78
TaLTP2.43	chr2A	691140275	691140592	1	M-27-C-9-C-16-CC-9-C-1-C-26-C-7-C-1	28	78	8.31	9.23
TaLTP2.44	chr2A	691169089	691169406	1	M-27-C-9-C-16-CC-9-C-1-C-26-C-7-C-1	28	78	8.33	8.32
TaLTP2.45	chr2A	741373075	741373470	1	M-46-C-9-C-18-CC-13-C-1-C-25-C-9-C-1	24	108	10.68	4.73
TaLTP2.46	chr2A	747697212	747697613	-1	M-49-C-10-C-15-CC-11-C-1-C-24-C-9-C-5	32	102	11.06	9.6
TaLTP2.47	chr2A	747723957	747724358	-1	M-49-C-10-C-15-CC-11-C-1-C-24-C-9-C-5	32	102	11.00	9.81

TaLTP2.48	chr2A	747727094	747727495	-1	M-49-C-10-C-15-CC-11-C-1-C-24-C-9-C-5	32	102	11.00	9.81
TaLTP2.49	chr2A	747730232	747730633	-1	M-49-C-10-C-15-CC-11-C-1-C-24-C-9-C-5	32	102	10.98	9.81
TaLTP2.50	chr2A	747733420	747733821	-1	M-49-C-10-C-15-CC-11-C-1-C-24-C-9-C-5	32	102	11.00	9.81
TaLTP2.51	chr2A	747739744	747740145	-1	M-49-C-10-C-15-CC-11-C-1-C-24-C-9-C-5	32	102	10.98	9.81
TaLTP2.52	chr2A	747742933	747743334	-1	M-49-C-10-C-15-CC-11-C-1-C-24-C-9-C-5	32	102	11.01	10.14
TaLTP2.53	chr2A	747773829	747774230	-1	M-49-C-10-C-15-CC-11-C-1-C-8-C-15-C-15	32	102	11.18	7.01
TaLTP2.54	chr2A	747777016	747777417	-1	M-49-C-10-C-15-CC-11-C-1-C-24-C-9-C-5	32	102	10.98	9.81
TaLTP2.55	chr2A	747780203	747780604	-1	M-49-C-10-C-15-CC-11-C-1-C-24-C-9-C-5	32	102	11.00	9.81
TaLTP2.56	chr2A	747809997	747810398	-1	M-49-C-10-C-15-CC-11-C-1-C-8-C-15-C-15	32	102	11.19	7.01
TaLTP2.57	chr2A	747819511	747819912	-1	M-60-C-3-C-11-CC-11-C-1-C-24-C-9-C-5	32	102	10.96	9.74
TaLTP2.58	chr2A	747874783	747875184	-1	M-49-C-10-C-15-CC-11-C-1-C-24-C-9-C-5	32	102	11.12	9.69
TaLTP2.59	chr2A	749626244	749626534	-1	M-26-C-7-C-13-CC-8-C-1-C-23-C-6-C-3	25	72	8.03	5.62
TaLTP2.60	chr2A	749855016	749855327	-1	M-26-C-9-C-15-CC-10-C-1-C-23-C-7-C-3	24	80	8.87	8.24
TaLTP2.61	chr2B	618873204	618873581	-1	M-41-C-9-C-18-CC-13-C-1-C-25-C-9-C-0	18	108	11.11	9.39
TaLTP2.62	chr2B	618968168	618968563	-1	M-47-C-9-C-18-CC-13-C-1-C-25-C-9-C-0	24	108	11.14	9.59
TaLTP2.63	chr2B	619044574	619044969	-1	M-47-C-9-C-18-CC-13-C-1-C-25-C-9-C-0	24	108	11.15	9.89
TaLTP2.64	chr2B	637444754	637445248	-1	M-78-C-9-C-19-CC-13-C-1-C-24-C-9-C-2	23	142	14.21	8.92
TaLTP2.65	chr2B	654545867	654546184	-1	M-27-C-9-C-16-CC-9-C-1-C-26-C-7-C-1	28	78	8.31	9.6
TaLTP2.66	chr2B	654588167	654588484	-1	M-27-C-9-C-16-CC-9-C-1-C-26-C-7-C-1	28	78	8.53	6.77
TaLTP2.67	chr2B	654648916	654649233	-1	M-27-C-9-C-16-CC-9-C-1-C-26-C-7-C-1	28	78	8.24	9.52
TaLTP2.68	chr2B	654652893	654653210	-1	M-27-C-9-C-16-CC-9-C-1-C-26-C-7-C-1	28	78	8.29	9.78
TaLTP2.69	chr2B	654681164	654681481	-1	M-27-C-9-C-16-CC-9-C-1-C-26-C-7-C-1	28	78	8.32	9.78
TaLTP2.70	chr2B	654702996	654703313	-1	M-27-C-9-C-16-CC-9-C-1-C-26-C-7-C-1	28	78	8.29	9.78
TaLTP2.71	chr2B	654730472	654732231	-1	M-27-C-9-C-16-CC-9-C-1-C-26-C-7-C-1	28	78	8.38	9.78
TaLTP2.72	chr2B	732839527	732839826	-1	M-26-C-7-C-13-CC-8-C-1-C-23-C-6-C-6	24	76	8.30	9.63
TaLTP2.73	chr2B	743695125	743695514	1	M-44-C-9-C-18-CC-13-C-1-C-25-C-9-C-1	26	104	10.41	4.94
TaLTP2.74	chr2B	755158846	755159136	-1	M-26-C-7-C-13-CC-8-C-1-C-23-C-6-C-3	25	72	7.95	8.29
TaLTP2.75	chr2B	755404195	755404482	-1	M-26-C-7-C-13-CC-8-C-1-C-23-C-5-C-3	25	71	8.15	5.73
TaLTP2.76	chr2B	756156764	756157078	-1	M-26-C-9-C-15-CC-10-C-1-C-23-C-7-C-4	22	83	9.22	6.09
TaLTP2.77	chr2D	524002804	524003199	-1	M-47-C-9-C-18-CC-13-C-1-C-25-C-9-C-0	24	108	11.08	9.59
TaLTP2.78	chr2D	535751756	535752250	-1	M-78-C-9-C-19-CC-13-C-1-C-24-C-9-C-2	23	142	14.23	9.16
TaLTP2.79	chr2D	547774709	547775026	-1	M-27-C-9-C-16-CC-9-C-1-C-26-C-7-C-1	28	78	8.25	9.31
TaLTP2.80	chr2D	547790937	547791254	-1	M-27-C-9-C-16-CC-9-C-1-C-26-C-7-C-1	28	78	8.25	9.52
TaLTP2.81	chr2D	547806114	547806431	-1	M-27-C-9-C-16-CC-9-C-1-C-26-C-7-C-1	28	78	8.32	9.78
TaLTP2.82	chr2D	609425079	609425471	1	M-31-C-9-C-18-CC-13-C-1-C-25-C-9-C-1	24	93	9.17	4.06
TaLTP2.83	chr2D	618868170	618868481	-1	M-26-C-9-C-15-CC-10-C-1-C-23-C-7-C-3	24	80	8.89	8.39
TaLTP2.84	chr3A	29048596	29048943	1	M-27-C-9-C-14-CC-19-C-1-C-19-C-13-C-4	26	90	8.94	10.67
TaLTP2.85	chr3A	29351629	29351976	-1	M-27-C-9-C-14-CC-19-C-1-C-19-C-13-C-4	26	90	8.95	10.67
TaLTP2.86	chr3A	484634127	484634414	1	M-28-C-7-C-13-CC-8-C-1-C-23-C-6-C-0	22	74	8.25	11.59
TaLTP2.87	chr3A	661655290	661655586	1	M-37-C-3-C-12-CC-9-C-1-C-21-C-6-C-0	25	74	7.71	9.51
TaLTP2.88	chr3A	661787323	661787640	1	M-44-C-3-C-12-CC-9-C-1-C-21-C-6-C-0	32	74	7.73	9.58
TaLTP2.89	chr3B	3092002	3092337	-1	M-26-C-9-C-18-CC-13-C-1-C-24-C-9-C-2	25	87	9.03	4.64
TaLTP2.90	chr3B	9427199	9427477	-1	M-25-C-7-C-13-CC-8-C-1-C-23-C-6-C-0	25	68	7.10	10.55
TaLTP2.91	chr3B	35037705	35038052	1	M-27-C-9-C-14-CC-19-C-1-C-19-C-13-C-4	26	90	8.77	10.52
TaLTP2.92	chr3B	35119171	35119518	1	M-27-C-9-C-14-CC-19-C-1-C-19-C-13-C-4	26	90	8.77	10.52
TaLTP2.93	chr3B	35212403	35212750	1	M-27-C-9-C-14-CC-19-C-1-C-19-C-13-C-4	26	90	8.66	10.75

TaLTP2.94	chr3B	35288587	35288934	1	M-27-C-9-C-14-CC-19-C-1-C-19-C-13-C-4	26	90	8.66	10.75
TaLTP2.95	chr3B	35697822	35698169	1	M-27-C-9-C-14-CC-19-C-1-C-19-C-13-C-4	26	90	8.73	10.75
TaLTP2.96	chr3B	35701446	35701793	1	M-27-C-9-C-14-CC-19-C-1-C-19-C-13-C-4	26	90	8.63	10.45
TaLTP2.97	chr3B	35754310	35754657	1	M-27-C-9-C-14-CC-19-C-1-C-10-C-8-C-18	26	90	8.72	10.46
TaLTP2.98	chr3B	35769759	35770106	1	M-27-C-9-C-14-CC-19-C-1-C-19-C-13-C-4	26	90	8.73	10.75
TaLTP2.99	chr3B	35773382	35773729	1	M-27-C-9-C-14-CC-19-C-1-C-19-C-13-C-4	26	90	8.66	10.75
TaLTP2.100	chr3B	35813194	35813541	1	M-27-C-9-C-14-CC-19-C-1-C-19-C-13-C-4	26	90	8.70	10.75
TaLTP2.101	chr3B	35823275	35823622	1	M-27-C-9-C-14-CC-19-C-1-C-10-C-8-C-18	26	90	8.70	10.46
TaLTP2.102	chr3B	35837851	35838198	1	M-27-C-9-C-14-CC-19-C-1-C-19-C-13-C-4	26	90	8.66	10.75
TaLTP2.103	chr3B	35839140	35839487	1	M-27-C-9-C-14-CC-19-C-1-C-19-C-13-C-4	26	90	8.72	10.75
TaLTP2.104	chr3B	473691569	473691859	1	M-29-C-7-C-13-CC-8-C-1-C-23-C-6-C-0	23	74	8.21	10.86
TaLTP2.105	chr3B	696672997	696673308	1	M-38-C-3-C-12-CC-9-C-1-C-23-C-8-C-0	22	82	8.61	11.5
TaLTP2.106	chr3B	696778128	696778445	1	M-44-C-3-C-12-CC-9-C-1-C-21-C-6-C-0	32	74	7.77	6.28
TaLTP2.107	chr3B	696788089	696788403	-1	M-43-C-3-C-12-CC-9-C-1-C-21-C-6-C-0	31	74	7.68	9.58
TaLTP2.108	chr3D	7430150	7430404	-1	M-17-C-7-C-13-CC-8-C-1-C-23-C-6-C-0	17	68	7.10	10.55
TaLTP2.109	chr3D	21328598	21328945	-1	M-27-C-9-C-14-CC-19-C-1-C-19-C-13-C-4	26	90	8.73	10.75
TaLTP2.110	chr3D	363593703	363593990	1	M-28-C-7-C-13-CC-8-C-1-C-23-C-6-C-0	22	74	8.26	11.24
TaLTP2.111	chr3D	526995531	526995842	1	M-38-C-3-C-12-CC-9-C-1-C-23-C-8-C-0	22	82	8.58	10.87
TaLTP2.112	chr3D	527126755	527127075	1	M-45-C-3-C-12-CC-9-C-1-C-21-C-6-C-0	33	74	7.67	8.11
TaLTP2.113	chr3D	527135956	527136279	1	M-46-C-3-C-12-CC-9-C-1-C-21-C-6-C-0	34	74	7.67	9.52
TaLTP2.114	chr4A	476142148	476142510	-1	M-30-C-9-C-13-CC-19-C-1-C-22-C-13-C-4	29	92	9.11	11.41
TaLTP2.115	chr4A	684448840	684449261	-1	M-28-C-9-C-19-CC-13-C-1-C-24-C-3-C-9	26	90	9.30	6.17
TaLTP2.116	chr4A	684471199	684471624	1	M-54-C-9-C-19-CC-13-C-1-C-24-C-3-C-9	23	119	12.33	6.37
TaLTP2.117	chr4A	694676879	694677172	1	M-26-C-7-C-13-CC-8-C-1-C-23-C-6-C-4	25	73	7.87	8.31
TaLTP2.118	chr4B	603025686	603026111	-1	M-54-C-9-C-19-CC-13-C-1-C-24-C-3-C-9	23	119	12.29	6.7
TaLTP2.119	chr4B	603144552	603144977	-1	M-54-C-9-C-19-CC-13-C-1-C-24-C-3-C-9	23	119	12.37	6.37
TaLTP2.120	chr4B	603148473	603148898	1	M-54-C-9-C-19-CC-13-C-1-C-24-C-3-C-9	23	119	12.31	5.89
TaLTP2.121	chr4B	613905713	613906024	1	M-27-C-9-C-17-CC-9-C-1-C-24-C-7-C-0	28	76	8.13	4.34
TaLTP2.122	chr4B	654440796	654441242	1	M-61-C-9-C-21-CC-13-C-1-C-24-C-9-C-1	25	124	12.11	8.92
TaLTP2.123	chr4B	654453330	654453749	-1	M-53-C-9-C-19-CC-13-C-1-C-24-C-9-C-2	23	117	11.35	6.9
TaLTP2.124	chr4B	654560940	654561404	-1	M-69-C-9-C-18-CC-13-C-1-C-24-C-3-C-8	23	132	13.11	4.93
TaLTP2.125	chr4B	654592596	654593027	-1	M-58-C-9-C-18-CC-13-C-1-C-24-C-3-C-8	23	121	12.04	4.92
TaLTP2.126	chr4B	654606592	654607062	-1	M-81-C-5-C-17-CC-13-C-1-C-19-C-3-C-8	26	131	13.47	4.44
TaLTP2.127	chr4B	654699101	654699538	-1	M-50-C-9-C-18-CC-13-C-1-C-24-C-3-C-8	23	113	11.61	4.92
TaLTP2.128	chr4B	654719678	654720109	-1	M-58-C-9-C-18-CC-13-C-1-C-24-C-3-C-8	23	121	12.08	4.92
TaLTP2.129	chr4B	654728109	654731861	-1	M-43-C-9-C-18-CC-13-C-1-C-24-C-3-C-8	24	123	11.04	9
TaLTP2.130	chr4B	654731472	654731861	-1	M-43-C-9-C-18-CC-13-C-1-C-25-C-3-C-8	24	106	10.98	9
TaLTP2.131	chr4B	654734070	654734513	-1	M-72-C-5-C-17-CC-13-C-1-C-19-C-3-C-8	26	122	12.57	4.44
TaLTP2.132	chr4B	654751596	654752033	-1	M-50-C-9-C-18-CC-13-C-1-C-24-C-3-C-8	23	113	11.41	4.86
TaLTP2.133	chr4B	654761835	654762272	-1	M-60-C-9-C-18-CC-13-C-1-C-24-C-3-C-8	23	123	12.37	4.93
TaLTP2.134	chr4B	654774041	654774478	-1	M-60-C-9-C-18-CC-13-C-1-C-24-C-3-C-8	23	123	12.38	4.93
TaLTP2.135	chr4B	654793453	654793885	-1	M-47-C-9-C-18-CC-13-C-1-C-24-C-3-C-8	23	110	11.27	7.85
TaLTP2.136	chr4B	654806594	654806983	-1	M-43-C-9-C-18-CC-13-C-1-C-25-C-3-C-8	24	106	11.00	7.76
TaLTP2.137	chr4B	654810532	654811005	-1	M-82-C-5-C-17-CC-13-C-1-C-19-C-3-C-8	26	132	13.47	4.11
TaLTP2.138	chr4B	654925077	654925481	-1	M-58-C-5-C-18-CC-13-C-1-C-19-C-3-C-8	27	108	11.04	4.92
TaLTP2.139	chr4B	654965422	654965826	-1	M-58-C-5-C-18-CC-13-C-1-C-19-C-3-C-8	27	108	11.10	4.63

TaLTP2.140	chr4B	655000545	655000949	-1	M-58-C-5-C-18-CC-13-C-1-C-19-C-3-C-8	27	108	11.07	4.93
TaLTP2.141	chr4B	655036289	655036693	-1	M-58-C-5-C-18-CC-13-C-1-C-19-C-3-C-8	27	108	11.11	4.63
TaLTP2.142	chr4B	655091831	655092268	-1	M-60-C-9-C-18-CC-13-C-1-C-24-C-3-C-8	19	127	12.73	6.94
TaLTP2.143	chr4B	655111018	655111407	-1	M-43-C-9-C-18-CC-13-C-1-C-25-C-3-C-8	24	106	11.05	8.62
TaLTP2.144	chr4B	656326666	656327079	1	M-62-C-5-C-17-CC-13-C-1-C-19-C-3-C-8	26	112	11.68	4.23
TaLTP2.145	chr4B	667648816	667649091	1	M-24-C-7-C-13-CC-8-C-1-C-23-C-6-C-0	25	67	6.96	9.52
TaLTP2.146	chr4B	667855279	667855569	-1	M-29-C-7-C-13-CC-8-C-1-C-23-C-6-C-0	30	67	6.98	9.4
TaLTP2.147	chr4B	667859023	667859307	-1	M-27-C-7-C-13-CC-8-C-1-C-23-C-6-C-0	28	67	7.09	7.07
TaLTP2.148	chr4D	100336137	100336499	1	M-30-C-9-C-13-CC-19-C-1-C-22-C-13-C-4	29	92	9.10	11.41
TaLTP2.149	chr4D	477543091	477543516	-1	M-54-C-9-C-19-CC-13-C-1-C-24-C-3-C-9	21	121	12.37	6.7
TaLTP2.150	chr4D	477559039	477559464	1	M-54-C-9-C-19-CC-13-C-1-C-24-C-3-C-9	23	119	12.16	6.37
TaLTP2.151	chr4D	483179528	483179824	-1	M-22-C-9-C-17-CC-9-C-1-C-24-C-7-C-0	23	76	8.13	4.34
TaLTP2.152	chr4D	507124730	507125155	1	M-56-C-9-C-19-CC-13-C-1-C-24-C-9-C-1	23	119	11.38	8
TaLTP2.153	chr4D	507163625	507164068	-1	M-60-C-9-C-21-CC-13-C-1-C-24-C-9-C-1	26	122	11.89	9.37
TaLTP2.154	chr5A	78368993	78369310	1	M-27-C-9-C-16-CC-9-C-1-C-26-C-7-C-1	28	78	8.30	6.78
TaLTP2.155	chr5A	78474456	78474773	1	M-27-C-9-C-16-CC-9-C-1-C-26-C-7-C-1	22	84	8.90	6.07
TaLTP2.156	chr5A	78480627	78480944	1	M-27-C-9-C-16-CC-9-C-1-C-26-C-7-C-1	28	78	8.29	9.87
TaLTP2.157	chr5A	547658439	547658837	1	M-46-C-9-C-18-CC-13-C-1-C-25-C-9-C-2	23	110	11.53	4.95
TaLTP2.158	chr5A	547711278	547711676	1	M-46-C-9-C-18-CC-13-C-1-C-25-C-9-C-2	23	110	11.51	6.76
TaLTP2.159	chr5A	653281499	653281903	-1	M-42-C-10-C-21-CC-11-C-1-C-25-C-9-C-6	30	105	11.09	5.01
TaLTP2.160	chr5A	653284131	653284535	-1	M-42-C-10-C-21-CC-11-C-1-C-25-C-9-C-6	30	105	11.09	5.01
TaLTP2.161	chr5A	663375905	663376207	-1	M-24-C-9-C-17-CC-9-C-1-C-24-C-7-C-0	25	76	8.13	4.34
TaLTP2.162	chr5A	691976837	691977286	1	M-62-C-9-C-21-CC-13-C-1-C-24-C-9-C-1	26	124	12.01	9.19
TaLTP2.163	chr5A	692057989	692058417	-1	M-56-C-9-C-19-CC-13-C-1-C-24-C-9-C-2	23	120	11.44	8
TaLTP2.164	chr5A	692163190	692163696	-1	M-83-C-9-C-18-CC-13-C-1-C-24-C-3-C-8	23	146	14.40	4.86
TaLTP2.165	chr5A	692179351	692179782	-1	M-58-C-9-C-18-CC-13-C-1-C-24-C-3-C-8	23	121	12.08	4.92
TaLTP2.166	chr5A	692236726	692237106	-1	M-40-C-9-C-18-CC-13-C-1-C-25-C-3-C-8	24	103	10.52	7.96
TaLTP2.167	chr5A	692261839	692262243	-1	M-58-C-5-C-18-CC-13-C-1-C-19-C-3-C-8	24	111	11.34	4.63
TaLTP2.168	chr5A	706270655	706270945	1	M-29-C-7-C-13-CC-8-C-1-C-23-C-6-C-0	30	67	7.01	9.4
TaLTP2.169	chr5B	90988334	90988651	1	M-27-C-9-C-16-CC-9-C-1-C-26-C-7-C-1	28	78	8.28	6.77
TaLTP2.170	chr5B	91108881	91109198	1	M-27-C-9-C-16-CC-9-C-1-C-26-C-7-C-1	28	78	8.40	5.66
TaLTP2.171	chr5B	91112112	91112429	1	M-27-C-9-C-16-CC-9-C-1-C-26-C-7-C-1	28	78	8.26	9.87
TaLTP2.172	chr5B	526597643	526598041	1	M-46-C-9-C-18-CC-13-C-1-C-25-C-9-C-2	23	110	11.45	5.55
TaLTP2.173	chr5B	526633884	526634274	1	M-32-C-9-C-18-CC-13-C-1-C-25-C-9-C-2	27	92	9.69	5.55
TaLTP2.174	chr5B	526654817	526655215	1	M-46-C-9-C-18-CC-13-C-1-C-25-C-3-C-8	23	110	11.51	6.92
TaLTP2.175	chr5B	689336940	689337224	-1	M-26-C-7-C-13-CC-8-C-1-C-23-C-6-C-1	27	68	7.06	8.49
TaLTP2.176	chr5B	689340369	689340656	-1	M-28-C-7-C-13-CC-8-C-1-C-23-C-6-C-0	29	67	7.03	9.4
TaLTP2.177	chr5D	84185677	84185994	1	M-27-C-9-C-16-CC-9-C-1-C-26-C-7-C-1	28	78	8.31	9.87
TaLTP2.178	chr5D	433058166	433058564	1	M-46-C-9-C-18-CC-13-C-1-C-25-C-9-C-2	23	110	11.48	5.55
TaLTP2.179	chr5D	433109024	433109422	1	M-46-C-9-C-18-CC-13-C-1-C-25-C-9-C-2	23	110	11.59	6.03
TaLTP2.180	chr6A	65073332	65073841	-1	M-68-C-9-C-15-CC-12-C-1-C-27-C-11-C-17	25	145	14.92	9.74
TaLTP2.181	chr6A	65133550	65134074	-1	M-73-C-9-C-15-CC-12-C-1-C-27-C-11-C-17	25	150	15.45	8.16
TaLTP2.182	chr6A	459677544	459677924	-1	M-42-C-9-C-18-CC-13-C-1-C-24-C-9-C-1	23	104	10.47	5.57
TaLTP2.183	chr6B	121529231	121529737	-1	M-69-C-9-C-15-CC-12-C-1-C-27-C-9-C-17	25	144	14.69	9.36
TaLTP2.184	chr6B	123724068	123724529	1	M-47-C-9-C-15-CC-12-C-1-C-27-C-11-C-22	27	127	13.13	4.49
TaLTP2.185	chr6B	501128173	501128553	1	M-42-C-9-C-18-CC-13-C-1-C-24-C-9-C-1	23	104	10.41	5.61

TaLTP2.186	chr6D	47810554	47811000	-1	M-48-C-9-C-15-CC-12-C-1-C-27-C-11-C-16	22	127	13.09	4.02
TaLTP2.187	chr6D	49848829	49849353	1	M-73-C-9-C-15-CC-12-C-1-C-27-C-11-C-17	25	150	15.35	9.8
TaLTP2.188	chr6D	49855206	49855724	1	M-73-C-9-C-15-CC-12-C-1-C-27-C-9-C-17	25	148	15.14	9.8
TaLTP2.189	chr7A	81607073	81607384	-1	M-26-C-9-C-16-CC-9-C-1-C-26-C-7-C-0	27	77	8.10	10.59
TaLTP2.190	chr7A	498593990	498594400	-1	M-45-C-17-C-15-CC-9-C-1-C-22-C-15-C-3	31	106	10.63	4.27
TaLTP2.191	chr7A	674505756	674506154	-1	M-47-C-9-C-18-CC-13-C-1-C-24-C-3-C-8	23	110	11.33	6.3
TaLTP2.192	chr7A	674520709	674521107	-1	M-47-C-9-C-18-CC-13-C-1-C-24-C-3-C-8	23	110	11.20	7.91
TaLTP2.193	chr7A	674737358	674737756	-1	M-47-C-9-C-18-CC-13-C-1-C-24-C-3-C-8	23	110	11.28	5.05
TaLTP2.194	chr7A	674752092	674752490	-1	M-47-C-9-C-18-CC-13-C-1-C-24-C-3-C-8	23	110	11.28	5.05
TaLTP2.195	chr7A	674796419	674796820	-1	M-48-C-9-C-18-CC-13-C-1-C-24-C-3-C-8	23	111	11.37	6.73
TaLTP2.196	chr7A	674802099	674802500	-1	M-48-C-9-C-18-CC-13-C-1-C-24-C-3-C-8	23	111	11.36	9.03
TaLTP2.197	chr7B	25403834	25404145	-1	M-26-C-9-C-16-CC-9-C-1-C-26-C-7-C-0	27	77	8.10	10.27
TaLTP2.198	chr7B	464548398	464548811	-1	M-44-C-17-C-15-CC-9-C-1-C-22-C-17-C-3	32	106	10.84	4.51
TaLTP2.199	chr7B	558759919	558760203	-1	M-27-C-7-C-13-CC-8-C-1-C-23-C-6-C-0	27	68	6.93	11.31
TaLTP2.200	chr7B	558992275	558992559	-1	M-27-C-7-C-13-CC-8-C-1-C-23-C-6-C-0	27	68	6.99	11.31
TaLTP2.201	chr7B	650294286	650294684	-1	M-47-C-9-C-18-CC-13-C-1-C-24-C-3-C-8	23	110	11.24	7.91
TaLTP2.202	chr7B	650300433	650300831	-1	M-47-C-9-C-18-CC-13-C-1-C-24-C-3-C-8	23	110	11.28	7.91
TaLTP2.203	chr7B	650317214	650317612	-1	M-47-C-9-C-18-CC-13-C-1-C-24-C-3-C-8	23	110	11.38	7.91
TaLTP2.204	chr7B	650361486	650361884	-1	M-47-C-9-C-18-CC-13-C-1-C-24-C-3-C-8	23	110	11.32	8.58
TaLTP2.205	chr7B	650408469	650408867	-1	M-47-C-9-C-18-CC-13-C-1-C-24-C-3-C-8	23	110	11.31	8.58
TaLTP2.206	chr7B	650455225	650455623	-1	M-47-C-9-C-18-CC-13-C-1-C-24-C-3-C-8	21	112	11.45	7.91
TaLTP2.207	chr7B	650539649	650540050	-1	M-48-C-9-C-18-CC-13-C-1-C-24-C-3-C-8	23	111	11.43	8.97
TaLTP2.208	chr7B	650550199	650550600	-1	M-48-C-9-C-18-CC-13-C-1-C-24-C-3-C-8	23	111	11.41	8.97
TaLTP2.209	chr7B	650561737	650562138	-1	M-48-C-9-C-18-CC-13-C-1-C-24-C-3-C-8	23	111	11.47	8.58
TaLTP2.210	chr7B	650573579	650573980	-1	M-48-C-9-C-18-CC-13-C-1-C-24-C-3-C-8	23	111	11.40	8.97
TaLTP2.211	chr7B	650584509	650584910	-1	M-48-C-9-C-18-CC-13-C-1-C-24-C-3-C-8	23	111	11.41	8.97
TaLTP2.212	chr7D	5277144	5277443	1	M-29-C-5-C-16-CC-9-C-1-C-18-C-3-C-9	26	74	7.92	10.57
TaLTP2.213	chr7D	15402480	15402749	-1	M-26-C-8-C-17-CC-9-C-1-C-15-C-4-C-0	26	64	6.92	5.48
TaLTP2.214	chr7D	447061732	447062142	-1	M-44-C-17-C-15-CC-9-C-1-C-22-C-16-C-3	31	106	10.87	4.47
TaLTP2.215	chr7D	523392670	523392951	1	M-26-C-7-C-13-CC-8-C-1-C-23-C-6-C-0	26	68	6.99	11.31
TaLTP2.216	chr7D	582544930	582545331	-1	M-48-C-9-C-18-CC-13-C-1-C-24-C-3-C-8	21	113	11.66	6.27
TaLTP2.217	chr7D	582556602	582557002	-1	M-31-C-9-C-18-CC-13-C-1-C-24-C-3-C-8	23	94	9.82	6.74
TaLTP2.218	chr7D	582561126	582561526	-1	M-25-C-5-C-18-CC-13-C-1-C-24-C-3-C-8	23	84	8.79	9.19
TaLTP2.219	chr7D	582650386	582650787	-1	M-48-C-9-C-18-CC-13-C-1-C-24-C-3-C-8	23	111	11.52	5.04
TaLTP2.220	chr7D	582661777	582662177	-1	M-28-C-9-C-18-CC-13-C-1-C-24-C-3-C-8	23	91	9.54	6.27
TaLTP2.221	chr7D	582747483	582747878	-1	M-47-C-9-C-18-CC-13-C-1-C-23-C-3-C-8	23	109	11.22	5.61
TaLTP2.222	chrUn	29789284	29789571	1	M-28-C-7-C-13-CC-8-C-1-C-23-C-6-C-0	29	67	7.14	7.11
TaLTP2.223	chrUn	29798592	29798882	1	M-29-C-7-C-13-CC-8-C-1-C-23-C-6-C-0	30	67	7.05	9.4
TaLTP2.224	chrUn	29990173	29990454	-1	M-26-C-7-C-13-CC-8-C-1-C-23-C-6-C-0	27	67	6.87	8.49
TaLTP2.225	chrUn	43664829	43665176	1	M-27-C-9-C-14-CC-19-C-1-C-19-C-13-C-4	26	90	8.68	10.75
TaLTP2.226	chrUn	43770507	43770854	1	M-27-C-9-C-14-CC-19-C-1-C-19-C-13-C-4	26	90	8.64	10.75
TaLTP2.227	chrUn	44271349	44271696	1	M-27-C-9-C-14-CC-19-C-1-C-19-C-13-C-4	26	90	8.62	10.75
TaLTP2.228	chrUn	44297183	44297530	1	M-27-C-9-C-14-CC-19-C-1-C-19-C-13-C-4	26	90	8.62	10.75
TaLTP2.229	chrUn	44500426	44500773	-1	M-27-C-9-C-14-CC-19-C-1-C-19-C-13-C-4	26	90	8.62	10.75
TaLTP2.230	chrUn	44529121	44529468	-1	M-27-C-9-C-14-CC-19-C-1-C-19-C-13-C-4	26	90	8.62	10.75
TaLTP2.231	chrUn	60683260	60683673	1	M-62-C-5-C-17-CC-13-C-1-C-19-C-3-C-8	26	112	11.68	4.23

TaLTP2.232	chrUn	60741011	60741424	1	M-62-C-5-C-17-CC-13-C-1-C-19-C-3-C-8	26	112	11.66	4.17
TaLTP2.233	chrUn	154527864	154528298	1	M-69-C-5-C-17-CC-13-C-1-C-19-C-3-C-8	24	121	12.48	4.83
TaLTP2.234	chrUn	154531224	154531760	1	M-69-C-5-C-17-CC-13-C-1-C-36-C-3-C-25	24	155	16.42	9.3
TaLTP2.235	chrUn	154535835	154536257	1	M-65-C-5-C-17-CC-13-C-1-C-19-C-3-C-8	24	117	12.19	5.53
TaLTP2.236	chrUn	154542607	154542996	1	M-43-C-9-C-18-CC-13-C-1-C-25-C-3-C-8	24	106	10.82	7.95
TaLTP2.237	chrUn	154586875	154587306	1	M-58-C-9-C-18-CC-13-C-1-C-24-C-3-C-8	23	121	12.10	6.21
TaLTP2.238	chrUn	154601510	154601974	1	M-58-C-9-C-18-CC-13-C-1-C-24-C-3-C-8	23	121	12.00	6.18
TaLTP2.239	chrUn	154617362	154617793	1	M-58-C-9-C-18-CC-13-C-1-C-24-C-3-C-8	23	121	12.16	4.86
TaLTP2.240	chrUn	154629667	154630185	1	M-87-C-9-C-18-CC-13-C-1-C-24-C-3-C-8	23	150	14.67	6.18
TaLTP2.241	chrUn	168641413	168641760	-1	M-27-C-9-C-14-CC-19-C-1-C-19-C-13-C-4	26	90	8.66	10.75
TaLTP2.242	chrUn	168644994	168645341	-1	M-27-C-9-C-14-CC-19-C-1-C-19-C-13-C-4	26	90	8.70	10.75
TaLTP2.243	chrUn	168709387	168709734	-1	M-27-C-9-C-14-CC-19-C-1-C-19-C-13-C-4	26	90	8.66	10.75
TaLTP2.244	chrUn	189561514	189561903	-1	M-43-C-9-C-18-CC-13-C-1-C-25-C-3-C-8	24	106	10.79	7.95
TaLTP2.245	chrUn	189575201	189575590	-1	M-43-C-9-C-18-CC-13-C-1-C-25-C-3-C-8	24	106	10.80	7.95
TaLTP2.246	chrUn	189578553	189578939	-1	M-53-C-5-C-17-CC-13-C-1-C-19-C-3-C-8	24	105	11.14	4.9
TaLTP2.247	chrUn	201362401	201362823	1	M-65-C-5-C-17-CC-13-C-1-C-19-C-3-C-8	24	117	12.27	4.9
TaLTP2.248	chrUn	201365776	201366210	1	M-69-C-5-C-17-CC-13-C-1-C-19-C-3-C-8	24	121	12.58	4.18
TaLTP2.249	chrUn	201369161	201369550	1	M-43-C-9-C-18-CC-13-C-1-C-25-C-3-C-8	24	106	10.77	8.04
TaLTP2.250	chrUn	201383979	201384413	1	M-69-C-5-C-17-CC-13-C-1-C-19-C-3-C-8	24	121	12.61	4.17
TaLTP2.251	chrUn	201387365	201387784	1	M-64-C-5-C-17-CC-13-C-1-C-19-C-3-C-8	24	116	12.15	4.5
TaLTP2.252	chrUn	201389948	201390382	1	M-69-C-5-C-17-CC-13-C-1-C-19-C-3-C-8	24	121	12.63	4.5
TaLTP2.253	chrUn	202839683	202840030	-1	M-27-C-9-C-14-CC-19-C-1-C-19-C-13-C-4	26	90	8.70	10.75
TaLTP2.254	chrUn	248122351	248122668	-1	M-27-C-9-C-16-CC-9-C-1-C-26-C-7-C-1	28	78	8.24	9.52
TaLTP2.255	chrUn	248126327	248126644	-1	M-27-C-9-C-16-CC-9-C-1-C-26-C-7-C-1	28	78	8.29	9.78
TaLTP2.256	chrUn	272422375	272422794	-1	M-64-C-5-C-17-CC-13-C-1-C-19-C-3-C-8	24	116	12.13	4.5
TaLTP2.257	chrUn	272425745	272426164	1	M-64-C-5-C-17-CC-13-C-1-C-19-C-3-C-8	24	116	12.15	4.5
TaLTP2.258	chrUn	279539920	279540339	1	M-64-C-5-C-17-CC-13-C-1-C-19-C-3-C-8	24	116	12.22	4.5
TaLTP2.259	chrUn	279543298	279543687	1	M-43-C-9-C-18-CC-13-C-1-C-25-C-3-C-8	24	106	10.81	7.96
TaLTP2.260	chrUn	281905703	281906020	1	M-27-C-9-C-16-CC-9-C-1-C-26-C-7-C-1	28	78	8.22	9.52
TaLTP2.261	chrUn	291090280	291090702	1	M-65-C-5-C-17-CC-13-C-1-C-19-C-3-C-8	24	117	12.14	4.83
TaLTP2.262	chrUn	316645401	316645748	1	M-27-C-9-C-14-CC-19-C-1-C-19-C-13-C-4	26	90	8.77	10.52
TaLTP2.263	chrUn	352901801	352902148	-1	M-27-C-9-C-14-CC-19-C-1-C-19-C-13-C-4	26	90	8.70	10.75
TaLTP2.264	chrUn	363336879	363337268	1	M-43-C-9-C-18-CC-13-C-1-C-25-C-3-C-8	24	106	10.82	7.95
TaLTP2.265	chrUn	382657136	382657570	1	M-69-C-5-C-17-CC-13-C-1-C-19-C-3-C-8	24	121	12.63	4.5
TaLTP2.266	chrUn	384745684	384746118	1	M-69-C-5-C-17-CC-13-C-1-C-19-C-3-C-8	24	121	12.65	4.5
TaLTP2.267	chrUn	386578210	386578557	-1	M-27-C-9-C-14-CC-19-C-1-C-19-C-13-C-4	26	90	8.66	10.75
TaLTP2.268	chrUn	390420707	390421054	-1	M-27-C-9-C-14-CC-19-C-1-C-19-C-13-C-4	26	90	8.70	10.75
TaLTP2.269	chrUn	391869713	391870147	1	M-69-C-5-C-17-CC-13-C-1-C-19-C-3-C-8	24	121	12.63	4.43
TaLTP2.270	chrUn	405745791	405746225	1	M-69-C-5-C-17-CC-13-C-1-C-19-C-3-C-8	24	121	12.61	4.17
TaLTP2.271	chrUn	410676270	410676689	1	M-64-C-5-C-17-CC-13-C-1-C-19-C-3-C-8	24	116	12.22	4.5
TaLTP2.272	chrUn	411262600	411263034	1	M-69-C-5-C-17-CC-13-C-1-C-19-C-3-C-8	24	121	12.67	4.5
TaLTP2.273	chrUn	413773129	413773542	1	M-62-C-5-C-17-CC-13-C-1-C-19-C-3-C-8	26	112	11.72	4.52
TaLTP2.274	chrUn	416009590	416010006	1	M-63-C-5-C-17-CC-13-C-1-C-19-C-3-C-8	26	113	11.79	5.47
TaLTPc.1	chr5A	524240635	524241108	1	M-37-C-9-C-19-CC-9-C-1-C-12-C-6-C-31	33	101	10.57	9.82
TaLTPc.2	chr5B	496521936	496522402	1	M-37-C-9-C-19-CC-9-C-1-C-12-C-6-C-30	33	100	10.47	9.62
TaLTPc.3	chr5D	412360925	412361358	1	M-36-C-9-C-19-CC-9-C-1-C-12-C-6-C-1	32	71	7.11	9.97

TaLTPc.4	chr7A	275916291	275916705	1	M-33-C-9-C-14-CC-9-C-1-C-12-C-6-C-2	30	66	6.80	10.61
TaLTPc.5	chr7B	234590456	234590876	1	M-33-C-9-C-14-CC-9-C-1-C-12-C-6-C-2	30	66	6.73	10.61
TaLTPd.1	chr1A	42670763	42671250	1	M-21-C-10-C-17-CC-9-C-1-C-11-C-10-C-19	21	87	9.88	9.38
TaLTPd.2	chr1A	42695478	42695965	1	M-21-C-10-C-17-CC-9-C-1-C-11-C-10-C-19	21	87	9.83	6.78
TaLTPd.3	chr1A	42721347	42721834	1	M-21-C-10-C-17-CC-9-C-1-C-11-C-10-C-19	21	87	9.87	9.38
TaLTPd.4	chr1A	43270923	43271411	-1	M-21-C-10-C-17-CC-9-C-1-C-11-C-10-C-19	20	88	9.86	8.69
TaLTPd.5	chr1A	292077106	292077622	1	M-27-C-10-C-16-CC-9-C-1-C-23-C-7-C-5	25	83	8.61	4.24
TaLTPd.6	chr1B	63202243	63202730	1	M-21-C-10-C-17-CC-9-C-1-C-11-C-10-C-19	21	87	9.78	8.71
TaLTPd.7	chr1B	63468788	63469269	1	M-21-C-10-C-17-CC-9-C-1-C-11-C-10-C-17	21	85	9.59	9
TaLTPd.8	chr1B	63480020	63480507	1	M-21-C-10-C-17-CC-9-C-1-C-11-C-10-C-19	21	87	9.79	9
TaLTPd.9	chr1B	63614431	63614918	1	M-21-C-10-C-17-CC-9-C-1-C-11-C-10-C-19	21	87	9.80	9.02
TaLTPd.10	chr1B	63809033	63809520	1	M-21-C-10-C-17-CC-9-C-1-C-11-C-10-C-19	21	87	9.79	8.68
TaLTPd.11	chr1B	63889321	63889808	1	M-21-C-10-C-17-CC-9-C-1-C-11-C-10-C-19	21	87	9.79	9
TaLTPd.12	chr1B	325818004	325818534	-1	M-28-C-10-C-16-CC-9-C-1-C-23-C-7-C-5	25	84	8.83	4.56
TaLTPd.13	chr1B	645244411	645244868	1	M-21-C-10-C-17-CC-9-C-1-C-11-C-10-C-19	21	87	10.04	9.48
TaLTPd.14	chr1D	43306213	43306700	1	M-21-C-10-C-17-CC-9-C-1-C-11-C-10-C-19	21	87	9.81	8.71
TaLTPd.15	chr1D	43823484	43823971	1	M-21-C-10-C-17-CC-9-C-1-C-11-C-10-C-19	21	87	9.79	8.68
TaLTPd.16	chr1D	44275397	44275864	1	M-21-C-10-C-17-CC-9-C-1-C-11-C-10-C-20	21	88	9.99	9
TaLTPd.17	chr1D	44310595	44311158	1	M-21-C-10-C-17-CC-9-C-1-C-11-C-10-C-30	21	98	10.75	7.93
TaLTPd.18	chr1D	44629280	44629767	1	M-21-C-10-C-17-CC-9-C-1-C-11-C-10-C-19	21	87	9.80	8.68
TaLTPd.19	chr1D	225710372	225710900	-1	M-27-C-10-C-16-CC-9-C-1-C-23-C-7-C-5	20	88	9.03	4.52
TaLTPd.20	chr2A	25449735	25450711	-1	M-96-C-9-C-17-CC-12-C-1-C-27-C-9-C-40	23	198	20.97	4.55
TaLTPd.21	chr2A	158073110	158073760	-1	M-84-C-9-C-17-CC-12-C-1-C-27-C-9-C-17	27	159	16.79	5.29
TaLTPd.22	chr2A	511095229	511095672	1	M-29-C-14-C-14-CC-12-C-1-C-24-C-10-C-6	28	92	9.30	9.85
TaLTPd.23	chr2A	511114764	511115263	1	M-29-C-14-C-14-CC-12-C-1-C-24-C-10-C-12	28	98	10.45	5.04
TaLTPd.24	chr2A	684199222	684199709	1	M-26-C-13-C-14-CC-12-C-1-C-23-C-4-C-6	25	84	8.58	11.45
TaLTPd.25	chr2B	36915011	36916039	-1	M-99-C-9-C-17-CC-12-C-1-C-27-C-9-C-43	26	201	21.72	4.59
TaLTPd.26	chr2B	36920840	36921868	-1	M-99-C-9-C-17-CC-12-C-1-C-27-C-9-C-43	26	201	21.73	4.59
TaLTPd.27	chr2B	36926736	36927764	-1	M-99-C-9-C-17-CC-12-C-1-C-27-C-9-C-43	26	201	21.73	4.59
TaLTPd.28	chr2B	36938142	36939170	-1	M-99-C-9-C-17-CC-12-C-1-C-27-C-9-C-43	26	201	21.73	4.59
TaLTPd.29	chr2B	36944050	36945078	-1	M-99-C-9-C-17-CC-12-C-1-C-27-C-9-C-43	26	201	21.72	4.59
TaLTPd.30	chr2B	200896772	200897422	1	M-82-C-9-C-17-CC-12-C-1-C-27-C-11-C-18	27	160	17.05	8.41
TaLTPd.31	chr2B	448778246	448778688	1	M-29-C-14-C-14-CC-12-C-1-C-24-C-10-C-6	28	92	9.38	9.85
TaLTPd.32	chr2B	448870450	448870945	1	M-29-C-14-C-14-CC-12-C-1-C-24-C-10-C-12	28	98	10.51	8.97
TaLTPd.33	chr2B	646066328	646066819	1	M-26-C-12-C-14-CC-12-C-1-C-24-C-4-C-6	25	84	8.69	10.4
TaLTPd.34	chr2D	143221549	143222200	1	M-84-C-9-C-17-CC-12-C-1-C-27-C-9-C-17	27	159	16.79	5.29
TaLTPd.35	chr2D	143236318	143236976	1	M-85-C-9-C-17-CC-12-C-1-C-27-C-9-C-17	27	160	17.09	8.76
TaLTPd.36	chr2D	377150417	377150853	1	M-27-C-14-C-14-CC-12-C-1-C-24-C-10-C-6	26	92	9.35	9.85
TaLTPd.37	chr2D	377156149	377156644	1	M-29-C-14-C-14-CC-12-C-1-C-24-C-10-C-12	28	98	10.48	8.19
TaLTPd.38	chr3A	574864267	574864817	1	M-48-C-10-C-17-CC-9-C-1-C-11-C-10-C-20	21	115	12.10	4.77
TaLTPd.39	chr3A	574866319	574866734	1	M-20-C-10-C-17-CC-9-C-1-C-11-C-10-C-20	20	88	9.55	9.08
TaLTPd.40	chr3A	613171334	613171851	-1	M-27-C-14-C-14-CC-11-C-1-C-24-C-10-C-14	26	99	10.28	11.84
TaLTPd.41	chr3B	571809668	571810254	1	M-60-C-10-C-17-CC-9-C-1-C-11-C-10-C-20	21	127	13.39	4.58
TaLTPd.42	chr3B	571811742	571812157	1	M-20-C-10-C-17-CC-9-C-1-C-11-C-20-C-10	20	88	9.79	9.4
TaLTPd.43	chr3B	625332980	625333477	-1	M-27-C-14-C-14-CC-11-C-1-C-24-C-10-C-30	26	115	12.38	10.27
TaLTPd.44	chr3D	436042498	436043075	1	M-57-C-10-C-17-CC-9-C-1-C-11-C-10-C-20	21	124	13.00	5.07

TaLTPd.45	chr3D	436044575	436044990	1	M-20-C-10-C-17-CC-9-C-1-C-11-C-10-C-20	20	88	9.61	9.08
TaLTPd.46	chr3D	436163790	436164205	1	M-20-C-10-C-17-CC-9-C-1-C-11-C-10-C-20	20	88	9.56	8.74
TaLTPd.47	chr3D	470888758	470889215	-1	M-27-C-14-C-14-CC-11-C-1-C-24-C-10-C-6	26	91	9.28	11.65
TaLTPd.48	chr5B	600728083	600728567	1	M-21-C-10-C-17-CC-9-C-1-C-11-C-10-C-19	21	87	9.84	8.71
TaLTPd.49	chr5D	488203890	488204374	1	M-21-C-10-C-17-CC-9-C-1-C-11-C-10-C-19	21	87	9.85	9.22
TaLTPd.50	chr6B	17036701	17037146	-1	M-27-C-14-C-14-CC-12-C-1-C-24-C-10-C-6	26	92	9.34	9.7
TaLTPd.51	chr7A	644845693	644846250	1	M-29-C-14-C-14-CC-11-C-1-C-24-C-10-C-6	26	93	9.55	8.4
TaLTPd.52	chr7A	656982419	656982982	1	M-32-C-10-C-18-CC-10-C-1-C-17-C-4-C-41	26	117	12.91	9.47
TaLTPd.53	chr7A	676065583	676066434	-1	M-87-C-9-C-17-CC-12-C-1-C-27-C-9-C-5	28	149	15.68	7.89
TaLTPd.54	chr7A	676277892	676278720	1	M-87-C-9-C-17-CC-12-C-1-C-27-C-9-C-5	29	148	15.57	7.83
TaLTPd.55	chr7B	608470317	608470782	1	M-29-C-14-C-14-CC-11-C-1-C-24-C-10-C-6	22	97	9.80	8.34
TaLTPd.56	chr7D	560706749	560708577	-1	M-29-C-14-C-14-CC-11-C-1-C-24-C-10-C-32	22	123	12.54	8.87
TaLTPd.57	chr7D	585603227	585604080	-1	M-87-C-9-C-17-CC-12-C-1-C-27-C-9-C-4	28	148	15.67	7.89
TaLTPg.1	chr1A	30196854	30197476	-1	M-29-C-9-C-14-CC-12-C-1-C-26-C-9-C-61	25	120	11.70	8.34
TaLTPg.2	chr1A	498174489	498175684	-1	M-59-C-9-C-16-CC-12-C-1-C-25-C-9-C-74	34	156	15.27	8.28
TaLTPg.3	chr1B	48346465	48347106	1	M-25-C-9-C-14-CC-12-C-1-C-26-C-9-C-79	22	143	13.77	9.23
TaLTPg.4	chr1B	541011245	541012356	1	M-59-C-9-C-16-CC-12-C-1-C-25-C-9-C-74	34	156	15.26	8.28
TaLTPg.5	chr1D	30107700	30108330	-1	M-31-C-9-C-14-CC-12-C-1-C-26-C-9-C-61	28	119	11.56	8.34
TaLTPg.6	chr1D	403059303	403060402	-1	M-60-C-9-C-16-CC-12-C-1-C-25-C-9-C-74	34	157	15.34	8.28
TaLTPg.7	chr2A	113928376	113929907	-1	M-37-C-9-C-16-CC-14-C-1-C-22-C-9-C-62	26	127	11.87	9.46
TaLTPg.8	chr2A	349721024	349721944	1	M-23-C-9-C-14-CC-12-C-1-C-25-C-9-C-62	21	115	11.84	4.45
TaLTPg.9	chr2A	571149720	571150423	-1	M-37-C-9-C-14-CC-12-C-1-C-26-C-10-C-78	26	146	14.66	4.75
TaLTPg.10	chr2A	674493788	674494564	-1	M-29-C-10-C-18-CC-12-C-1-C-24-C-8-C-57	25	123	12.47	8.59
TaLTPg.11	chr2B	162928065	162929589	-1	M-36-C-9-C-16-CC-14-C-1-C-22-C-9-C-62	25	127	11.98	9.46
TaLTPg.12	chr2B	318204810	318206745	-1	M-23-C-9-C-14-CC-12-C-1-C-25-C-9-C-62	21	115	11.89	4.45
TaLTPg.13	chr2B	491022663	491023363	1	M-34-C-9-C-14-CC-12-C-1-C-26-C-10-C-78	23	146	14.66	4.45
TaLTPg.14	chr2B	629693498	629694274	-1	M-29-C-10-C-18-CC-12-C-1-C-24-C-8-C-78	25	144	14.51	6.28
TaLTPg.15	chr2D	112719725	112721413	-1	M-36-C-9-C-16-CC-14-C-1-C-22-C-9-C-62	25	127	11.90	9.46
TaLTPg.16	chr2D	279055262	279056172	-1	M-23-C-9-C-14-CC-12-C-1-C-25-C-9-C-62	19	117	11.95	4.45
TaLTPg.17	chr2D	419024868	419025582	1	M-37-C-9-C-14-CC-12-C-1-C-26-C-10-C-78	26	146	14.54	4.65
TaLTPg.18	chr2D	529657261	529658067	-1	M-29-C-10-C-18-CC-12-C-1-C-24-C-8-C-80	25	144	14.52	6.28
TaLTPg.19	chr3A	395763172	395764865	-1	M-32-C-9-C-20-CC-19-C-1-C-24-C-20-C-79	24	165	16.53	5.26
TaLTPg.20	chr3A	584766039	584767648	1	M-41-C-9-C-16-CC-12-C-1-C-25-C-9-C-67	27	136	13.54	5.12
TaLTPg.21	chr3B	581663498	581664752	1	M-41-C-9-C-16-CC-12-C-1-C-25-C-9-C-67	27	136	13.53	5.68
TaLTPg.22	chr3D	298061090	298062754	-1	M-32-C-9-C-20-CC-19-C-1-C-24-C-20-C-79	24	159	15.88	5.25
TaLTPg.23	chr3D	443628687	443630068	1	M-41-C-9-C-16-CC-12-C-1-C-25-C-9-C-68	27	137	13.62	5.68
TaLTPg.24	chr4A	14835749	14837105	-1	M-33-C-9-C-14-CC-12-C-1-C-26-C-9-C-83	22	144	14.60	6.98
TaLTPg.25	chr4A	30399234	30400445	-1	M-32-C-9-C-16-CC-12-C-1-C-24-C-9-C-77	23	142	13.87	5.68
TaLTPg.26	chr4A	168545335	168546427	1	M-42-C-9-C-16-CC-12-C-1-C-24-C-9-C-63	26	131	12.68	4.65
TaLTPg.27	chr4A	596215050	596215755	1	M-47-C-9-C-14-CC-12-C-1-C-21-C-6-C-87	31	148	14.01	4.14
TaLTPg.28	chr4A	596238542	596239241	-1	M-46-C-9-C-14-CC-12-C-1-C-21-C-6-C-86	31	147	13.91	4.14
TaLTPg.29	chr4A	596298088	596299944	1	M-31-C-12-C-8-CC-14-C-1-C-24-C-13-C-110	24	174	17.05	6.03
TaLTPg.30	chr4B	13125606	13127461	-1	M-27-C-12-C-8-CC-14-C-1-C-24-C-13-C-112	24	172	16.76	6.19
TaLTPg.31	chr4B	13277411	13278102	-1	M-46-C-9-C-14-CC-12-C-1-C-21-C-6-C-83	28	146	13.77	3.85
TaLTPg.32	chr4B	565313012	565314547	1	M-33-C-9-C-14-CC-12-C-1-C-26-C-9-C-83	27	139	14.08	6.08
TaLTPg.33	chr4D	7215791	7217463	1	M-31-C-12-C-8-CC-14-C-1-C-24-C-13-C-111	24	175	17.16	6.19

TaLTPg.34	chr4D	7409439	7410145	1	M-47-C-9-C-14-CC-12-C-1-C-21-C-6-C-86	32	147	13.82	4.14
TaLTPg.35	chr4D	7411916	7412692	1	M-30-C-9-C-14-CC-12-C-1-C-24-C-6-C-122	24	179	17.75	4.08
TaLTPg.36	chr4D	308544569	308545738	-1	M-42-C-9-C-16-CC-12-C-1-C-24-C-9-C-63	26	133	12.82	4.61
TaLTPg.37	chr4D	437683745	437685153	1	M-40-C-9-C-16-CC-12-C-1-C-24-C-9-C-73	31	139	13.61	5.18
TaLTPg.38	chr4D	451801760	451803035	-1	M-23-C-9-C-14-CC-12-C-1-C-26-C-9-C-83	17	139	14.05	6.08
TaLTPg.39	chr5A	491948772	491949564	-1	M-35-C-9-C-14-CC-12-C-1-C-26-C-9-C-82	22	151	15.25	4.17
TaLTPg.40	chr5A	616909276	616909794	-1	M-30-C-9-C-14-CC-12-C-1-C-26-C-9-C-62	29	118	11.75	8.3
TaLTPg.41	chr5A	616914032	616914550	-1	M-30-C-9-C-14-CC-12-C-1-C-26-C-9-C-62	29	118	11.68	8.27
TaLTPg.42	chr5A	616919394	616919912	-1	M-30-C-9-C-14-CC-12-C-1-C-26-C-9-C-62	29	118	11.58	9.16
TaLTPg.43	chr5A	616981829	616982464	-1	M-26-C-9-C-14-CC-12-C-1-C-26-C-9-C-66	25	122	11.84	9.6
TaLTPg.44	chr5A	617173798	617174627	-1	M-26-C-10-C-17-CC-12-C-1-C-24-C-8-C-80	21	143	14.35	8.74
TaLTPg.45	chr5A	617175190	617175916	1	M-38-C-9-C-14-CC-12-C-1-C-25-C-9-C-64	20	132	12.59	4.93
TaLTPg.46	chr5A	617188181	617188922	1	M-44-C-9-C-14-CC-12-C-1-C-25-C-9-C-61	20	138	13.27	4.46
TaLTPg.47	chr5A	634077376	634079042	1	M-33-C-9-C-16-CC-12-C-1-C-26-C-8-C-77	27	137	14.50	8.97
TaLTPg.48	chr5A	634086223	634087886	1	M-30-C-9-C-16-CC-12-C-1-C-26-C-8-C-74	24	132	13.87	8.18
TaLTPg.49	chr5B	467227042	467227827	-1	M-33-C-9-C-14-CC-12-C-1-C-26-C-9-C-56	29	116	11.84	4.16
TaLTPg.50	chr5B	609927335	609927847	-1	M-30-C-9-C-14-CC-12-C-1-C-26-C-9-C-60	29	116	11.47	8.24
TaLTPg.51	chr5B	609935235	609935753	-1	M-30-C-9-C-14-CC-12-C-1-C-26-C-9-C-62	29	118	11.74	8.27
TaLTPg.52	chr5B	610007128	610007768	-1	M-36-C-9-C-14-CC-12-C-1-C-26-C-9-C-53	35	108	10.52	9.31
TaLTPg.53	chr5B	610022234	610022905	-1	M-36-C-9-C-14-CC-12-C-1-C-26-C-9-C-66	35	122	11.88	9.78
TaLTPg.54	chr5B	610081075	610081832	-1	M-36-C-9-C-14-CC-12-C-1-C-26-C-9-C-96	35	178	17.65	9.01
TaLTPg.55	chr5B	610085156	610085805	-1	M-36-C-9-C-14-CC-12-C-1-C-26-C-9-C-61	35	117	11.34	9.23
TaLTPg.56	chr5B	610293664	610294516	-1	M-30-C-10-C-17-CC-12-C-1-C-24-C-8-C-80	25	143	14.33	8.74
TaLTPg.57	chr5B	610295057	610295797	1	M-44-C-9-C-14-CC-12-C-1-C-25-C-9-C-63	31	132	12.78	5.55
TaLTPg.58	chr5B	637143796	637145288	1	M-35-C-9-C-16-CC-12-C-1-C-26-C-8-C-76	29	135	14.35	9.3
TaLTPg.59	chr5B	637158254	637159814	1	M-30-C-9-C-16-CC-12-C-1-C-26-C-8-C-72	24	131	13.78	8.18
TaLTPg.60	chr5D	388830376	388831166	-1	M-33-C-9-C-14-CC-12-C-1-C-26-C-9-C-81	29	141	14.35	4.37
TaLTPg.61	chr5D	493997499	493998137	1	M-26-C-9-C-14-CC-12-C-1-C-26-C-9-C-66	25	122	11.88	9.6
TaLTPg.62	chr5D	494033291	494033910	1	M-26-C-9-C-14-CC-12-C-1-C-26-C-9-C-66	25	122	11.80	9.6
TaLTPg.63	chr5D	494042019	494042570	1	M-26-C-9-C-14-CC-12-C-1-C-26-C-9-C-77	25	133	13.21	9.63
TaLTPg.64	chr5D	494052848	494053351	1	M-25-C-9-C-14-CC-12-C-1-C-26-C-9-C-62	24	118	11.68	8.27
TaLTPg.65	chr5D	494181604	494182457	-1	M-26-C-10-C-17-CC-12-C-1-C-24-C-8-C-80	21	143	14.34	8.74
TaLTPg.66	chr5D	494183026	494183762	1	M-44-C-9-C-14-CC-12-C-1-C-25-C-9-C-61	29	129	12.38	4.93
TaLTPg.67	chr5D	506269882	506271676	1	M-36-C-9-C-16-CC-12-C-1-C-26-C-8-C-77	30	137	14.44	8.97
TaLTPg.68	chr5D	506290475	506292167	1	M-33-C-9-C-16-CC-12-C-1-C-26-C-8-C-71	27	130	13.68	8.18
TaLTPg.69	chr5D	506946614	506947460	1	M-34-C-9-C-16-CC-12-C-1-C-26-C-8-C-66	28	125	13.05	6.06
TaLTPg.70	chr6A	484065309	484067524	-1	M-32-C-9-C-14-CC-12-C-1-C-26-C-8-C-77	22	138	14.10	5.28
TaLTPg.71	chr6B	518601609	518604075	-1	M-28-C-9-C-14-CC-12-C-1-C-26-C-8-C-77	22	134	13.77	6.41
TaLTPg.72	chr6B	612197715	612199721	1	M-37-C-9-C-16-CC-14-C-1-C-23-C-9-C-53	24	122	11.91	9.17
TaLTPg.73	chr6B	645490602	645491359	-1	M-33-C-10-C-15-CC-12-C-1-C-25-C-8-C-83	27	147	14.29	10.83
TaLTPg.74	chr6D	343636222	343638515	-1	M-28-C-9-C-14-CC-12-C-1-C-26-C-8-C-77	22	134	13.77	6.41
TaLTPg.75	chr6D	428902991	428903766	-1	M-33-C-10-C-15-CC-12-C-1-C-25-C-8-C-85	27	149	14.34	11.55
TaLTPg.76	chr7A	76182477	76183163	1	M-45-C-6-C-13-CC-12-C-1-C-25-C-5-C-32	22	127	13.02	8.46
TaLTPg.77	chr7A	257147699	257152247	1	M-29-C-9-C-14-CC-12-C-1-C-29-C-9-C-61	24	125	13.35	5.38
TaLTPg.78	chr7A	589453828	589455189	1	M-47-C-6-C-13-CC-12-C-1-C-25-C-8-C-41	34	99	9.91	8.3
TaLTPg.79	chr7A	641425898	641428573	-1	M-30-C-6-C-15-CC-12-C-1-C-25-C-8-C-44	25	101	10.27	9.4

TaLTPg.80	chr7B	12149409	12150113	1	M-41-C-6-C-13-CC-12-C-1-C-25-C-5-C-32	22	123	12.73	6.76
TaLTPg.81	chr7B	216815633	216818509	-1	M-29-C-9-C-14-CC-12-C-1-C-29-C-9-C-61	24	125	13.39	5.14
TaLTPg.82	chr7B	548162279	548163672	1	M-47-C-6-C-13-CC-12-C-1-C-25-C-8-C-64	34	122	11.73	5.09
TaLTPg.83	chr7D	69631912	69632637	1	M-43-C-6-C-13-CC-12-C-1-C-25-C-5-C-64	22	133	13.55	6.75
TaLTPg.84	chr7D	241176510	241179983	-1	M-29-C-9-C-14-CC-12-C-1-C-29-C-9-C-137	24	201	21.55	6.31
TaLTPg.85	chr7D	515821376	515822755	1	M-47-C-6-C-13-CC-12-C-1-C-25-C-8-C-64	34	123	11.80	5.09
TaLTPg.86	chr7D	554563423	554565727	1	M-30-C-6-C-15-CC-12-C-1-C-25-C-8-C-51	25	108	10.89	9.4

[1]8CM, eight cysteine motif

[2]AA, number of amino acid

[3]Mw, molecular weight in kiloDalton

[4]pI, isoelectric point (cysteine residues engaged in disulphide bridges were removed prior pI calculation)

Table S2 | Ka/Ks analysis and estimated divergence time for the some *TaLTP* duplicated pairs.

Chr	Gene 1	Position gene 1	Gene 2	Position gene 2	Ka	Ks	Ka/Ks	Identity (%)	Age (MYA)
Chr2A	TaLTP2.48	747727094	TaLTP2.55	747780203	0.0000	0.0000	-	100	0
Chr2A	TaLTP2.55	747780203	TaLTP2.50	747733420	0.0000	0.0000	-	100	0
Chr2A	TaLTP2.50	747733420	TaLTP2.47	747723957	0.0069	0.0000	-	99.5	0
Chr2A	TaLTP2.47	747723957	TaLTP2.54	747777016	0.0103	0.0000	-	99.3	0
Chr2A	TaLTP2.54	747777016	TaLTP2.49	747730232	0.0069	0.0095	0.7267	99.3	0.72978
Chr2A	TaLTP2.49	747730232	TaLTP2.51	747739744	0.0000	0.0000	-	100	0
Chr2A	TaLTP2.51	747739744	TaLTP2.52	747742933	0.0103	0.0096	1.0805	99	0.7354
Chr2A	TaLTP2.52	747742933	TaLTP2.57	747819511	0.0205	0.0536	0.3822	97.3	4.12243
Chr2A	TaLTP2.57	747819511	TaLTP2.58	747874783	0.0446	0.0794	0.5614	94.8	6.10727
Chr2A	TaLTP2.58	747874783	TaLTP2.46	747697212	0.0780	0.1349	0.5785	91.3	10.3785
Chr2A	TaLTP2.46	747697212	TaLTP2.53	747773829	0.0935	0.1160	0.8059	90.8	8.92169
Chr2A	TaLTP2.53	747773829	TaLTP2.56	747809997	0.0034	0.0199	0.1696	99.3	1.5343
Chr3B	TaLTP2.91	35037705	TaLTP2.92	35119171	0.0000	0.0000	-	100	0
Chr3B	TaLTP2.95	35697822	TaLTP2.98	35769759	0.0000	0.0000	-	100	0
Chr3B	TaLTP2.93	35212403	TaLTP2.94	35288587	0.0000	0.0000	-	100	0
Chr3B	TaLTP2.94	35288587	TaLTP2.96	35701446	0.0079	0.0232	0.3394	98.9	1.78377
Chr3B	TaLTP2.96	35701446	TaLTP2.99	35773382	0.0039	0.0000	-	99.7	0
Chr3B	TaLTP2.99	35773382	TaLTP2.97	35754310	0.0380	0.4167	0.0912	90.5	32.0504
Chr3B	TaLTP2.97	35754310	TaLTP2.101	35823275	0.0075	0.0135	0.5555	99.1	1.03502
Chr3B	TaLTP2.101	35823275	TaLTP2.100	35813194	0.0150	0.0278	0.5399	98.3	2.13643
Chr3B	TaLTP2.100	35813194	TaLTP2.102	35837851	0.0150	0.0000	-	98.9	0
Chr3B	TaLTP2.102	35837851	TaLTP2.103	35839140	0.0075	0.0000	-	99.4	0
Chr7B	TaLTP2.204	650361486	TaLTP2.205	650408469	0.0059	0.0191	0.3086	99.2	1.4689
Chr7B	TaLTP2.205	650408469	TaLTP2.203	650317214	0.0179	0.1037	0.1723	97.2	7.974
Chr7B	TaLTP2.203	650317214	TaLTP2.202	650300433	0.0089	0.0816	0.1090	98.2	6.27413
Chr7B	TaLTP2.202	650300433	TaLTP2.206	650455225	0.0090	0.0188	0.4752	99	1.44915
Chr7B	TaLTP2.206	650455225	TaLTP2.201	650294286	0.0089	0.0000	-	99.2	0
Chr7B	TaLTP2.201	650294286	TaLTP2.207	650539649	0.0338	0.7009	0.0482	90.5	53.9148
Chr7B	TaLTP2.207	650539649	TaLTP2.209	650561737	0.0151	0.2535	0.0595	95.5	19.5028
Chr7B	TaLTP2.209	650561737	TaLTP2.208	650550199	0.0030	0.0508	0.0594	99	3.90868
Chr7B	TaLTP2.208	650550199	TaLTP2.210	650573579	0.0030	0.0509	0.0592	99	3.91853
Chr7B	TaLTP2.210	650573579	TaLTP2.211	650584509	0.0060	0.0165	0.3631	99.3	1.26751

Table S3 | Gene expression data from RNA-seq in log2 FPKM.

	Choulet et al. (2014)										Yang et al. (2016)														
	CSTP_stamen	CSTP_pistil	triplo_dia_rep1	triplo_dia_rep2	...ent_lepto_rep1	...ent_lepto_rep2	...taphasel_rep1	...taphasel_rep2	...go_pachy_rep1	...go_pachy_rep2	spike_Z32	spike_Z39	spike_Z65	leaf_Z10	leaf_Z23	leaf_Z71	root_Z10	root_Z13	root_Z39	stem_Z30	stem_Z32	stem_Z65	grain_Z71	grain_Z75	grain_Z85
TaLTP1.1	0	6.89	-2.98	0	0	0	0	-0.91	0	0	-4.68	0	0.48	-1.66	0	-1.39	-0.97	0	0	-2.16	-2.55	0	-1	-2.65	0.17
TaLTP1.10	11.4	0	11.1	11.3	11.5	10.7	10.3	0	11.2	10.8	2.76	0	0	0	0	0	0	0	0	0	0	0	2.55	0	0
TaLTP1.11	7.79	2.92	8.18	7.95	8.19	8.43	8.6	10.1	8	7.11	7.51	0	0	-0.48	8.73	8.12	4.35	-2.42	7.58	7.13	6.79	0	7.38	6.08	5.22
TaLTP1.12	11.3	7.65	11.1	11.3	11.5	10.8	10.1	-0.53	10.9	10.8	2.8	0	0	0	0	0	0	0	-3.31	0	0	0	3.2	-3.27	0
TaLTP1.13	6.48	2.54	6.73	6.75	6.87	7.22	7.08	8.6	6.68	5.93	6.11	-3.83	-3.4	-1.84	7.65	6.6	4.27	0	5.62	6.17	5.57	0	5.77	4.35	4.22
TaLTP1.14	11.1	2.69	10.8	11	11.3	10.6	9.8	0	10.6	10.6	2.92	0	0	0	0	0	0	0	0	0	0	0	2.92	0	0
TaLTP1.15	7.63	7.62	7.99	8.02	8.02	8.28	8.29	9.43	8.03	7.09	7.51	-0.62	0	-1.6	8.52	7.92	3.98	-1.13	6.93	7.14	6.67	-1.14	7.23	5.68	5.29
TaLTP1.16	6.7	8.26	6.66	7.22	7.03	7.01	7.26	6.73	7.05	6.29	5.06	-1.94	-1.51	0	6.12	4.91	5.61	-1.98	4.08	4.68	4.02	-3.25	5.77	2.97	3.7
TaLTP1.17	5	7.14	4.87	5.47	4.96	4.7	4.67	4.71	4.65	4.86	2.22	-3.52	0	-3.7	5.43	3.72	5.36	-1.98	2.19	4.07	2.62	0	3.22	1.15	3.39
TaLTP1.18	2.15	0	2.13	1.87	2.72	1.36	2.14	0	3.12	2.22	-3.72	0	0	0	0	0	0	0	0	0	0	0	0	0	0
TaLTP1.19	0	0	0	0	0	0	0	0	0	0	0	0.69	0	1.42	0	0	0	1.07	0	0	0	0	0	0	0
TaLTP1.2	0	5.83	0	0	0	-2.67	-3.01	-1.11	0	0	-2.04	-3.75	1.14	-2.92	-0.93	-2.65	0	0	0	-3.69	0	0	-0.53	-1.27	-1.58
TaLTP1.20	7.05	9.39	6.82	7.71	7.27	7.07	7.01	6.99	7.21	6.7	4.91	-3.52	-3.1	-1.11	6.85	5.15	6.12	0	4.63	5.46	4.36	-2.25	5.54	3.4	4.09
TaLTP1.21	2.1	-1.08	1.01	1.53	2.21	1.32	1.34	0	2.68	1.79	-3.1	0	0	0	0	0	0	0	0	0	0	0	0	0	0
TaLTP1.22	-5.56	0.78	-5.3	-5.5	-4.86	-5.38	-4.74	-1.82	-4.85	-5.36	-5.08	-10.4	0.41	-9.14	0	-3.02	-3.41	-9.25	0.33	-1.25	-0.85	-0.38	-1.49	-0.94	-2.07
TaLTP1.23	1.64	8.56	1.24	1.19	1.79	2.12	2.42	5.86	1.98	1.56	1.97	-4.52	7.78	-2.7	7.01	4.29	3.83	-4.57	7.22	5.85	6.52	6.91	5.61	6.23	5.23
TaLTP1.24	0	0	0	0	0	-1.28	0	-0.45	0	0	0	0	0	-1.19	0	-1.26	4.07	-1.78	-3.23	-1.71	0	-2.06	-0.12	-2.19	0.13
TaLTP1.25	4.23	0	4.28	3.4	4.65	3.32	3.7	0	4.29	3.82	-2.7	0	0	0	0	0	0	0	0	0	0	0	0	0	0
TaLTP1.26	-2.66	7.95	-1.13	-1.9	0.08	1.05	-0.79	4.07	1.02	-2.57	-0.28	0	7.74	0	7.83	4.88	1.43	-3.57	8.1	5.72	7.69	6.05	6.23	7.29	6.17
TaLTP1.27	0	0	0	0	0	0	0	0	0	0	0	0	-2.92	0.39	0	-0.94	13.8	-0.78	0	0	0	0	4.32	0	10.2
TaLTP1.28	0	0	0	0	0	0	0	0	0	0	0	0	0	-1.52	0	-2.26	13.3	-2.36	-3.23	0	0	0	3.56	0	8.47
TaLTP1.29	1.09	9.43	0.77	0.71	0.88	2.09	2.04	5.55	1.7	1.12	2.48	-0.92	6.86	-2.09	8.55	5.27	4.69	-3.54	8.03	6.24	7.6	5.67	6.3	7.03	5.84
TaLTP1.3	0	6.53	0	0	0	0	0	-1.05	0	0	-4.56	0	-0.35	-3.86	0	0	0	0	0	-3.63	0	0	-1.14	0	-1.14
TaLTP1.30	4.65	9.25	3.98	5.14	4.7	3.2	3.34	3.38	4.85	4.28	-0.93	0	0	0	4.47	0	0	0	1.04	0	0	0	2.65	0	-3.07
TaLTP1.31	0	0	0	0	0	0	0	-1.61	0	0	0	0	0	0	0	0	0	0	0	0	0	0	0	0	0
TaLTP1.32	0	0	0	0	0	0	0	0	0	0	0	0	0	0	0	-3.38	0	0	-3.35	0	0	0	0	0	0
TaLTP1.33	0	0	0	0	0	0	0	0	0	0	0	1.88	0	1.78	0	-2.39	0	2.07	0	-1.42	-2.21	0	0	0	0
TaLTP1.34	0	0	0	0	0	0	0	0	0	0	0	0.13	-3.53	1.5	0	-3.87	0.88	1.19	-3.86	-2.9	-1.38	-3.69	0	-2.22	-4.11
TaLTP1.35	0	0	0	0	0	0	0	-2.03	0	0	0	0	0	-4.52	0	0	0	-3.47	0	0	0	0	0	0	0
TaLTP1.36	0	0	-3.32	0	0	0	0	-3.85	0	0	0	-4.15	0	0	-2.33	0	0	-2.69	0	0	0	0.28	0	-4	0
TaLTP1.37	-3.93	0	0	0	0	0	0	-3.8	0	0	0	0.98	-1.68	2.23	0	-2.43	0	1.02	-1.2	0.41	-1.26	0.74	-2.31	0.13	0
TaLTP1.38	0	0	0	0	0	0	0	-0.5	0	0	0	0	0	0	0	0	-1.29	0	-3.7	0	0	0	0	0	-3.96
TaLTP1.39	0	0	0	-2.27	0	0	0	0	0	0	0	1.69	0	1.91	0	0	0	1.13	0	0	0	0	0	-3.32	0
TaLTP1.4	8.16	11	8.06	8.38	8.52	8.72	8.26	10	8.48	7.8	6.24	-1.43	-3	0	8.82	7.04	0.9	-1.28	7.6	7.25	9.09	0.31	9.43	7.65	4.98
TaLTP1.5	2.67	3.44	2.72	1.03	3.08	3.61	3.38	6.1	2.43	2.39	1.46	0	0	-1.6	5.93	3.43	0	0	4.22	3.24	3.83	0	4.83	1.05	0
TaLTP1.6	0.43	-2.94	-0.86	3.14	0.55	4.13	3.2	4.86	3.51	0.55	0.86	0	0	0	0.57	0.86	0	0	-1.19	1.66	1	0	6.62	0.68	0
TaLTP1.7	1.76	-1.52	-0.5	4.5	1.62	4.84	3.96	5.41	4.56	1.55	2.06	0	0	0	5.58	2.14	0	0	3.05	3.37	1.31	-3.2	6.75	0.85	0
TaLTP1.8	7.78	9.12	7.59	8.12	8.1	8.1	8.11	8.82	8.19	7.25	5.81	0	0	-3.65	7.87	5.88	-2.96	0	6.58	6.9	6.63	-0.87	8.55	6.22	2.72
TaLTP1.9	6.69	10.2	6.57	7.04	7.15	7.43	6.77	8.74	6.98	6.35	5.15	0	0	0	7.19	5.58	0	-4.45	5.89	5.56	6.45	-1.56	8.16	6.04	3.66
TaLTP2.1	9.82	5.02	9.41	9.61	10.1	9.25	8.3	-0.02	9.29	9.14	1.47	0	0	-1.82	0.73	0	0	0	-1.54	-2.64	0	0	1.95	0	-1.29
TaLTP2.10	0.5	-2.85	0.3	-0.66	0.98	0	-0.28	0	0.39	0.37	0.99	1.84	0	2.37	-0.56	0.98	0	1.69	-0.66	3.32	-0.07	2.55	-0.24	-0.83	-0.67
TaLTP2.100	0	0	0	0	0	0	0	0	0	0	0	0	0	0	0	0	0	0	0	0	0	0	0	0	0
TaLTP2.101	0	0	0	0	0	-3.87	0	0	0	0	0	0	0	0	0	0	0	0	0	0	0	0	0	0	0
TaLTP2.102	0	0	0	-2.74	0	0	0	0	-3	0	0	0	0	0	-4.02	0	0	0	-4.81	-4.07	-3.21	-4.65	0	-2.19	0
TaLTP2.103	0	0	0	0	0	0	0	0	0	0	0	0	0	0	-5.43	0	0	0	0	0	0	0	0	0	0
TaLTP2.104	0	0	0	0	0	0	0	0	-1.86	0	0	-1.14	0	-0.87	0	-2.65	0	-1.02	0	0	0	0	0	0	0
TaLTP2.105	1.55	0	1.51	1.35	2.03	-0.92	1.73	-1.66	0.72	1.97	-0.04	2.11	0	4.16	0	0.1	0	3.52	0	-0.35	0	0	0	0	-3.17
TaLTP2.106	4.4	3.76	4.41	4.33	4.64	4.2	4.1	4.85	4.23	4.08	4.1	5.1	0	5.86	1.77	4.85	0	5.52	-1.34	2.73	-0.78	0	3.5	1.92	2.32
TaLTP2.107	0	-3.06	0	0	0	0	0	0	0	0	-2.88	-1.43	1.66	4.9	0	2.27	0	3.12	-2.89	2.79	0.25	0	0	2.79	0
TaLTP2.108	0	0	0	0	0	0	0	0	0	0	0	0	0	0	-1.89	0	0	0	0	0	0	0	0	0	0
TaLTP2.109	-1.65	5.08	-0.22	0.66	-0.98	0	0	-0.03	0	-1.82	-0.89	-3.35	8.54	-3.52	5.24	5.61	2.26	0	6.14	6.52	7.94	7.69	0.05	8.56	2.61
TaLTP2.11	-3.72	-0.81	0	0	-0.88	0	-3.05	0	-1.9	-3.29	-2.03	-1.76	0	-2.91	-1.52	0	0	0	0	-2.13	-3.49	-2.45	0	-3.6	-1.95
TaLTP2.110	0	0	0	0	0	0	0	0	0	0	0	0.32	0	0.18	0	0	0	-0.97	0	0	0	0	0	0	-2.88
TaLTP2.111	1.41	0	-0.61	1.76	0.1	-1.92	0.06	-2.66	0.72	-0.17	-0.84	1.6	0	2.79	0	-0.9	0	2.75	0	-1.94	0	0	0	0	0
TaLTP2.112	6.02	4.35	5.9	6.2	6.26	6.26	5.95	7.06	6.19	5.66	5.18	5.77	0	7.46	2.83	6.1	0	6.75	0.37	3.77	4.41	0	4.59	3.21	2.41
TaLTP2.113	0	0	0	0	0	0	0	0	-1.2	0	0.48	0.59	3.91	4.25	-1.88	3.03	0	2.94	-1.99	2.89	-2.84	0	0	4.16	0
TaLTP2.114	0	0	0	0	0	0	0	0	-0.94	-2.94	-3.35	0	0	0	2.01	0	0	0	0	-3.42	0	0	-3.25	0	-1.32
TaLTP2.115	0	0	0	0	0	0	0	0	0	0	0	-1.68	0	-1.24	0	0	0	-0.97	0	0	0	0	0	0	0
TaLTP2.116	0	0	0	0	0	0	0	0	0	0	0	3.16	0	2.81	0	-3.82	0	2.25	0	0	-3.66	0	0	0	0
TaLTP2.117	0	-2.81	0	0	0	0	0	1.16	0	0	0	0	0	0	-1.52	0	0	0	-1.04	0	0	0	0	0	0
TaLTP2.118	0	0	0	0	0	0	0	0	0	0	0	0	0	0	0	0	0	0	0	0	0	0	0	0	0
TaLTP2.119	0	0	0	0	0	0	0	0	0	0	0	5.98	0	5.57	0	-1.82	0	5.68	0	-3.86	-3.66	0	0	0	0

TaLTP2.12	9.06	7.33	8.59	8.97	9.33	8.61	7.72	-1.35	8.56	8.26	1.79	0	0	0	-0.12	-2.6	0	0	-0.54	0	0	0	2.31	0	0
TaLTP2.120	0	0	0	0	0	0	0	0	0	0	0	7.94	0	7.15	0	1.85	0	7.43	0	1.05	2.15	0	0	-2.76	0
TaLTP2.121	4.84	5.41	4.45	4.86	4.78	4.46	4.22	7.12	4.34	4.31	3.9	5.18	-2.56	6.47	3.8	5.47	-0.87	5.13	1.88	2.4	3.56	-1.1	3.71	1.22	4.01
TaLTP2.122	4.84	7.66	4.61	3.73	5.03	5.07	4.78	6.26	4.47	4.68	4.31	3.84	-3.62	0.1	2.84	7.57	-3.53	0.94	2.06	5.73	8.81	2.63	5.72	5.99	0
TaLTP2.123	0	-0.22	0	0	0	-2.81	0	-1.25	0	0	0	0	-3.46	0	0	0.46	0	0	-1.78	-0.82	0.38	0	0	0.27	0
TaLTP2.124	0	0	0	0	0	0	0	0	0	0	0	0	-1.71	0	0	0	0	0	0	0	0	0	0	-2.4	0
TaLTP2.125	0	0	0	0	0	0	0	0	0	0	0	-0.25	0	0	0	0	0	-4.06	0	0	4.62	0	0	0.45	0
TaLTP2.126	0	0	0	0	0	0	0	0	0	0	0	-0.47	0	-1.19	0	0	0	-0.59	0	0	0	0	0	0	0
TaLTP2.127	0	0	0	0	0	0	0	0	0	0	0	0	0	0	0	0	0	0	0	0	0	0	0	0	0
TaLTP2.128	0	0	0	0	0	0	0	0	0	0	0	-2.37	-2.53	0	0	0	0	-3.06	0	0	2.15	0	0	-0.99	0
TaLTP2.129	0	0	0	0	0	0	0	0	0	0	0	-3.17	0	0	0	0	0	0	0	0	-2.9	0	0	0	0
TaLTP2.13	1.82	6.36	2.07	2.18	1.54	2.46	2.37	4.71	2.78	1.75	0.97	-0.18	5.78	-0.05	3.95	4.97	0.05	1.67	3.86	5.12	6.69	5.65	3.59	5.93	-0.38
TaLTP2.130	0	0	0	0	0	0	0	0	0	0	0	-2.68	0	4.26	0	0	0	3.1	0	0	0	0	0	0	0
TaLTP2.131	0	0	0	0	0	0	0	0	0	0	0	0.06	0	0.31	0	0	0	2.07	0	0	0	0	0	0	0
TaLTP2.132	0	0	0	0	0	0	0	0	0	0	0	4.47	0	2.6	0	-2.07	0	2.76	0	-3.11	2.58	-1.28	0	-0.19	0
TaLTP2.133	0	0	0	0	0	0	0	0	0	0	0	3.74	0	2.12	-4.76	-1.44	0	2.35	0	-3.93	1.85	-2.72	0	-1.25	0
TaLTP2.134	0	0	0	0	0	0	0	0	0	0	0	4.64	0	2.8	-4.76	-1.19	0	3.47	0	0	2.42	-1.72	0	-1.03	0
TaLTP2.135	0	0	0	0	0	0	0	-2.52	0	0	0	-1.27	0	0	0	0	0	0	0	0	3.59	0	0	-2.69	0
TaLTP2.136	0	0	0	0	0	0	0	0	0	0	0	0	0	3.73	0	0	2.67	2.54	0	0	0	0	0	0	0
TaLTP2.137	0	0	0	0	0	0	0	0	0	0	0	-0.6	0	-1.2	0	0	0	0.62	0	0	0	0	0	0	0
TaLTP2.138	0	0	0	0	0	0	0	0	0	0	0	-0.66	0	0.26	0	-4.69	0	-0.22	0	-1.92	0	0	0	0	0
TaLTP2.139	0	0	0	0	0	0	0	0	0	0	0	-2.98	0	-3.23	0	-4.69	0	-2.28	0	-2.41	0	0	0	0	0
TaLTP2.14	7.2	2.67	6.69	6.6	7.49	6.42	6.2	0.46	7.26	6.49	-0.21	-0.68	0	-1.24	0	-2.6	0	0.25	0	0	-0.4	-0.78	-0.86	0	0
TaLTP2.140	0	0	0	0	0	0	0	0	0	0	0	-3.46	0	-3.23	0	0	0	-3.87	0	-2.73	0	0	0	0	0
TaLTP2.141	0	0	0	0	0	0	0	0	0	0	0	-0.43	0	-0.64	0	-3.69	0	-0.47	0	-0.92	0	0	0	0	0
TaLTP2.142	0	0	0	0	0	0	0	0	0	0	0	-3.99	0	0	0	0	0	0	0	0	0	0	0	0	0
TaLTP2.143	0	0	0	0	0	0	0	0	0	0	0	0	0	1.63	0	0	-0.58	-0.58	0	0	0	0	0	0	0
TaLTP2.144	0	0	0	0	0	0	0	0	0	0	0	0.61	0	0.17	0	-4.63	0	0.97	0	0	-7.49	0	0	0	0
TaLTP2.145	0	0	0	0	0	0	0	0	0	0	0	0	0	0	4.83	0	0	0	0	0	0	0	0	0	-2.71
TaLTP2.146	0.64	9.16	0.64	1.99	1.61	1.14	2.16	7.31	2.38	-2.25	0.23	0	2.29	0	6.57	1.6	7	0	5.57	2.02	0.14	0	3.35	-0.97	6.28
TaLTP2.147	0	-2.68	0	0	0	0	0	0	0	0	0	0	0	0	-2.4	0	0.91	0	0	0	0	0	0	0	6.63
TaLTP2.148	0	0	0	0	0	0	0	0	0	0	0	0	0	-2.06	3.4	0	-2.96	0	0	0	0	0	0	0	-1.32
TaLTP2.149	0	0	0	0	0	0	0	0	0	0	0	5.46	0	5.41	0	0	0	5.29	0	-3.86	0	0	0	-2.76	0
TaLTP2.15	0	0	0	0	0	0	0	0	0	0	0	4.83	0	2.97	0	-1.56	0	3.17	0	-3.91	0	0	0	0	0
TaLTP2.150	0	0	0	0	0	0	0	0	0	0	0	4.06	0	4.26	0	0	0	3.1	0	0	0	0	0	0	0
TaLTP2.151	4.88	3.14	4.43	4.56	4.24	4.19	4.2	6.54	4.37	4.21	3.84	5	0	5.32	2.69	5.13	0	4.51	0.8	2.27	2.81	-2.49	2.29	1.57	2.28
TaLTP2.152	-3.76	-2.38	0	0	0	0	0	-1.29	0	0	0	0	-1.17	0	-1.1	0	-2.4	0	0	-2.28	0.66	0	0	-0.76	0
TaLTP2.153	6.26	8.64	5.9	5.2	6.39	6.19	6.03	7.39	5.73	6.01	5.19	4.29	0	2.52	4.68	8.22	0	3.09	4.17	7.14	9.43	2.5	6.94	6.65	-0.53
TaLTP2.154	0	0	0	0	0	0	0	0	0	0	-1.33	0	0	0	0	0	0	0	0	3.63	0	2.86	0	-2.89	0
TaLTP2.155	0	0	0	0	0	-1.99	0	0	0	0	-2.91	-0.24	2.42	0.96	0	-0.38	0	0.58	-0.92	4.86	0	4.3	0	-2.89	0
TaLTP2.156	0	0	0	0	0	0	0	0	0	0	-1.33	0	-2.63	1.79	0	0.49	0	-0.2	-1.34	3.77	0	1.64	0	-2.89	0
TaLTP2.157	0	0	0	0	0	0	0	0	0	0	0	0	0	0	2.9	0	0	0	0	0	0	0	0	0	0
TaLTP2.158	0	0	0	0	0	0	0	0	0	0	0	0	0	0	2.24	0	0	0	0	0	0	0	0	0	0
TaLTP2.159	0	0	0	0	0	0	0	0	0	0	0	0	-1.55	0	0	0	0	0	1.49	0	0	0	-0.76	-1.31	0
TaLTP2.16	0	0	0	0	0	0	0	0	0	0	0	3.99	0	2.68	0	-0.05	0	2.44	0	-2.9	0	0	0	0	-4.11
TaLTP2.160	0	0	0	0	0	0	0	0	0	0	0	0	-2.04	0	0	0	0	0	1.45	0	0	0	-0.76	-1.31	0
TaLTP2.161	5.26	2.94	5.05	4.42	5.41	3.84	4.49	7.44	4.64	4.87	4.32	3.95	0	5.12	3.38	5.08	0	4.42	2.04	1.92	2.46	0	2.85	1.09	2.84
TaLTP2.162	5.3	8.01	4.88	4.43	5.5	5.13	4.68	6.09	4.7	5	4.21	3.68	0	0.46	2.6	7.28	0	1.9	2.18	5.3	8.46	1.81	6.46	5.87	-2.4
TaLTP2.163	-1.19	0	-3.11	-2.69	-2.12	-2.86	-3.2	0	-1.95	0	0	-3.94	-3.51	-3.12	-1.38	-2.26	0	0	-2.25	-1.56	-1.09	-3.67	0	-2.2	0
TaLTP2.164	0	0	0	0	0	0	0	0	0	0	0	-2.76	0.54	-0.44	0	-4.24	0	-1.89	0	-3.28	0	0	0	-3.19	0
TaLTP2.165	0	0	0	0	-2.14	0	0	0	0	0	0	2.47	-2.53	-2.14	0	-2.28	0	-0.89	0	-2.9	6.42	0	0	0.78	0
TaLTP2.166	0	0	0	0	0	0	0	0	0	0	0	-3.62	0	0	0	0	0	0	0	0	0	0	0	0	0
TaLTP2.167	0	0	0	0	0	0	0	0	0	0	0	0	0	-3.97	0	0	0	0	0	-2.14	0	0	0	0	0
TaLTP2.168	2.07	-2.77	0.64	3.73	1.61	1.92	3.12	-0.07	3.18	1.07	-1.57	0	1.7	-2.87	7.33	-0.65	7.11	0	4.67	0.32	-2.44	-1.41	1.6	-0.56	8.48
TaLTP2.169	0	0	0	0	0	0	0	0	0	0	0	-0.46	-0.04	0.38	0	-1.97	0	-0.69	0	5.2	0	4.07	0	0	0
TaLTP2.17	0	0	0	0	0	-2.36	0	0	0	0	0	7.72	0	7.13	-3.19	1.36	0	7.1	0	-2.37	1.09	0	-1.2	-0.46	-1.59
TaLTP2.170	0	0	0	0	0	0	0	0	0	0	0	0.65	0.18	-2.21	0	0	0	-0.69	-0.6	6.2	0	5.84	0	-1.31	0
TaLTP2.171	0	0	0	0	0	0	0	0	0	0	0	0.65	1.46	3.83	0	1.79	-2.52	3.64	-0.92	6.82	-1.78	4.47	0	0.28	0
TaLTP2.172	0	0	0	0	0	0	0	0	0	0	0	0	0	0	0	0	0	0	0	0	0	0	0	0	0
TaLTP2.173	0	0	0	0	0	0	0	0	0	0	0	0	0	0	-2.88	0	0	0	0	0	0	0	0	0	0
TaLTP2.174	0	0	0	0	0	0	0	0	0	0	0	0	0	0	1.85	0	0	0	0	0	0	0	0	0	0
TaLTP2.175	1.56	5.14	1.59	2.57	2.65	2.12	0.65	-0.72	1.53	0.4	0	0	0	0	7.93	-2.56	0	0	3.21	0	0	0	0.41	0	-1.25
TaLTP2.176	1.05	6.66	2	1.9	1.87	1.55	0.83	3.56	0.98	-1.22	-2.53	0	-2.25	0	5.38	1.3	1.18	0	2.75	0.53	-2.4	-2.36	1.64	-1.52	6.14
TaLTP2.177	0	0	0	0	0	0	0	0	0	0	0	-1.46	-0.04	4.57	0	2.2	0	3.89	-1.92	5.13	0	3.6	0	-0.57	0
TaLTP2.178	0	0	0	0	0	0	0	0	0	0	0	0	0	0	2.07	0	0	0	0	0	0	0	0	0	0
TaLTP2.179	0	0	0	0	0	0	0	0	0	0	0	0	0	0	0.74	0	0	0	0	0	0	0	0	0	0
TaLTP2.18	0	0	0	0	0	0	0	0	0	0	0	0	0	0	0	0	0	0	0	0	0	0	0	-3.55	0
TaLTP2.180	-2.16	10.3	-3.52	-4.09	0	-3.28	-2.61	1.93	-3.34	0	0	0	0	0	-4.12	-4.26	-2.84	0	0	0	0	0	0	5.34	0
TaLTP2.181	0	9.68	0	-4.15	0	0	0	0.58	0	0	-2.31	0	0	0	0	0	0	0	0	0	0	0	0	6.45	0
TaLTP2.182	4.36	0.29	4.11	3.17	4.42	3.98	2.72	5.39	3.63	3.81	2.96	-0.03	0	-0.21	2.77	4.21	-3.1	-0.5	1.14	3.82	1.29	0.57	1.81	1.79	-3.78
TaLTP2.183	-3.15	6.62	-3.51	-2.07	-1.51	-1.68	-3.59	-0.87	-3.32	-2.76	-1.91	-4.34	-2.92	0	-3.11	0	-2.24	0	-2.66	0	0	0	3.58	0	0

TaLTP2.184	0	2.71	0	0	0	-3.05	0	0	0	0	-4.01	0	0	0	0	0	0	0	0	0	0	0	1.05	0	0
TaLTP2.185	6.72	4.22	6.66	5.94	6.73	6.24	5.22	6.77	6.05	6.25	4.8	0	0	-2.79	5.55	5.58	0	-3.67	3.62	4.74	6.36	-2.34	4.19	4.64	0
TaLTP2.186	0	6.15	0	0	0	0	0	-3.73	0	0	-2.92	0	0	0	0	0	0	0	0	0	0	0	5.95	0	0
TaLTP2.187	0	9.81	0	0	0	-3.34	0	0.74	-2.81	0	-3.31	0	0	0	0	0	-3.91	0	0	0	0	0	5.44	0	0
TaLTP2.188	0	10.5	0	-2.12	0	-1.73	0	2	-2.79	-3.81	0	0	0	0	0	0	-2.88	0	0	0	0	0	5.45	0	0
TaLTP2.189	0	-1.44	0	0	0	0	0	0	0	0	0	0	0	1.32	0	0	0	-0.6	0	-0.94	0	0	0	0	0
TaLTP2.19	2.22	1.93	2.22	1.21	2.39	1.34	0.79	-0.39	1.94	1.25	-2.57	1.86	0	4.53	0	2.11	0	3.53	-0.99	2.88	0	4.41	0.32	-2.56	0
TaLTP2.190																									
TaLTP2.191	0	0	0	0	0	0	0	0	0	0	0	4.99	0	5.36	0	-0.65	0	4.5	0	-0.88	0.52	-2.47	0	0	0
TaLTP2.192	0	0	0	0	0	0	0	0	0	0	-3.62	6.77	0	6.07	0	-0.19	0	5.45	0	0	-1.16	0	0	0	0
TaLTP2.193	0	0	0	0	0	0	0	0	0	0	-3.04	5.86	0	4.73	0	1.72	0	4.35	0	-2.1	-2.9	0	0	0	0
TaLTP2.194	0	0	0	0	0	0	0	0	0	0	-3.04	5.86	0	4.73	0	1.72	0	4.35	0	-2.1	-2.9	0	0	0	0
TaLTP2.195	0	0	0	0	0	0	0	0	0	0	-2.64	6.12	0	7.15	0	0.03	0	6.2	0	-3.71	2.62	0	-3.55	-1.61	-0.75
TaLTP2.196	0	0	0	0	0	0	0	0	0	0	0	6.41	0	7.47	0	-2.67	0	6.27	0	0	0.95	0	0	0	-3.92
TaLTP2.197	0	0	0	0	0	0	0	0	0	0	0	0	0	3.18	0	0	0	0.07	0	-0.94	0	-1.68	0	0	-3.17
TaLTP2.198	6.32	0	6.16	5.98	6.74	5.72	5.38	-3.53	6.11	5.86	-1.72	0	0	-2.44	0	0	0	0	0	0	0	0	-2.63	0	0
TaLTP2.199	0	-0.68	0	0	-1.9	0	0	0	0	0	0	0	0	0	0	-0.98	1.23	0	0	1.65	-2.36	0	0	0	0
TaLTP2.2	1.89	8.78	2.26	2.29	2.81	3.76	3.2	6.21	2.57	2.11	2.4	0	5.03	0	4.69	4.88	-1.95	0	5.21	5.64	5.56	5.62	4.21	5.46	-0.12
TaLTP2.20	4.64	4.41	4.05	4.37	4.86	4.64	3.39	2.63	4.42	4.1	2.01	6.38	-2.3	8.77	0	5.14	0	8.17	0.39	6.74	1.4	6.79	3.95	1.25	0
TaLTP2.200	0	0	0	0	0	0	0	0	0	0	0	0	0	0	0	0	0	0	0	0	0	0	0	0	0
TaLTP2.201	0	0	0	-3.51	0	0	0	0	0	0	0	6.7	0	6.17	0	0	-3.23	5.76	0	0	0	0	0	0	0
TaLTP2.202	0	0	0	0	0	0	0	0	0	0	0	5.15	0	3.56	0	-2.65	-2.23	3.84	0	0	0	0	0	0	-2.9
TaLTP2.203	0	0	0	0	0	0	0	0	0	0	0	6.61	0	4.62	0	-1.07	-2.23	5.02	0	0	0	0	0	0	0
TaLTP2.204	0	0	0	0	0	0	0	0	0	0	0	5.41	0	3.77	0	-3.65	-3.23	4.28	0	0	0	0	0	0	0
TaLTP2.205	0	0	0	0	0	0	0	0	0	0	0	5.57	0	3.78	0	0	0	4.34	0	0	0	0	0	0	0
TaLTP2.206	0	0	0	-3.51	0	0	0	0	0	0	0	6.31	0	4.49	0	0	0	4.3	0	0	0	0	0	0	0
TaLTP2.207	0	0	0	0	0	0	0	0	0	0	0	7.36	0	6.51	0	2.41	0	6.23	0	0.54	1.5	-1.91	-3.55	-2.03	-2.92
TaLTP2.208	0	0	0	0	0	0	0	0	0	0	-3.64	7.08	0	7.27	0	2.55	0	6.58	0	0.16	1.17	-3.49	0	-1.61	0
TaLTP2.209	0	0	0	0	0	0	0	0	0	0	0	6.33	0	5.72	0	0.33	0	5.57	0	-2.97	-1.18	0	0	-2.61	-3.92
TaLTP2.21	1.32	6.19	0.64	0.99	1.83	0.92	-0.43	1.07	1.14	-2.25	-2.57	4.37	-2.3	5.14	-1.48	3.56	0	4.11	-1.58	4.33	-2.44	3.84	0.97	-2.56	0
TaLTP2.210	0	0	0	0	0	0	0	0	0	0	-3.64	6.78	0	6.46	0	2.04	0	6.28	0	-0.32	0.4	-3.49	0	-2.61	-3.92
TaLTP2.211	0	0	0	0	0	0	0	0	0	0	0	5.06	0	5.24	0	0.63	0	4.84	0	-1.65	-0.6	0	0	0	0
TaLTP2.212	-2.79	0	0	0	-2.09	0	-1.13	-1.51	-1.97	0	-2.7	2.16	0	2.6	0	1.05	0	3.2	0	1.21	-1.56	0	0	-2.68	0
TaLTP2.213	0	0	0	0	0	0	0	0	0	0	0	2.18	0	0.63	0	-2.34	0	1.49	0	-1.37	0	0	0	0	0
TaLTP2.214	6.46	0	6.11	6.27	6.9	6.1	5.54	-3.52	6.24	6.08	-0.9	0	0	0	0	0	0	0	0	0	0	0	-1.02	0	0
TaLTP2.215	0	0	0	0	0	0	0	0	0	0	0	0	0	0	0	0	0	0	0	0	0	0	0	0	0
TaLTP2.216	0	0	0	0	0	0	0	0	0	0	0	6.86	0	6.95	0	-2.67	0	6.36	0	0	0	0	0	0	0
TaLTP2.217	0	0	0	0	0	0	0	0	0	0	0	1.12	0	1.7	0	0	0	2.12	0	0	0	0	0	0	0
TaLTP2.218	0	0	0	0	0	0	0	0	0	0	0	3.64	0	2.22	0	0	0	1.53	0	0	0	0	0	0	0
TaLTP2.219	0	0	0	0	0	0	0	0	0	0	0	7.34	0	7.63	0	-0.67	0	6.98	0	0	-1.92	0	0	0	0
TaLTP2.22	0	0	0	0	0	0	0	0	0	0	-2.15	0	0	-0.85	0	0	0	0	0	0	0	0	0	0	0
TaLTP2.220	0	0	0	0	0	0	0	0	0	0	0	0.41	0	3.13	0	0	0	0.89	0	0	0	0	0	0	0
TaLTP2.221	0	0	0	0	0	0	0	0	0	0	0	-0.4	0	0	0	0	0	-2.8	0	0	0	0	0	0	0
TaLTP2.222	0	0	0	0	0	0	0	0	0	0	0	0	0	0	0	0	-0.14	0	0	0	0	0	0	0	7.71
TaLTP2.223	2.49	8.85	2.76	3.41	3.23	2.04	1.99	7.22	3.38	1.83	0	0	0.7	0	7.87	1.52	5.27	0	6.9	3.08	2.26	1.29	3.07	0	7.72
TaLTP2.224	3.45	5.88	2.7	3.42	2.57	2.63	2.11	-0.26	3	2.25	-2.44	0	0	0	7.54	-1.52	0	0	2.46	0	0.01	0	1.73	-0.11	0.67
TaLTP2.225	2.44	4.09	3.5	5.01	3.81	4.39	4.75	4.98	4.91	2.64	3.83	1.05	5.89	1.24	8.57	6.9	3.11	0.96	7.48	7.86	8.74	6.31	7.01	8.18	3.49
TaLTP2.226	1.47	3.91	2.67	4.41	3.37	3.45	4.41	2.29	3.75	1.27	2.71	0	3.45	0	6.63	6.01	4.32	0	5.3	6.11	7.44	3.63	5.48	6.8	2.07
TaLTP2.227	0	-2.58	0	0	0	0	0	0	-3.41	0	-1.89	0	3.82	0	0.61	0.94	0	-3.36	1.19	3.27	5.21	4.53	-1.9	6.17	-0.82
TaLTP2.228	0	-2.58	0	0	0	0	0	0	-3.41	0	-1.89	0	3.82	0	0.61	0.94	0	-3.36	1.19	3.27	5.21	4.53	-1.9	6.17	-0.82
TaLTP2.229	0	-5.39	0	0	0	0	0	0	0	0	-3.22	0	3.6	0	-0.24	0.26	0	-3.36	0.36	2.37	5.05	4.08	-1.8	5.87	-2.52
TaLTP2.23	-2.72	-1.81	0	0	-4.34	0	-3.05	0	0	0	0	-1.18	0	-0.1	0	-0.68	0	-0.33	-2.62	4.52	0	3.76	-1.53	0	0
TaLTP2.230	0	-5.39	0	0	0	0	0	0	0	0	-1.22	0	3.97	0	0.11	0.72	0	-3.36	0.97	2.58	5.06	4.62	-2.25	6.07	-2.52
TaLTP2.231	0	0	0	0	0	0	0	0	0	0	0	2.47	0	1.61	0	-3.17	0	2.84	0	0	0	0	0	0	0
TaLTP2.232	0	0	0	0	0	0	0	0	0	0	0	-0.89	0	-0.86	0	0	0	-0.93	0	0	0	0	0	0	0
TaLTP2.233	0	0	0	0	0	0	0	0	0	0	0	-3.97	0	-3.16	0	0	0	-1.75	0	0	0	0	0	0	0
TaLTP2.234	0	0	0	0	0	0	0	0	0	0	0	-4.47	0	0	0	0	0	-4.62	0	0	0	0	0	0	0
TaLTP2.235	0	0	0	0	0	0	0	0	0	0	0	0	0	0	0	0	0	0	0	0	0	0	0	0	0
TaLTP2.236	0	0	0	0	0	0	0	0	0	0	0	-5.27	0	0.93	0	0	-4.17	0.36	0	0	0	0	0	0	0
TaLTP2.237	0	0	0	0	0	0	0	0	0	0	0	4.09	-3.53	0.82	0	-3.86	0	1.56	0	-3.9	7.17	0	-3.74	2.91	0
TaLTP2.238	0	0	0	0	0	0	0	0	0	0	0	-1.72	0.51	0	0	0	0	-1.02	0	-2.68	0	0	0	-2.56	0
TaLTP2.239	0	0	0	0	0	0	0	0	0	0	0	0	0	0	0	0	0	0	0	0	0	0	0	0	0
TaLTP2.24	-0.18	7.25	0.26	0.92	0	0.55	0.78	2.84	1.78	0.75	-0.77	0	5	0	3.52	4.71	0	0	3.26	5.42	6.28	5.61	2.69	5.19	-2.71
TaLTP2.240	0	0	0	0	0	0	0	0	0	0	0	0	0.62	-4.59	0	-4.3	0	-3.54	0	-0.43	-4.14	0	0	-1.07	0
TaLTP2.241	-2.39	-1.99	-2.86	0.08	-0.6	-0.25	0.11	0.96	0.78	-1.56	-0.58	-2.58	3.86	-3.38	4.66	3.75	-0.58	-5.68	3.87	4.11	5.97	2.42	2.99	6.12	-0.38
TaLTP2.242	-5.23	0	0	-2.15	-2.98	-2.7	-1.81	-2.03	-1.83	-3.24	-2.63	-3.35	2.68	0.13	3.78	2.09	-0.12	-0.84	2.64	2.98	3.78	2.53	1.4	4.68	-0.87
TaLTP2.243	0	0	0	-2.74	0	-3.87	0	0	-3	0	0	0	0	0	-4.02	0	0	0	-4.81	-4.07	-3.21	-4.65	0	-2.19	0

TaLTP2.244	0	0	0	0	0	0	0	0	0	0	0	-3.27	0	0.39	0	0	0	0.59	0	0	0	0	0	0	0
TaLTP2.245	0	0	0	0	0	0	0	0	0	0	0	0	0	1.42	0	0	0	-0.85	0	0	0	0	0	0	0
TaLTP2.246	0	0	0	0	0	0	0	0	0	0	0	0	0	0	0	0	0	0	0	0	0	0	0	0	0
TaLTP2.247	0	0	0	0	0	0	0	0	0	0	0	0	0	0	0	0	0	0	0	0	0	0	0	0	0
TaLTP2.248	0	0	0	0	0	0	0	0	0	0	0	0	0	0	0	0	0	-4.08	0	0	0	0	0	0	0
TaLTP2.249	0	0	0	0	0	0	0	0	0	0	0	0	0	-1.1	0	0	0	-2.91	0	0	0	0	0	0	0
TaLTP2.25	9.06	1.92	8.72	9.32	9.37	8.25	8	0.46	9.12	8.2	1.37	0	0	0	-2.44	0	0	0	0	0	0	0	1.36	0	0
TaLTP2.250	0	0	0	0	0	0	0	0	0	0	0	0	0	0	0	0	0	0	0	0	0	0	0	0	0
TaLTP2.251	0	0	0	0	0	0	0	0	0	0	0	0	0	0	0	0	0	0	0	0	0	0	0	0	0
TaLTP2.252	0	0	0	0	0	0	0	0	0	0	0	0	0	0	0	0	0	0	0	0	0	0	0	0	0
TaLTP2.253	-5.23	0	0	-2.15	-2.98	-2.7	-1.81	-2.03	-1.83	-3.24	-2.63	-3.35	2.68	0.13	3.78	2.09	-0.12	-0.84	2.64	2.98	3.78	2.53	1.4	4.68	-0.87
TaLTP2.254	0	0	0	0	0	0	0	0	0	0	0	-3.05	0.94	3.64	0	0.77	0	3.22	1.02	5.76	0	4.87	0	-1.72	0
TaLTP2.255	0	0	0	0	0	0	0	0	0	0	-2.5	0	-2.63	1.44	0	0.15	0	0.53	0.82	3.6	0	2.1	0	0	0
TaLTP2.256	0	0	0	0	0	0	0	0	0	0	0	0	0	0	0	0	0	-2.39	0	0	0	0	0	0	0
TaLTP2.257	0	0	0	0	0	0	0	0	0	0	0	0	0	0	0	0	0	0	0	0	0	0	0	0	0
TaLTP2.258	0	0	0	0	0	0	0	0	0	0	0	0	0	0	0	0	0	0	0	0	0	0	0	0	0
TaLTP2.259	0	0	0	0	0	0	0	0	0	0	0	-5.27	0	-5.44	0	0	0	-1.16	0	0	0	0	0	0	0
TaLTP2.26	-3.96	0	0	0	0	-0.74	0	0	-1.13	0	0	0	0	0	0	0	0	0	0	0	-1.56	0	-3.92	-2.4	0
TaLTP2.260	0	0	0	0	0	0	0	0	0	0	0	0.2	-0.51	3.49	0	0.51	0	2.78	-0.05	5.78	0	5.12	0	-2.57	0
TaLTP2.261	0	0	0	0	0	0	0	0	0	0	0	0	0	0	0	0	0	0	0	0	0	0	0	0	0
TaLTP2.262	0	-3.39	0	0	-3.15	-2.87	0	-3.03	-3	0	-1.63	0	7.45	-4.1	4.76	4.71	-0.09	0	5.56	5.66	6.51	6.3	-1.54	7.78	2.91
TaLTP2.263	-5.23	0	0	-2.15	-2.98	-2.7	-1.81	-2.03	-1.83	-3.24	-2.63	-3.35	2.68	0.13	3.78	2.09	-0.12	-0.84	2.64	2.98	3.78	2.53	1.4	4.68	-0.87
TaLTP2.264	0	0	0	0	0	0	0	0	0	0	0	0	0	1.16	0	0	-4.17	0.36	0	0	0	0	0	0	0
TaLTP2.265	0	0	0	0	0	0	0	0	0	0	0	0	0	0	0	0	0	0	0	0	0	0	0	0	0
TaLTP2.266	0	0	0	0	0	0	0	0	0	0	0	-3.97	0	0	0	0	0	-4.08	0	0	0	0	0	0	0
TaLTP2.267	-2.39	-1.99	-2.86	0.08	-0.6	-0.25	0.11	0.96	0.78	-1.56	-0.58	-2.58	3.86	-3.38	4.66	3.75	-0.58	-5.68	3.87	4.11	5.97	2.42	2.99	6.12	-0.38
TaLTP2.268	-5.23	0	0	-2.15	-2.98	-2.7	-1.81	-2.03	-1.83	-3.24	-2.63	-3.35	2.68	0.13	3.78	2.09	-0.12	-0.84	2.64	2.98	3.78	2.53	1.4	4.68	-0.87
TaLTP2.269	0	0	0	0	0	0	0	0	0	0	0	0	0	0	0	0	0	0	0	0	0	0	0	0	0
TaLTP2.27	0	0	0	0	0	0	0	0	0	0	0	6.9	0	5.14	0	1.96	0	5.62	0	0.05	0	0	0	0	0
TaLTP2.270	0	0	0	0	0	0	0	0	0	0	0	0	0	0	0	0	0	0	0	0	0	0	0	0	0
TaLTP2.271	0	0	0	0	0	0	0	0	0	0	0	0	0	0	0	0	0	0	0	0	0	0	0	0	0
TaLTP2.272	0	0	0	0	0	0	0	0	0	0	0	0	0	0	0	0	0	0	0	0	0	0	0	0	0
TaLTP2.273	0	0	0	0	0	0	0	0	0	0	0	1.62	0	-0.08	0	0	0	1.06	0	0	0	0	0	0	0
TaLTP2.274	0	0	0	0	0	0	0	0	0	0	0	1.57	0	0.61	0	-4.77	0	1.66	0	0	0	0	0	0	0
TaLTP2.28	0	0	0	0	0	0	0	0	0	0	0	6.24	0	4.73	0	-0.22	-1.96	5.07	0	-2.42	0	0	0	0	0
TaLTP2.29	0	0	0	0	0	0	0	-2.95	0	0	0	6.9	0	5.62	0	0.41	0	6.09	0	-2.21	0	0	0	0	0
TaLTP2.3	-0.01	0	-2.26	0.49	0.05	-0.01	-2.35	-3.78	-0.28	-1.2	0	0	0	-0.47	0	0	0	0	0	0	-0.51	0	-2.29	-1.94	0
TaLTP2.30	-3.21	0	0	0	0	0	0	0	0	0	0	6.39	0	5.68	0	0.57	0	5.98	0	-3.27	-3.05	0	0	0	0
TaLTP2.31	0	0	0	0	0	0	0	0	0	0	0	6.46	0	5.35	0	1.01	0	5.95	0	-2.27	0	0	0	0	0
TaLTP2.32	0	0	0	0	0	0	0	0	0	0	0	0	0	0	0	0	0	0	0	0	-1.18	0	-3.55	0	0
TaLTP2.33	1.42	3.23	1.38	2.75	0.88	1.82	0.53	0.61	2.01	1.59	-0.25	6.1	0.29	8.13	0	3.69	0	7.86	1.49	6.43	1.97	6.67	2.74	0.44	-2.91
TaLTP2.34	2.57	6.14	2.91	2.41	3.15	3.09	1.69	2.14	2.89	2.83	0.6	6.1	0	7.15	-0.48	4.29	0	6.44	1.01	4.94	2.64	4.24	2.52	0.61	-0.33
TaLTP2.35	0.25	2.61	0.56	1.66	1.67	0.58	-0.77	-0.15	-1.93	0.26	0.15	3.41	0	3.2	-1.56	0.74	0	1.76	0	2.47	-2.53	0.32	0.89	0	-2.99
TaLTP2.36	0	-0.52	0	0	0	0	0	-2.47	0	0	-1.66	-2.8	0	-1.95	0	-2.72	0	0	0	-0.76	0	0	0	0	0
TaLTP2.37	0	0	0	0	0	0	0	0	0	0	0	0	0	0	0	0	0	0	0	0	0	0	0	0	0
TaLTP2.38	0	0	0	0	-3.92	0	0	0	0	0	0	0	-0.29	2.42	0	0	0	-0.49	-0.56	3.33	0	-1.96	0	-2.14	0
TaLTP2.39	0	0	0	0	0	0	0	0	-2.65	0	0	4.72	0	3.88	0	0	0	3.57	0	0	0	0	0	0	0
TaLTP2.4	0	0	0	0	0	0	0	0	0	0	0	6.92	0	5.55	0	1.5	0	5.98	0	0.61	0	0	-3.75	-3.82	-4.12
TaLTP2.40	0	0	0	0	0	0	0	0	0	0	0	7.81	0	6.44	0	-1.63	0	7.06	0	0	0	0.25	0	-1.99	0
TaLTP2.41	0	0	0	0	0	0	-4.54	-3.98	0	0	-4.17	0	1.78	0	0	2.83	0	-3.42	-4.19	0.66	4.25	0	-2.26	5.4	0
TaLTP2.42	0	0	0	0	0	0	0	0	0	0	0	-0.24	0	-1.62	0	-0.16	0	-0.42	0	4.45	0	4.04	0	-2.89	0
TaLTP2.43	0	0	0	0	0	0	0	0	0	0	-1.91	1.86	-2.63	2.11	0	-1.38	0	1.75	-1.92	5.52	0	5.47	0	-2.89	0
TaLTP2.44	0	0	0	0	0	0	0	0	0	0	-2.91	-0.46	-0.3	1.25	0	1.12	0	-0.01	0.08	6.55	0	5.98	-2.82	-1.31	0
TaLTP2.45	0	0	0	0	-1.67	0.98	0	-1.04	-1.58	-1.96	0	0	0	0	-2.15	-2.32	0	0	0	-2.35	3.65	0	-2.15	-1.23	0
TaLTP2.46	0	0	0	0	0	0	0	0	0	0	0	0	0	0	0	0	0	0	0	0	0	0	0	-0.03	0
TaLTP2.47	0	0	0	0	0	0	0	0	0	0	0	0	-5.34	0	0	0	0	0	0	0	0	0	0	0.45	0
TaLTP2.48	0	0	0	0	0	0	0	0	0	0	0	0	-5.34	0	0	0	0	0	0	0	0	0	0	-0.24	0
TaLTP2.49	0	0	0	0	0	0	0	0	0	0	0	0	0	0	0	0	0	0	0	0	0	0	0	0.12	0
TaLTP2.5	0	0	0	0	0	0	0	-3.16	0	0	-3.35	6.47	0	6.07	-3.24	0.07	-2.96	6.08	0	-1.84	1.83	0	0	0.26	-1.06
TaLTP2.50	0	0	0	0	0	0	0	0	0	0	0	0	-5.34	0	0	0	0	0	0	0	0	0	0	-0.24	0
TaLTP2.51	0	0	0	0	0	0	0	0	0	0	0	0	0	0	0	0	0	0	0	0	0	0	0	0.12	0
TaLTP2.52	0	0	0	0	0	0	0	0	0	0	0	0	0	0	0	0	0	0	0	0	0	0	0	1.44	0
TaLTP2.53	0	0	0	0	0	0	0	0	0	0	0	0	0	0	0	0	0	0	0	0	0	0	0	0	0
TaLTP2.54	0	0	0	0	0	0	0	0	0	0	0	0	0	0	0	0	0	0	0	0	0	0	0	-1.61	0
TaLTP2.55	0	0	0	0	0	0	0	0	0	0	0	0	-5.34	0	0	0	0	0	0	0	0	0	0	-0.24	0
TaLTP2.56	0	0	0	0	0	0	0	0	0	0	-3.64	0	0	0	0	0	0	0	0	0	0	0	0	0	0
TaLTP2.57	0	0	0	0	0	0	0	0	0	0	-3.64	0	0	0	0	0	0	0	0	0	0	0	0	-0.09	0
TaLTP2.58	0	0	0	0	0	0	0	0	0	0	0	0	0	0	0	0	0	0	0	0	0	0	0	-0.61	0
TaLTP2.59	0	0	0	0	0	0	0	0	0	0	0	0	0	0	0.52	0	0	0	0	0	0	0	0	0	0
TaLTP2.6	0	0	0	-2.13	0	0	-2.59	0	0	0	0	5.3	0	4.91	0	-1.65	0	5.09	0	-1.27	0	0	0	-2.16	0
TaLTP2.60	0	0	0	0	0	0	0	0	0	0	0	0	0	0	0	0	0	0	0	0	0	0	0	0	1.53

TaLTP2.61	0	0	0	0	0	0	0	0	0	0	0	0	0	0	0	0	0	0	0	0	0	0	0	0
TaLTP2.62	0	0	0	0	0	0	0	0	0	0	0	5.92	0	4.68	0	3.07	0	5.12	-3.61	0.58	-1.88	1.87	-3.5	-1.99	0
TaLTP2.63	0	0	0	0	0	0	0	0	0	0	0	7.69	0	6.44	0	-0.17	0	6.7	0	0	-3.46	0	0	0	0
TaLTP2.64	0	0	0	0	0	0	-4.54	0	0	0	-4.17	0	4.61	0	-4.05	2.59	0	-4.42	-4.19	-1.32	4.91	-3.03	-1.9	6.43	0
TaLTP2.65	0	0	0	0	0	0	0	0	0	0	-1.91	1.34	1.46	3.12	0	1.73	0	3.72	1.78	6.31	0	5.92	0	-1.31	0
TaLTP2.66	0	0	0	0	0	0	0	0	0	0	0	0	0	0	0	0	0	0	0	0	0	0	0	0	0
TaLTP2.67	0	0	0	0	0	0	0	0	0	0	0	-3.05	0.94	3.64	0	0.77	0	3.22	1.02	5.76	0	4.87	0	-1.72	0
TaLTP2.68	0	0	0	0	0	0	0	0	0	0	-3.18	0	0	1.65	0	0.15	0	-0.81	-0.81	2.45	0	1.66	0	0	0
TaLTP2.69	0	0	0	0	0	0	0	0	0	0	0	0	0	1.44	0	0.35	0	-0.92	0.25	2.76	0	1.59	0	0	0
TaLTP2.7	0	0	0	0	0	0	0	0	0	0	0	0	0	0	0	0	0	0	0	0	0	0	0	0	0
TaLTP2.70	0	0	0	0	0	0	0	0	0	0	-3.18	0	0	1.65	0	0.15	0	-0.81	-0.81	2.45	0	1.66	0	0	0
TaLTP2.71	0	0	0	0	0	0	0	0	0	0	-5.56	-6.64	0	0	0	0	0	0	-6.56	0	0	-4.82	0	0	0
TaLTP2.72	0	0	0	0	0	0	0	0	0	0	0	0	0	0	-2.6	0	0	0	0	0	0	0	0	0	0
TaLTP2.73	-3.54	0	0	0	-2.88	-1.61	-1.95	-1.37	0	-2.13	-3.56	0	0	0	-2.45	-1.59	0	0	0	-2.63	0.58	0	-3.46	-1.94	0
TaLTP2.74	0	0	0	0	0	0	0	0	0	0	0	0	0	0	1.33	0	0	0	0	0	0	0	0	0	0
TaLTP2.75	0	0	0	0	0	0	0	2.65	0	0	0	0	0	0	-2.44	0	0	0	0.27	0	0	0	0	0	0
TaLTP2.76	0	0	0	0	0	0	0	0	0	0	0	0	0	0	0	0	0	0	0	0	0	0	0	0	3.94
TaLTP2.77	0	0	0	0	0	0	0	0	0	0	0	8.47	0	6.61	0	4.56	0	7.06	0	-3.67	0.54	2.48	0	-1.25	0
TaLTP2.78	0	-3.33	0	0	0	0	0	-3.98	0	0	0	0	5.62	-2.48	-1.47	0.34	-3.77	0	-3.19	1.58	5.28	-0.33	-2.07	6.46	0
TaLTP2.79	0	0	0	0	0	0	0	0	0	0	-1.33	1.12	0.18	0.79	0	1.56	0	0.31	-0.34	6.78	0	5.93	0	-0.89	0
TaLTP2.8	5.02	5.88	4.58	4.8	5.32	5.11	3.65	3.85	4.42	4.56	1.82	6.48	-0.71	9.04	-0.89	5.41	0	8.13	2.75	6.68	1.67	6.94	3.52	2.73	-1.91
TaLTP2.80	0	0	0	0	0	0	0	0	0	0	0	0.47	-1.63	1.48	0	0.95	0	1.72	0.08	5.51	0	4.92	0	-1.72	0
TaLTP2.81	0	0	0	0	0	0	0	0	0	0	0	0.86	0	-0.62	0	-1.38	0	-1.01	-1.34	5.14	0	5.3	0	0	0
TaLTP2.82	0	0	-1.63	-1.31	-1.67	0	-1.7	0.54	-1.58	-1.96	0	0	0	0	-2.15	0.26	0	0	0	0	3.02	0	0	-1.23	0
TaLTP2.83	0	0	0	0	0	0	0	0	0	0	0	0	0	0	0	0	0	0	0	0	0	0	0	0	3.43
TaLTP2.84	0	0	0	0	0	0	0	0	0	0	0	0	0	-3.52	1.47	-3.26	0	0	-1.64	0	4.01	0	-3.12	4.19	-2.52
TaLTP2.85	0	0	0	0	0	0	0	0	0	0	0	0	0	0	-3.11	0	0	0	-2.23	0	3.41	0	0	1.33	0
TaLTP2.86	-1.06	-1.14	-1.91	0	-1.94	-1.62	0	-1.35	0	0	0	-1.09	-2.25	0.18	0	0	-2.14	-0.55	0	0	0	0	0	0	0
TaLTP2.87	4.9	3.3	4.69	5.53	5.12	4.99	5.19	5.73	5.36	4.74	4.74	5.64	0	6.47	2.44	6.05	0	6.25	-0.08	3.81	2.56	0	4.27	3.14	1.71
TaLTP2.88	-1.97	1.49	-2.26	0	-2.28	0	0	-2.73	0	0	0	1.65	4.44	5.81	0	1.28	0	4.5	0.4	3.13	-2.78	-1.75	-0.82	3.22	-0.91
TaLTP2.89	0	0	0	0	0	0	0	0	0	0	0	-2.23	0	-2.4	0	0	0	-0.64	0	0	0	0	0	0	0
TaLTP2.9	1.84	0	1.38	1.99	2.41	1.51	1.16	0	2.38	2.39	-2.57	5.55	-2.3	6.26	-2.48	3.08	0	5.73	-0.99	5.07	0.14	3.88	0.52	-0.97	0
TaLTP2.90	0	0	0	0	0	0	0	0	0	0	0	0	0	0	0	0	0	0	0	0	0	0	0	0	0
TaLTP2.91	0	-3.39	0	0	-3.15	-2.87	0	-3.03	-3	0	-1.63	0	7.45	-4.1	4.76	4.71	-0.09	0	5.56	5.66	6.51	6.3	-1.54	7.78	2.91
TaLTP2.92	0	-3.39	0	0	-3.15	-2.87	0	-3.03	-3	0	-1.63	0	7.45	-4.1	4.76	4.71	-0.09	0	5.56	5.66	6.51	6.3	-1.54	7.78	2.91
TaLTP2.93	-1.75	0.69	-1.34	1.13	-0.13	1.37	0.94	2.5	1.52	-0.53	1.19	-3.08	5.72	-3.38	6.05	4.46	-0.69	-3.1	5.55	5.34	6.71	4.35	4.97	6.87	0.75
TaLTP2.94	-1.75	0.69	-1.34	1.13	-0.13	1.37	0.94	2.5	1.52	-0.53	1.19	-3.08	5.72	-3.38	6.05	4.46	-0.69	-3.1	5.55	5.34	6.71	4.35	4.97	6.87	0.75
TaLTP2.95	0	-4.39	0	-3.15	0	0	-2.03	-2.03	-1.83	0	-2.63	-2.02	1.36	-4.52	3.71	1.89	-1.82	-2.04	1.86	2.5	4.45	0.79	1.27	4.92	-0.82
TaLTP2.96	0	-5.39	0	-3.15	-1.98	-3.28	-3.62	0.37	-1.83	-3.82	-4.22	-4.35	1.66	-4.52	3.88	3.06	-1.82	-1.36	3.13	3.25	5.61	-2.26	1.11	5.97	-3.52
TaLTP2.97	0	0	0	0	0	-3.87	0	0	0	0	0	0	0	0	0	0	0	0	0	0	0	0	0	0	0
TaLTP2.98	0	-4.39	0	-3.15	0	0	-2.03	-2.03	-1.83	0	-2.63	-2.02	1.36	-4.52	3.71	1.89	-1.82	-2.04	1.86	2.5	4.45	0.79	1.27	4.92	-0.82
TaLTP2.99	-2.39	-1.99	-2.86	0.08	-0.6	-0.25	0.11	0.99	0.86	-1.29	-0.47	-2.58	3.91	-3.38	4.69	3.81	-0.58	-5.68	3.96	4.17	6.03	2.4	3.02	6.16	-0.38
TaLTPc.1	10.1	4.45	9.28	9.66	9.94	8.59	8.04	0	9.47	9.23	0.7	0	0	0	0	0	0	0	0	0	0	0	2.31	0	0
TaLTPc.2	9.36	4.74	8.32	9.08	9.05	7.57	7.43	-1.89	8.86	8.47	-1.07	0	0	0	0	0	0	0	0	0	0	0	1.88	0	0
TaLTPc.3	0	0	0	0	0	0	0	0	0	0	0	0	0	0	0	0	0	0	0	0	0	0	0	0	0
TaLTPc.4	12.4	5.77	12.4	12.1	12.7	11.2	10.7	-1.36	11.6	11.8	2.66	0	0	0	0	0	0	0	0	0	0	0	5.27	0	0
TaLTPc.5	10.7	4.36	9.96	10.8	10.6	9.4	9.27	0	10.6	9.85	1.7	0	0	0	0	0	0	0	0	0	0	0	4.14	0	0
TaLTPd.1	0	0	0	0	0	0	0	0	0	0	-2.7	0	0	-2.99	6.14	0	0	0	0	-2.79	0	0	0	0	4.32
TaLTPd.10	0	0	0	0	0	0	0	0	0	0	0	0	0	0	3.63	0	0	0	0	0	0	0	0	0	0.43
TaLTPd.11	0	0	0	0	0	0	0	0	0	0	0	0	0	0	5.22	0	0	0	0	0	0	0	0	0	1.97
TaLTPd.12	-3.3	10.7	0	-2.22	-1.05	-2.36	-1.7	2.25	-0.48	-2.89	-0.98	0	0	-3.6	0	0	0	-3.45	0	0	0	0	7.6	0	0
TaLTPd.13	0	0	0	0	0	0	0	0	0	0	0	0	0	0	-2.88	0	0	0	0	0	0	0	0	0	0
TaLTPd.14	0	0	0	0	0	0	0	0	0	0	0	0	0	0	5.1	0	0	0	0	0	0	0	0	0	1.14
TaLTPd.15	0	0	0	0	0	0	0	0	0	0	0	0	0	0	6.39	0	-1.3	0	0	0	0	0	0	0	6.49
TaLTPd.16	0	0	0	0	0	0	0	0	-1.97	0	-2.11	0	0	0	6.1	0	0	0	0	0	0	0	0	0	5.23
TaLTPd.17	0	0	0	0	0	0	0	0	0	0	0	0	0	0	2.13	0	0	0	0	0	0	0	0	0	0
TaLTPd.18	0	0	0	0	0	0	0	0	-1.97	0	-3.7	0	0	0	6.29	0	0	0	-2.7	0	0	0	0	0	4.47
TaLTPd.19	0	10.8	0	0	0	0	0	2.01	0	0	-1.1	0	-3.12	0	0	-3.46	0	0	-3.43	0	-3.28	-3.27	6.67	-3.39	0
TaLTPd.2	0	0	0	0	0	0	0	0	0	0	0	0	0	0	-1.6	0	0	0	0	0	0	0	0	0	1.73
TaLTPd.20	0	4.79	0	0	0	0	0	-3.62	0	0	0	0	0	0	0	0	0	0	-4.83	0	0	0	-4.71	0	0
TaLTPd.21	0	5.31	0	0	0	0	0	0	0	0	-4.35	-4.46	0	0	0	0	0	0	0	0	0	0	-4.25	0	0
TaLTPd.22	2.69	4.15	2.03	0.05	3.55	1.84	1.71	0.3	2.52	2.31	0.9	5.19	0	5.43	2.03	3.37	-1.37	4.94	-1.36	4.1	-1.63	5.4	-0.08	0.38	1.4
TaLTPd.23	-3.46	8.03	0	-1.8	-1.8	-0.95	0	0.3	0	0	-2.48	0	0	0	0	-3.51	0	0	0	0	0	0	0.98	0	0
TaLTPd.24	0	0	0	0	-2.43	0	0	0	0	0	0	-0.88	0	0	-0.16	0	0	-0.61	0	0	-2.94	0	0	0	-2.38
TaLTPd.25	0	4.99	0	0	0	0	0	-4.09	0	0	0	-5.98	0	-3.17	0	0	0	0	-5.88	0	0	0	0	0	0
TaLTPd.26	0	2.59	0	0	0	0	0	-6.26	0	0	0	0	0	0	0	0	0	0	0	0	0	0	0	0	0
TaLTPd.27	0	2.55	0	0	0	0	0	-6.26	0	0	0	0	0	0	0	0	0	0	0	0	0	0	0	0	0

TaLTPd.28	0	2.59	0	0	0	0	0	-6.26	0	0	0	0	0	0	0	0	0	0	0	0	0	0	0	0
TaLTPd.29	0	4.99	0	0	0	0	0	-4.09	0	0	0	-5.98	0	-3.17	0	0	0	0	-5.88	0	0	0	0	0
TaLTPd.3	0	0	0	0	0	0	0	0	0	0	0	0	0	0	0	0	0	0	0	0	0	0	0	-1.03
TaLTPd.30	0	5.85	-2.74	0	-2.74	0	0	-1.95	0	-3.98	0	0	0	0	-2.76	0	0	0	-1.67	0	0	0	-2.36	0	0
TaLTPd.31	-1.76	3.96	-0.66	-2.26	0.02	-2.4	-1.74	-3.15	-1.2	-0.76	-1.17	6.21	0	6.1	0	2.67	0	5.92	-0.35	3.94	0	4.54	-1.24	-3.31	-3.63
TaLTPd.32	-3.46	6.05	0	0	-1.8	0	-2.87	0	-2.64	0	0	0	-3.18	0	0	0	-2.08	0	0	0	0	0	-2.38	0	-3.76
TaLTPd.33	0.73	0	-0.06	1	1.06	-0.11	-0.45	0	0.91	0.14	0	3.22	0	0.12	0	-1.51	0	1.54	0	0.68	-0.91	0	0	0	0
TaLTPd.34	0	6.34	0	0	0	0	0	-3.15	0	0	0	0	0	0	0	0	0	0	0	-4.4	0	0	-0.66	0	0
TaLTPd.35	0	-0.81	0	0	0	0	0	0	0	0	0	0	0	0	0	0	0	0	0	0	0	0	0	0	0
TaLTPd.36	0.4	2.78	1.08	0.59	1.22	-0.36	-0.37	0	-0.67	-0.19	0.23	6.67	0	5.91	-2.61	2.59	-1.9	4.92	-0.99	4.78	-1.58	5.31	1.8	-1.68	-0.01
TaLTPd.37	-3.46	8.41	-1.2	-0.21	0	-1.53	0	-0.29	-0.64	-2.06	0	0	0	0	-1.78	-2.51	0	-3.66	0	-3.55	0	0	1.64	0	-3.76
TaLTPd.38	-2.47	-2.07	0	0	-2.81	-1.54	0	0	0	-3.06	0	0	0	0	0	0	0	0	0	-3.56	0	0	-3.39	0	0
TaLTPd.39	0	0	0	0	0	0	0	0	0	0	0	0	0	0	3.92	0	0	0	0	0	0	0	0	0	0
TaLTPd.4	0	0	0	0	0	0	0	0	0	0	-2.7	0	0	0	4.89	0	0	0	0	0	0	0	0	0	4.68
TaLTPd.40	-2.44	-0.16	-1.76	-0.03	0.55	0.5	-1.84	-0.94	-2.61	-2.03	0.95	3.8	0.18	3.11	0	4.08	0	2.82	-0.14	4.59	2.08	5.54	0.97	1.79	-2.73
TaLTPd.41	-2.7	-3.9	-3.03	-2.62	-3.05	-2.78	0	0	0	-3.3	0	0	0	0	-2.04	0	0	0	-2.16	0	0	0	0	0	0
TaLTPd.42	0	0	0	0	0	0	0	0	0	0	0	0	0	0	5.01	0	0	0	0	0	0	0	0	0	-2.99
TaLTPd.43	-2.15	-1.62	-0.76	-1.07	0.61	-0.5	-3.16	-2.01	-2.91	-1.34	0.92	2.64	-3.47	2	-2.08	4.45	-1.39	1.91	-2.79	4.06	-0.06	3.44	1.22	0.16	-3.05
TaLTPd.44	-2.64	-2.84	0	0	-1.99	-1.73	-3.06	0	0	0	0	0	0	0	0	0	0	0	0	0	0	0	0	0	-3.95
TaLTPd.45	0	0	0	0	0	0	0	0	0	0	0	0	0	0	4.59	0	0	0	0	0	0	0	0	0	0
TaLTPd.46	0	0	0	0	0	0	0	0	0	0	-2.66	0	0	0	3.98	0	0	-2.7	0	0	0	0	0	0	0
TaLTPd.47	0.9	0.96	0.01	1.14	1.49	1.01	-0.33	0.52	-0.86	0.15	2.17	2.73	-1.96	3.74	-3.15	5.71	0.14	2.6	-0.26	5.76	1.64	5.43	2.4	1.47	-0.55
TaLTPd.48	0	0	0	0	0	0	0	0	0	0	-0.7	0	0	0	4.39	0	-1.3	0	0	0	0	0	0	0	5.82
TaLTPd.49	0	0	0	0	0	0	0	0	0	0	-1.11	0	0	0	4.88	0	-0.72	0	0	0	0	0	0	0	6.89
TaLTPd.5	0	9.85	0	0	-2.48	-2.2	-2.54	0.86	0	0	-1.13	-1.68	0	-0.43	0	0	0	-3.26	-3.14	0	0	0	6.97	0	0
TaLTPd.50	0	0	0	0	0	-2.41	-2.75	0	-1.53	-2.94	-2.35	4.55	0	3.21	0	-1.07	0	2.58	0	-2.42	-3.21	0	0	0	-1.32
TaLTPd.51	2.77	5.07	2.07	2.39	2.78	2.74	1.78	1.71	1.88	1.92	2.6	6.65	-1.17	9.51	-1.36	6.07	0	8.41	4.37	7.02	0.51	8.3	4.17	2.78	0
TaLTPd.52	0	0	0	0	0	0	0	0	0	0	0	0	0	0	0	0	0	0	0	0	0	0	0	0	0
TaLTPd.53	0	2.55	0	0	0	0	0	0	0	0	0	0	0	0	0	0	0	0	0	0	0	0	0	0	0
TaLTPd.54	0	6.09	0	0	0	0	0	-1.83	0	0	0	0	0	0	0	0	0	0	0	0	0	0	-4.24	0	0
TaLTPd.55	2.79	3.96	2.73	3.06	2.99	3.13	2.32	1.32	2.82	2.39	3.36	6.95	0	9.01	-3.4	6.15	0	8.27	2.81	6.94	2.21	8.07	3.25	2.74	0.01
TaLTPd.56	1.9	3.8	1.58	2.27	2.33	1.34	0.94	0.91	2.08	1.63	1.7	6.78	-0.3	9.84	0	6.43	0	9.15	2.24	7.33	2.04	8.77	2.12	4	-1.9
TaLTPd.57	0	0	0	0	0	0	0	0	0	0	0	0	0	0	0	0	0	0	0	0	0	0	0	0	0
TaLTPd.6	0	0	0	0	0	0	0	0	0	0	0	0	0	0	5.2	0	0	0	0	0	0	0	0	-1.09	-2.03
TaLTPd.7	0	0	0	0	0	0	0	0	0	0	0	0	0	0	5.15	0	0	0	0	0	0	0	0	0	4.11
TaLTPd.8	0	0	0	0	0	0	0	0	0	0	-2.7	0	0	0	5.01	0	-1.3	0	0	0	0	0	0	0	7.28
TaLTPd.9	0	0	0	0	0	0	0	0	0	0	0	0	0	0	3.83	0	-2.3	0	0	0	0	0	0	0	4.79
TaLTPg.1	0.8	3.19	1.3	0.05	1.76	0.39	-0.06	-3.09	0.72	0.9	-0.47	5.79	-0.27	5.83	-1.84	1.84	0	5.45	0.03	2.74	2.19	0.26	0.58	0.89	2.9
TaLTPg.10	0	-4.39	0	-3.08	0	0	0	0	0	0	0	0.58	0	1.76	0	-2.25	0	1.53	0	-4.29	-0.51	-4.09	0	-1.61	-4.49
TaLTPg.11	3.55	3.38	3.05	3.59	3.46	3.91	3.16	3.96	3.52	2.8	1.61	2.06	0	2.61	2.56	2.84	-2.78	3.03	1.67	1.88	1.95	-1.04	1.71	0.74	0.92
TaLTPg.12	0	0	0	0	0	0	0	0	0	0	0	0	0	0	0	0	0	0	0.4	0	0	0	0	0	0
TaLTPg.13	-2.86	-0.79	-1.23	-1.79	0.35	3.76	-2.91	0	-1.3	3.15	0.51	0	-4.23	0	-4.42	0	0	0	0	0	-4.4	0	-0.86	0	-4.79
TaLTPg.14	0	0.56	0	0	0	0	0	0	0	-4.01	0	1.25	0	2.97	-3.38	-1.34	0	2.01	-4.51	-1.09	-0.65	-4.35	-4.4	-2.13	-2.75
TaLTPg.15	3.78	4.98	3.13	3.71	3.83	3.82	3.17	4.55	3.2	3.36	1.39	1.52	-2.87	2.85	2.86	1.86	-1.78	2.65	2.11	0.62	1.35	-0.95	1.53	-0.19	0.61
TaLTPg.16	0	0	-3.48	0	0	0	-3.57	0	0	0	0	0	0	0	-4.08	0	-3.8	0	0.18	0	0	0	-4.1	0	0
TaLTPg.17	-3.48	-1.56	-2.26	-2.4	0.4	2.84	-3.94	-4.39	0	2.72	0.64	-4.69	0	-2.08	0	0	0	0	0	0	0	0	-2.48	0	0
TaLTPg.18	0	-3.09	0	0	0	0	0	0	0	0	0	0.25	0	2.45	0	-1.53	0	1.82	-4.54	-3.57	-0.68	-3.38	-4.42	-1.67	-1.96
TaLTPg.19	2	-0.49	1.46	1.18	2	1.74	1.34	1.23	1.87	1.56	-0.71	-4.62	0	-2.82	-1.22	-2.52	-1.53	-4.78	-2.21	-4.56	-4.37	0	-4.41	-4.47	-2.44
TaLTPg.2	0.14	4.82	0.09	-0.2	0.32	0.2	0.39	0.92	0.43	-0.76	-1.7	0	-2.14	-5.08	0.48	-4.2	2.16	0	-0.68	-4.82	-1.54	-3.31	-2.22	-2.41	1.6
TaLTPg.20	2.76	4.31	1.86	2.75	2.85	2.46	2.59	3.79	2.74	1.73	0.69	0	-0.87	0	2.57	1.58	-4.11	0	1.13	0.49	3.73	-2.37	2.73	1.96	-2.76
TaLTPg.21	2.14	4.02	1.69	2.74	2.28	2.21	2.43	3.51	2.7	0.89	1.18	0	-2.04	0	2.46	0.95	-3.76	0	0.55	0.51	3.37	-2.69	2.2	1.37	0
TaLTPg.22	0.62	0.71	0.3	0.01	0.62	0.3	0.06	-0.86	0.76	-0.17	-1.6	-2.87	-2.86	-1.89	-2.63	-2.44	-1.55	-3.04	-3.19	0	0	-1.81	0	-2.71	-5
TaLTPg.23	2.18	3.38	1.72	2.27	2.17	2.31	2.71	3.21	2.49	1.42	1.2	0	-3.62	0	2.12	1.39	-4.12	-4.79	1.02	-0.08	3.31	-2.21	2.39	1.67	-2.18
TaLTPg.24	3.14	4.32	2.51	3.69	3.12	3.45	4.07	4.74	3.79	2.12	2.85	-2.24	0	-1.37	0.43	1.56	-1.73	-2.54	0.15	0.84	1.01	0	2.74	0.31	-0.51
TaLTPg.25	0.13	0.79	-0.06	-0.15	0.56	0.18	-0.68	-3.3	0.24	0.16	-0.59	2.5	-4.18	3.74	0	1.52	-4.09	2.85	-2.92	1.53	-0.35	0.7	1	-0.36	-4.74
TaLTPg.26	-1.56	0.71	-2.15	0.41	-1.15	-2.49	-0.82	-2.27	0.16	-2.98	-4.47	0	0	0	-3.34	-4.47	0	-3.14	0	-4.51	-1.51	0	-2.36	-3.42	0
TaLTPg.27	0	0	0	0	0	0	0	0	0	0	0	-4.5	0	0	0	0	0	-4.21	0	0	0	-5.45	0	-5.57	0
TaLTPg.28	0	0	0	0	0	0	0	0	0	0	0	-0.21	0	-1.36	0	-3.63	0	-1.45	0	0	-2.46	-4.23	-5.09	-4.35	0
TaLTPg.29	-3.4	-4.98	-1.64	-4.65	-3.22	-3.27	-4.19	0	-3.31	-2.46	0	0	0	0	0	0	0	0	0	0	0	0	0	0	0
TaLTPg.3	-2.04	2.15	-1.4	-2.28	-0.73	-1.9	-1.49	-1.67	-1.53	-1.97	-2.14	4.6	-0.23	5.56	0.25	1.8	-3.05	5.01	-0.3	1.63	1.34	-0.61	0.46	-0.09	-1.24
TaLTPg.30	3.69	0	3.24	2.75	3.85	2.51	2.76	-4.62	3.83	3.37	-0.74	0	0	0	0	0	0	0	0	0	0	0	-4.71	0	-5.06
TaLTPg.31	0	0	0	0	0	0	0	-3.43	-3.7	0	0	0.07	0	-0.18	-4.5	-4.63	0	-0.09	0	0	-1.48	-4.48	-4.52	-2.58	-4.87
TaLTPg.32	4.12	6.77	3.71	4.54	3.96	4.17	4.7	5.41	4.32	3.52	3.49	0.97	0	2.12	3.28	3.19	2.89	1.69	1.73	2.38	2.42	-4.44	3.83	1.7	1.74
TaLTPg.33	0	-4.13	0	0	0	0	0	0	0	0	0	0	0	0	0	0	0	0	0	0	0	0	0	0	0
TaLTPg.34	####	0	0	0	0	0	0	0	0	0	0	0	0	0	0	0	0	0	0	0	0	0	0	0	0
TaLTPg.35	0	0	0	0	0	0	0	-3.47	0	0	0	1.94	0	1.9	0	-2.67	0	1.51	0	0	-0.06	-4.52	-4.56	-1.62	-2.59
TaLTPg.36	-0.72	2.33	-2.15	0.52	-0.65	-1.91	-1.5	-0.06	0.21	-2.65	-2.14	-3.57	-3.15	-3.76	-4.34	-3.47	0	-4.73	-2.48	-1.7	-0.27	-3.32	-1.27	-1.25	0
TaLTPg.37	-1.29	-0.49	-1.95	0	-0.15	-2.69	-0.71	-3.46	-0.2	-2.21	-0.84	1.14	-3.34	3.39	-3.53	1.08	0	3.56	-2.07	2.48	-0.92	1.15	1.31	-0.29	0
TaLTPg.38	2.98	6.54	2.78	3.24	3.05	3.43	3.77	5.46	3.24	2.26	2.6	0.23	0	0.6	2.97	1.58	1.55	0.39	1.01	0.18	1.33	0	3.03	0.91	1.1

Table S4 | Motif enrichment analysis of *cis*-regulatory elements in anther-specific promoter regions.

Box	Consensus sequence	Enrichment *P*-value [a]	Reference
5256BOXLELAT5256	TGTGGTTATATA	-	Zhou, 1999
5659BOXLELAT5659	GAAWTTGTGA	-	Zhou, 1999
GBOX10NT	GCCACGTGCC	-	Ishige *et al.*, 1999
GTGANTG10	GTGA	-	Rogers *et al.*, 2001
POLLEN1LELAT52	AGAAA	6.72×10^{-3}	Bate and Twell, 1998
POLLEN2LELAT52	TCCACCATA	-	Bate and Twell, 1998
PSREGIONZMZM13	TCGGCCACTATTTCTACGGGCAGCCAGACAAA	-	Halmilton *et al.*, 1998
QELEMENTZMZM13	AGGTCA	-	Halmilton *et al.*, 1998
VOZATVPP	GCGTNNNNNNNACGC	-	Mitsuda *et al.*, 2004

[a] The enrichment *p*-value of the motif that are enriched in 17 the anther-specific gene promoter regions compared with promoter sequences of the remaining 444 identified *nsLTPs*. The p-value was calculated for the Wilcoxon rank-sum test implemented in AME tool (Analysis of Motif Enrichment)

Table S5 | Identification of wheat anther-specific nsLTPs orthologues in rice, maize and sorghum.

	Wheat		Rice[2]		Maize[3]		Sorghum[4]	
Gene	Chr.	Position	Chr.	Position	Chr.	Position	Chr.	Position
TaLTP2.25	chr1D	2.35E+08	Chr10	19288018	Chr5	23858169	Chr1	18191249
TaLTP2.14	chr1B	3.4E+08	Chr10	19288018	Chr5	23858169	Chr1	18191249
TaLTP2.1	chr1A	3.13E+08	Chr10	19288018	Chr5	23858169	Chr1	18191249
TaLTP2.214	chr7D	4.47E+08	-	-	-	-	-	-
TaLTP2.93	chr7A	4.99E+08	-	-	-	-	-	-
TaLTP2.198	chr7B	4.65E+08	-	-	-	-	-	-
TaLTPg.30	chr4B	13125606	Chr3	26073641	Chr2	48052056	Chr6	45983685
TaLTP1.25	chr5A	6.8E+08	Chr7	16294810	-	-	Chr2	17997167
TaLTP1.18	chr4B	6.42E+08	Chr7	16294810	-	-	Chr2	17997167
TaLTP1.21	chr4D	4.99E+08	Chr7	16294810	-	-	Chr2	17997167
TaLTPc.3	chr5D	4.12E+08	Chr9	20534165	Chr7	1.42E+08	Chr2	65407147
TaLTPc.1	chr5A	5.24E+08	Chr9	20534165	Chr7	1.42E+08	Chr2	65407147
TaLTPc.2	chr5B	4.97E+08	Chr9	20534165	Chr7	1.42E+08	Chr2	65407147
TaLTPc.4	chr7A	2.76E+08	Chr8	27364161	Chr4	1.95E+08	Chr7	61403378
TaLTPc.5	chr7B	2.35E+08	Chr8	27364161	Chr4	1.95E+08	Chr7	61403378
TaLTP1.14	chr3D	1.19E+08	Chr1	6541005	Chr8	25951054	Chr3	1451110
TaLTP1.12	chr3B	1.72E+08	Chr1	6541005	Chr8	25951054	Chr3	1451110
TaLTP1.10	chr3A	1.26E+08	Chr1	6541005	Chr8	25951054	Chr3	1451110
TaLTPg.19	chr3A	3.96E+08	Chr1	23919358	Chr10	15009187	Chr6	49389699

[2] Ouyang *et al.*, 2007

[3] Schnable *et al.*, 2009

[4] McCormick *et al.*, 2018

Table S6 | Primers used for qRT-PCR.

Gene	Forward primer (5' to 3')	Reverse primer (5' to 3')
TaGAPDH	TTCAACATCATTCCAAGCAGCA	CGGACAGCAAAACGACCAAG
TaActin	GACAATGGAACCGGAATGGTC	GTGTGATGCCAGATTTTCTCCAT
Ta13-3-3	ACGCAGCTACCTGTATCATTC	CGACGATGTCCACATGACC
TaLTP1.15	ATGAACCCTGAGATCGGACC	GGCCCTTGATTCAATCTTATAG
TaLTP2.102	TGCAACGTAGCATGTAGCAGC	TGGTGCTTGGGTTAGATCAAC
TaLTP2.93	GACAGCGACCTGCGTCAG	TGTCACAAACTGAAGGAGAAGG
TaLTP2.94	GCACTGCAACGTAGCATGTAG	GGTGCCTGGGTTGGATTAG
TaLTPc.1	CGAAGAAACGATGCGAGTC	GGCGAAGAGGCAGACATG
TaLTPc.2	ATGGGCATCATCAACAGCA	CAACAACGGCAGAATGACA
TaLTPc.3	AAGAAGACGATGATGAATAAGAGC	GACATGAGAGCCTCTAATGGC
TaLTPc.4	ATGAATAAGAAGCTCGATGGC	ATGAATAAGAAGCTCGATGGC
TaLTPc.5	AGGAGGAACTGAAGAAGACGAC	TGCAAATTGGTTTCATTACTATTG
TaLTP2.74	GACGGTTCTCAGCCTCGG	CCGGTAGCAAAGCAAGATCAC
TaLTP2.87	CGCGGTCACCTACTGCAAC	TCCACAGTTCCATGAAACTAACAG
TaLTP1.14	CGCAACGTACACAGAGGAAG	CATCGGGATAACAATTGAATTAC
TaLTP2.89	AGGCAACCGACGATTTCAG	AGCTACGTGATCCAGTTTTCG
TaLTP1.13	TACGGATGAACCCTGAGATG	AGGCCCTTGATTCAATCTTATAC

Chapter 5

Towards identification of a fertility modifier in the wheat ms1c

Statement of Authorship

Title of Paper	Towards identification of a fertility modifier in the wheat ms1c mutant
Publication Status	☐ Published ☐ Accepted for Publication ☐ Submitted for Publication ☑ Unpublished and Unsubmitted work written in manuscript style
Publication Details	Chapter written in publication format for future submission.

Principal Author

Name of Principal Author (Candidate)	Allan Kouidri
Contribution to the Paper	Conducted the study, analysed data and wrote the manuscript.
Overall percentage (%)	60 %
Certification:	This paper reports on orginal research I conducted during the period of my Higher Degree by Research candidature and is not subject to any obligations or contractual agreements with a third party that would constrain its inclusion in this thesis. I am the primary author of this paper.
Signature	Date 28/05/2018

Co-Author Contributions

By signing the Statement of Authorship, each author certifies that:

i. the candidate's stated contribution to the publication is accurate (as detailed above);

ii. permission is granted for the candidate in include the publication in the thesis; and

iii. the sum of all co-author contributions is equal to 100% less the candidate's stated contribution.

Name of Co-Author	Elise J. Tucker
Contribution to the Paper	Help in conceiving the project and data interpretation. Contributed to the QTL analysis. Reviewed and edited the manuscript.
Signature	Date 28.5.18

Name of Co-Author	Patricia Warner
Contribution to the Paper	Contributed to the *ms1d* x Gladius penetrance test by growing and genotyping plants.
Signature	Date 28/5/2018

Name of Co-Author	Paul Eckermann
Contribution to the Paper	Performed linkage map and contributed to the QTL analysis.
Signature	Date 28/5/18

Name of Co-Author	Nathan Watson-Haigh
Contribution to the Paper	Performed the SNP marker identification from the GBS reads.
Signature	Date 30/5/18.

Name of Co-Author	Margaret Pallotta
Contribution to the Paper	Contributed in data interpretation. Provided help with the Southern blot analysis
Signature	Date 28.5.18

Name of Co-Author	Ute Baumann
Contribution to the Paper	Supervised development of the work, help in data interpretation. Reviewed and edited the manuscript.
Signature	Date 28/5/18

Name of Co-Author	Ryan Whitford
Contribution to the Paper	Supervised development of the work, help in data interpretation. Reviewed and edited the manuscript.
Signature	Date 27/5/2018

Chapter 5

Towards identification of a fertility modifier in the wheat *ms1c* mutant

Allan Kouidri[1], Elise J. Tucker[1,2], Patricia Warner[1], Paul Eckermann[1], Nathan Watson-Haigh[1], Margaret Pallotta[1], Ute Baumann[1], Ryan Whitford[1*]

[1]University of Adelaide, School of Agriculture, Food and Wine, Waite Campus, Urrbrae, South Australia 5064, Australia.

[2]Current address Commonwealth Scientific and Industrial Research Organization, Agriculture and Food, Waite Campus, Urrbrae, South Australia 5064, Australia.

[*]Correspondence**:** ryan.whitford@adelaide.edu.au

5.1 Abstract

To date, hybrid breeding is limited in wheat due to its strong self-pollinating nature. The use of *Tams1,* non-specific lipid transfer protein (*nsLTP*)*,* as a recessive mutant sterility locus coupled with its cognate dominant fertility restorer sequence (*TaMs1)* are promising elements towards controlling cross-pollination in wheat. A cost-effective wheat hybrid seed production system requires completely penetrant male sterility across various genotypic backgrounds.

Here, we report variability in phenotypic sterility penetrance between *ms1d* and *ms1c* mutant alleles. We show that *ms1d* (cv. Chris)-induced sterility is highly penetrant across all backgrounds tested. This contrasts with low phenotypic sterility penetrance observed for *ms1c* (cv. Cornerstone) consistent with previous reports of a modifier gene (*Mod*) affecting fertility restoration in this particular genetic background. We present a linkage map derived from a *ms1c*-P5 x Gladius biparental F_2 population (*N* = 122), generated using 1247 single nucleotide polymorphisms identified by genotyping-by-sequencing (GbS). Thereafter, quantitative trait loci (QTL) mapping for the modifiers contributing to incomplete sterility penetrance was performed. Two QTLs were identified, one on the long arm of chromosome 4A (QMod_4A) explaining 17.7 % of the phenotypic variance and another on the short arm of chromosome 2B (QMod_2B) responsible for 12.2 % of phenotypic variance. The QMod_4A was delimited to a 36 cM interval, a region containing three nsLTPs, each of type G and including the A-genome homeologue of *TaMs1* (*TaMs1-A*). The QMod_2B spans an interval of 42.5 cM and contains two nsLTPs (Type D and Type G).

The genome-wide SNP identification, linkage map and QTL analysis undertaken within this study now permits the identification of *Mod* candidates that could be responsible for incomplete sterility penetrance in the *ms1c* mutant background.

5.2 Introduction

It has been estimated that worldwide crop production would need to double from 2013 to 2050 to meet the demand of the growing population (Ray *et al.*, 2013). However, the current yield gain increase is insufficient to feed the predicted 9 billion by 2050 (FAOSTAT, 2013). Wheat is one of the major staple food crops, providing approximately 18 % of daily calorie intake by humans (FAOSTAT, 2013). Therefore boosting wheat yield is of high priority, which will in part rely on the development of new breeding technologies (Tester, 2011). The development and application of hybrid seed production technologies have contributed greatly to yield increases for rice and maize among others (Kim and Zhang, 2017). In the past decades, hybrid rice has boosted yields by approximately 20 % compared to inbred varieties (Cheng *et al.,* 2007). In addition, maize hybrids have been shown to outperform inbred line varieties by approximately 50 % to 100 % (Duvick, 2004).

The use of nuclear male sterility (NMS) based systems have long been recognised as a promising approach to producing hybrid wheat (Driscoll and Qualset, 1986). NMS refers to mutations in nuclear encoded genes that are essential for the development of viable pollen. In principle, a NMS system uses maintainer lines which are male fertile, and when crossed as a pollen donor to a male-sterile produce 100 % male-sterile progenies (Prat and van Lookeren Campagne, 2002). Such systems are based on the complementation of recessive mutant male steriles by a maintainer locus that harbours the cognate dominant wild-type fertility restorer sequence. This method was first described as the XYZ system, and was proposed for up-scaling the production of male-sterile female inbreds (Driscoll, 1972). This system proposed to use the ionizing radiation-induced male-sterile wheat mutant (cv. Cornerstone), *ms1c*, which is a large deletion of the *Ms1* locus (Driscoll and Barlow, 1976). In this system, the fertility restorer is located on a 5R addition chromosome derived from rye (*Secale cereale*), which additionally possesses the visual marker hairy peduncle (*hp*).

A cost-effective wheat hybridisation system relies upon completely penetrant male sterility in the female inbred. Incomplete sterility would otherwise result in selfed progenies being present in the F1. These inbred progenies would not possess the desired hybrid vigour, and

would therefore compromise both hybrid seed purity and therefore yield potential. Poor sterility penetrance (partial fertility) has previously been reported for particular *ms1* mutant alleles. These include *ms1c* (cv. Cornerstone) (Islam and Driscoll, 1984; Driscoll, 1985; Tucker *et al.*, 2017), and a deletion of chromosome 4BS (DT4BL) (cv. Chinese Spring) (Joshi *et al.*, 2014). Because incomplete sterility penetrance was observed in deletion lines for the *Ms1* locus (*ms1c*, DT4BL), we inferred fertility restoration could be a consequence of functional homeoalleles in some genetic backgrounds, as opposed to the presence of residual B-derived-genome TaMs1 activity.

TaMs1 homeoalleles from A- and D-genomes are each predicted to encode similar proteins to TaMs1, as there is no difference in predicted motifs or structure, suggesting that these homeoalleles would have a function related to TaMs1-B under similar spatio-temporal expression profile (Tucker *et al.*, 2017; Wang *et al.,* 2017). Additionally, promoter sequence analysis at the nucleotide level for *TaMs1* and its homeologues showed no easily discernible differences that could explain why only the *TaMs1-B* copy is expressed (Chapter 3). However, epigenetic mark analysis of *TaMs1* -A and -D sub-genomes revealed a hyper-methylation of their promoter sequences, suggesting that both homeoalleles are epigenetically silenced (Wang *et al.*, 2017).

Here we show that male sterility penetrance is variable depending upon the *ms1* mutant allele and genetic background; suggestive of the presence of a *Modifier* (*Mod*) gene in *cv.* Cornerstone (Driscoll, 1977). To elucidate the genetic context of the *Mod* gene we developed a SNP-based linkage map by genotyping-by-sequencing (GbS) a *ms1c*-P5 x Gladius biparental F_2 mapping population. Quantitative trait loci (QTL) mapping revealed two loci that are responsible for fertility restoration and are present on chromosomes and 4A (*QMod-4A*) and 2B (QMod-2A), spanning 37 cM and 49.7 cM respectively. Within the QMod-2B interval two predicted lipid transfer proteins (LTPs) were identified, whereas three nsLTPs were identified within QMod-4A. Interestingly, the QMod-4A interval contained the *TaMs1-A* homeoallele*,* making it a strong candidate for the *Mod* gene. Our results provide valuable information towards selecting or creating highly penetrant male sterile mutants required for cost-effective hybrid seed production.

5.3 Materials and Methods

5.3.1 Plant growth condition and F_2 populations

The soil mix consisted of 75 % (v/v) Coco Peat, 25 % (v/v) nursery cutting sand (sharp), 750 mg/L $CaSO_4.2H_2O$ (gypsum) 750 mg/L $Ca(H_2PO_4)_2.H20$ (superphosphate), 1.9 g/L $FeSO_4$, 125 mg/L FeEDTA, 1.9 g/L $Ca(NO_3)$, 2.750 mg/L Scotts Micromax micronutrients, and 2.5 g/L Osmocote Plus slow release fertilizer (16:3:9) (Scotts Australia Pty. Ltd.). pH was adjusted to between 6.0 and 6.5 using 2 parts agricultural lime to 1 part hydrated lime. Potted plants were grown either in controlled environment growth rooms at 23 °C (day) and 16 °C (night) or similarly temperature moderated glasshouses in which photoperiod was extended using 400 W high pressure sodium lamps in combination with metal halide lamps to 12 hours over winter months.

Six separate F_2 mapping populations were developed by crossing the male sterile cv. Chris-EMS mutagenized line FS2 (*ms1d*) (Sasakuma *et al.*, 1978) with male fertile cultivars H45, Mace, Pastor, RAC875, Westonia and Gladius (Pedigrees are provided in supplemental Table S1). Additionally an F_2 population derived from a cross between the male sterile deletion mutant *ms1c* (cv. Cornerstone, line P5) and the male fertile cv. Gladius was generated. Finally, a deletion mutant line *ms1c* (line P10) was also used for the penetrance test and qRT-PCR analysis.

5.3.2 Genotyping at the *Ms1* locus

The *Ms1* allele from the *ms1d* x cultivars F_2 populations was genotyped using a KBioscience Competitive Allele-Specific Polymerase chain reaction (KASP™) assay targeting the causative mutation (forward primers, 5'-GAAGGTGACCAAGTTCATGCTGGAGGAGGCGGACAACGTAC-3' and 5'-GAAGGTCGGAGTCAACGGATTGGAGGAGGCGGACAACGTAT-3', and common reverse primer CTCGCCGCCGCCTGCGAA). For *ms1c*-P10 and *ms1c*-P5 x Gladius F_2 population, the presence/absence of the *Ms1* chromosome B locus was genotyped using a PCR-based marker targeting both the 4B *ms1c* deletion and an orthologous locus on 4A hit (Chr4A:596161853-596162127) that provided a positive control for the PCR amplification, yielding a 277bp amplicon (5'-GGTACCGGGAAATGATCTTCGACGAGGC-3' and 5'-CGTCGAACATCTTTCAGTGATTCAGAGG-3') compared with an amplicon of 288 bp from wildtype 4B.

5.3.3 Phenotyping and penetrance

Plant fertility was assessed based on seed counting from 3 to 5 heads. Over each head a glassine bag was placed and sealed before anthesis to avoid potential cross pollination. The two basal and two apical spikelets per head were eliminated from the analysis due to their incomplete development. Total seed set and numbers of florets were counted on a per head basis. The fertility score for each spike or plant was calculated as follows:

$$\text{Fertility} = \frac{\text{Total number of seed per spike}}{\text{Total number of 1°, 2° and 3° florets per spike}}$$

The penetrance percentage of the *ms1* mutation was calculated based on the proportion of individual homozygous *ms1* showing full sterility.

$$\text{Penetrance} = \frac{\text{Total number of genotypically sterile } \textit{ms1} \text{ homozygous plants}}{\text{Total number of phenotyped } \textit{ms1} \text{ homozygous plants}} \text{ x } 100$$

5.3.4 Nucleic acid extraction

DNA were extracted using either a phenol/chloroform or freeze-dried protocol. For phenol phenol/chloroform DNA extraction, a 15 cm long piece leaf was frozen in liquid nitrogen, and tissues were ground to fine powder using shakers (Retsch® MM 300) and ball bearings. 700 µL of extraction buffer (1% sarkosyl, 100 mM Tris-HCl pH 8.5, 100 mM NaCl, 10mM EDTA, 2% PVPP) was added and samples were mixed on a rotary shaker. Then 700 µL of phenol/chloroform/iso-amylalcohol (25:24:1) was added, briefly vortexed, transferred to a silica matrix phase lock tubes (BD Vacutainer®, *No.* 367958) and centrifuged at 4000 rpm for 10 min. DNA was precipitated by adding 60 µL 3M sodium acetate pH 4.8 and 600 µL isopropanol and centrifuged at 13 000 rpm for 10 min. The DNA pellet was washed with 1 mL 70% ethanol, centrifuged for 2 min at 13 000 rpm and air dried for 20 min. The purified DNA was resuspended in 50 µL of R40 (1x TE, 40 µg mL^{-1} RNase A).

For freeze-dried DNA extraction, a 4-5 cm long leaf from a 2-3 week old seedling was freeze-dried overnight and grinded using ball bearings. 600 µL of extraction buffer (0.1 M Tris-HCl, 0.05 M EDTA-pH 8.0 and 1.25 % SDS) and incubated at 65 °C for 30 min. After cooling the samples 15 min on ice, 300 µL of 6 M ammonium acetate was added and samples were centrifuged 15 min at 3750 rpm. DNA was precipitated using 400 µL of 70 % ethanol. The purified DNA was resuspended in 50 µL of R40 (1x TE, 40 µg mL^{-1} RNase A).

5.3.5 5-azacitidine demethylation treatment

The DNA demethylating reagent, 5-azacytidine (5-azaC) (Sigma, Sydney, Australia) was applied to seeds of fertile and sterile segregants from heterozygous *Ms1d*/*ms1d* line (cv. Chris). Seeds were treated at room temperature in a petri dish with a daily fresh solution of 5-azaC in water solution for 5 days. Three concentrations of 5-azaC were tested: 125 µM, 250 µM and 500 µM of 5-azaC. After 5 days, seedling were transferred into pots and were grown as described in section 3.1. The control plants were treated with water in the same manner.

5.3.6 Southern hybridization

Initially 10 µg of DNA (cv. Chinese Spring, cv. Gladius, Chinese Spring-derived nullisomic tetrasomic stocks (Cenci *et al*., 2003) (N4AT4D, N4BT4Aand N4DT4B), cv. Cornerstone (*ms1c*-P4, *ms1c*-P5, *ms1c*-P10) were digested overnight with HindIII and BamHI restriction enzymes. Digested DNA was run on a 1.2 % agarose/Tris-acetate-EDTA gel and stained with ethidium bromide. DNA fragments were transferred to nylon membrane for Southern hybridisation using standard methods (Brown, 2001). Membranes were probed with a ^{32}P-labelled probe from a 353 base pair (bp) PCR fragment amplified with 3'- GCCTTCTTCTTCGTCGCCAC -5' and 5'- CCATTTCCATTCAGATCATACCG-3. The probe sequence was amplified from the last exon to the 3' UTR of *TaMs1-B* with a sequence identity of 76.8 % and 68.4 % to *TaMs1-D* and *TaMs1-A*, respectively. The membrane was washed at room temperature twice in 2x SSC + 0.1 % SDS for 20 min each, followed by once in 1x SSC+ 0.1 % SDS for 20 min at 65 °C, once in 0.5x SSC+ 0.1 % SDS for 20 min at 65°C, once in 0.2x SSC + 0.1% SDS and once in 0.1x SSC + 0.1% SDS. Membranes were exposed to X-ray film for 24–48 h at -80 °C.

5.3.7 Expression analysis

Total RNA was isolated using ISOLATE II RNA Mini Kit (Bioline, Sydney, Australia) from wheat tissues: anthers containing meiotic microspores and uninucleate microspores. Quantitative real-time (qRT)-PCR was perform according to Burton *et al*., (2004) using the primer combinations shown in Table 1. Anthers containing developing microspores were staged by acetocarmine staining. 0.6 µg of RNA was used to synthesise the oligo-(dT)-primed first strand cDNA using the superscript IV reverse transcriptase (Thermo Fisher, Adelaide, Australia). 2 µL of the RT product diluted 1:20 was then used as template for conventional and quantitative real-time PCR. TaGAPdH, TaActin and Ta14-3-3 were used as reference genes.

Table 1 | List of primers used for qRT-PCR.

Gene	Forward primer (5' to 3')	Reverse primer (5' to 3')
TaGAPdH	TTCAACATCATTCCAAGCAGCA	CGGACAGCAAAACGACCAAG
TaActin	GACAATGGAACCGGAATGGTC	GTGTGATGCCAGATTTTCTCCAT
Ta13-3-3	ACGCAGCTACCTGTATCATTC	CGACGATGTCCACATGACC
TaMs1-B	CCTCTACATCATCCTCTGAGTCGC	GTACGAGCGGACAGAAACGATAG
TaMs1-A	CCTCTACATCATCCTCTGAGTCGC	TGAACATACTGCTGCTACCAGACACTA
TaMs1-D	CCTCTACATCATCCTCTGAGTGGC	TCCATACTCCTGCCAACGACAG

5.3.8 GbS library construction, SNP identification and QTL analysis

5.3.8.1 SNP marker identification

Genomic DNA isolated from 122 *ms1c*-P5 x Gladius F_2 individuals as well as Gladius and *ms1c-P5* parents were used to prepare PstI-MspI reduced representation libraries. Reads from the two parents (*ms1c*-P5 and Gladius) were mapped to the *Triticum aestivum* (Chinese Spring) genome assembly (IWGSC WGA v0.3) using BioKanga (Stephen *et al.*, 2012). Default mapping parameters were used except for mapping in paired-end mode and allowing a maximum of 2 mismatches per 100bp of alignment. Pileups were generated from the resulting BAM files and SNPs called using an in-house tool. Only homozygous and polymorphic SNPs were used for further analysis. A SNP was called homozygous if all reads at a position agreed with each other and there were at least 3 and 2 reads covering the position in the *Ms1c*-P5 and Gladius parents respectively. There were 30,651 positions in the wheat genome identified as polymorphic in either *ms1c*-P5 and/or Gladius. Of these, 2,157 met the above thresholds required for being called homozygous and polymorphic between the two parents.

5.3.8.2 Genotyping in *ms1c*-P5 *x* Gladius biparental F_2 population

Reads were mapped to the reference genome using the same procedure as for the parent samples. Pileups were generated from the resulting BAM files, restricted to the 2,157 positions previously identified as being homozygous and polymorphic between the two parents. SNP calling was performed using an in-house tool and required a minimum coverage of 5 reads to have the genotype called. For a position to be called heterozygous, a minimum coverage of 2 reads coverage for both alleles was required. The genotype calls were translated into AB format, where the A allele is from *ms1c*-P5 and the B allele is from Gladius. Of the 2,157 SNP markers identified in the parents, 29 had missing genotype calls across all 122 F_2's. This left 2,128 SNP markers for input into the map construction stage.

5.3.8.3 Fertility score, linkage map construction and QTL analysis

Phenotypic data for four traits were considered including, (i) average fertility (fertility score average from three heads), (ii) transformed average fertility, (iii) maximum fertility (the highest fertility score among the three heads) and, (iv) transformed maximum fertility. Transformed data of average and maximum fertility were calculated using the empirical logit transformation (Haldane, 1955); this was used taking into account the number of infertile spikelet per head to spread out the zero values.

The linkage map was constructed using the R package ASMap (Taylor and Butler, 2017), with additional functions in R used for quality control of the data. The input data consisted of 2128 GbS markers scored on 122 lines. Markers with high rates of missing values or segregation distortion were removed, leaving 1240 GbS markers in the final map. No lines were found to be clonal or had other anomalies such as high rates of double crossovers, so all 122 were retained in the final map. Chromosome assignments were checked against the Chinese Spring genome assembly (IWGSC WGA v0.4) and used to verify marker locations. The final map included 1247 markers anchored in all 21 wheat chromosomes.

5.4 Results

5.4.1 *ms1c* male sterility is not fully penetrant

We first investigated the phenotypic penetrance of male sterility in homozygous *ms1d* and *ms1c* mutants. The sterility penetrance for *ms1d* was tested in six F_2 populations derived from crosses with the following cultivars: H45, Mace, Pastor, RAC875, Westonia and Gladius (Table 2). Sterility for genotypic homozygotes (*ms1d*/*ms1d*), as assessed based on lack of selfed seed-set, was identified to range between 98.52 % to 100 %, and therefore was deemed highly penetrant. In contrast, low sterility penetrance of 42.11 % for genotypic homozygotes derived from the *ms1c*-P5 x Gladius F_2 population was observed. Unexpectedly, high phenotypic variability between three heads of the same individual was observed for some homozygote individuals derived from the *ms1c* x Gladius F_2 population (Table S2). In addition, of the 48 lines genotyped as homozygous *ms1c/ms1c*, only 12.5 % exhibited some level of fertility across all assessed spikes of the same plant. Additionally, incomplete sterility penetrance (0 %) was observed for the *ms1c*-P10 individual (*ms1c*/*ms1c*), in addition to partial to full fertility in all of its selfed *ms1c*/*ms1c* progenies.

Table 2 | Phenotypic penetrance of *ms1d* and *ms1c* in various cultivars.

Genotype	Allele at the *Ms1* locus	Number phenotyped	Number of fertile	Penetrance	Fertile plants	
					seed/floret average	seed/floret range
ms1d x H45	*ms1d/ms1d*	79	1	98.73%	0.03	0.03
	Ms1/Ms1	8	8		1.42	0.15 - 1.88
ms1d x Mace	*ms1d/ms1d*	69	0	100%	-	-
	Ms1/Ms1	7	7		1.55	0.96 - 2.11
ms1d x Pastor	*ms1d/ms1d*	68	1	98.53%	0.02	0.02
	Ms1/Ms1	8	8		1.67	0.88 - 2.33
ms1d x RAC875	*ms1d/ms1d*	71	0	100%	-	-
	Ms1/Ms1	8	8		1.44	0.81 - 1.8
ms1d x Westonia	*ms1d/ms1d*	70	0	100%	-	-
	Ms1/Ms1	8	8		1.46	0.5 – 2.11
ms1d x Gladius	*ms1d/ms1d*	109	1	99%	0.024	0.024
	Ms1/Ms1	37	37		2.55	1.5 – 3.7
ms1c-P5 x Gladius	*ms1c/ms1c*	114	48	42.11%	0.24	0.022 – 0.8
	Ms1/Ms1	14	14		1.55	1.00-2.23
ms1c-P10	*ms1c/ms1c*	11	11	0%	1.72	1.14-2.11

5.4.2 Epigenetic regulation of the modifier gene

The sterility penetrance for the *ms1c* homozygote deletion mutants derived from *ms1c*-P5 x Gladius F_2 population was shown to be highly variable between individuals and tillers from the same plant (Table 2; Figure S2 and Table S2). This indicates the presence of another locus, outside *TaMs1-B* genome deleted region, able to partially restore fertility in the *ms1c* background. Some observations suggest that *TaMs1*-A and -D homeologues as likely candidates for the modifier gene. First, *TaMs1* -A and *TaMs1*-D are predicted to encode proteins highly identical to TaMs1-B, suggesting that they could complement TaMs1-B function if expressed (Figure S2). Second, *TaMs1*-A and *TaMs1*-D derived-genomes were suggested to be transcriptionally repressed, as evidenced by a hypermethylation of their promoter sequences (Wang *et al.*, 2017) and negligible transcript abundance (Tucker *et al.*, 2017; Wang *et al.*, 2017).

Therefore, to evaluate a potential role for DNA demethylation in the mechanism underlying the observed self-fertility in homozygous mutants across different genetic backgrounds (poor penetrance), we tested whether the demethylation agent, 5-azacitidine (5-azaC) could alter the observed incidence of self-fertility. Treatment with 5-azaC was performed on seeds of fertile and sterile segregants derived from heterozygous *Ms1d/ms1d* individuals of the cv.

Chris. Whilst all seeds germinated, early abortion of seedling development was typically observed, resulting in a survival rate of 25 % for 125 µM 5-acaC treatment, 2.1 % for 250 µM and 16.6 % for 500 µM (Table 3).

The length of roots and hypocotyls of treated seeds were reduced, but no morphological abnormalities were observed at plant maturity (data not shown). From a total of 192 treated seeds, only four homozygous mutants survived treatment, this included two for each that were treated with 125 µM and 500 µM 5-azaC. All WT (*Ms1*/*Ms1*) and heterozygotes (*Ms1*/*ms1c*) were observed to be fully fertile, with no reduction in fertility relative to non-treated controls. In addition, all *ms1d* homozygotes exhibited complete sterility. These results suggest that the 5-acaC treatment strongly reduces plant growth and survival particularly at the germination stage of development. However, no obvious phenotypic effects were observed on treated plants relative to controls later in plant development (after potting out). Importantly, no changes in the degree of self-fertility was observed for any of the *ms1d* homozygous mutants.

Table 3 | Effect of the DNA demethylating reagent, 5-azacytidine, sterile and fertile segregants derived from *Ms1/ms1d* individuals.

5-azaC concentration (µM)	Number of seeds	Number of survival	Survival rate	Allele at the Ms1 locus	Number of plants	Number of fertile individuals	Seed/floret average
125[a]	48	12	25%	*ms1d*	2	0	0
				Het	5	5	1.98
				WT	2	2	2.02
250[b]	48	1	2.08%	*ms1d*	0	-	-
				Het	0	-	-
				WT	1	1	2.2
500[a]	100	15	15%	*ms1d*	2	0	0
				Het	8	8	2.08
				WT	2	2	2.3
Control	12	12	100%	*ms1d*	2	0	0
				Het	8	8	2.05
				WT	2	2	1.99

[a] and [b]: alternate batches of 5-acaC used.

5.4.3 No additional *TaMs1*-homologous sequence was detected in *ms1c*

To further investigate the basis for self-fertility in *ms1c*-P10 derived individuals, we determined whether additional *TaMs1*-like sequences (outside its direct 4A and 4D homeologues) are present in this *ms1c*-P10 background. Southern blot hybridisation, using a probe designed to discern *TaMs1* from other nsLTP genes was used to assess *TaMs1* copy number for the cultivars Gladius, Chinese Spring (CS) as well as homeogroup 4 nulli-tetrasomics and homozygous *ms1c* deletion mutant lines (Figure 1).

Nulli-tetrasomics (N4A-T4D, N4B-T4A and N4D-T4B) were used to identify *TaMs1*-A, -*B* and -*D* derived sequences (Figure 1). As expected, three major hybridization bands were detected for Gladius and Chinese Spring (CS), each corresponding to the three *TaMs1* homeoalleles. The B locus copy was absent in the *ms1c*-P5 and *ms1c*-P10 mutants confirming deletion of the *Ms1* locus. Importantly, no additional strongly-hybridising bands were detected in these mutant backgrounds.

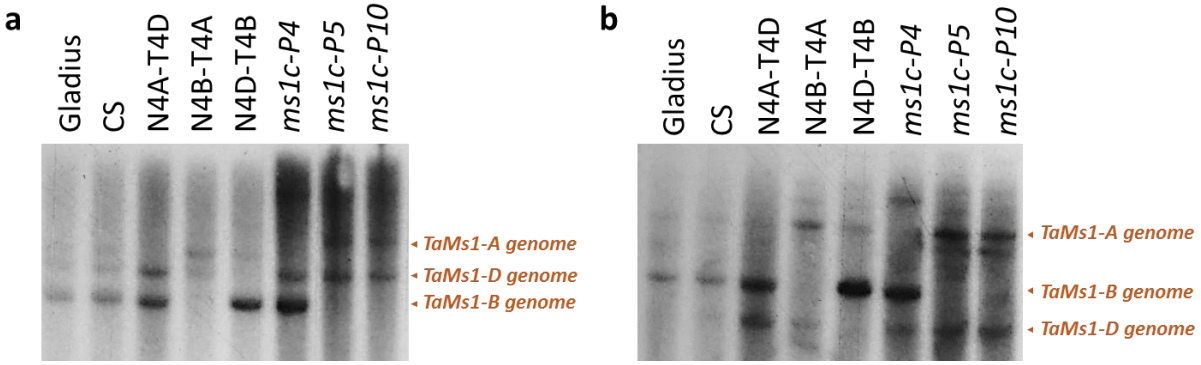

Figure 1 | Southern blot hybridization of *TaMs1* in Gladius, Chinese Spring and *ms1c* mutant lines. DNA digested with (a) BamH I and (b) Hind III restriction enzymes. CS, Chinese Spring; N4A/T4D, nullisomic for 4A and tetrasomic for 4D; N4B/T4A, nullisomic for 4B and tetrasomic for 4A; N4D/T4B, nullisomic for 4D and tetrasomic for 4B; *ms1c*-P4, *ms1c*-P5 and *ms1c*-P10, cv. Cornerstone homozygote *ms1c* deletion mutants. Full image in supplementary Figure S3.

5.4.4 Identification of two QTLs associated with restoration fertility in *ms1c*

Genotyping-by-sequencing (GbS)-SNP based linkage map was generated in order to identify QTL associated with modifier(s) of fertility in the *ms1c* background. For the final map, 1247 markers were contained within 31 linkage groups that could then be anchored to their physical position of the reference chromosome sequence from IWGSC refseq V0.4 (Figure 2 and Table 4). Highly variable SNP distribution across the genetic map was observed, with 10 – 126 binned SNPs per chromosome spanning an average distance of 2.2 cM and with a maximum distance of 47.5 cM.

Two QTLs, on chromosome 4A (*QMod-4A*) and chromosome 2B (*QMod-2B*), were significantly associated (*P* ≤1.44e-05) value with self-fertility in the *ms1c*-P5 x Gladius F_2 biparental population (Table 5). *QMod-4A* explained 17.7 % of the phenotypic variance and was mapped to an interval of 36 cM that is predicted to span approximately 30.5 Mb of chromosome 4A. *QMod-2B* explained 12.2 % of the phenotypic variance, spanning a predicted 167.5 Mb interval from 25.8 cM to 68.3 cM on chromosome 2B.

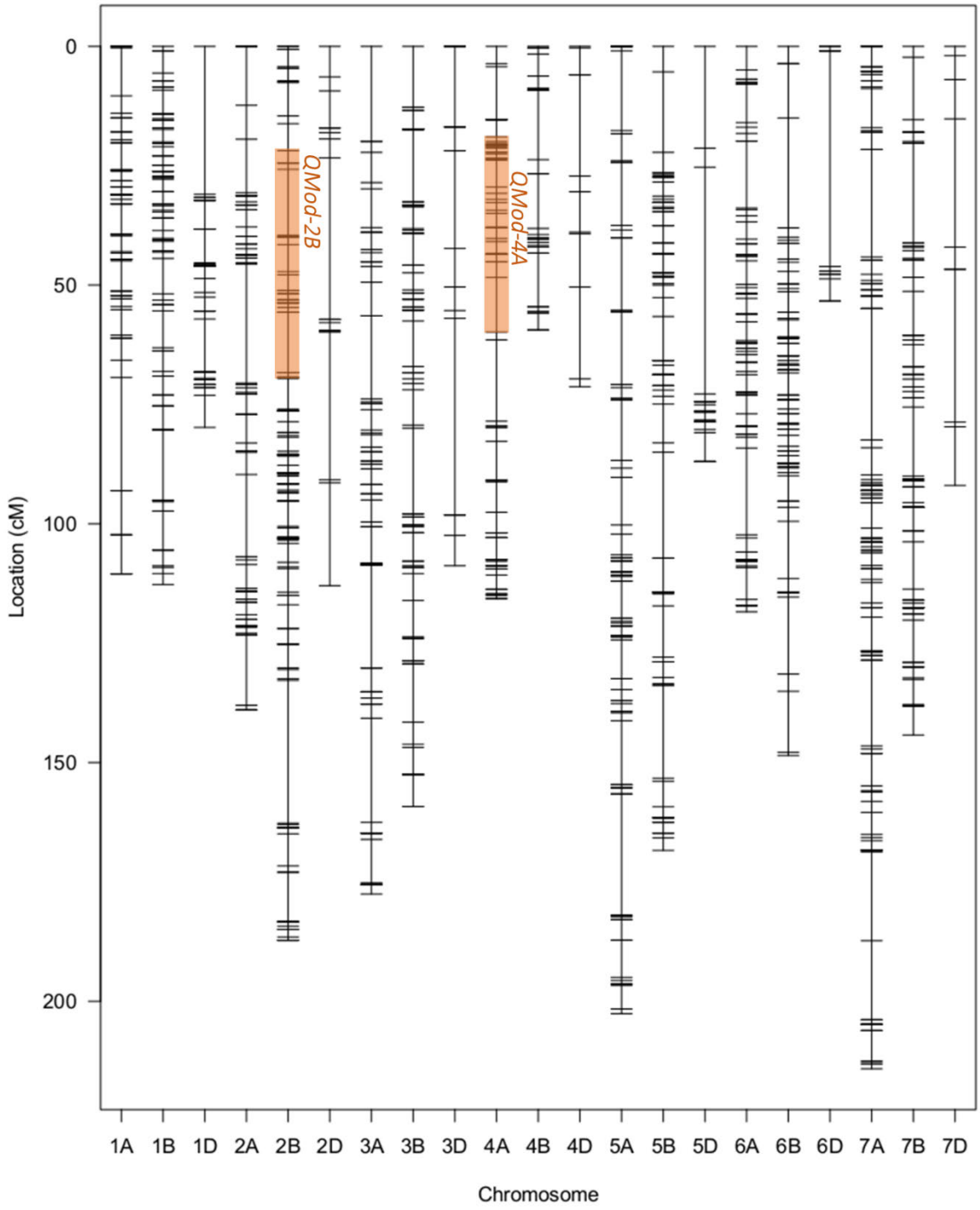

Figure 3 | *ms1c*-P5 x Gladius linkage map with 1247 binned SNPs. The genetic position (cM) of SNPs is labelled on the left of the chromosomes. Vertical orange bars on linkage groups indicate the QTLs with interval LOD above 3.8 (*P* ≤1.44e-05).

Table 4 | Summary of the *ms1c*-P5 x Gladius genetic linkage map.

Chromosome	No Markers	Length (cM)	Average distance between SNPs (cM)	Maximum distance between SNPs (cM)
1A	60	110.5	1.9	23.7
1B	78	112.7	1.5	14.8
1D	37	79.8	2.2	31
2A	77	139	1.8	24.9
2B	126	187.2	1.5	29.9
2D	20	113	5.9	33.9
3A	71	177.5	2.5	21.8
3B	81	159.2	2	18
3D	17	108.8	6.8	41.2
4A	76	115.7	1.5	17
4B	31	59.4	2	14.6
4D	11	71.3	7.1	21.2
5A	87	202.6	2.4	25.4
5B	80	168.4	2.1	22.2
5D	21	86.9	4.3	47.5
6A	82	118.4	1.5	18.2
6B	74	148.5	2	23
6D	14	53.3	4.1	45.1
7A	109	214.1	2	27.5
7B	85	144.2	1.7	20.9
7D	10	92	10.2	32
overall	1247	2662.6	2.2	47.5

Table 5 | Quantitative trait loci (QTL) associated with restored self-fertility in *ms1c*-P5 x Gladius F_2 population (*N*=114).

Trait	Chr	Peak (cM)	Closest Marker to QTL (scaffold:position-bps)	Range (cM)	LOD score	% VP[a]
Transformed Maximum	4A	45.1	chr4A:612662402	23.8-59.8	5.73	17.7
Transformed Average	4A	45.1	chr4A:612662402	29.5-59.8	5.19	15.9
Transformed Average	2B	53.1	chr2B:96600851	25.8-68.3	4.07	12.2

[a] Percent of the phenotypic variance explained by the QTL.

5.4.5 Candidate genes

To identify candidate genes for the fertility restoration in *ms1c* background we investigated all predicted genes within the *QMod-2B* and *QMod-4A* intervals. Using high confidence annotated genes from the IWGSC Ref1.0 assembly (URGI), we identified that the *QMod-2B* interval chr2B:44755839-210251654 contained 1394 predicted genes and that *QMod-4A*

interval chr4A:584720304-625798187 contained 724 predicted genes (data not shown). To narrow down the number of candidate genes within the two QTL intervals, we selected annotated genes with predicted function for pollen and anther development involved in lipid synthesis and transport (Table S3). A total of 39 genes involved in lipid biosynthesis or lipid transport were identified. Because male sterility in an *ms1* background has previously been shown to be the result of GPI-anchor nsLTP (TaMs1) loss of function, type G *nsLTPs* are likely candidates for the fertility modifier as they may complement the function of the absent *TaMs1* gene. A total of seven predicted nsLTPs were retrieved within the QTL intervals, including five nsLTPs within the *QMod-2B* (TraesCS2B01G138300.1_nsLTPg, TraesCS2B01G187600.1_nsLTPg, TraesCS2B01G215400.1_nsLTP1, TraesCS2B01G215500.1_nsLTP1, TraesCS2B01G215600.1_nsLTPd) and two nsLTPs on *QMod-4A* (TraesCS4A01G295600.1_nsLTPg, TraesCS4A01G295800.1_nsLTPg) (Figure 3a). Moreover, we identified that *TaMs1-A*, while not annotated as a high confidence gene, was also present within the *QMod-4A* interval. Furthermore, because the lipid binding domain (LBD) of nsLTPs has been reported to be essential for protein function (Salminen *et al.*, 2016), we aligned the LBD amino acid sequence of candidate *Mod's* with the TaMs1-B derived amino acid sequence (Figure 3b). As expected, high sequence identity (98.8 %) was observed between the TaMs1-B and TaMs1-A proteins across the eight-cysteine motif (8CM). In contrast, an identity of only 20.2 % to 25.9 % was found between TaMs1 and the other nsLTPs of the QTL intervals. In addition, protein domains normally present in nsLTPs were analysed, this included the N-terminal signal peptide (SP) and the 8CM (Table S4). All candidate nsLTPs were predicted to contain the SP, however, TraesCS2B01G138300.1_nsLTPg did not possess the characteristic 8CM of nsLTPs and therefore should not be annotated as such.

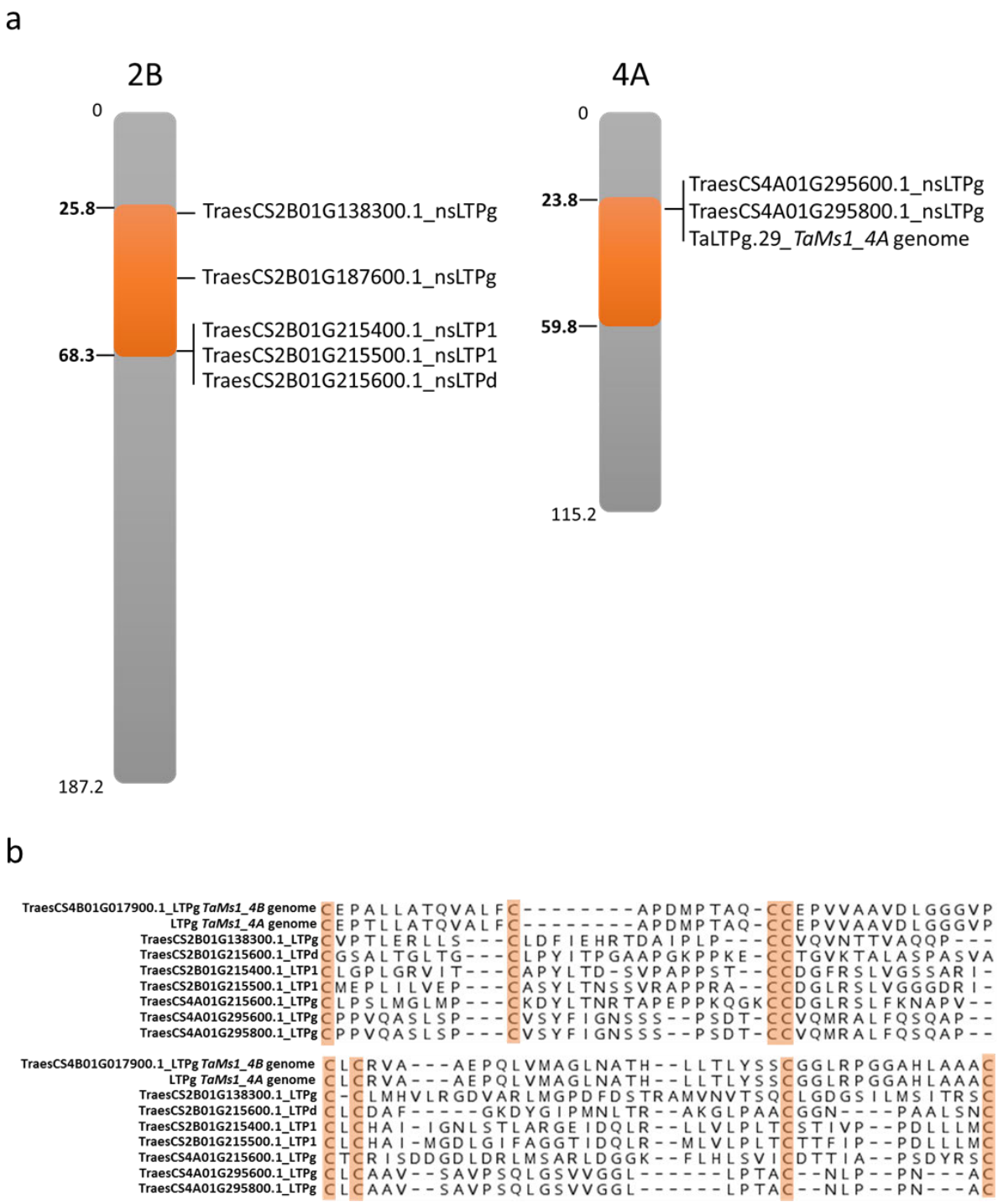

Figure 3 | Identification of putative candidate genes within the *QMod-2B* and *QMod-4A* intervals. (a) *nsLTPs* present within the QTL intervals. (b) Amino acid sequence alignments of the candidate nsLTP- eight cysteine motif (8CM).

5.5 Discussion

The expressivity of *ms1*-induced male sterility varies depending upon the genetic background

In this study, we showed variability in sterility penetrance across *ms1* mutant alleles and genetic backgrounds (Table 2); while the *ms1d* allele showed near-complete sterility penetrance (> 98.53%) across all backgrounds tested (H45, Mace, Pastor, RAC875, Westonia and Gladius), low sterility penetrance was observed for deletion mutant *ms1c* (*ms1c*-P5 and *ms1c*-P10 individuals). Self-fertility in the *ms1c* mutant background was highly variable between plants as well as tillers of the same plant, suggesting self-fertility is modulated either by environmental conditions/developmental timing or other genetic factors. Interestingly tiller variability in self-fertility, and previous reports of *TaMs1* homeologue silencing would indicate a possible epigenetic regulation.

***TaMs1-A* derived-genome as likely candidate for the modifier gene**

Here we identified two QTLs associated with selfed seed-set in *ms1c* homozygotes derived from an *ms1c*-P5 x Gladius F_2 population. These included a QTL on chromosome 4A (*QMod-4A*) and another on chromosome 2B (*QMod-2B*). *QMod-4A* (36 cM) and *QMod-2B* (42.5 cM) explain 17.7 % and 12.2 % of the phenotypic variance respectively (Figure 2, Table 5). This suggests polygenic inheritance of self-seed set. Increasing population size must be considered for narrowing down the QTL intervals and more precisely defining their relative effects on self-fertility. Narrowing these regions would also prove linked molecular markers that can be used for counter selecting these self-fertility inducing loci in a hybrid breeding program, albeit this would add to the costs of hybrid seed production. Additionally, self-fertility assessment under a range of environmental conditions should be investigated through replicated field trials across multiple environments. This is a pre-requisite for commercial deployment in a hybrid breeding program.

It is reasonable to assume that the incomplete sterility penetrance might be a consequence of residual functionality of a TaMs1-like protein. Interestingly, seven nsLTP sequences within the two major effect QTL intervals (*QMod-4A* and *QMod-2B*) sequences were retrieved from the Chinese Spring reference genome (Table S3). Considering the *TaMs1-A* homeologue was present within the *QMod-4A* interval, it makes it a strong candidate for a fertility modifier (Figure 3a). The expression of the *TaMs1-A* homeologue has previously been investigated in anthers derived from *ms1c*-P10. Results of this study revealed that *TaMs1-A* transcripts in pools of anthers containing meiotic and uninucleate microspores were below reasonable

detection levels (Tucker *et al.*, 2017). It would be informative to analyse the expression by qRT-PCR of all seven nsLTPs present within these QTL intervals, particularly within the *ms1c*-P5 x Gladius individuals, considering this particular genetic background exhibits homozygote mutant self-fertility. Anthers containing pre-meiotic to meiotic microspores would need to be assessed.

Interestingly, Wang *et al.* (2017) recently suggested that *TaMs1* homeologues from -A and -D genome sequences were epigenetically silenced due to hypermethylation of their promoters in allohexaploid wheat. While no DNA methylation in *TaMs1* orthologue promoters was observed in diploid and tetraploid ancestors, and these orthologues were shown to be expressed. Therefore, *TaMs1* (B genome) dominance in allohexaploid wheat is likely due to epigenetic repression of its homeoalleles. Moreover, no deleterious SNP was detected in the coding sequence of *TaMs1*-A and -D genome sequences (Figure S2). Taking together, we suggest that both homeoalleles represent strong candidates for the modifier genes. Other 4B deletion male sterile mutants have been previously reported, this include the ditelosomic 4BL line and, *ms1a* (spontaneous mutant cv. Pugsley) and *ms1b* (ionising radiation mutant, cv. Probus) which both contain a 4BS deletion smaller than *ms1c* (4BS-8, cv. Chinese Spring (CS)) (Pugsley and Oram, 1959; Fossati and Ingold, 1970; Joshi *et al.*, 2014). All these mutant lines were reported to be completely male sterile. However, the selfed-progeny between the ditelosomic 4BL (4BS-8) and the cultivar Norin 61 (N61) resulted in fertile 4BS deletions lines (Joshi *et al*., 2013). Some nullisomic-4B lines were found fertile among F_2 plants derived from a cross between CS and monosomic line of N61, suggesting the presence of a modifier gene on a chromosome other than 4B in N61 background (Joshi *et al.*, 2014). A targeted DNA demethylation approach (i.e. CRISPR-based approach, Xu *et al.*, 2016) could provide evidence for an epigenetic regulation and correct function of *TaMs1* homeologues.

Furthermore, allopolyploidization has been shown to be associated with gene silencing in *A. thaliana* and wheat (Comai *et al.*, 2000; Lee and Chen, 2001; Madlung, 2002). Homeologous gene silencing in newly synthesized polyploids occurs at a frequency of 5 % in wheat from early stages of allopolyploid formation (Kashkush *et al.*, 2002) and 7-8 % of genes in established wheat hexaploids. In each of these cases, gene silencing was shown to be associated with cytosine methylation. Similarly, aneuploidy (loss of whole chromosomes, chromosome arms, or variable sizes of chromosomal segments (Tang and Amon, 2013) resulted in extensive changes of gene expression and chromatin condensation resulting from

epigenetic mark modifications (Huettel *et al.*, 2008; Gao *et al.*, 2016). In wheat, these epigenetic changes were studied using whole-chromosome aneuploidy of 1A, 1B and 1D (Gao *et al.*, 2016). Monosomic 1A lines were observed to contain significantly lower total GC methylation than WT and that this alteration in DNA methylation was heritable. This suggest a possible transcriptional activation of genes within the demethylated regions. However, the chromosomal location of loci with DNA demethylation changes in these aneuploidy lines could not be precisely identified. How the loss of a whole-chromosome or chromosome fragment affect the transcriptional regulation of their homeologue counterparts in polyploid species remains largely unknown. Interestingly, the conversion from hexaploid wheat (BBAADD) to extracted tetraploid wheat (BBAA) results in viable plants (Zhang *et al.*, 2017). This possible ploidy-reversion suggests a conservation of integrity of the sub-genomes.

A pilot experiment of whole-genome demethylation did not induce fertility restoration of *ms1d* lines

DNA methylation plays an important role in regulating gene expression, with DNA methylation preventing gene expression and DNA demethylation conferring relative gene activation (Vanyushin *et al.*, 2002). This epigenetic regulation of gene expression was in part demonstrated by the use of the demethylation reagent 5-azaC, an analogue of cytosine that cannot be methylated at the 5' position. It has been shown to activate transcriptionally repressed genes (Jones, 1985; John and Amasino, 1989; Klaas *et al.*, 1989; Weber and Graessmann, 1989). Differences in ripeness, height and number of tillers were the most striking reported effect of 5-azaC treatment of *triticale* seeds (Heslop-Harrison, 1990; Amado *et al.*, 1997). The meiotic transmission of hypomethylation is thought to result from the demethylation of loci controlling phenotypic traits (Vyskot *et al.*, 1995). To study a potential epigenetic regulation of self-seed set, we treated *ms1d* seeds with the DNA demethylation agent, 5-azaC. Germinating seeds treated with 5-azaC showed significant reduction in root and coleoptile growth. Such inhibiting effects of 5-azaC have already been reported for wheat (Aleksandrushkina *et al.*, 1989; Shkute and Stivrina, 2005). The 5-azaC treatment did not induce self-fertility in *ms1d* mutants (Table 3). The lack of induced self-fertility by 5-azaC would either suggest that the chemical dosage was not sufficient or that self-fertility is not responsive to demethylation. Additionally demethylation may not have persisted through till anthesis and seed-set considering is has previously been reported to occur from early meristem development through to early flowering (Yang *et al.*, 2015). It is also worth noting that only four 5-azaC-treated homozygote *ms1d* mutant seeds were grown to maturity,

therefore this sample size is small for which no definite conclusion can be drawn. To confirm the results obtained in this study, an increased number of replicates (>20 homozygote *ms1d* plants) and doses would be required. In addition, whilst the 5-azaC treatment protocol conducted in this study has been successfully used to assess DNA degradation in *triticale* seedlings (Vanyushin *et al.*, 2002; Shkute and Stivrina, 2005); an alternative treatment might be more appropriate for this study. For example, effects on flowering were studied using 5-azaC diluted with ethanol and applied directly onto shoot apical meristems (Kondo *et al.*, 2006, 2007). Such an approach could provide a more direct assessment on self-fertility.

In this study, we conducted a GBS-SNP linkage map and identified two QTL associated with the incomplete male sterility penetrance in *ms1c*-P5 x Gladius F_2 population. The developed markers within the QTL have potential use for counter-selecting these self-fertility inducing loci in a hybrid breeding program. Screening more F_2 individuals will allow us to narrow down the QTL intervals and identify any potential additional loci.

5.6 Declarations

5.6.1 Acknowledgment

We thank Sue Manning and Lorelei Arbeile for growing, phenotyping and genotyping the plant material used in this work. This research was funded by DuPont Pioneer Hi-Bred International Inc. We are grateful for the support provided by The University of Adelaide.

5.6.2 Author contributions

Experimental design: AK, EJT, MP, UB, RW; Performed the experiment: AK, EJT, PW, SM, LA, MP; Analysed data: AK, EJT, PE, MP, NW-H, UB, RW; Manuscript preparation: AK, PE, NW-H; Manuscript editing: AK, EJT, MP PE, NW-H, UB, RW.

5.7 References

Aleksandrushkina NI, Kirnos MD, Rotaenko EP, Vanyushin BF. 1989. Inhibition of nuclear DNA synthesis and methylation by 5-azacytidine during successive cell cycles in dividing cells of the first leaf of etiolated wheat seedlings. Biokhimiya **54**, 355–360.

Amado L, Abranches R, Neves N, Viegas W. 1997. Development-dependent inheritance of 5-azacytidine-induced epimutations in triticale: analysis of rDNA expression patterns. Chromosome research : an international journal on the molecular, supramolecular and evolutionary aspects of chromosome biology **5**, 445–50.

Brown T. 2001. Southern Blotting. Current Protocols in Immunology. John Wiley & Sons, Inc.

Burton RA. 2004. The CesA Gene Family of Barley. Quantitative Analysis of Transcripts Reveals Two Groups of Co-Expressed Genes. Plant Physiology **134**, 224–236.

Cenci A, Chantret N, Kong X, Gu Y, Anderson OD, Fahima T, Distelfeld A, Dubcovsky J. 2003. Construction and characterization of a half million clone BAC library of durum wheat (Triticum turgidum ssp. durum). Theoretical and Applied Genetics **107**, 931–939.

Comai L, Tyagi AP, Winter K, Holmes-Davis R, Reynolds SH, Stevens Y, Byers B. 2000. Phenotypic instability and rapid gene silencing in newly formed Arabidopsis allotetraploids. The Plant Cell **12**, 1551–1567.

Driscoll CJ. 1972. XYZ system of producing hybrid wheat. Crop Science **12**, 516–517.

Driscoll CJ. 1977. Registration of cornerstone male sterile wheat germplasm (reg. no. GP 74). Crop Science **17**, 190.

Driscoll CJ. 1985. Modified XYZ system of producing hybrid wheat. Crop Science, 1115–1116.

Driscoll CJ, Barlow KK. 1976. Male sterility in plants. Induction, isolation and utilization. Induced mutations in cross-breeding.

Driscoll CJ, Qualset CO. 1986. Nuclear male sterility systems in seed production of hybrid varieties. Critical Reviews in Plant Sciences **3**, 227–256.

Duvick DN. 2004. *Hybrid Maize Breeding Program*. Plant Breeding Reviews.

FAO. 2013. Food and Agriculture Organization of the United Nations. FAOSTAT, http://faostat.fao.org.

Fossati A, Ingold M. 1970. A male-sterile mutant in Triticum aestivum. Wheat Information Service (Kyoto), 8–10.

Gao L, Diarso M, Zhang A, Zhang H, Dong Y, Liu L, Lv Z, Liu B. 2016. Heritable alteration of DNA methylation induced by whole-chromosome aneuploidy in wheat. New Phytologist **209**, 364–375.

Haldane JBS. 1955. The measurement of variation. Evolution **9**, 484–484.

Heslop-Harrison JS. 1990. Gene expression and parental dominance in hybrid plants. Development **108**, 21–28.

Huettel B, Kreil DP, Matzke M, Matzke AJM. 2008. Effects of aneuploidy on genome structure,

expression, and interphase organization in Arabidopsis thaliana. PLoS Genetics **4**.

Islam A, Driscoll C. 1984. Latent male fertility in 'Cornerstone' chromosome 4A. Can. J. Genet. Cytol. **26**, 98–99.

John MC, Amasino RM. 1989. Extensive changes in DNA methylation patterns accompany activation of a silent T-DNA ipt gene in Agrobacterium tumefaciens-transformed plant cells. Molecular and cellular biology **9**, 4298–303.

Jones PA. 1985. Effects of 5-Azacytidine on Cell Differentiation and DNA methylation. Pharmac. Ther. **28**, 17–22.

Joshi GP, Li J, Nasuda S, Endo TR. 2014. Development of a self-fertile ditelosomic line for the long arm of chromosome 4B and its characterization using SSR markers. , 311–314.

Kashkush K, Feldman M, Levy AA. 2002. Gene loss, silencing and activation in a newly synthesized wheat allotetraploid. Genetics **160**, 1651–1659.

Kim YJ, Zhang D. 2017. Molecular Control of Male Fertility for Crop Hybrid Breeding. Trends in Plant Science **23**, 53–65.

Klaas M, John MC, Crowell DN, Amasino RM. 1989. Rapid induction of genomic demethylation and T-DNA gene expression in plant cells by 5-azacytosine derivatives. Plant Molecular Biology **12**, 413–423.

Kondo H, Miura T, Wada KC, Takeno K. 2007. Induction of flowering by 5-azacytidine in some plant species: relationship between the stability of photoperiodically induced flowering and flower-inducing effect of DNA demethylation. Physiologia plantarum **131**, 462–9.

Kondo H, Ozaki H, Itoh K, Kato A, Takeno K. 2006. Flowering induced by 5-azacytidine, a DNA demethylating reagent in a short-day plant, Perilla frutescens var. crispa. Physiologia Plantarum **127**, 130–137.

Kovalchuk N. 2014. High-Throughput Analysis Pipeline for Achieving Simple Low-Copy Wheat and Barley Transgenics. In: Whitford R,, In: Fleury D, eds. Crop Breeding. Methods and Protocols.239–252.

Lee HS, Chen ZJ. 2001. Protein-coding genes are epigenetically regulated in Arabidopsis polyploids. Proceedings of the National Academy of Sciences of the United States of America **98**, 6753–6758.

Madlung A. 2002. Remodeling of DNA Methylation and Phenotypic and Transcriptional Changes in Synthetic Arabidopsis Allotetraploids. Plant Physiology **129**, 733–746.

Pugsley A, Oram R. 1959. Genic male sterility in wheat. Australian Plant Breeding and Genetics Newsletter **14**, 10–11.

Ray DK, Mueller ND, West PC, Foley JA. 2013. Yield Trends Are Insufficient to Double Global Crop Production by 2050. PLoS ONE **8**.

Salminen TA, Blomqvist K, Edqvist J. 2016. Lipid transfer proteins: classification, nomenclature, structure, and function. Planta **244**, 971–997.

Sasakuma T, Maan SS, Williams ND. 1978. EMS-Induced Male-Sterile Mutants in Euplasmic and Alloplasmic Common Wheat1. Crop Science **18**, 850.

Shkute N, Stivrina N. 2005. 5-Azacytidine decreases fragmentation of nuclear DNA and pigment formation in first leaf cells of barley seedlings. Cell Biology International **29**, 1025–1031.

Stephen S, Cullerne D, Spriggs A, Helliwell C, Lovell D, Taylor J. 2012. BioKanga: a suite of high performance bioinformatics applications.

Tang YC, Amon A. 2013. Gene copy-number alterations: A cost-benefit analysis. Cell **152**, 394–405.

Taylor J, Butler D. 2017. R Package ASMap: Efficient Genetic Linkage Map Construction and Diagnosis.

Tester M. 2011. Breeding Technologies to Increase. Science **818**, 818–822.

Tucker EJ, Baumann U, Kouidri A, *et al.* 2017. Molecular identification of the wheat male fertility gene Ms1 and its prospects for hybrid breeding. Nature Communications **8**, 869.

Vanyushin BF, Shorning BY, Seredina A V., Aleksandrushkina NI. 2002. The effects of phytohormones and 5-azacytidine on apoptosis in etiolated wheat seedlings. Russian Journal of Plant Physiology **49**, 501–506.

Vyskot B, Koukalová B, Kovařík A, Sachambula L, Reynolds D, Bezděk M. 1995. Meiotic transmission of a hypomethylated repetitive DNA family in tobacco. Theoretical and Applied Genetics **91**, 659–664.

Wang Z, Li J, Chen S, *et al.* 2017. Poaceae-specific *MS1* encodes a phospholipid-binding protein for male fertility in bread wheat. Proceedings of the National Academy of Sciences, 201715570.

Weber H, Graessmann A. 1989. Biological activity of hemimethylated and single-stranded DNA after direct gene transfer into tobacco protoplasts. FEBS Letters **253**, 163–166.

Xu X, Tao Y, Gao X, Zhang L, Li X, Zou W, Ruan K, Wang F, Xu GL, Hu R. 2016. A CRISPR-based approach for targeted DNA demethylation. Cell Discovery **2**.

Yang H, Chang F, You C, Cui J, Zhu G, Wang L, Zheng Y, Qi J, Ma H. 2015. Whole-genome DNA methylation patterns and complex associations with gene structure and expression during flower development in Arabidopsis. The Plant Journal **81**, 268–281.

Zhang A, Li N, Gong L, Gou X, Wang B, Deng X, Li C, Dong Q, Zhang H, Liu B. 2017. Global analysis of gene expression in response to whole-chromosome aneuploidy in hexaploid wheat. Plant Physiology **175**, pp.00819.2017.

Zhou K, Wang S, Feng Y, Ji W, Wang G. 2007. A new male sterile mutant LZ in wheat (Triticum aestivum L.). Euphytica **159**, 403–410.

5.8 Additional files

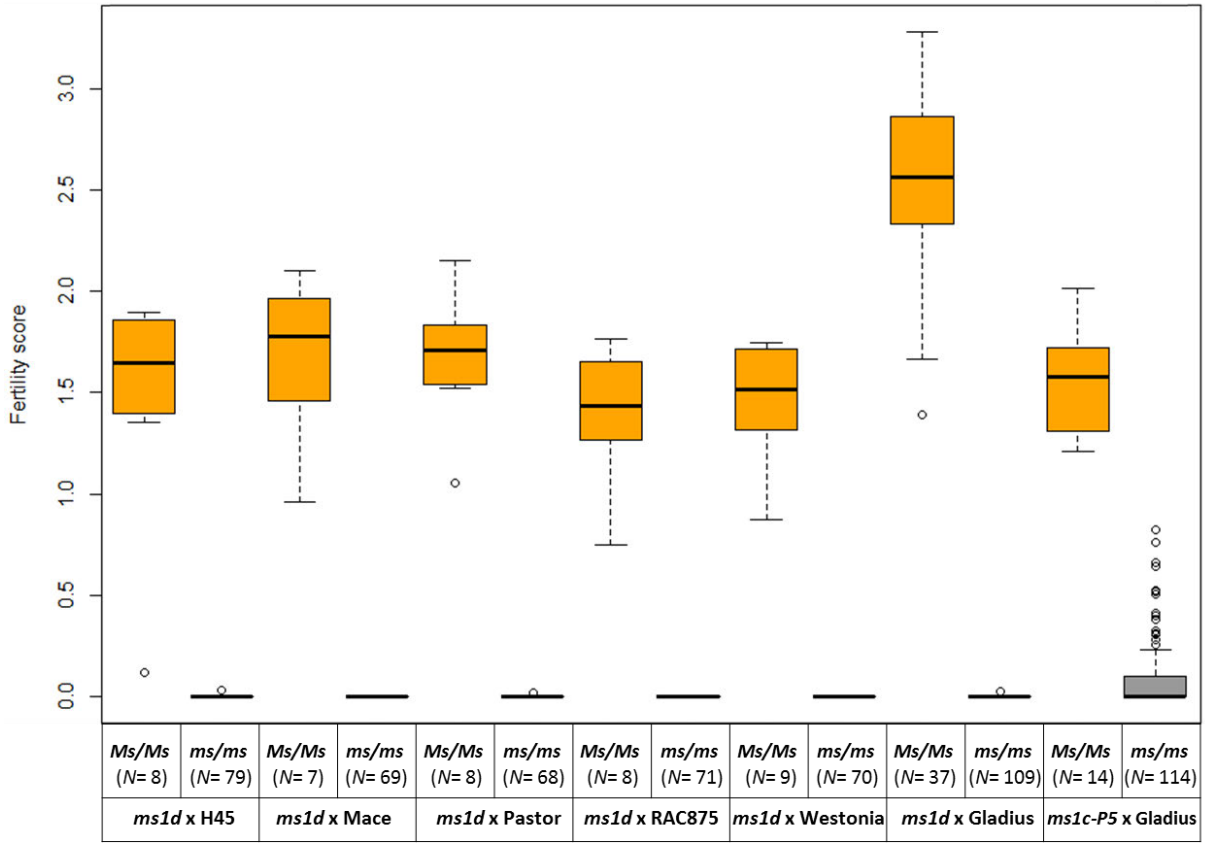

Figure S1 | Box plots of the distributions highlighting the fertility scores from *ms1* x varieties F_2 individuals. Average fertility score was calculated from two or three heads per individuals. The fertility score distributions of the F_2 populations are presented for *ms1d* x H45, *ms1d* x Mace, *ms1d* x Pastor, *ms1d* x Westonia, *ms1d* x Gladius and *ms1c-P5* x Gladius.

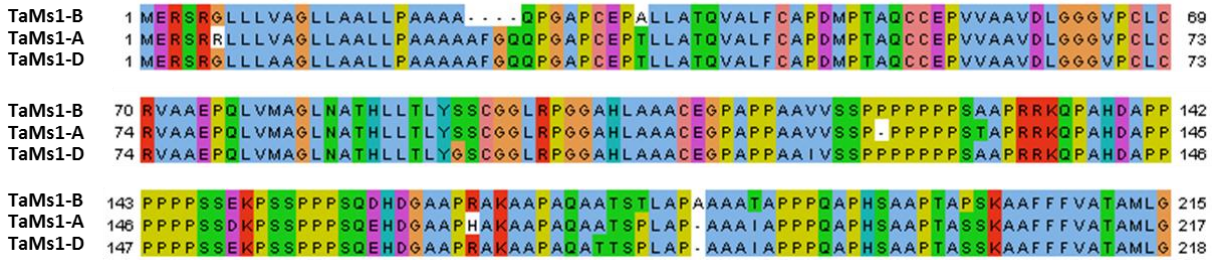

Figure S2 | Amino acid sequence alignment of TaMs1 and its homeologues. Multiple sequence alignment of TaMs1-A, TaMs1-B and TaMs1-D derived-genomes coloured by amino acid similarity.

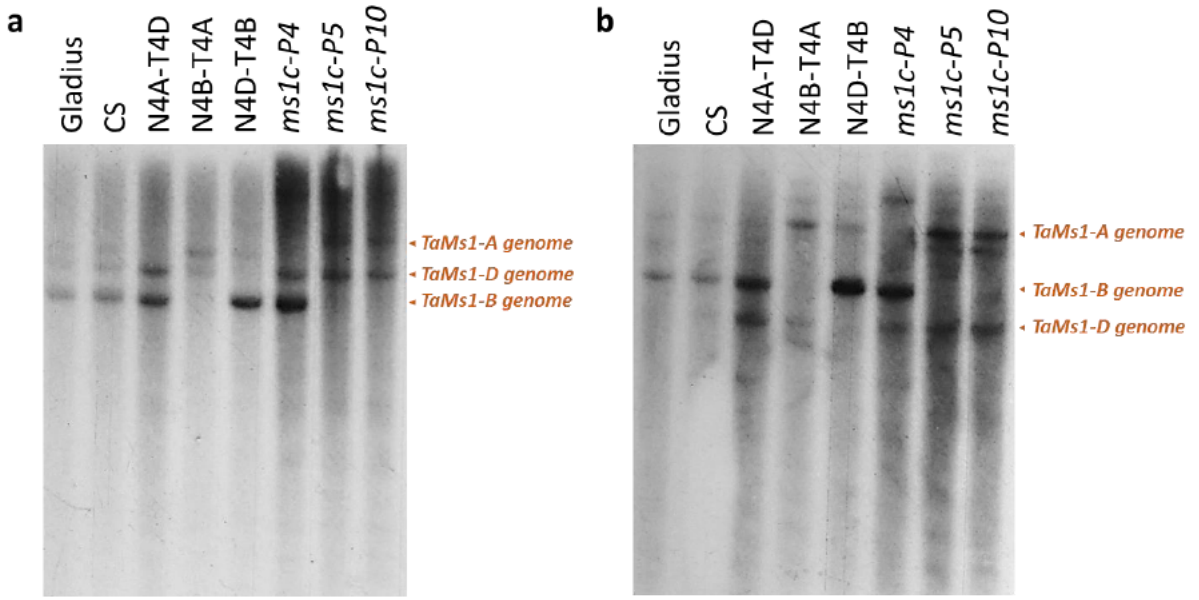

Figure S3 | Southern blot hybridization of *TaMs1* in Gladius, Chinese spring and *ms1c* mutant lines. DNA digested with (a) BamH I and (b) Hind III restriction enzymes. CS, Chinese Spring; N4A/T4D, nullisomic for 4A and tetrasomic for 4D; N4B/T4A, nullisomic for 4B and tetrasomic for 4A; N4D/T4B, nullisomic for 4D and tetrasomic for 4B; *ms1c*-P4, *ms1c*-P5 and *ms1c*-P10, cv. Cornerstone homozygote *ms1c* deletion mutants.

Table S1 | List of pedigree used crosses with *ms1* to generate F_2 populations

Name	Pedigree
Gladius	CO-1190-203/84-W-127-501[3767][4094]
H45	B-1814//WW-15/QT-7605[3770]
Mace	WYALKATCHEM/STYLET//WYALKATCHEM [3798]
Pastor	PFAU/SERI-82(CID-93300//BOBWHITE[2964]
RAC875	RAC-655/3/Sr21/4*LANCE//4*BAYONET
Westonia	CO-1190-203/84-W-127-501[3767][4094]

Table S2 | Fertility scores from *ms1c* x Gladius F_2 individuals.

	Fertility score			
Plant ID	Head 1	Head 2	Head 3	average
1	0.000	0.000	0.000	0.000
2	0.000	0.000	0.000	0.000
3	0.000	0.000	0.000	0.000
4	0.643	0.000	0.000	0.214
5	0.000	0.000	0.000	0.000
6	0.000	0.000	0.167	0.056
7	0.000	0.000	0.000	0.000
8	0.091	0.000	0.000	0.030
9	0.000	0.000	0.000	0.000
10	0.000	0.000	0.000	0.000
11	0.000	0.000	0.000	0.000
12	0.000	0.000	0.000	0.000
13	0.000	0.000	0.000	0.000
14	0.222	0.000	0.750	0.324
15	0.000	0.000	0.000	0.000
16	0.000	0.000	0.000	0.000
17	0.000	0.000	0.000	0.000
18	0.000	0.000	0.000	0.000
19	0.000	0.000	0.154	0.051
20	0.000	0.000	0.125	0.042
21	0.000	0.000	0.000	0.000
22	0.000	0.000	0.000	0.000
23	0.000	0.000	0.000	0.000
24	0.167	0.385	0.000	0.184
25	0.000	0.417	0.000	0.139
26	0.000	0.000	0.000	0.000
27	0.286	0.000	0.000	0.095
28	0.000	0.000	0.000	0.000
29	0.000	0.000	0.000	0.000
30	0.000	0.000	0.000	0.000
31	0.000	0.250	0.000	0.083
32	0.091	0.600	0.000	0.230
33	0.750	0.900		0.825
34	0.167	0.294	0.063	0.174
35	0.000	0.000	0.000	0.000
36	0.000	0.000	0.000	0.000
37	0.000	0.000	0.000	0.000
38	0.000	0.000	0.000	0.000
39	0.636	1.286	0.000	0.641
40	0.000	0.000	0.000	0.000
41	0.000	0.000	0.000	0.000
42	0.000	0.000	0.000	0.000
43	0.167	0.000	0.000	0.056
44	0.067	0.000	0.000	0.022
45	0.000	0.000	0.000	0.000
46	0.833	0.300	0.000	0.378
47	1.000	0.556	0.000	0.519
48	0.000	0.000	0.000	0.000
49	0.091	0.500	0.000	0.197
50	0.000	0.000	0.000	0.000
51	0.167	0.000	0.000	0.056
52	0.000	0.000	0.167	0.056
53	0.000	0.000	0.000	0.000
54	0.000	0.000	0.000	0.000
55	0.000	0.000	0.000	0.000
56	0.333	0.000	0.111	0.148
57	0.111	0.143	0.000	0.085

	Fertility score			
Plant ID	Head 1	Head 2	Head 3	average
58	0.333	0.000		0.167
59	0.500	0.000	0.333	0.278
60	0.000	0.143	0.000	0.048
61	0.000	0.000	0.000	0.000
62	0.000	0.000	0.000	0.000
63	0.000	0.000	0.091	0.030
64	0.500	0.125		0.313
65	0.000	0.000	0.000	0.000
66	0.000	0.000	0.000	0.000
67	0.000	0.000	0.000	0.000
68	0.000	0.000	0.000	0.000
69	0.000	0.000	0.000	0.000
70	0.000	0.000	0.000	0.000
71	0.000	0.000	0.000	0.000
72	0.000	0.000	0.000	0.000
73	1.333	0.182	0.000	0.505
74	0.000	0.000	0.000	0.000
75	0.000	0.667	0.000	0.222
76	0.357	0.000	0.000	0.119
77	0.000	0.188	0.000	0.063
78	0.000	0.000	0.000	0.000
79	0.000	0.000	0.000	0.000
80	0.000	0.000	0.000	0.000
81	0.294	0.063	0.000	0.119
82	0.091	0.000	0.000	0.030
83	0.889	0.583	0.500	0.657
84	0.000	0.000	0.000	0.000
85	0.000	0.000	0.000	0.000
86	0.000	0.000	0.000	0.000
87	0.000	0.000	0.000	0.000
88	0.000	0.000	0.000	0.000
89	0.067	0.000	0.000	0.022
90	0.000	0.000	0.000	0.000
91	1.538	0.100		0.800
92	0.000	0.000	0.000	0.000
93	0.500	0.222	0.500	0.407
94	1.462	0.111	0.000	0.524
95	0.000	0.000	0.000	0.000
96	0.909	0.000	0.286	0.398
97	0.000	0.000		0.000
98	0.313	0.000	0.333	0.215
99	0.000	0.000	0.154	0.051
100	1.786	0.000	0.500	0.762
101	0.000	0.000	0.250	0.083
102	0.000	0.000	0.000	0.000
103	0.000	0.000	0.000	0.000
104	0.000	0.000	0.000	0.000
105	0.000	0.000	0.000	0.000
106	0.000	0.000	0.000	0.000
107	0.000	0.000	0.000	0.000
108	0.917	0.000	0.000	0.306
109	0.533	0.000	0.231	0.255
110	0.000	0.143	0.000	0.048
111	0.000	0.000	0.000	0.000
112	0.154	0.000	0.077	0.077
113	0.000	0.000	0.000	0.000
114	0.000	0.000	0.000	0.000

Table S3 | List of candidate genes within QTL *QMod-2B* and *QMod-4A* associated with the fertility restoration in *ms1c* x Gladius F_2 population.

QTL	Gene ID	Chr	Start	End	Strand	Predicted function
QMod-2B	TraesCS2B01G096400.1	chr2B	56714333	56715260	-	Tapetum determinant 1
QMod-2B	TraesCS2B01G099500.1	chr2B	58843918	58846788	-	Omega-3 fatty acid desaturase
QMod-2B	TraesCS2B01G110900.1	chr2B	72760663	72761079	+	ATP-binding-cassette transporter family protein
QMod-2B	TraesCS2B01G121000.1	chr2B	88618432	88622044	-	Cytochrome P450 family protein, expressed
QMod-2B	TraesCS2B01G128400.1	chr2B	96084601	96090792	-	ABC transporter G family member
QMod-2B	TraesCS2B01G128700.1	chr2B	96100271	96110906	-	ABC transporter G family member
QMod-2B	TraesCS2B01G128800.1	chr2B	96236555	96240339	-	ABC transporter G family member
QMod-2B	TraesCS2B01G136500.1	chr2B	103923350	103925242	+	Cytochrome P450 family protein, expressed
QMod-2B	TraesCS2B01G136600.1	chr2B	103960587	103962566	+	Cytochrome P450 family protein, expressed
QMod-2B	TraesCS2B01G138300.1	chr2B	105477534	105478669	+	Lipid transfer protein
QMod-2B	TraesCS2B01G138800.1	chr2B	105895427	105896920	+	Cytochrome P450 family protein
QMod-2B	TraesCS2B01G147600.1	chr2B	113912189	113915288	+	Cytochrome P450, putative, expressed
QMod-2B	TraesCS2B01G167500.1	chr2B	140750519	140756635	-	Cytochrome P450, putative
QMod-2B	TraesCS2B01G187600.1	chr2B	162928065	162929589	-	Lipid transfer protein
QMod-2B	TraesCS2B01G201900.1	chr2B	181119111	181120782	-	Cytochrome P450 protein
QMod-2B	TraesCS2B01G213000.1	chr2B	197681873	197686903	+	Fatty-acid desaturase
QMod-2B	TraesCS2B01G213000.2	chr2B	197683500	197686903	+	Fatty-acid desaturase
QMod-2B	TraesCS2B01G215400.1	chr2B	200690011	200690854	-	Lipid transfer protein
QMod-2B	TraesCS2B01G215500.1	chr2B	200863705	200864349	-	Non-specific lipid-transfer protein-like protein
QMod-2B	TraesCS2B01G215600.1	chr2B	200896772	200897422	+	Lipid transfer protein
QMod-A4	TraesCS4A01G276900.1	chr4A	585027950	585031394	-	polyketide cyclase/dehydrase/lipid transport superfamily protein
QMod-A4	TraesCS4A01G276900.2	chr4A	585027950	585032610	-	polyketide cyclase/dehydrase/lipid transport superfamily protein
QMod-A4	TraesCS4A01G276900.3	chr4A	585027950	585033320	-	polyketide cyclase/dehydrase/lipid transport superfamily protein
QMod-A4	TraesCS4A01G276900.4	chr4A	585027950	585033320	-	polyketide cyclase/dehydrase/lipid transport superfamily protein
QMod-A4	TraesCS4A01G277900.1	chr4A	585539981	585541802	+	Cytochrome P450 family protein, expressed
QMod-A4	TraesCS4A01G295600.1	chr4A	596214978	596215939	+	Lipid transfer protein
QMod-A4	TraesCS4A01G295800.1	chr4A	596238333	596239331	-	Lipid transfer protein
QMod-A4	TraesCS4A01G304400.1	chr4A	599842221	599846313	+	Fatty acyl-CoA reductase
QMod-A4	TraesCS4A01G307600.1	chr4A	601337777	601338814	+	Cytochrome P450 family protein, expressed
QMod-A4	TraesCS4A01G307700.1	chr4A	601338817	601339314	+	Cytochrome P450 family protein, expressed
QMod-A4	TraesCS4A01G308200.1	chr4A	602053534	602061759	+	ABC transporter G family member
QMod-A4	TraesCS4A01G308600.1	chr4A	602248955	602250749	-	Cytochrome P450 family protein, expressed
QMod-A4	TraesCS4A01G315900.1	chr4A	605744972	605749290	+	ABC transporter G family member
QMod-A4	TraesCS4A01G336400.1	chr4A	618620274	618626659	-	Long-chain-fatty-acid CoA ligase, putative
QMod-A4	TraesCS4A01G336400.2	chr4A	618620274	618626705	-	Long-chain-fatty-acid CoA ligase, putative
QMod-A4	TraesCS4A01G336400.3	chr4A	618620274	618627913	-	Long-chain-fatty-acid CoA ligase, putative
QMod-A4	TraesCS4A01G336400.4	chr4A	618620274	618627946	-	Long-chain-fatty-acid CoA ligase, putative
QMod-A4	TraesCS4A01G336500.1	chr4A	618660637	618665413	-	Long-chain-fatty-acid CoA ligase, putative
QMod-A4	TraesCS4A01G336500.2	chr4A	618660637	618674099	-	Long-chain-fatty-acid CoA ligase, putative

Table S4 | Structural features of the predicted nsLTPs within the *QMod-2B* and *QMod-4A* intervals.

Gene ID	Signal peptide	8 cysteine motif	GPI
TraesCS4B01G017900.1_LTPg_TaMs1_B	24	Yes	195
TaMs1_A-genome_LTPg	24	Yes	197
TraesCS2B01G138300.1_LTPg	27	No	153
TraesCS2B01G187600.1_LTPg	25	Yes	151
TraesCS2B01G215400.1_LTP1	19	Yes	No
TraesCS2B01G215500.1_LTP1	20	Yes	No
TraesCS2B01G215600.1_LTPd	27	Yes	No
TraesCS4A01G295600.1_LTPg	31	Yes	176
TraesCS4A01G295800.1_LTPg	31	Yes	178

Chapter 6

General discussion

Chapter 6
General discussion

This PhD project was designed to:

1. Understand the biological function of TaMs1 in pollen exine development.
2. Investigate male sterility penetrance of *ms1* mutant alleles across germplasm and identify candidate genes for incomplete sterility penetrance.
3. Identify *nsLTPs* within the wheat genome (cv. Chinese Spring), and analyse their gene structure, expression and evolution of family members.
4. Identify additional wheat *nsLTPs* involved in pollen and anther development.

The main empirical findings are chapter-specific and are presented and discussed in each chapter/paper.

This chapter discusses the significance of outcomes generated in this PhD project with considerations for future research directions.

Non-specific lipid transfer proteins (nsLTPs) and pollen development

Increasing our understanding of the process of pollen development is of great interest for yield improvement through hybrid breeding. Morphology of anthers and pollen grains show considerable similarities across monocots and dicots. A high degree of conservation of the regulatory pathways controlling the development of these reproductive organs has also been observed and previously described in *A. thaliana* and rice (Ariizumi and Toriyama, 2011; Zhang and Yang, 2014; Gómez *et al.*, 2015). Among these pathways, lipid metabolism represents an important regulatory network for pollen wall development. It involves the biosynthesis of sporopollenin within the tapetal cells and its subsequent transport to the developing microspores. The suggested function of nsLTPs for cargo transport of sporopollenin precursors from the tapetal cells to the developing microspores has been reported based on analyses of *nsLTPs* knock-out mutants and the fact they often result in defective exine and therefore male sterility (Zhang *et al.*, 2010; Huang *et al.*, 2013; Edstam and Edqvist, 2014; Tucker *et al.*, 2017; Wang *et al.*, 2017). Taken together these studies describe in detail phenotypic defects in pollen development, expression profiles of *nsLTPs* and their likely lipid binding activities.

In this PhD project, the characterisation of TaMs1 provides valuable information toward understanding the role of this protein within the biological process of pollen wall formation (Chapter 3). *TaMs1* was reported to be expressed in anthers containing pre-meiotic

microspores, which was unexpected considering the genes deemed necessary for the production and transport of sporopollenin precursors were shown to be up-regulated at a later meiotic stage (Chapter 3). This finding is suggestive of a role for TaMs1 very early in the process of sporopollenin deposition onto the developing exine. Sporopollenin build up requires correct primexine and callose wall formation that subsequently provide receptive substructures for sporopollenin deposition (Ariizumi and Toriyama, 2011). Whilst no phenotypic defects were observed in *ms1* callose structures relative to wild-type (Tucker *et al.*, 2017; Wang *et al.*, 2017), an in-depth analysis of primexine development may provide evidence of the function of TaMs1 in the formation of this layer. However, the timing of gene expression does not always directly relate to the timing of protein function, as proteins are often subject to post-translational modification or regulation. TaMs1, for instance has a GPI-anchor, which has been demonstrated to be essential for its function (Tucker *et al.*, 2017; Wang *et al.*, 2017). GPI-anchor proteins are typically subject to the specific activity of a suite of phospholipases (Low, 1989). Therefore one could hypothesise that TaMs1 is secreted to the tapetum cell surface at pre-meiosis, but the protein would only be released through the activity of a phospholipase at a stage latter in development, co-ordinating with the presence of sporpollenin precursor gene expression. At this point, lipidic precursors would be bound and transported by TaMs1 from the tapetal cell surface to the microspore cell surface. Alternatively, in addition to the role of GPI anchors as membrane tethers, they are suggested to act as determinants of signalling activity (Saha *et al.*, 2016). GPI-anchored proteins have been reported to be associated with lipid rafts which organise the plasma membrane into smaller domains that can serve as platforms for signal transduction (Rajendran, 2005). GPI-anchors may act as an intermediary between the exterior cell surface and internal molecules, resulting in Ca^{2+} fluxes, protein tyrosine phosphorylation or cytokine secretion (Robinson, 1997; Jones and Varela-Nieto, 1998). Despite the fact that GPI-anchors do not completely cross the cell membrane, it is hypothesized the signal transduction occurs through raft-associated interactions with other transmembrane proteins involved in intracellular signalling (Simons and Toomre, 2000). In order to determine whether TaMs1 functions either as a transporter of sporopollenin precursors or as a signalling molecule, further research is necessary. Particularly studies that investigate TaMs1 subcellular localisation and targeting *in planta*. For this purpose, the use of a fluorescent translational reporter or immunological detection of TaMs1 in anthers could be undertaken.

Toward a cost-effective hybrid seed production platform in wheat

The rate of yield gain in wheat has declined in many areas of the world, and is predicted to be aggravated by climate change. Increasing productivity whilst having an environmentally sustainable food system will predominantly rely on the breeding of new high-performance varieties. The use of hybrids represents a promising approach to increase yield potential and yield stability in wheat. An important prerequisite for the large-scale commercial deployment of wheat hybridization platforms is the need for sufficient heterotic yield advantage that can counteract the high costs of hybrid seed production to obtain an attractive commercial return on investment (Oettler *et al.*, 2005; Longin and Würschum, 2014). Reducing hybrid seed production costs relies on efficient and inexpensive systems to multiply male sterile lines and promote outcrossing (Whitford *et al.*, 2013; Chapter 2). Several platforms for producing hybrid seeds are commercially available and either rely on chemical hybridizing agents (CHA) or cytoplasmic male sterility (CMS). However, the use of such systems account for only 1% of the cultivated wheat area. A proposed alternative relies on the use of a non-conditional nuclear-encoded recessive male sterile which has the advantage of overcoming many of the limitations inherent to the use of CHAs or CMS. For example, the use of an NMS-based system does not require chemical applications to induce male sterility. Chemical application under field conditions can be unreliable as both application and efficacy are highly dependent upon the weather. Furthermore, all wheat genotypes can effectively restore fertility to recessive male steriles in the F_1 therefore broadening germplasm base utility. This contrasts with alloplasmic lines where often many loci need to be introgressed and tracked to ensure full fertility restoration in the F_1. Additionally NMS systems do not possess yield penalties often inherent to CMS-based systems. In rice and maize, a NMS-based platform called “seed production technology” (SPT) has been successfully implemented for large scale and cost-effective production of hybrid seed. The development of a similar platform in wheat was previously limited by the lack of genic identification of a non-conditional nuclear encoded male sterile; which was recently overcome with the identification of *TaMs1* (Tucker *et al.*, 2017; Wang *et al.*, 2017).

The discovery of *TaMs1* represents a key step toward the development of a SPT hybridisation platform in wheat; nevertheless, much research and development remains to be done before large-scale commercialisation becomes feasible. The development of genetically distinct heterotic pools is critical towards maximising heterotic yield potential (Longin *et al.*, 2012). In

order to effectively exploit this germplasm base for heterosis, complete penetrance of the nuclear recessive male sterility is needed across the female germplasm pool. This study, for the first time, demonstrated variability in male sterility penetrance dependent upon background and mutant allele (Chapter 5). Based on the mutants investigated in this study, it was concluded that further research is crucial in order to identify, breed or engineer additional mutant alleles or combinations thereof in order to induce the necessary degree of sterility penetrance across germplasm. Here, a hybridization platform based on *ms1* male sterility would need to ensure the production of at least 90 % F_1 hybrid seed across a range of environments prior to deployment of the platform internationally (OECD, 2018).

The SPT platform results in the production of non-GM F_1 hybrids but also relies on a transgenic maintainer line (Wu *et al.*, 2016). The use of transgenic lines in the field would instil an additional cost to production considering the requirements of biotechnology trait deregulation. The cost of a biotechnological trait was estimated at $136m between 2008 and 2012 (survey involving BASF Corporation, Bayer CropScience, Dow AgroSciences, Dupont-Pioneer Hi-Bred, Monsanto Company and Syngenta AG; (Mcdougall, 2011)). While the step of gene discovery accounted for an estimated 22.8 % of the total costs and 23.0 % of the time from project initiation to commercialisation, regulatory processes are estimated to account for 25.8 % of the cost and 36.7 % of the total time (Figure 1).

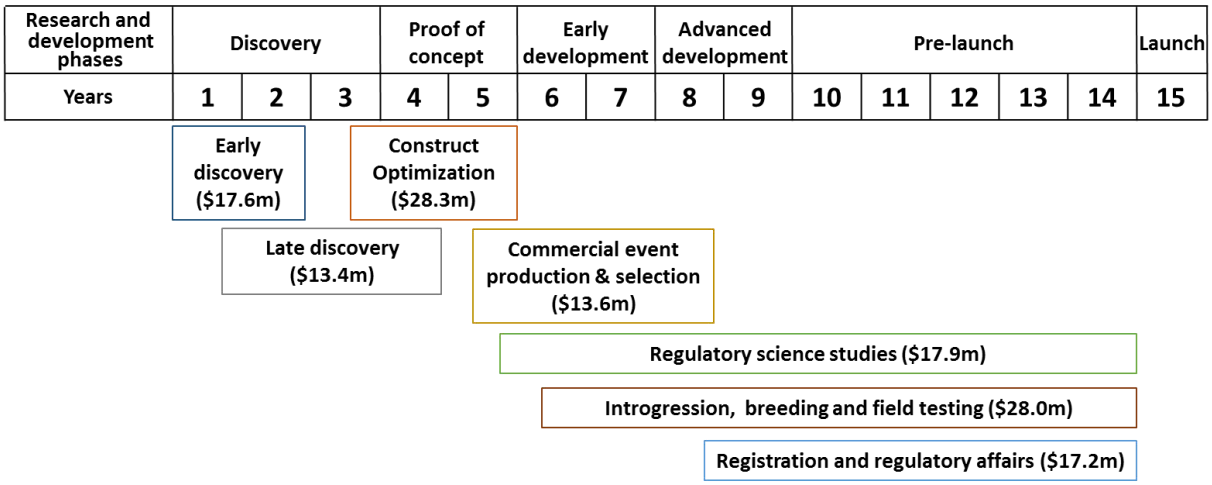

Figure 1 | Timeline, activity stages and costs for biotech crop discovery and development (image modified from Mcdougall, 2011).

Wheat's floral architecture strongly favours self-pollination. Converting wheat to an obligate cross-pollinator is necessary for efficient hybrid seed production. In contrast to maize and rice, one disadvantage of wheat is the limited amount and dispersion of pollen (Pickett, 1993). This

would require the use of a large ratio of male versus female lines to produce hybrids, thereby resulting in a higher cost of hybrid seed production (Kempe and Gils, 2011). In addition, making hybrid wheat seed is also limited by pollen viability with its longevity being approximately 0.5-3 h compared to 72 h for rye (Fritz and Lukaszewski, 1989). Hybrid seed production in wheat is not only constrained by pollen number and viability, but is also restricted in stigma receptivity duration. For instance, whilst male-sterile plants have florets fully open for 6 days in the absence of cross-pollination, the stigma receptivity decreases rapidly post anthesis (De Vries, 1971; Okada *et al.*, 2018). As a consequence, hybrid breeding requires an optimized nick of flowering time in parental pairs in order to ensure cross-pollination (Pickett, 1993). Research towards the development of male and female idiotypes is required in order to reduce the cost of hybrid seed production (Whitford *et al.*, 2013). In this case male parents would be taller with high anther extrusion producing large quantities of pollen that are easily dispersed by wind over large distances. The female would be shorter with open florets, long stigmatic branches and hairs that are receptive for extended durations. Variation in these traits relevant for successful hybridization have been reported, suggesting that substantial research could allow breeding of desired traits into germplasm of interest (Virmani and Edwards, 1983; Pickett, 1993).

Heterotic yield gain in wheat was shown to be limited relative other species. For instance, an estimated heterotic yield gain of approximately 10 % has been reported in wheat (Jiang *et al.*, 2017), whilst a yield improvement of 55 % has been observed in rice and 68 % in foxtail millet (Siles *et al.*, 2004; Chen and Liu, 2014). The lower yield benefits observed in wheat could be explained by its genomic composition. Bread wheat is an allohexaploid containing three closely related genomes (AABBDD, 2n = 6x = 42) (IWGSC, 2014). Its polyploidy nature causes some degree of epistatic interactions between genes and sub-genomes resulting in homoeologous gene silencing and differential gene expressions. Such epistatic interactions are analogous to what has been observed during heterosis and has been termed “fixed heterosis” (Ellstrand and Schierenbeck, 2000; Mochida *et al.*, 2003). In short, wheat could already be expressing heterosis due to its polyploid state. The presence of three homoeologous alleles in elite varieties may already impart significant hybridity, and therefore subsequent crosses perhaps may fail to bring in as much desirable hybridity across all loci compared to other species such as rice and foxtail millet.

Overall, stable yield improvement offered by wheat hybrids have to be justified in the context of longer breeding times and larger breeding pools which ultimately contribute to higher costs of seed production. The higher capital investment of buying hybrid seed relative to inbred seed could be a major constraint for hybrid adoption by farmers. Furthermore, because self-pollination of hybrids results in yield reduction and loss of uniformity due to inbreeding depression (Charlesworth and Willis, 2009) farmers would need to buy new seed every planting season in order to ensure consistency of production. Moreover, while hybrids might perform well under optimum growing conditions, inadequate use of fertiliser inputs or poor irrigation systems could result in little yield advantage relative to conventional inbred lines. This could pose an additional commercial risk for farmers.

Improvement of crop breeding technologies

Increasing yield potential through hybrids may be a promising approach to rise the yield potential of wheat. Nevertheless, concurring approaches are required to ensure a sustainable yield increase. The development of pre-selection methods to predict best hybrids in the field would allow the acceleration of selection gain, save time and resources that can be focussed on materials predicted to harbour this higher yield potential (Mühleisen *et al.*, 2014; Longin *et al.*, 2015). The development of the integrative "omics" technologies represents valuable tools for plant breeding and are gaining more popularity as the cost of applying these technologies decreases. One clear example of this is the implementation of genomic selection (GS) in many crops. This has emerged from the significant reduction in cost for genotyping and sequencing combined with the development and accessibility of software for prediction of benefit. Alongside genomics, the ascent of high-throughput phenotypic screening into breeding schemes enables more accurate prediction of elite lines (Brown *et al.*, 2014; Cooper *et al.*, 2014). Another example is the use of metabolomic data for trait prediction (Riedelsheimer *et al.*, 2012).

Additionally, another major advance is the development of speed breeding to accelerate the rate of crop improvement (Watson *et al.*, 2018). By growing cereals in a controlled-environment room with extended photoperiod (22 hours light/2 hours dark), the authors demonstrated the possibility to achieve up to 6 generation cycles per year instead of the 2 – 3 generations usually obtained for wheat in common glasshouse conditions (10 – 16 hours

photoperiod). Further, a theoretical framework reducing the generation cycle down to one week was proposed by (De La Fuente *et al.*, 2013). This was proposed through rapid cycles of meiosis and mitosis *in vitro*. Although this approach is not currently feasible for any crop due to technological limitations, it could revolutionize the speed of the breeding process. Lastly, genome editing represents a promising technology to introduce precise mutations into plant genomes (Gao, 2018). This offers tremendous potential to rapidly breed lines with desired traits. One example is the use of CRISPR/Cas9 for generation of powdery mildew resistance in wheat (Zhang *et al.*, 2017).

International collaborations

Increasing crop productivity is a long and costly process that would require collaborative efforts. This is especially relevant for wheat in which the implementation of genomic tools has lagged behind compared to other cereals such as maize and rice, mostly due to its large genome size (17 Gb), its hexaploid nature and high content of repetitive DNA (IWGSC, 2014). In order to accelerate wheat improvement, a reference sequence for wheat was much needed. In 2005, the International *Wheat Genome Sequencing* Consortium (IWGSC) was established from a collaboration of 64 countries. In 2008, this led to the first physical map of the 3B chromosome and to the production of a first draft genome of cv. Chinese Spring in 2014 (Paux *et al.*, 2008; IWGSC, 2014). Finally, in 2018, a high-quality reference sequence cv. Chinese Spring, IWGSC Ref 1.0 was released. These developments have, and will, enable more rapid genetic marker development, more precise breeding and quicker cloning of genes relevant to agriculture. The reference genome sequence also provides opportunity to deepen our understanding of the evolution and function of the gene families for wheat development (Chapter 5).

In order to further co-ordinate efforts among researchers, funding organisations and governments, the Wheat Initiative (www.wheatinitiative.org) was established in 2011. The Wheat Initiative aims to promote collaborative research towards the increase of yield potential and yield stability, increase the sustainability of wheat production systems and ensure the supply of high quality varieties across the world. It also facilitates the exchange of knowledge within the wheat research community by providing accessibility to wheat omics

datasets and analytic tools. Coordinated efforts will undoubtedly help accelerate wheat research in the coming years.

The challenges of reaching sustainable food security

Despite recent productivity gains, the agricultural production system is failing to meet the population demand. Approximately 800 million people are lacking access to food and do not meet the daily energy requirement (Liu, 2017). Meanwhile, increasing population and consumption is raising pressure for the intensification of agriculture systems that already account for 24% of the global greenhouse gas (GHG) emissions (IPCC, 2014). In addition, these GHG emissions are a likely cause of climate change which is projected to jeopardize global food production (Porter, 2014). Therefore, increasing yield alone is unlikely to solve food security in the long run and concurrent strategies need to be developed (Foley *et al.*, 2011). First, with the recent increase in agriculture productivity, it is estimated that enough food is produced to meet the dietary needs of the entire population (Liu, 2017). However, due to overconsumption of the wealthiest countries, political instabilities, inequality in incomes and food accessibility, hundreds of millions of people are undernourished. Reducing disparities in income both globally and within-countries along with improved food distribution access are key steps toward eradicating hunger. Second, over 30% of all food intended for consumption is lost or wasted along the food chain; this occurs at all steps from production to consumption in both low- and high- income countries (HPLE, 2014) . Reducing food losses and waste would increase food supply viability and strengthen food security. Third, only 62% of the global crop production is allocated to human food, and less efficiently, about one third is used for animal feed. In US, where meat accounts for a large part in diet, shifting dietary habits by replacing all animal-based products by plant-based alternatives is projected to feed an additional 350 million people. This represents more benefits than eliminating all food waste from the supply chain (Shepon *et al.*, 2018). While it is possible to meet the dietary requirements of an individual in a plant-based diet, it can be challenging to achieve this for an entire population (White and Hall, 2017). Overall, to ensure food security and environmental sustainability, no single strategy is sufficient, and solving global agricultural challenges would require integrated policy approaches at national and international levels.

6.1 References

Ariizumi T, Toriyama K. 2011. Genetic Regulation of Sporopollenin Synthesis and Pollen Exine Development. Annual Review of Plant Biology **62**, 437–460.

Brown TB, Cheng R, Sirault XRR, Rungrat T, Murray KD, Trtilek M, Furbank RT, Badger M, Pogson BJ, Borevitz JO. 2014. TraitCapture: Genomic and environment modelling of plant phenomic data. Current Opinion in Plant Biology **18**, 73–79.

Charlesworth D, Willis JH. 2009. The genetics of inbreeding depression. Nature Reviews Genetics **10**, 783–796.

Chen L, Liu Y-G. 2014. Male Sterility and Fertility Restoration in Crops. Annual Review of Plant Biology **65**, 579–606.

Cooper M, Messina CD, Podlich D, Totir LR, Baumgarten A, Hausmann NJ, Wright D, Graham G. 2014. Predicting the future of plant breeding: Complementing empirical evaluation with genetic prediction. Crop and Pasture Science **65**, 311–336.

Edstam MM, Edqvist J. 2014. Involvement of GPI-anchored lipid transfer proteins in the development of seed coats and pollen in Arabidopsis thaliana. Physiologia Plantarum **152**, 32–42.

Ellstrand NC, Schierenbeck KA. 2000. Hybridization as a stimulus for the evolution of invasiveness in plants? Euphytica **148**, 35–46.

Foley JA, Ramankutty N, Brauman KA, *et al.* 2011. Solutions for a cultivated planet. Nature **478**, 337.

Fritz SE, Lukaszewski AJ. 1989. Pollen Longevity in Wheat, Rye and Triticale. Plant Breeding **102**, 31–34.

Gao C. 2018. The future of CRISPR technologies in agriculture. Nature Reviews Molecular Cell Biology **19**, 275–276.

Gómez JF, Talle B, Wilson ZA. 2015. Anther and pollen development: A conserved developmental pathway. Journal of Integrative Plant Biology **57**, 876–891.

HPLE. 2014. Food losses and waste in the context of sustainable food systems. A report by the High Level Panel of Experts on Food Security and Nutrition of the Committee on World Food Security. Rome.

Huang M-D, Chen T-LL, Huang AHC. 2013. Abundant Type III Lipid Transfer Proteins in Arabidopsis Tapetum Are Secreted to the Locule and Become a Constituent of the Pollen Exine. Plant Physiology **163**, 1218–1229.

IPCC. 2014. *Climate Change 2014: Mitigation of Climate Change. Summary for Policymakers and Technical Summary*.

IWGSC. 2014. A chromosome-based draft sequence of the hexaploid bread wheat (Triticum aestivum) genome Ancient hybridizations among the ancestral genomes of bread wheat Genome interplay in the grain transcriptome of hexaploid bread wheat Structural and functional pa. Science (New York, N.Y.) **345**, 1250092.

Jiang Y, Schmidt RH, Zhao Y, Reif JC. 2017. Quantitative genetic framework highlights the role of epistatic effects for grain-yield heterosis in bread wheat. Nature Genetics **49**, 1741–1746.

Jones DR, Varela-Nieto I. 1998. The role of glycosyl-phosphatidylinositol in signal transduction. International Journal of Biochemistry and Cell Biology **30**, 313–326.

Kempe K, Gils M. 2011. Pollination control technologies for hybrid breeding. Molecular Breeding **27**, 417–437.

De La Fuente GN, Frei UK, Lübberstedt T. 2013. Accelerating plant breeding. Trends in Plant Science **18**, 667–672.

Liu P. 2017. *The future of food and agriculture: Trends and challenges.*

Longin CFH, Mi X, Würschum T. 2015. Genomic selection in wheat: optimum allocation of test resources and comparison of breeding strategies for line and hybrid breeding. Theoretical and Applied Genetics.

Longin CFH, Mühleisen J, Maurer HP, Zhang H, Gowda M, Reif JC. 2012. Hybrid breeding in autogamous cereals. Theoretical and Applied Genetics **125**, 1087–1096.

Longin CFH, Würschum T. 2014. Genetic variability, heritability and correlation among agronomic and disease resistance traits in a diversity panel and elite breeding material of spelt wheat. Plant Breeding **133**, 459–464.

Low MG. 1989. Glysosylphosphatidylinositol: a versatile anchor for cell surface proteins. Faseb J. **3**, 1600–1608.

Mcdougall P. 2011. The cost and time involved in the discovery , development and authorisation of a new plant biotechnology derived trait A Consultancy Study for Crop Life International September 2011. Vineyard Business Centre United Kingdom, 1–24.

Mochida K, Yamazaki Y, Ogihara Y. 2003. Discrimination of homoeologous gene expression in hexaploid wheat by SNP analysis of contigs grouped from a large number of expressed sequence tags. Molecular Genetics and Genomics **270**, 371–377.

Mühleisen J, Piepho HP, Maurer HP, Longin CFH, Reif JC. 2014. Yield stability of hybrids versus lines in wheat, barley, and triticale. Theoretical and Applied Genetics.

OECD. 2018. Organisation for Economic Co-operation and Development. Annex Xi To the Decision Oecd Scheme for the Varietal Certification of Maize and Sorghum Seed.

Oettler G, Tams SH, Utz HF, Bauer E, Melchinger AE. 2005. Prospects for hybrid breeding in winter triticale: I. Heterosis and combining ability for agronomic traits in European elite germplasm. Crop Science **45**, 1476–1482.

Okada T, Jayasinghe JEARM, Nansamba M, Baes M, Warner P, Kouidri A, Correia D, Nguyen V, Whitford R, Baumann U. 2018. Unfertilized ovary pushes wheat flower open for cross-pollination. Journal of Experimental Botany **69**, 399–412.

Paux E, Sourdille P, Salse J, *et al.* 2008. A physical map of the 1-gigabase bread wheat chromosome 3B. Science **322**, 101–104.

Pickett AA. 1993. Hybrid Wheat: Results and Problems.

Porter. 2014. Part A: Global and Sectoral Aspects. (Contribution of Working Group II to the Fifth Assessment Report of the Intergovernmental Panel on Climate Change). Climate Change 2014: Impacts, Adaptation, and Vulnerability., 1132.

Rajendran L. 2005. Lipid rafts and membrane dynamics. Journal of Cell Science **118**, 1099–1102.

Riedelsheimer C, Czedik-Eysenberg A, Grieder C, Lisec J, Technow F, Sulpice R, Altmann T, Stitt M, Willmitzer L, Melchinger AE. 2012. Genomic and metabolic prediction of complex heterotic traits in hybrid maize. Nature Genetics **44**, 217–220.

Robinson PJ. 1997. Signal Transduction Via GPI-Anchored Membrane Proteins. In: Haag F,, In: Koch-Nolte F, eds. ADP-Ribosylation in Animal Tissues: Structure, Function, and Biology of Mono (ADP-ribosyl) Transferases and Related Enzymes. Boston, MA: Springer US, 365–370.

Saha S, Anilkumar AA, Mayor S. 2016. GPI-anchored protein organization and dynamics at the cell surface. Journal of Lipid Research **57**, 159–175.

Shepon A, Eshel G, Noor E, Milo R. 2018. The opportunity cost of animal based diets exceeds all food losses. Proceedings of the National Academy of Sciences, 201713820.

Siles MM, Russell WK, Baltensperger DD, Nelson LA, Johnson B, Van Vleck LD, Jensen SG, Hein G. 2004. Heterosis for grain yield and other agronomic traits in foxtail millet. Crop Science **44**, 1960–1965.

Simons K, Toomre D. 2000. Lipid rafts and signal transduction. Nature Reviews Molecular Cell Biology **1**, 31–39.

Tucker EJ, Baumann U, Kouidri A, *et al.* 2017. Molecular identification of the wheat male fertility gene Ms1 and its prospects for hybrid breeding. Nature Communications **8**, 869.

Virmani SS, Edwards IB. 1983. *Current Status and Future Prospects for Breeding Hybrid Rice and Wheat*.

De Vries AP. 1971. Flowering biology of wheat, particularly in view of hybrid seed production --- A review. Euphytica **20**, 152–170.

Wang Z, Li J, Chen S, *et al.* 2017. Poaceae-specific *MS1* encodes a phospholipid-binding protein for male fertility in bread wheat. Proceedings of the National Academy of Sciences, 201715570.

Watson A, Ghosh S, Williams MJ, *et al.* 2018. Speed breeding is a powerful tool to accelerate crop research and breeding. Nature Plants **4**, 23–29.

White RR, Hall MB. 2017. Nutritional and greenhouse gas impacts of removing animals from US agriculture. Proceedings of the National Academy of Sciences, 201707322.

Whitford R, Fleury D, Reif JC, Garcia M, Okada T, Korzun V, Langridge P. 2013. Hybrid breeding in wheat: technologies to improve hybrid wheat seed production. Journal of experimental botany **64**, 5411–28.

Wu Y, Fox TW, Trimnell MR, Wang L, Xu R ji, Cigan AM, Huffman GA, Garnaat CW, Hershey H, Albertsen MC. 2016. Development of a novel recessive genetic male sterility system for hybrid seed production in maize and other cross-pollinating crops. Plant Biotechnology Journal **14**, 1046–1054.

Zhang Y, Bai Y, Wu G, Zou S, Chen Y, Gao C, Tang D. 2017. Simultaneous modification of three homoeologs of TaEDR1 by genome editing enhances powdery mildew resistance in wheat. Plant Journal **91**, 714–724.

Zhang D, Liang W, Yin C, Zong J, Gu F, Zhang D. 2010. OsC6, encoding a lipid transfer protein, is required for postmeiotic anther development in rice. Plant physiology **154**, 149–62.

Zhang D, Yang L. 2014. Specification of tapetum and microsporocyte cells within the anther. Current Opinion in Plant Biology **17**, 49–55.

Appendix

Appendix 1

Molecular idenfication of the wheat male fertility gene *Ms1 and its prospects for hybrid breeding*

nature COMMUNICATIONS

ARTICLE

DOI: 10.1038/s41467-017-00945-2 OPEN

Molecular identification of the wheat male fertility gene *Ms1* and its prospects for hybrid breeding

Elise J. Tucker[1], Ute Baumann[1], Allan Kouidri[1], Radoslaw Suchecki[1], Mathieu Baes[1], Melissa Garcia[1], Takashi Okada[1], Chongmei Dong[2], Yongzhong Wu[3], Ajay Sandhu[3], Manjit Singh[3], Peter Langridge[1], Petra Wolters[3], Marc C. Albertsen[3], A. Mark Cigan[3] & Ryan Whitford[1]

The current rate of yield gain in crops is insufficient to meet the predicted demands. Capturing the yield boost from heterosis is one of the few technologies that offers rapid gain. Hybrids are widely used for cereals, maize and rice, but it has been a challenge to develop a viable hybrid system for bread wheat due to the wheat genome complexity, which is both large and hexaploid. Wheat is our most widely grown crop providing 20% of the calories for humans. Here, we describe the identification of *Ms1*, a gene proposed for use in large-scale, low-cost production of male-sterile (*ms*) female lines necessary for hybrid wheat seed production. We show that *Ms1* completely restores fertility to *ms1d*, and encodes a glycosylphosphatidylinositol-anchored lipid transfer protein, necessary for pollen exine development. This represents a key step towards developing a robust hybridization platform in wheat.

[1] Australian Centre for Plant Functional Genomics, School of Agriculture, Food & Wine, University of Adelaide, Waite Campus, Urrbrae, SA 5064, Australia. [2] Plant Breeding Institute, University of Sydney, PMB 4011, Narellan, NSW 2567, Australia. [3] DuPont Pioneer Hi-Bred International Inc., 7250 NW 62nd Avenue, Johnston, IA 50131-0552, USA. Elise J. Tucker and Ute Baumann contributed equally to this work. Correspondence and requests for materials should be addressed to R.W. (email: Ryan.Whitford@adelaide.edu.au)

With the predicted growth in world population to over nine billion by 2050, the Food and Agriculture Organization of the United Nations (July 2005) set a target of 60% increased food production by that year. This is an ambitious target for two reasons: there are serious concerns about the viability of existing production systems and the sustainability of current growth rates in crop production, and the predicted environmental changes are expected to have an overall negative effect on agricultural production, with serious crop declines in some countries. Wheat is grown more widely than any other crop and delivers around 20% of our food calories and protein[1]. To increase global production by 60% will require a lift in the rates of gain from the current 1 to 1.6% per annum. Improvements in disease resistance and stress tolerance offer opportunities for small increases in productivity but major jumps in yield are hard to achieve and are expected to come through shifts in the way we breed wheat and other crops. However, many important new genetic and genomic technologies are difficult to apply to wheat since this plant has a large complex genome, an allohexaploid, which is 50 times larger than rice.

One of the most promising options for achieving significant boosts in yield across diverse production environments is through hybrid breeding. Hybrids offer two important advantages: first, heterotic yield gains of well over 10%, and improved yield stability have been reported[2–4], and second, hybrid seed production would act as a major stimulant for investment in wheat improvement from both the public and private sectors. However, the competitiveness of wheat hybrids relative to line varieties will depend on hybrid seed production costs[5].

Lowering hybrid seed production costs depends on a reliable and inexpensive system that forces outcrossing. Wheat male sterility and restoration systems were first developed in the 1960s, but many of them were proved to be impractical and deemed commercially high risk[6]. Relative to systems based on chemical hybridizing agents and cytoplasmic male sterility, the use of non-conditional nuclear-encoded recessive male steriles (*ms*) would offer major advantages for hybrid breeding. The value of recessive male steriles was first recognised in 1972 with the proposal of the XYZ system[7]. This system aimed to overcome the costs associated with propagating pure stands of male steriles by cytogenetic chromosomal manipulation[7, 8]. A further advantage of recessive male steriles came through the opportunity to broaden parental line choice, avoid negative alloplasmic and cytoplasmic yield penalties, as well as alleviate the problems associated with incomplete fertility restoration. A cost-effective and flexible hybridization platform that uses a recessive male sterile is Seed Production Technology (SPT)[9] developed for maize and rice hybrid seed production (Supplementary Fig. 1). This platform overcomes many of the problems with large-scale production of male steriles for use as female parents in hybrid breeding. SPT uses a maintainer line solely for the propagation of non-GM homozygous recessive male-sterile parents; therefore, F_1 hybrids provided to farmers are considered to be non-GM.

Developing an equivalent platform for hybrid wheat breeding requires the identification of a suitable non-conditional, nuclear-encoded recessive male sterile. These types of mutants are particularly rare and difficult to detect in polyploids due to genetic redundancy. Many of our major crops and food plants are polyploids, including wheat, oats, potato, sweet potato, peanut, sugarcane, cotton, kiwifruit, strawberry, and plums. For example, only ten nuclear-encoded wheat male-sterile mutants have been identified to date[6], in contrast to 108 mutants in diploid barley[10, 11]. Polyploidy not only makes it difficult to find suitable male-sterile mutations but also complicates deploying mutants since multiple mutations would be needed to deal with genetic redundancy[12] and this increases breeding costs and population sizes needed for introgression of each additional mutation. The most cost-effective mutants would be single locus encoded. In wheat, only two of the ten mutant loci are reported to fit this criterion. These are *ms1* and *ms5* located on chromosomes 4BS and 3AL, respectively[13].

The first *ms1* mutant was observed in Australia in the late 1950s[14]. This spontaneous mutant named *Pugsley's* male sterile was followed by the identification of *Probus* and *Cornerstone* male steriles from an X-ray-induced wheat mutant population[15, 16]. Cytogenetic and linkage analysis showed these to be allelic and they were designated as *ms1a*, *ms1b* and *ms1c*, respectively[15, 17–19]. In 1976, additional monogenic recessive male steriles were identified from an ethyl methanesulfonate (EMS)-treated population[20]. Three mutants were allelic to *ms1*, and designated as *ms1d*, *ms1e* and *ms1f*[13, 21] while the fourth mutant was nonallelic to *ms1* and designated as *ms5*[13]. However, even for *ms1*, the variability between backgrounds and mutant alleles, and problems with male sterility penetrance were reported[22–24]. In order to address these problems, it is necessary to identify the gene underlying the *Ms1* locus and explain its function.

Here, we describe the identification of the *Ms1* gene sequence (*TaMs1*) by map-based cloning and demonstrate its function in male fertility by complementation of the *ms1d* mutant. *TaMs1* encodes a glycosylphosphatidylinositol (GPI)-anchored lipid transfer protein, which is necessary for pollen exine development. The identification of the *Ms1* gene sequence represents a key step towards developing a robust hybridization platform in wheat similar to the maize SPT.

Results

***Ms1* encodes a GPI-anchored lipid transfer protein**. We followed a map-based cloning approach to isolate the *Ms1* gene sequence (chr. 4BS). Using syntenic regions on chromosomes 1, 3 and 4 from rice, *Brachypodium* and barley, respectively, we generated markers and tested their presence or absence in male-sterile mutants *ms1a*, *ms1b* and *ms1c*. The results revealed that *ms1a* and *ms1c* are terminal deletions while *ms1b* is an interstitial deletion of the chromosome 4BS covering approximately 14 centimorgans (cM) (Fig. 1). *Ms1*-flanking markers were identified by their presence in *ms1b* and their absence from *ms1c*. Using a population representing 7000 meioses and segregating for *ms1d*, we delimited the *Ms1* locus to a 0.5 cM interval between markers ×27140346 and ×12360198. Probes designed within the region bounded by these markers, were used to isolate and sequence BACs from durum and hexaploid wheat. Marker development from BAC-derived sequences and analysis of 14 recombinants across the region, further delimited *Ms1* between markers 007.033.1 and 007.0046.1. The mapped 251- Kb interval contains eight intact genes and one likely pseudogene (Supplementary Table 1).

RNAseq-based expression profiling identified one of these eight genes to be preferentially expressed in floral tissues (Supplementary Table 1). This gene (*TaMs1*) is predicted to encode a 219 amino acid polypeptide with a similarity to a large family of GPI-anchored lipid transfer proteins (LTPGs), for which it is a member of a Poaceae-specific clade (Supplementary Fig. 2). This gene was confirmed as *Ms1* through in planta complementation of the *ms1d* mutation and identification of the causative lesions in *ms1d*, *ms1e*, *ms1f* and a newly identified TILLING mutant (described below).

***TaMs1* is necessary for pollen exine integrity**. *Arabidopsis* harbours over 20 LTPG genes for which only two of them have been characterised[25, 26]. *AtLTPG1* and *AtLTPG2* are required for cuticular wax accumulation or for export onto stem and silique

surfaces. Epicuticular wax has lipid precursors common to sporopollenin, the major constituent of pollen exine, which is produced in sporophytic tapetal cells and transported to developing microspores in structures called orbicules. The analysis of *ms1* anthers revealed a disrupted orbicule and a pollen exine structure (Fig. 2a), which was first observed in early uninucleate microspores and typified by ectopic exine deposition and reduced electron-dense materials at the tapetal cell surface (Supplementary Figs. 3 and 4). No differences in the surface cuticle layer were observed between *ms1* and wild-type anthers (Supplementary Fig. 5). Furthermore, metabolomic profiling revealed that *ms1* anthers accumulate lipid monomers of sporopollenin (C16 and C18 long-chain fatty acids) relative to the wild type (Supplementary Fig. 6). Taken together, this suggests that *Ms1* is necessary for sporopollenin biosynthesis or transport. Transcriptional β-glucuronidase fusions and homeologue-specific qRT-PCR revealed only the B-genome-derived *TaMs1* is to be expressed during early microspore development (Fig. 2b, c).

***TaMs1* exhibits functional divergence from its homeologues.** Since no obvious differences in *TaMs1* coding potential were detected between homeoloci, the basis for *TaMs1*'s subfunctionalization between homeoloci is likely to be due to variation in transcription. We suggest that functional homeoalleles may still exist in the cultivated germplasm pool and this could account for the reports of poor sterility penetrance dependent upon the genotype and the mutant allele[22–24]. In each of these cases, the loss of *Ms1* is either via a large deletion (*ms1a* and *ms1c*) or chromosome arm (DT4BL) replacement; therefore, restoration of fertility is unlikely to be a consequence of the B-genome-derived *TaMs1*. By performing a *TaMs1* homeologue-specific qRT-PCR on anthers isolated from a partially fertile homozygote for *ms1c*, we attempted to answer the question on whether *TaMs1* homeoalleles can transcriptionally compensate for the loss of *TaMs1*-B. However, this does not seem to be the case since *TaMs1* and homeologous transcripts from cv. *Cornerstone* were all below the detection limits (Supplementary Fig. 7). It is, therefore, possible that other genomic loci are associated with fertility restoration in lines carrying *ms1* deletions.

The variable penetrance of *ms1* large-deletion mutants led us to investigate the utility of the available *Ms1* mutant alleles derived from an EMS-treated population[27]. Chromosome 4BS-specific full-length coding sequences from wild-type (*Ms1*) fertiles and the EMS-derived *ms1d*, *ms1e* and *ms1f* steriles were isolated and sequenced. A comparison of *Ms1* to *ms1*-derived sequences identified unique single-nucleotide transitions for each mutant allele (Fig. 3a). Transition G329A is unique to *ms1d* and unlikely to be a natural allelic variant, considering that the wild-type G is detected in all 192 spring wheat varieties tested (Supplementary

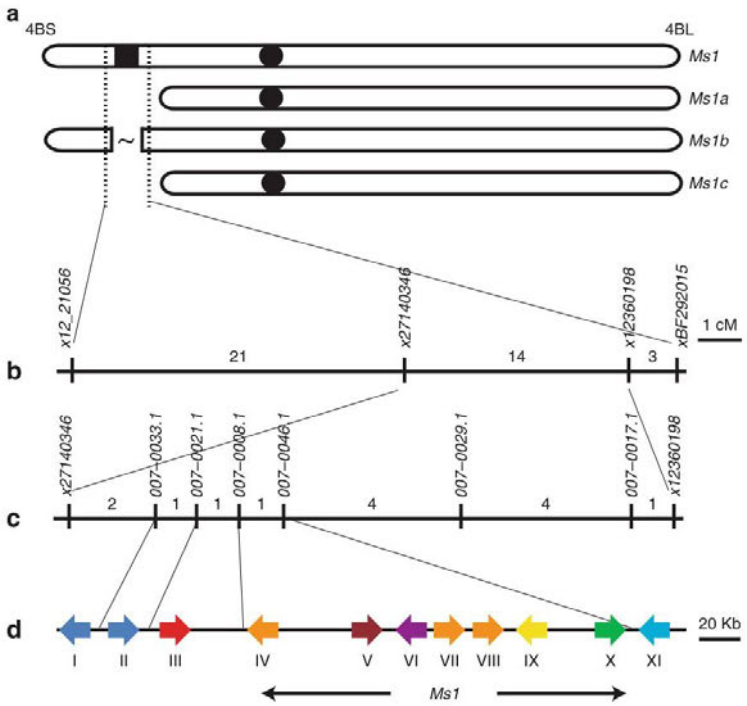

Fig. 1 Map-based cloning of the *Male sterility 1* locus on chromosome 4BS. *Ms1* was initially mapped to the interval between ×*12_21056* and *xBF292015* based on genotyping a (**a**) deletion mutant allele series, and then to an (**b**) ~0.5 cM interval between ×*27140346* and ×*12360198* based on 7000 F_2 segregants. **c** Fine mapping using 14 recombinants deliminated *Ms1* to a (**d**) 251-Kb genomic region in wheat. Marker names are in italics. The numbers indicate recombinants identified for each marker interval. Coloured arrows I to XI denote the position and orientation of predicted wheat genes with a similarity to *Brachypodium* genes Bradi1g13040 (Cupin domain-containing protein), Bradi1g13040 (Cupin domain-containing protein), Bradi2g05445 (60S ribosomal protein), Bradi1g13030 (Lipid Transfer Protein-Like 94), Bradi4g44760 (F-box/LRR-repeat protein 3), Bradi1g69240 (U-box domain-containing protein), Bradi1g13000 (Lipid Transfer Protein-Like 72), Bradi1g12990 (Lipid Transfer Protein-Like 71), Bradi1g12980 (Putative Parafibromin), Bradi1g12970 (Putative GNAT family acetyltransferase) and Bradi1g12960 (DUF581 domain-containing protein), respectively. The sequence is available via NCBI GenBank accession code KX447407

Table 2). This SNP, at the first *Ms1* exon–intron boundary induces a cryptic splice site in the first intron, resulting in a coding sequence frame shift (Fig. 3b). *ms1e* transition C1435T is coupled with a 1 bp deletion in the second exon, resulting in a frame shift prior to the predicted C-terminal GPI anchor domain. *ms1f* transition G155A changes a highly conserved cysteine residue to a tyrosine (C52Y). This site is one of the eight cysteine motifs characteristic of LTP domains that appear to be important for the structural scaffold necessary for lipid binding[28]. In a parallel approach, we identified a G178A transition (designated as *ms1h*) in a TILLING screen of a soft wheat cultivar *QAL2000*, that induced male sterility similar to other mutant alleles (Supplementary Fig. 8) when it was in the homozygous condition (Fig. 3a)[29]. This mutation changes an aspartic acid to an asparagine (D60N) within the conserved LTP domain. Taken together, these findings indicate that both the GPI anchor and putative lipid-binding domains are necessary for Ms1 functionality.

***TaMs1* functionally complements *ms1d*.** The SPT hybridization platform incorporates a maintainer line (Supplementary Fig. 1) capable of propagating non-GM nuclear male-sterile lines for use as female parents in hybrid production. The SPT maintainer line is a homozygous recessive male sterile transformed with a SPT construct containing (i) a complementary wild-type male fertility gene to restore fertility, (ii) an α-amylase gene to disrupt pollination and (iii) a seed colour marker gene. We demonstrated that the α-amylase gene and seed colour marker function in wheat (Supplementary Fig. 9). However, the remaining key component of the SPT hybridization platform requires the demonstration of complementation of male sterility to fully restore fertility[9]. Therefore, we tested the ability of this gene sequence to complement *ms1d*. A 4.4-Kb genomic fragment containing *Ms1* was synthesised (*TaMs1*) and introduced into the wheat cultivar *Gladius* segregating for *ms1d*. Eleven independent *Agrobacterium*-mediated T_0 transformants were generated (Supplementary Table 3). Four SNP markers closely flanking the *Ms1* locus allowed the selection of T_0 regenerants that were homozygous for *ms1d*, whilst a seed-screenable marker (*DsRed*) was used to confirm the presence of *TaMs1*. SNP and seed colour detection identified six homozygous *ms1d* T_0 regenerants with the introduction of the *TaMs1* gene. Selfed seed set analysis showed that all six T_0 regenerants were fully fertile (Fig. 3c, Supplementary Table 3). Seventeen T_1 progenies for two independent T_0 lines (Event 1 and Event 7) were assayed for both the copy number and zygosity of the introduced *TaMs1* (Supplementary Table 4). The results revealed that all progenies were homozygous for *ms1d* with either zero, one or two copies of the exogenous *TaMs1*. Those progenies with no detectable introduced *TaMs1* were male sterile whilst those containing either one or two copies of the *TaMs1* transgene were self-fertile. These findings demonstrate that *Ms1* can fully restore fertility to the homozygous *ms1d* mutant.

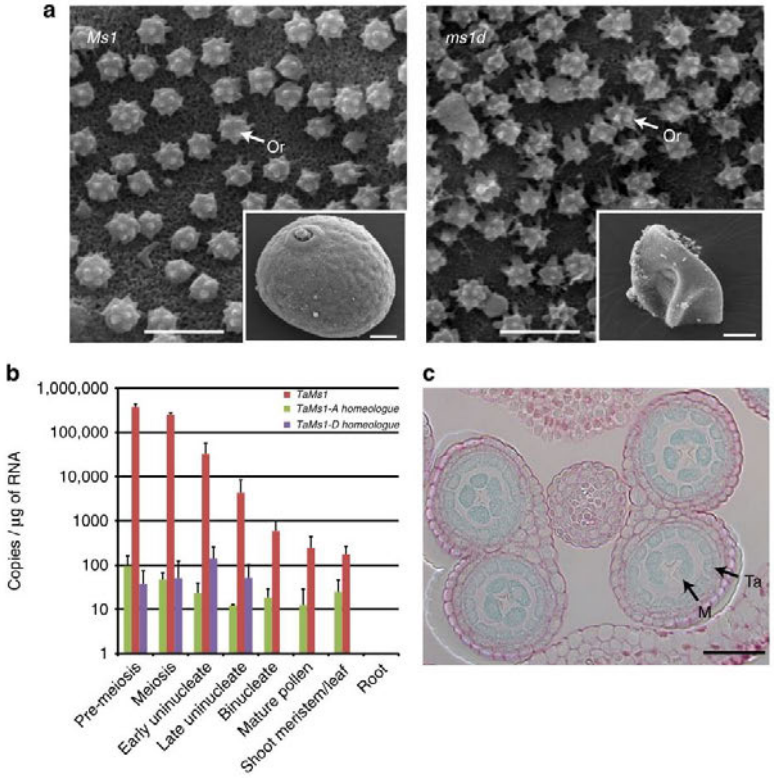

Fig. 2 *TaMs1* confers male fertility and is expressed in developing wheat anthers. **a** Scanning electron micrographs showing the defects in tapetal cell surface-localised orbicule (Or) structures and pollen coat (inset) within male sterile (*ms1d*) vs. wild-type anthers (*Ms1*). Scale bars: 2 µm (inset 10 µm). **b** *TaMs1* and homeologue mRNA levels as detected by qRT-PCR in premeiotic to mature pollen-containing anthers, leaf/shoot apical meristem and roots. The data are means ± s.e.m (n = 3 biological replicates). **c** Histochemical GUS analysis of wheat anthers expressing a translational GUS fusion with *TaMs1* (native promoter). Transverse section of a wheat anther containing microspores undergoing meiosis showing cell-type-specific GUS expression. Ruthenium red-stained cell walls (pink). Scale bar: 50 µm. (Ta Tapetal cell, M Microspore)

NATURE COMMUNICATIONS | DOI: 10.1038/s41467-017-00945-2 ARTICLE

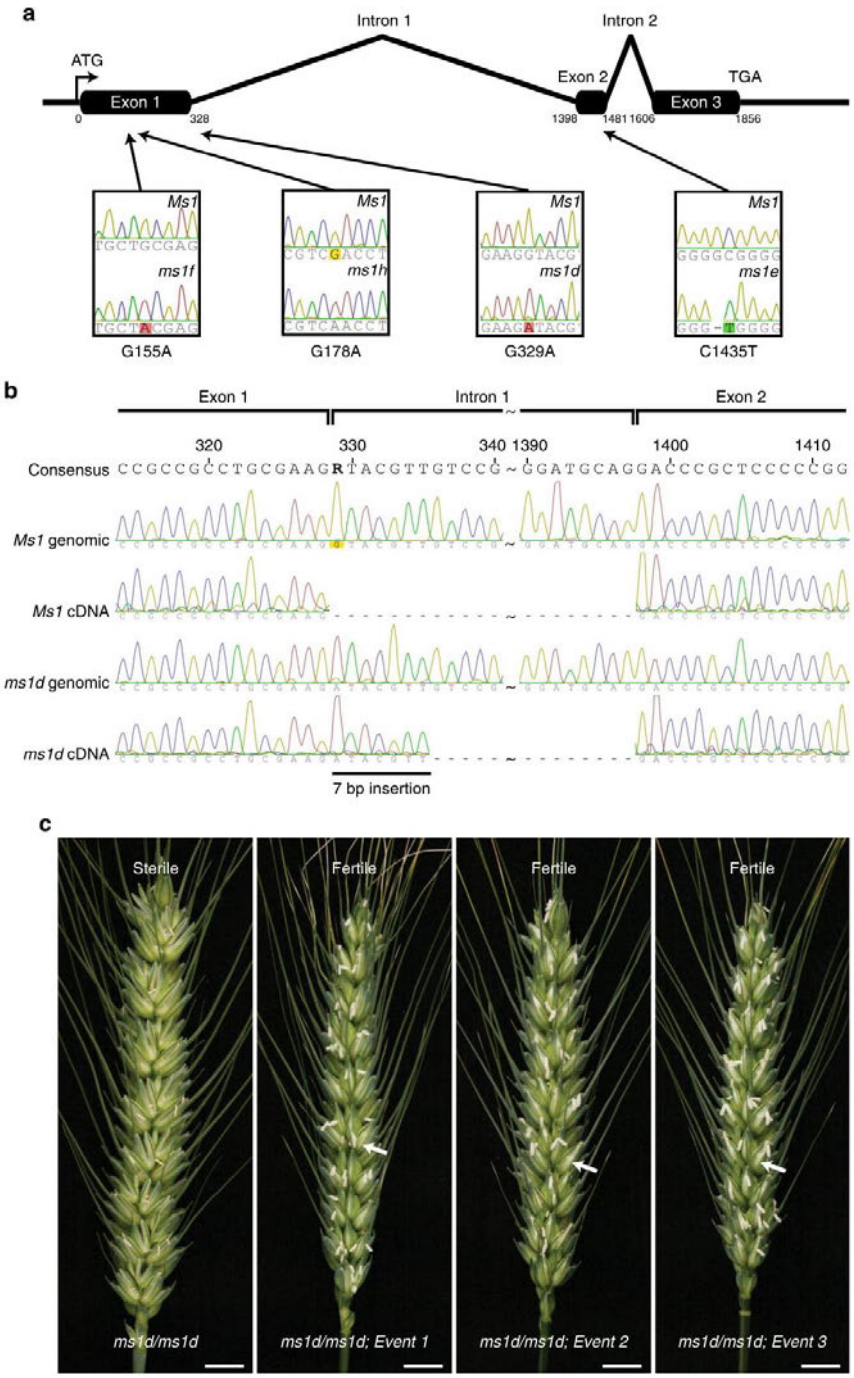

Fig. 3 Identity of male sterility inducing lesions within *TaMs1* and in vivo complementation of *ms1d/ms1d* by *TaMs1*. **a** Schematic representation of the *TaMs1* (the three exons are shown as black boxes) gene depicting the relative positions (indicated by solid lines with arrowheads) of EMS-derived lesions (chromatogram insets) for *ms1d*, *ms1e*, *ms1f* and *ms1h*. Polymorphisms cause either a frame shift (*ms1d*, *ms1e*) or an amino acid transition in a conserved residue of TaMs1 (*ms1f*, *ms1h*). **b** Sequence chromatogram comparison between both mutant (*ms1d*) and wild-type genomic cDNAs. Polymorphism G329A of *ms1d* induces the use of a cryptic splice site (highlighted by a 7 bp insertion) within *TaMs1*. **c** Stable complementation of the *ms1d* mutant by *TaMs1*. Mature inflorescences of male-sterile *ms1d/ms1d*, and three independent transformants (Events 1–3), each homozygous for *ms1d*, and showing a self-seed set (arrow). Scale bars: 1 cm

Discussion

An ambitious target of a 60% increase in wheat production by 2050 has been set to meet the predicted demand for this crop (FAO). A viable hybrid seed production system could deliver a third or more of this gain and currently, it is difficult to see any other technology that could achieve an equivalent impact. Several components are needed for an efficient hybrid system, which include optimising hybrid gains through defining heterotic pools and improving pollen vectoring by transitioning from a self-pollinating flower structure to the one that facilitates outcrossing. Based on experience in other hybrid systems, these components can be generated through targeted selection. However, forcing outcrossing through a reliable and manageable male sterility system requires the development of systems that are able to cope with the complexity of the hexaploid wheat genome.

The use of recessive male sterility has been an attractive prospect for hybrid seed production in wheat since it was first proposed in the 1950s but translating the concept to reality has proved to be elusive. The conundrum has been to maintain the male-sterile lines for use as pollen acceptors in commercial hybrid seed production fields. For example, the cytogenetic 4E-*ms* system, which utilises the novel mutant *ms1g* allele and a fertility-restoring chromosome from *Agropyron elongatum* ssp. *ruthenicum* Beldie (4E)[30] was initially reported to be successful in enabling the production of a male-sterile seed. However, reports have since indicated residual pollen transmissibility of chromosome 4E,[31] resulting in a selfed seed set within the male-sterile stands and thus reducing the purity of the hybrid seed produced. Therefore, alternate approaches are being sought to enhance this system. Now, with the isolation of *Ms1* and characterisation of most known mutations at this locus, we finally have the tools needed to develop an efficient means of bulking a male-sterile female-inbred seed (*ms1*/*ms1*), as is the case for SPT in maize. This represents a major cost saving for hybrid seed production and can overcome the seed purity issues inherent to the 4E-*ms* system. Coupled with a functional α-amylase gene for wheat pollen disruption and a seed-selectable marker, the identity and ability of the *TaMs1* gene sequence to completely restore viable pollen production in *ms1* plants represents the last critical step towards developing SPT for wheat.

To our knowledge, this study is the first to report a role of a GPI-anchored LTP in pollen exine development[32]. Given the observation that *ms1d* anthers contain pollen deficient in exine structural integrity, and that metabolomic profiling revealed a significant accumulation in free C16 and C18 fatty acids, it is reasonable to expect this to be a consequence of disruption in sporopollenin precursor transport from sporophytic tapetal cells to developing microspores. The finding that anther epidermal wax layers were not disrupted in *ms1d* anthers also indicates that TaMs1's role is specific to exine development. Further studies are needed to elucidate the subcellular localisation of TaMs1 and its direct involvement in lipid binding.

TaMs1's identification now also raises the question on whether previously reported male-sterile mutants may represent additional mutant alleles of this gene or its homeologues. Apart from the dominant male-sterile mutants *Ms2*[33, 34] and *Ms4*[35], no other mutants have been reported on homeogroup four. Both *Ms2* and *Ms4* were reported to be located on chromosome 4DS. However, recent cloning and complementation of the *Ms2* gene sequence *WMS*, reveals that it does not encode a *TaMs1* homeologue, but represents a novel gene sequence expressed only in sterile anthers as a consequence of a transposon insertion[36, 37]. Further research is necessary to determine whether *Ms4* is a mutant of the *TaMs1*-D homeologous gene sequence.

From a traditional breeding perspective, the molecular identity of the *TaMs1* gene sequence now allows the development of germplasm-specific markers for fast-tracking *ms1* introgression into diverse female-inbred parental lines. Moreover, complementation studies demonstrate that *ms1* is unique and contrasts with other reported wheat *ms* mutant alleles[38] in that *ms1* behaves as a single-mutant locus in hexaploid wheat and a single copy of *Ms1* restores fertility. Given the characterisation of the *ms1* alleles described here and the observed variation in penetrance of sterility between these different alleles, understanding the relationship of these mutations to pollen production, as well as optimising *ms1* as a system for the production of a hybrid seed is now possible through the adoption of advanced breeding technologies such as gene editing[39, 40]. Gene editing would enable the generation of novel *ms1* alleles and allow simultaneous testing in different isogenic wheat backgrounds (e.g. spring and winter or hard and soft wheat). Further, once highly penetrant *ms1* alleles are identified, rather than introgression through conventional backcrossing, this new variant allele could be rapidly introduced into the most elite genetics by directly editing *TaMs1*. Adoption of new breeding technologies is likely to be particularly valuable in translating the results presented here in wheat to other polyploids suffering from a similar paucity of mutants. Such new technologies are necessary for the development of hybridisation systems to exploit heterosis as a means to increase seed production as global population increases.

Methods

Plant and DNA materials. Bread wheat lines used for fertility phenotyping, molecular marker development and genetic mapping were cv. Chinese Spring, Chinese Spring-derived nullisomic tetrasomic stocks[41] (N4AT4D, N4AT4B, N4BT4A, N4BT4D, N4DT4A and N4DT4B), cv. *Gladius*, cv. *Pugsley's* male sterile (*ms1a*)[14], cv. *Probus* (*ms1b*)[16], cv. *Cornerstone* (*ms1c*)[18], cv. *Chris* and *Chris*-EMS-mutagenised lines FS2 (*ms1d*), FS3 (*ms1e*) and FS24 (*ms1f*)[21]. All cultivars, breeders' lines or DNA samples for marker screening were obtained from various Australian wheat-breeding programmes, Australian Wheat and Barley Molecular Marker Program or the Australian Winter Cereals Collection (AWCC). The BAC library was derived from the *Triticum turgidum* ssp. durum cv. Langdon[42]. The EMS-mutagenised population used for TILLING was derived from the soft bread wheat cv. *QAL2000*[29].

Plant growth and phenotyping. Plants for genetic mapping, cytological examination, expression analysis, TILLING and transformation donor material were sown at 5–6 plants per 6 l (8-inches diameter) pot containing soil mix. The soil mix consisted of 75% (v v^{-1}) Coco Peat, 25% (v v^{-1}) nursery-cutting sand (sharp), 750 mg l^{-1} $CaSO_4.2H_2O$ (gypsum) 750 mg l^{-1} $Ca(H_2PO_4)_2.H_2O$ (superphosphate), 1.9 g l^{-1} $FeSO_4$, 125 mg l^{-1} FeEDTA, 1.9 g l^{-1} $Ca(NO_3)_2$, 750 mg l^{-1} Scotts Micromax micronutrients and 2.5 g l^{-1} Osmocote Plus slow-release fertilizer (16:3:9) (Scotts Australia Pty. Ltd.). The pH was adjusted between 6.0 and 6.5 using two parts of agricultural lime to one part of hydrated lime. Potted plants were grown either in controlled environment growth rooms at 23 °C (day) and 16 °C (night) or similarly temperature-moderated glasshouses in which the photoperiod was extended using 400 W high-pressure sodium lamps in combination with metal halide lamps to 12 h over winter months.

Individual plants were assessed for self-fertility by placing and sealing a glassine bag over each head before anthesis. Between three and ten heads per plant were collected for seed counting. The two basal and two apical sspikelets per head were eliminated from analysis due to their incomplete development. The total seed set and numbers of florets were counted on a per-head basis. The percentage of fertility for each spike or plant was calculated as follows:

$$\%\ \text{fertility} = \frac{\text{Total number of seeds per spike}}{\text{Total number of 1°, 2° and 3° florets per spike}} \times 100$$

A plant was deemed to be self-fertile if the total calculated percentage of fertility was greater than 60% or was equivalent to a wild-type control.

Pollen viability was assessed for three isolated anthers per plant (n = 3) by either acetocarmine–glycerin or Lugol (1% I_3K solution) staining. Dissected anthers were mounted on glass microscope slides and pollen grains ($n > 500$ per sample) counted for staining by visualising them on a Zeiss Axio Imager M2 optical microscope coupled with a CCD camera (The University of Adelaide microscopy). Stainable pollen is represented as the mean ± standard deviation for nine samples per genotype.

Histochemical staining cytological examination. Anthers containing premeiotic microspores to mature pollen were isolated from wheat plants identified to contain the *TaMs1::gusplus* cassette. Histochemical GUS activity was detected using 5-

bromo-4-chloro-3-indolyl-beta-D-glucuronic acid (Gold Biotechnology, Inc). The samples were incubated in a 1 mM X-Gluc solution in 100 mM sodium phosphate at pH 7.0, 10 mM sodium ethylenediaminetetraacetate, 2 mM $FeK_3(CN)_6$, 2 mM $K_4Fe(CN)_6$ and 0.1% Triton X-100. After vacuum infiltration at 2600 Pa for 20 min, the samples were incubated overnight at 37 °C. Anther samples were then immersed in a fixative solution of 4% sucrose, 1× PBS, 4% paraformaldehyde and 0.25% glutaraldehyde, at 4 °C overnight. The samples were then dehydrated in ethanol series of increasing concentrations (30, 50, 70, 85, 90, 95 and 100%). Tissues were embedded in Technovit® resin, then sectioned on a microtome to a thickness of 8–14 µm, counterstained with ruthenium red and DPX mounted (Sigma, St. Louis, MO) on glass slides. The sections were observed using a LEICA ASLMD laser dissection microscope coupled with a CCD camera (The University of Adelaide microscopy).

Electron and light microscopy. Sterile (*ms1d*) and fertile (*Ms1*) mature anthers before dehiscence were fixed with either 4% paraformaldehyde, 1.25% glutaraldehyde and 4% sucrose in phosphate-buffered saline (PBS) at pH 7.4, for 16 h at 4 °C for scanning electron microscopy (SEM) or 3% glutaraldehyde in 0.1 M phosphate buffer at pH 7.0 overnight for transmission electron (TEM) or light microscopy. The samples for SEM were rinsed twice with PBS at pH 7.4 for 5 min, whereas the samples for TEM and light microscopy were washed twice with 1 x PBS and embedded in 2% low melting point agarose (Sigma, St. Louis, MO) in 1 x PBS for sample orientation and sectioning, and then dehydrated using a series of graded ethanol solutions (30%, 50%, 70%, 85%, 90% and 95%) each for 60 min. The samples were then infiltrated 3 times, each for 60 min, in 100% ethanol. The samples were either embedded in LR white resin, sectioned (2 µm) and stained with 0.05% toluidine blue stain and mounted on slides in DPX solution (Sigma, St. Louis, MO) for light microscopy or dissected, then they were critical point dried and sputter coated with platinum (BalTec CPD030 Critical Point Dryer) for SEM. 70–80 nm ultrathin anther sections were prepared and stained in 4% uranyl acetate followed by Reynold's lead citrate (The University of Adelaide microscopy)[43]. SEM and image capture was performed at an accelerating voltage of 10 kV (Philips XL20 SEM w EDAX EDS), whereas TEM and image capture was performed on a Phillips CM-1000 TEM (The University of Adelaide microscopy). Light microscopy images were captured using a Zeiss Axio Imager M2 optical microscope (Zeiss, Germany).

Fatty acid profiling. Approximately 50 frozen anthers were transferred into pre-chilled cryogenic mill tubes and weighed accurately. A 300 µl aliquot of 1:3:1 chloroform:methanol:water containing a 30 µM internal standard ($^{13}C_1$ myristic acid) was added to each sample tube. Dried samples and a fatty acid calibration mix (Supelco®37 Component FAME Mix) was prepared by adding 25 µl of 2:1 chloroform:methanol followed by shaking at 37 °C for 30 min. The samples were then derivatised using 5 µl of Meth-Prep™ II (Grace Davison Discovery). 1 µl was injected onto the GC column. The GC-MS apparatus comprised of a Gerstel 2.5.2 autosampler, a 7890A Agilent gas chromatograph and a 5975C Agilent quadrupole mass spectrometer (Agilent, Santa Clara, USA). The mass spectrometer was calibrated according to the manufacturer's recommendations using *tris*-(perfluorobutyl)-amine (CF43).

Gas chromatography was performed on a VF-5ms column (Agilent Technologies, Australia). The injection temperature was set at 250 °C, with the MS transfer line at 280 °C, the ion source adjusted to 250 °C and the quadrupole at 150 °C. Helium was used as the carrier gas at a flow rate of 1.1 ml min^{-1}. The corresponding GC-MS method was performed using the following temperature programme; start at an injection of 50 °C, hold for 1 min, followed by a 15 °C min^{-1} oven temperature ramp to 230 °C; hold for 3 min, followed by a 10 °C ramp to 300 °C.

Mass spectra were recorded at 2 scans s^{-1} with an *m/z* value of 50–600 scanning range. Both chromatograms and mass spectra were evaluated using the MassHunter Workstation software version B.07.00 (Agilent, Santa Clara, USA). The retention times and mass spectra (unique qualifier ions) were identified and compared directly to standards from a commercially available fatty acid methyl ester mix (Supelco®37 Component FAME Mix, 47885-U, Sigma-Aldrich). All fatty acid methyl esters identified were quantified using prepared calibration curves from the stock Supelco®37 Component FAME Mix in the linear range from 2.5 to 150 µM for each lipid class.

Mapping *Ms1*. Using sequence collinearity among chromosomes 1, 3 and 4 from rice, *Brachypodium* and barley[44], respectively, we were able to identify gene sequences from these species and use them in a BLASTn search of ESTs and homeogroup four-derived genomic survey sequences from the bread wheat cv. Chinese Spring[45]. Chromosome arm 4AL, 4BS and 4DS-derived genomic sequence contigs were then used to develop PCR-based markers that were subsequently validated for sub-genome specificity by amplification from the Chinese Spring-derived nullisomic tetrasomic set (N4AT4D, N4AT4B, N4BT4A, N4BT4D, N4DT4A and N4DT4B). The region spanning *Ms1* was then identified by amplification of these markers on the sterile deletion mutant series *ms1a*, *ms1b* and *ms1c*[15–19] relative to their respective fertile wild-type (*Ms1*) controls[15–19].

An F_2-mapping population derived from a cross between the male sterile cv. *Chris*-EMS-mutagenised line FS2 (*ms1d*)[21] and male fertile cv. *Gladius*[46] was developed. *Ms1*-flanking markers identified by deletion mutant mapping were converted into high-resolution melting (HRM) markers[47] and tested for polymorphism between parental genotypes, and then assayed for segregation within the F_2 population. Recombinants within the *Ms1* region were identified from F_2- and F_3-derived individuals using a combination of both HRM markers and KBioscience competitive allele-specific polymerase chain reaction (KASPar) assays[48] based on SNPs used to develop both the 9K[49] and 90K[50] iSelect Beadchip Assay from Illumina. Primers used for either HRM or KASPar assays are listed in Supplementary Table 5 and 6. All recombinants for the region were marker selected, then fertility tested and not male sterile subsequently progeny tested for fertility in order to determine the zygosity.

BAC clone analysis. Eighteen probes were designed within the 0.5-cM region bounded by markers wsnp_Ex_c18318_27140346 (*x*27140346) and wsnp_Ku_c7153_12360198 (x12360198), using synteny to *Brachypodium* and rice. The probes were designed to be non-repetitive based on BLAST analysis of target sequences. The probes were then PCR amplified and separated by agarose gel electrophoresis with fragments of desired size being eluted from the gel using a Qiaquick Gel Extraction kit (Qiagen, Germantown, MD, USA). PCR fragments were pooled to an equimolar concentration and then ^{32}P-dATP radiolabelled by a NEBlot kit (New England Biolabs) using a manufacturer's protocol. The labelled probe was purified in a Sephadex G50 column (GE Healthcare) and denatured at 100 °C for 10 min. Twenty eight high-density BAC clone colony filters gridded onto Hybond N + nylon membranes (GE Healthcare, Piscataway, NJ, USA) were used for hybridisation. This represents a coverage of 5.1-genome equivalents from the *Triticum turgidum ssp.* durum wheat cv. Langdon[42]. For prehybridisation, overnight incubation of colony filters in a hybridisation solution (2x SSPE, 0.5% SDS, 5x Denhardt's reagent[51] and 40 µg ml^{-1} salmon sperm DNA) was done in rotary glass tubes at 65 °C. The labelled probe was mixed with 5 ml of hybridisation solution and colony filters were incubated at 65 °C overnight. To remove the unbound probe, the filters were washed twice in a washing solution containing 2x SSPE and 0.5% SDS and rinsed with 1x SSC. The washed filters were exposed to an X-ray film for 1–3days based on the signal intensity to identify positive clones. BAC clones that gave a positive signal were grown on single colonies from glycerol stabs and then DNA was extracted according to the BACMAX96™ DNA purification kit (Epicentre®, www.epicentre.com, Madison, Wisconsin, USA).

Restriction mapping, PCR experiments with primers corresponding to the markers previously used, determined the order of the BACs covering the region of interest. BAC libraries from the *Triticum turgidum ssp.* durum cv. Langdon and a bread wheat proprietary cultivar were screened with probes from the *Ms1* region, with positive clones being selected for sequencing. All BACs were sequenced using the Illumina MiSeq platform with paired-end (PE) reads of 250 bp. Quality-controlled PE reads were mapped in a single-end mode to the bread wheat cv. Chinese Spring chromosome arm survey sequencing using Biokanga 2.76.2 (https://github.com/csiro-crop-informatics/biokanga) allowing 2 mismatches per 100 bp to confirm that they were derived from homeogroup 4. The reads were then filtered for bacterial sequence contamination, and trimmed for a vector sequence using a combination of BLASTn-based filters and custom scripts. Before assembly, the overlapping PE reads were fused using FLASH 1.2.7 (https://sourceforge.net/projects/flashpage). The fused reads along with the remaining PE reads were then assembled into contigs using MIRA 4.0[52]. Contigs produced by MIRA were then scaffolded using SSPACE[53] using mate-pair anchors for each contig derived from a single mate-pair library for all samples. Single contiguous scaffolds for each homeolocus were manually finished using Gap5[54]. Highly repetitive regions on the BACs were masked based on a per-base depth of mapped reads (cv. *Excalibur*, cv. *Gladius*[55]) exceeding 1000. The alignments to the BACs of *Brachypodium* genes as well as mappings of publically available RNA-seq datasets from the bread wheat cv. Chinese Spring[56] facilitated gene prediction. Nucleotide sequences spanning the *Ms1* region were submitted to GenBank (accession codes KX447407, KX447408 and KX447409).

Nucleic acid extraction and expression analysis. DNA extractions from all bread wheat lines were performed using either a phenol/chloroform or freeze-dried extraction protocol[57]. A 15 cm leaf piece from a 2-week-old plant was frozen in liquid nitrogen, and the tissue was ground to a fine powder using one large (9 mm) and three small (3 mm) ball bearings and a vortex. 700 µl of the extraction buffer (1% sarkosyl, 100 mM Tris-HCl at pH 8.5, 100 mM NaCl, 10 mM EDTA and 2% PVPP) was added to each sample and the samples were mixed for 20 min on a rotary shaker. 700 µl of phenol/chloroform/iso-amylalcohol (25:24:1) was added and the extract was transferred to a silica matrix tube and spun at 4000 rpm for 10 min. DNA was precipitated by adding 60 µl of 3 M sodium acetate at pH 4.8 and 600 µl of isopropanol and centrifuged at 13 000 rpm for 10 min. The DNA pellet was washed with 1 ml of 70% ethanol, centrifuged for 2 min at 13 000 rpm and air dried for 20 min. The purified DNA was resuspended in 50 µl of R40 (1x TE, 40 µg ml^{-1} RNase A).

TaMs1 and homeologous transcripts were detected by qRT-PCR on cDNA using total RNA extracted from wheat of cv. *Chris* (wild type) using an ISOLATE II *RNA* Mini Kit (Bioline). For the anther developmental series, a single anther per floret was squashed in acetocarmine and mounted for microscopy. Microspores were cytologically examined for the stage of development. The remaining two

anthers from the same floret were isolated and snap frozen in liquid nitrogen. Developmentally equivalent anthers were pooled and RNA isolated. All total RNA samples were treated with DNase I (Qiagen). First-strand cDNA was synthesised using oligo dT[51] and Superscript III reverse transcriptase (Thermo Fisher). Amplification products from qRT-PCR on each tissue sample, three technical replicates and three biological replicates were used to estimate *TaMs1* and the homeologue transcript abundance relative to *TaEFA2*2*, *TaGAPdH 2*2* and *TaCyclophilin 2*2* reference transcripts. Standard qRT-PCR assays[58] were performed using primers, as listed in Supplementary Table 7.

RNA-seq expression analysis. RNA-seq reads derived from five organs (root, leaf, stem, spike and grain) at three developmental stages each from hexaploid wheat cv. Chinese Spring have been published previously[56]. The reads were aligned against the repeat-masked BAC assemblies with Bowtie2[59] and Tophat2[60]. The returned alignments were stringently filtered so as to remove ambiguously mapped reads and read pairs with conflicting alignments. Gene expression was computed on RNA-seq data by using Cufflinks and Cuffmerge v.3.0[61]. RNA-seq expression data for all predicted coding regions from the BAC assemblies are presented in Supplementary Table 1.

***TaMs1* sequence from mutant alleles**. To identify the *TaMs1* sequence variants in the *ms1d, ms1e* and *ms1f* alleles, the *TaMs1* coding region was amplified from 13 individuals segregating for the sterility phenotype for each mutant allele. PCR used Phusion High-Fidelity DNA Polymerase (NEB, M0530) with Phusion GC buffer, 5% DMSO and 1 M betaine using the primer *TaMs1* (coding region) listed in Supplementary Table 7. The fragments were subcloned into a pCR™8/GW/TOPO® TA Cloning Kit (Thermo Fisher Scientific, K250020) and Sanger sequencing of positive clones was performed by the Australian Genome Research Facility. Sequence chromatograms were compared using Geneious version 6.1.8[62]. Sequence analysis correlated a G-to-A transition at position 329 with the sterility phenotype in the *ms1d* mutant. A Kompetitive Allele-Specific PCR (KASP™) (LGC Genomics) was designed to this SNP transition using Primer Picker (LGC Genomics) (007-0091.1, Supplementary Table 6) and it was assayed using KASP Mastermix on the SNPline (LGC Genomics) on DNA from the *ms1d* x *Gladius* F_2-mapping population, the *ms1* mutant alleles and across a panel of 192 spring wheat germplasm.

Phylogenetic analysis. *TaMs1* homologous Poaceae sequences were retrieved from Phytozome (www.phytozome.net), TGAC *Triticum monococcum* Shotgun sequence, International Barley Genome Sequencing Consortium and Rice Genome Annotation Project (http://rice.plantbiology.msu.edu). All BLASTn, BLASTp, tBLASTn and BLASTx hits were retrieved using a cutoff e-value of $\leq 1 \times 10^{-5}$. Default BLAST settings were used for querying with complete sequences. Two prediction tools, PredGPI (gpcr.biocomp.unibo.it/predgpi/) and big-PI Plant Predictor (mendel.imp.ac.at/gpi/plant_server.html), were then used to determine whether primary peptide sequences contained a putative GPI-anchored motif at the C-termini. Protein multiple-sequence alignments (MSAs) were generated using MUSCLE (default settings) implemented in Geneious analysis package (www.geneious.com). Manual alignment was performed to improve the MSAs. The phylogenetic tree was computed with MEGA7 using the maximum likelihood method under default parameters (www.megasoftware.net).

Constructs. A 4.3-Kb genomic fragment containing approximately 1.5 Kb upstream of *TaMs1* start codon and 1 Kb downstream of the stop codon was synthesised and introduced upstream of the visible marker MoPAT-DsRED (a translational fusion of the bialaphos resistance gene, phosphinothricin-N-acetyl-transferase, and the red fluorescent protein DsRED) transcribed by the maize Ubiquitin promoter[63] and this 8.1 kb DNA fragment replaced the 2.1 kb *Hind III-Eco RI* DNA fragment from PHP43534[64]. This plasmid was introduced into *A. tumefaciens* strain LBA4404[65] by electroporation using a Gene Pulser II (Bio-Rad) [66] and used for complementing the *ms1d* mutant. A transcriptional reporter construct containing 1.5 Kb of *TaMs1* promoter sequence was fused to *gusplus*[67] and subcloned into the binary vector pMBC32.

Transformation and in vitro culture. Male-sterile transformation-amenable spring wheat lines, which contain the *ms1d* allele, were developed by backcrossing with pollen from the spring wheat-transformable cv. *Gladius*. Either immature embryos that segregated for the *ms1d* allele (3:1) or the cv. *Fielder* were used as donor materials for transformation. cv. *Fielder* donor material was used to test the transcriptional fusion construct with the *gusplus* reporter gene. Here, *A. tumefaciens* strain ALG0 (pBGXI) was engineered to contain a disarmed pTiBo542 carrying the *TaMs1::gusplus* cassette in a pMBC32 backbone. Segregating *ms1d* donor material enabled the transformation directly into a homozygous *ms1d* background to test for genetic complementation of the *ms1d* mutation with the putative *Ms1* allele in the transformed plants (T_0). To generate wheat transformants[68] for testing either complementation of the *ms1* mutation or the *TaMs1* transcriptional reporter, wheat (*Triticum aestivum* L., cv. *Gladius* or cv. *Fielder*) plants were grown in a growth chamber at 18/15 °C (day/night), with a 16-hr photoperiod (minimum of 1000 µmol s^{-1} m^{-2} light) or in a greenhouse. Immature seeds with immature embryos (IEs) of about 1.5–2.5 mm collected from spikes 12–14 days post anthesis were surface-sterilised for 20 min in 15% (v v^{-1}) bleach (5.25% sodium hypochlorite) plus one drop of Tween 20 followed by three washes in sterile water. IEs were isolated and placed in 1.0 ml of liquid infection medium (WI4; MS salt + vitamins (4.43 g l^{-1}), maltose (30 g l^{-1}), glucose (10 g l^{-1}), MES (1.95 g l^{-1}), 2,4-D (1 ml, 0.5 mg l^{-1}), Picloram (200 µl, 10 mg ml^{-1}) and BAP (0.5 ml, 1 mg l^{-1})) with 0.25 ml of autoclaved sand into 2 ml microcentrifuge tubes. IEs were treated by centrifuging at various strengths in an infection medium and then inoculated with *Agrobacterium*. The suspension of *Agrobacterium* and IEs was poured onto a co-cultivation medium (a WI4 medium containing 5.0 µM $CuSO_4$ without glucose solidified with 3.5 g l^{-1} of Phytagel). IEs were then placed on an embryo axis side down on the media, and incubated in the dark at 21 °C. After three days, IEs were transferred to a DBC4 medium containing 100 mg l^{-1} of cefotaxime (Phyto-Technology Lab., Shawnee Mission, KS) and then incubated at 26–28 °C under dim light for two weeks. The DBC4 medium is a DBC3 green-regenerative medium[69] modified with 1.0 mg l^{-1} of 6-benzylaminopurine (BAP). The tissues were then transferred to a DBC6 medium (a modified DBC3 medium with 0.5 mg l^{-1} of 2,4-dichlorophenoxyacetic acid and 2.0 mg l^{-1} of BAP) containing 150 mg l^{-1} of cefotaxime for another two weeks. Regenerable *DsRed*- expressing transgenic sectors were identified using a Leica M165 FC fluorescence microscope, cut from the non-transformed tissues and placed on a MSA regeneration medium [MSB[68] without indole-3-butyric acid] with 150 mg l^{-1} of cefotaxime, whereas *TaMs1::gusplus*-containing tissues were selected based on resistance to 100 mg l^{-1} of hygromycin B. After sectors have developed into small plantlets, they were transferred to an MSB-rooting medium. During each transfer, plantlets were checked for *DsRed* gene expression and any non-expressing or chimeric tissues were removed.

T_0 plantlet generation and analysis. T_0 wheat regenerants containing a single- or multicopy *TaMs1–DsRed* cassette(s) were identified by copy number qPCR[70] using the following forward, reverse and probe primers (Fwd: 5′-GACATCCCCGAC-TACAAGAAGCT-3′, Rev: 5′-CACGCGCTCCCACTTGA-3′ and Probe1-FAM MGB 5′-CCTTCCCCGAGGGC-3). Zygosity was shown of the *ms1d* mutation using flanking and linked markers (Supplementary Table 5 and 6). Plantlets were transferred to the glasshouse and assessed for self-fertility and expression of *DsRed* fluorescence in the resulting seed. Seed counts from these individual plants were counted as a qualitative measure of male fertility.

Molecular and phenotypic traits of T_1 plants. Inheritance of complementation by *TaMs1* T-DNA insertion was shown by analysing a selfed seed set on T_1 plants derived from two separate T_0 plants, each with independent T-DNA insertions (Event-1 and Event-7) (Supplementary Table 4). One set of T_1 progenies was derived from a T_0 plant homozygous for *ms1d* mutation (*ms1d/ms1d*) and containing the *TaMs1–DsRed* cassette (Event-1). The second set of T_1 progenies was derived from a T_0 plant heterozygous for *ms1d* mutation (*Ms1/ms1d*) and containing the *TaMs1–DsRed* cassette (Event-7). Genotyping for *ms1d* zygosity and the presence of the T-DNA insertion for plants derived from both sets were determined using flanking markers, as described above, and the expression of the *DsRed* seed colour marker.

Data availability. MiSeq BAC-sequencing data have been deposited in the NCBI SRA database under Bioproject ID PRJNA396428. The assembled genomic DNA of BACs derived from the *Ms1* locus (KX447407) as well as its A (KX447408) and D (KX447409) genome-derived homeoloci have been deposited in NCBI GenBank. Further data that support the findings of this study are available from the corresponding author upon reasonable request.

Received: 18 December 2016 Accepted: 8 August 2017
Published online: 11 October 2017

References

1. FAOSTAT. http://faostat3.fao.org (2013–2015).
2. HY-WHEAT. Scientific and technological cooperation in plant genome research as basis of the 'Knowledge-Based Bio-Economy' (Plant - KBBE) 2010 Project HY-WHEAT, http://www.agence-nationale-recherche.fr/?Project=ANR-10-KBBE-0004 (2010).
3. Longin, C. F. H. et al. Hybrid wheat: quantitative genetic parameters and consequences for the design of breeding programs. *Theor. Appl. Genet.* **126**, 2791–2801 (2013).
4. Muhleisen, J., Piepho, H. P., Maurer, H. P., Longin, C. F. & Reif, J. C. Yield stability of hybrids versus lines in wheat, barley, and triticale. *Theor. Appl. Genet.* **127**, 309–316 (2014).
5. Longin, C. F. H., Reif, J. C. & Würschum, T. Long-term perspective of hybrid versus line breeding in wheat based on quantitative genetic theory. *Theor. Appl. Genet.* **127**, 1635–1641 (2014).
6. Whitford, R. et al. Hybrid breeding in wheat: technologies to improve hybrid wheat seed production. *J. Exp. Bot.* **64**, 5411–5428 (2013).
7. Driscoll, C. J. XYZ system of producing hybrid wheat. *Crop Sci.* **12**, 516–517 (1972).
8. Driscoll, C. J. Modified XYZ system of producing hybrid wheat. *Crop Sci.* **25**, 1115–1116 (1985).

9. Wu, Y. et al. Development of a novel recessive genetic male sterility system for hybrid seed production in maize and other cross-pollinating crops. *Plant Biotechnol. J.* **14**, 1046–1054 (2015).
10. Druka, A. et al. Genetic dissection of barley morphology and development. *Plant Physiol.* **155**, 617–627 (2011).
11. Franckowiak, J. Revised linkage maps for morphological markers in barley, *Hordeum vulgare*. *Barley Genet. Newslett.* **26**, 9–21 (1997).
12. Cigan, A. M. et al. Targeted Mutagenesis of a conserved anther-expressed P450 gene confers male sterility in monocots. *Plant Biotechnol. J.* **15**, 379–389 (2016).
13. Klindworth, D. L., Williams, N. D. & Maan, S. S. Chromosomal location of genetic male sterility genes in four mutants of hexaploid wheat. *Crop Sci.* **42**, 1447–1450 (2002).
14. Pugsley, A. T. & Oram, R. N. Genetic male sterility in wheat. *Aust. Plant Breed. Genet. Newslett.* **14**, 10–11 (1959).
15. Driscoll, C. J. Cytogenetic analysis of two chromosomal male-sterility mutants in hexaploid wheat. *Aust. J. Biol. Sci.* **28**, 413–416 (1975).
16. Fossati, A. & Ingold, M. A male sterile mutant in Triticum aestivum. *Wheat Inform. Serv.* **30**, 8–10 (1970).
17. Barlow, K. K. & Driscoll, C. J. Linkage studies involving two chromosomal male-sterility mutants in hexaploid wheat. *Genetics* **98**, 791–799 (1981).
18. Driscoll, C. J. Registration of cornerstone male sterile wheat germplasm (reg. no. GP 74). *Crop Sci.* **17**, 190–190 (1977).
19. Kleijer, G. & Fossati, A. Chromosomal location of a gene for male sterility in wheat (*Triticum aestivum*). *Wheat Inform. Serv.* **41-42**, 12–13 (1976).
20. Endo, T. R., Mukai, Y., Yamamoto, M. & Gill, B. S. Physical mapping of a male-fertility gene of common wheat. *Jpn. J. Genet.* **66**, 291–295 (1991).
21. Sasakuma, T., Maan, S. S. & Williams, N. D. EMS-induced male-sterile mutants in euplasmic and alloplasmic common wheat. *Crop Sci.* **18**, 850–853 (1978).
22. Briggle, L. A recessive gene for male sterility in hexaploid wheat. *Crop Sci.* **10**, 693–696 (1970).
23. Islam, A. & Driscoll, C. Latent male fertility in'Cornerstone'chromosome 4A. *Can. J. Genet. Cytol.* **26**, 98–99 (1984).
24. Joshi, G. P., Li, J., Nasuda, S. & Endo, T. R. Development of a self-fertile ditelosomic line for the long arm of chromosome 4B and its characterization using SSR markers. *Genes Genet. Syst.* **88**, 311–314 (2013).
25. Borner, G. H. H., Lilley, K. S., Stevens, T. J. & Dupree, P. Identification of glycosylphosphatidylinositol-anchored proteins in *Arabidopsis*. A proteomic and genomic analysis. *Plant Physiol.* **132**, 568–577 (2003).
26. Kim, H. et al. Characterization of glycosylphosphatidylinositol-anchored lipid transfer protein 2 (*LTPG2*) and overlapping function between *LTPG/LTPG1* and *LTPG2* in cuticular wax export or accumulation in *Arabidopsis thaliana*. *Plant Cell Physiol.* **53**, 1391–1403 (2012).
27. Franckowiak, J. D., Maan, S. S. & Williams, N. D. A proposal for hybrid wheat utilizing *Aegilops squarrosa* L. cytoplasm. *Crop Sci.* **16**, 725–728 (1976).
28. José-Estanyol, M., Gomis-Rüth, F. X. & Puigdomènech, P. The eight-cysteine motif, a versatile structure in plant proteins. *Plant Physiol. Biochem.* **42**, 355–365 (2004).
29. Dong, C., Dalton-Morgan, J., Vincent, K. & Sharp, P. A modified TILLING method for wheat breeding. *Plant Genome* **2**, 39–47 (2009).
30. Zhou, K., Wang, S., Feng, Y., Liu, Z. & Wang, G. The 4E-system of producing hybrid wheat. *Crop Sci.* **46**, 250–255 (2006).
31. Wang, S., Zhou, K., Yang, W. & Wang, H. Technical difficulties and solutions of applying 4E-*ms* system in hybrid wheat production. *J. Triticeae Crops* **33**, 1312–1315 (2013).
32. Zhang, D., Shi, J. & Yang, X. in *Lipids in Plant and Algae Development*, 315–337 (Springer, 2016)
33. Yang, L. et al. *Induced Plant Mutations in the Genomics Era*. 370–372 (Food and Agriculture Organization of the United Nations, 2009).
34. Cao, W., Somers, D. J. & Fedak, G. A molecular marker closely linked to the region of *Rht-D1c* and *Ms2* genes in common wheat (*Triticum aestivum*). *Genome* **52**, 95–99 (2009).
35. Maan, S. & Kianian, S. Third dominant male sterility gene in common wheat. *Wheat Inform. Serv.* **93**, 27–31 (2001).
36. Ni, F. et al. Wheat *Ms2* encodes for an orphan protein that confers male sterility in grass species. *Nat. Commun.* **8**, 15121 (2017).
37. Xia, C. et al. A TRIM insertion in the promoter of *Ms2* causes male sterility in wheat. *Nat. Commun.* **8**, 15407 (2017).
38. Singh, M., Kumar, M., Thilges, K., Cho, M.-J. & Cigan, A. M. MS26/CYP704B is required for anther and pollen wall development in bread wheat (*Triticum aestivum* L.) and combining mutations in all three homeologs causes male sterility. *PLoS ONE* **12**, e0177632 (2017).
39. Voytas, D. F. & Gao, C. Precision genome engineering and agriculture: opportunities and regulatory challenges. *PLoS Biol.* **12**, e1001877 (2014).
40. Svitashev, S. et al. Targeted mutagenesis, precise gene editing, and site-specific gene insertion in maize using Cas9 and guide RNA. *Plant Physiol.* **169**, 931–945 (2015).
41. Sears, E. R. in *Chromosome Manipulations and Plant Genetics*, 29–45 (Springer, 1966).
42. Cenci, A. et al. Construction and characterization of a half million clone BAC library of durum wheat (*Triticum turgidum* ssp. durum). *Theor. Appl. Genet.* **107**, 931–939 (2003).
43. Reynolds, E. S. The use of lead citrate at high pH as an electron opaque stain in electron microscopy. *J. Cell. Biol.* **17**, 208 (1963).
44. Mayer, K. F. et al. Unlocking the barley genome by chromosomal and comparative genomics. *Plant Cell* **23**, 1249–1263 (2011).
45. Mayer, K. F. et al. A chromosome-based draft sequence of the hexaploid bread wheat (Triticum aestivum) genome. *Science* **345**, 1251788 (2014).
46. Australian, Grain Technologies Pty. Ltd. Gladius. *Plant Varieties J.* **20**, 41 (2007).
47. Tucker, E. J. & Huynh, B. L. Genotyping by high-resolution melting analysis. *Crop Breed. Methods Protoc.* **1145**, 59–66 (2014).
48. He, C., Holme, J. & Anthony, J. in *Methods in Molecular Biology*, Vol. 1145 (eds D. Fleury & R. Whitford) Ch. 7, 75-86 (Springer, 2014).
49. Cavanagh, C. R. et al. Genome-wide comparative diversity uncovers multiple targets of selection for improvement in hexaploid wheat landraces and cultivars. *Proc. Natl Acad. Sci.* **110**, 8057–8062 (2013).
50. Wang, S. et al. Characterization of polyploid wheat genomic diversity using a high-density 90 000 single nucleotide polymorphism array. *Plant. Biotechnol. J.* **12**, 787–796 (2014).
51. Green, M. R. & Sambrook, J. *Molecular Cloning: a Laboratory Manual*, Vol. 1 (Cold Spring Harbor Laboratory Press, 2012).
52. Chevreux, B., Wetter, T. & Suhai, S. in *German Conference on Bioinformatics*. 45–56. (Hannover, Germany, 1999)
53. Boetzer, M., Henkel, C. V., Jansen, H. J., Butler, D. & Pirovano, W. Scaffolding pre-assembled contigs using SSPACE. *Bioinformatics* **27**, 578–579 (2011).
54. Bonfield, J. K. & Whitwham, A. Gap5—editing the billion fragment sequence assembly. *Bioinformatics* **26**, 1699–1703 (2010).
55. Edwards, D. et al. Bread matters: a national initiative to profile the genetic diversity of Australian wheat. *Plant Biotechnol. J.* **10**, 703–708 (2012).
56. Choulet, F. et al. Structural and functional partitioning of bread wheat chromosome 3B. *Science* **345**, 1249721 (2014).
57. Kovalchuk, N. in *Methods in Molecular Biology*, Vol. 1145 (eds D. Fleury & R. Whitford) 239–252 (Springer, 2014).
58. Burton, R. A., Shirley, N. J., King, B. J., Harvey, A. J. & Fincher, G. B. The CesA gene family of barley. Quantitative analysis of transcripts reveals two groups of co-expressed genes. *Plant Physiol* **134**, 224–236 (2004).
59. Langmead, B. & Salzberg, S. L. Fast gapped-read alignment with Bowtie 2. *Nat. Methods* **9**, 357–359 (2012).
60. Kim, D. et al. TopHat2: accurate alignment of transcriptomes in the presence of insertions, deletions and gene fusions. *Genome Biol.* **14**, R36 (2013).
61. Trapnell, C. et al. Differential gene and transcript expression analysis of RNA-seq experiments with TopHat and Cufflinks. *Nat. Protoc.* **7**, 562–578 (2012).
62. Kearse, M. et al. Geneious basic: an integrated and extendable desktop software platform for the organization and analysis of sequence data. *Bioinformatics* **28**, 1647–1649 (2012).
63. Ananiev, E. V. et al. Artificial chromosome formation in maize (Zea mays L.). *Chromosoma* **118**, 157–177 (2009).
64. Rudrappa, T. & Girhepuje, P. V. Method of sunflower regeneration and transformation using radicle free embryonic axis. US patent US8901377 (2014).
65. Komari, T., Hiei, Y., Saito, Y., Murai, N. & Kumashiro, T. Vectors carrying two separate T-DNAs for co-transformation of higher plants mediated by Agrobacterium tumefaciens and segregation of transformants free from selection markers. *Plant J.* **10**, 165–174 (1996).
66. Gao, H. et al. Heritable targeted mutagenesis in maize using a designed endonuclease. *Plant J.* **61**, 176–187 (2010).
67. Vickers, C. E., Schenk, P. M., Li, D., Mullineaux, P. M. & Gresshoff, P. M. pGFPGUSPlus, a new binary vector for gene expression studies and optimising transformation systems in plants. *Biotechnol. Lett.* **29**, 1793–1796 (2007).
68. Ishida, Y., Tsunashima, M., Hiei, Y. & Komari, T. Wheat (Triticum aestivum L.) transformation using immature embryos. *Methods Mol. Biol.* **1**, 189–198 (2015).
69. Cho, M. J., Ellis, S. R., Gordon-Kamm, W. J. & Zhao, Z. Y. *Methods and compositions for producing and selecting transgenic plants* Worldwide patent WO2014093485 (2014).
70. Fletcher, S. J. qPCR for quantification of transgene expression and determination of transgene copy number. *Crop Breed. Methods Protoc.* **1145**, 213–237 (2014).

Acknowledgements

We thank J. Hayes for critical discussions and reading of the manuscript, P. Warner, M. Ovitigala, S. Manning, A. Okada, Y. Li, and M. Kumar for technical assistance. We also thank C. Kastner and M.-J. Cho for transgenic line generation, D. Dias and U. Roessner for metabolomic profiling and G. Mayo for microscopy assistance. This research was

funded by DuPont Pioneer Hi-Bred International Inc. We are grateful for the support provided by The University of Adelaide, Australian Research Council, Grains Research and Development Corporation and the South Australian State Government.

Author contributions

E.J.T., U.B., A.K., M.B., T.O., M.G., C.D., Y.W., A.S., P.L., P.W., M.C.A., A.M.C. and R.W.: Designed the experiments. E.J.T., A.K., M.B., T.O., C.D., R.S., A.S. and M.S.: Performed the experiments. E.J.T., U.B., A.K., C.D., R.S., A.M.C., and R.W.: Analysed the data. E.J.T., P.L., A.M.C., M.C.A., and R.W.: Wrote the manuscript.

Additional information

Supplementary Information accompanies this paper at doi:10.1038/s41467-017-00945-2.

Competing interests: M.A., U.B., M.C., M.S., E.T. and R.W. have filed a patent on this work. The remaining authors declare no competing financial interests.

Reprints and permission information is available online at http://npg.nature.com/reprintsandpermissions/

Publisher's note: Springer Nature remains neutral with regard to jurisdictional claims in published maps and institutional affiliations.